ROMP-processing of mono- and difunctional imidonorbornene derivatives

Thanawadee Leejarkpai

ROMP-processing of mono- and difunctional imidonorbornene derivatives

Thanawadee Leejarkpai

A thesis submitted for the degree of Doctor of Philosophy at the University of Durham

October 1999

Abstract

ROMP-processing of imidonorbornene derivatives
Thanawadee Leejarkpai Ph D Thesis October 1999

The work described in the thesis is concerned with making new polymeric materials via ring opening metathesis polymerisation (ROMP) using a well-defined ruthenium carbene as an initiator. The object of the study was to provide a process for producing shaped articles by introducing a reactive liquid mixture into a mould in which the reacting liquid mixture undergoes ROMP in the bulk to produce the moulded article. Mono- and difunctional imidonorbornene derivatives were used as monomer and crosslinker respectively. The properties of the cured samples were determined by sol-gel analysis, DSC, TGA, nmr and IR spectrometry. Gel fraction, Tg and content of unreacted monomer were used to characterise the cured samples. The results indicated a strong dependence of the polymers appearance and properties on the polymerisation formulation and protocol, i.e. the monomer, the crosslinker and the polymerisation conditions.

The relative reactivity of the *exo*- and *endo*-monomers was investigated using the ^{1}H nmr technique since the initiation and propagation steps of the polymerisations can be followed in detail by this technique. The results showed that the polymerisations are living and the *exo*-isomer is more reactive than *endo*-isomer. A wider range of polymers can be prepared from solution polymerisation as compared to bulk polymerisation. The polymers derived from solid monomers, the monofunctional monomer with short N-alkyl pendant groups and all the difunctional monomers, could be prepared more easily in solution than in bulk polymerisation. The *endo*-monomer and the monofunctional monomer with long N-alkyl pendant group showed very low reactivity and were not suitable for ROMP in bulk but underwent solution polymerisation. It was found that the thermal properties of the linear polymers depend upon the amount of each monomer isomer incorporated into the polymer chain and the length of the N-alkyl pendant groups. All linear polymers are soluble in chlorinated solvents from which clear films can be cast. The work described establishes conditions for production of fully crosslinked solids with only traces of the sol fraction.

Acknowledgements

First, I would like to thank my supervisor, Professor W. J. Feast for his unfailing guidance, support and encouragement throughout my stay in Durham. My thanks are also due to Dr. E. Khosravi for his help with ring opening metathesis polymerisation. I would also like to acknowledge all the support staff in Durham: Dr. Alan Kenwright for help with interpretation of the nmr spectra, Julia Say and Catherine Heffernan for recording them, Gordon Forrest and Andrew Bosanko for the DSC and GPC service, Ray Hart and Gordon Haswell for providing the glassware. I would like to thank Dr. Peter Hine and Dr. Alan Duckett for their assistance about the mechanical properties. Also I would like to thank my colleagues, past and present in the IRC for their support. Finally, I would like to thanks my parents and Chatrchai for their loving care, support, and encouragement.

Memorandum

The work reported in this thesis was carried out at the Interdisciplinary Research Centre in polymer Science and Technology at Durham University between September 1995 and September 1999. This work has not been submitted for any other degree and is in the original work of the author except where acknowledged by an appropriate reference.

Statement of copyright

Financial support

I gratefully acknowledge the funding provided by the Thai Government.

Contents page

Chapter 1

General introduction and background

1.1 Aims and objectives

The aim of the work described in this thesis was to synthesise new polymeric materials via ring opening metathesis polymerisation (ROMP) and to develop a process for producing shaped articles by polymerisation in a mould. The process might lend itself to reaction injection moulding (RIM) and/or resin transfer moulding (RTM) depending on the details of the system; for example, rate of reaction, viscosity profile, mixing, cure time, exothermicity and so on. For this work, we proposed to use a combination of monomers and an initiator for ROMP which had not been examined for these processes previously. Two types of polymer are considered. The first is made by ring opening metathesis polymerisation of monofunctional imidonorbornene derivatives using a well-defined ruthenium carbene initiator; this approach gives linear polymers. The second type involves copolymerisation of mono- and difunctional monomers so as to produce crosslinked polymers. Since the application of this polymerisation system to in-mould processing is new, the goals of the work were to find the guide lines and basic parameters for simulation of RIM and RTM. This kind of in-mould processing requires as high a conversion of monomer as possible, since incomplete reaction, and particularly residual monomer, will affect the physical and thermal properties of the product. The main purpose of this chapter is to present the necessary background information for the work described in this thesis. Thus, this chapter is divided into three parts; namely, descriptions of ring-opening metathesis polymerisation, polymer processing (RIM and RTM) and the application of ROMP-RIM and RTM. In general only information relevant to the work described in this thesis is discussed in detail, information on related topics can be found in the literature cited.

1.2 Ring Opening Metathesis Polymerisation (ROMP)

Definition and Historical Background

Olefin metathesis is a catalytically induced bond reorganisation process and involves exchange of carbon-carbon double bonds. For an acyclic olefin, this leads to exchange of alkylidene units. The reaction was first reported by Banks and Bailey in 1964 and termed 'olefin disproportionation'.[1] The process is summarised in Figure 1.1.

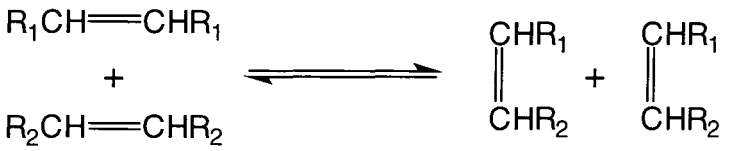

Figure1.1 General reaction scheme for the metathesis of acyclic olefins.

For a cyclic olefin, the metathesis reaction leads to ring scission and the formation of an unsaturated linear polymer.

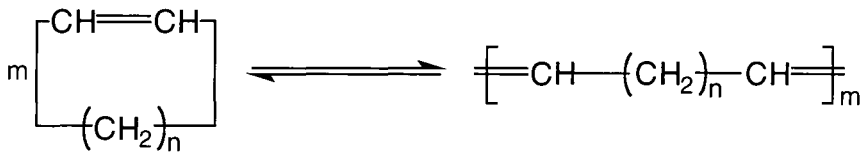

Figure 1.2 General reaction scheme for the metathesis of a cyclic olefin.

The first example of an olefin metathesis involving a cyclic olefin (in fact only recognised as such some years later) was reported by Anderson and Merkling in a Dupont patent in 1955.[2] They successfully polymerised norbornene using a mixture of titanium tetrachloride and ethylmagnesium bromide to initiate the process, see Figure 1.3. Calderon *et al.* recognised that disproportionation of acyclic olefins and ring opening polymerisations of cyclic olefins are examples of one and the same chemical reaction. They gave these types of reactions the name 'Olefin Metathesis'.[3-6]

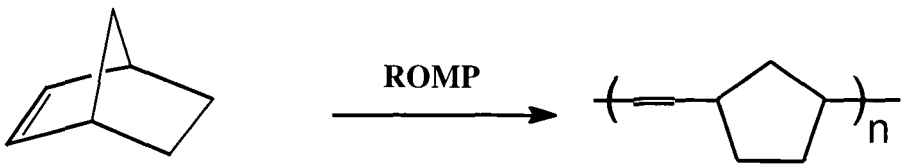

Figure 1.3 ROMP of norbornene.

Metathesis Initiators

In general the catalysts for olefin metathesis and ring-opening metathesis polymerisation are based on transition metals of groups IV to IX of the Periodic Table. However, Mo, W, Re and Ru compounds have been shown to be the most generally effective catalysts. Metathesis catalysts can be divided into two major categories;

namely, the ill-defined dual component systems, known as 'classical initiators', and single component 'well-defined initiators'. The well-defined initiators include transition metal carbenes and metallocyclobutanes, both were predicted by Chauvin when he proposed the mechanism for metathesis which is now established and accepted (see below). Various aspects of metathesis have been reviewed, most comprehensively in a recent book 'Olefin Metathesis and Metathesis Polymerisation' by Ivin and Mol.[7] Therefore, apart from a brief description of classical initiators, the remainder of this section is devoted to well-defined initiators, and particularly to the ruthenium carbene initiators, since they are of specific interest to the work discussed in this thesis.

Classical Initiators

Catalysts for a classical initiating system can either be homogeneous or heterogeneous and always contain a transition metal compound. Many of the commonly used catalyst systems are based on the chlorides, oxides or oxychlorides of Mo, W or Re. Although these compounds are sometimes effective by themselves, more commonly they require activation by a co-catalyst usually an organometallic compound or a Lewis acid. In some cases a third component called a promoter, is used as well. These promoters often contain oxygen; examples include O_2, EtOH and PhOH. Some typical homogeneous catalyst systems are $WCl_6/EtAlCl_2/EtOH$, $WOCl_4/Me_4Sn$, and $ReCl_5/Et_3Al/O_2$. Examples of heterogeneous supported catalyst systems include MoO_3/Al_2O_3, WO_3/SiO_2, and Re_2O_7/Al_2O_3.

However these classical initiators suffer from many disadvantages:-

- the precise nature of the active site at the metal centre is not known, thus the system is ill-defined,
- the metal carbene must be generated before initiation and subsequent propagation can commence and this process usually proceeds in a very low yield,
- the activity of a given initiating system is dependent upon its chemical, thermal and mechanical history, and upon the order and the rate of mixing of the catalyst, co-catalyst and monomer,

- they have limited tolerance towards functional groups in the monomer or solvent,
- there is a lack of control of molecular weight and molecular weight distribution due to intra- or intermolecular reactions with the double bonds, and
- they display an element of irreproducibility.

Well-Defined Initiators

Greater control over the reactivity of ROMP initiators became possible with the use of well-defined alkylidene complexes. These well-defined initiators allow, in favourable cases, the synthesis of polymers with narrow molecular weight distributions (M_w/ M_n <1.01) and control over tacticity. The first isolated metal carbene species, the Fischer carbene, was described in 1964.[8] It was a heteroatom stabilised complex and was shown to be reactive in olefin metathesis. It was found to react with highly strained olefins such as cyclobutene and norbornene derivatives. The diphenyl complex, first synthesised by Casey and Burkhardt in 1973, was not stabilised by a heteroatom and was much more reactive, initiating the polymerisation of less strained olefins.[9] These molecules are shown in Figure 1.4.

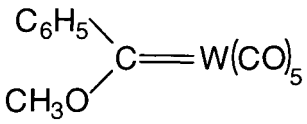

Fischer carbene

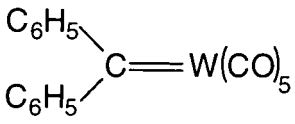

Casey carbene

Figure 1.4 Metal carbenes used to initiate metathesis.

Grubbs and co-workers isolated the first well defined metallacyclobutane complexes which were active as metathesis catalysts.[10] The reaction of Tebbe reagent with various olefins in the presence of nitrogen bases resulted in the formation of titanacyclobutane complexes. It has been shown that these titanacycles readily exchange with olefins via a rate determining loss of olefin from the titanacyclobutane ring to generate the transition metal methylidene species $Cp_2Ti{=}CH_2$ which is active in metathesis, see Figure 1.5. This type of catalyst is able to polymerise norbornene.[11]

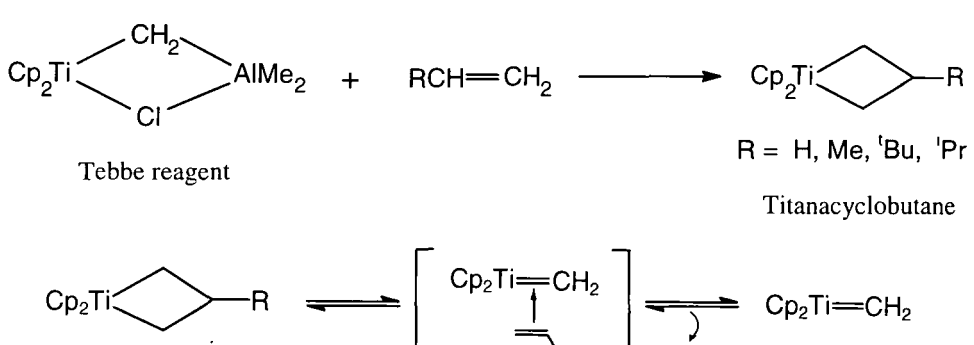

Figure 1.5 Formation of metallacyclobutane and methylidene species.

The first example of the living polymerisation of a cycloolefin was the polymerisation of norbornene by the titanacyclobutane complexes[12] shown in Figure 1.6.

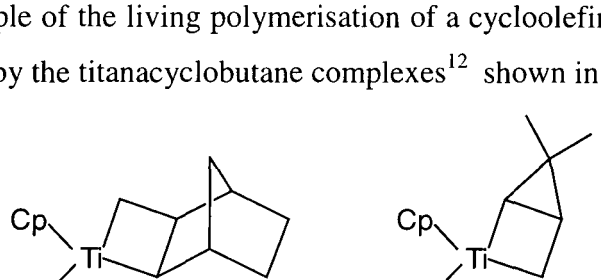

Figure 1.6 Grubbs' well-defined titanacyclobutane initiators.

In this case the polymerisation proceeds without termination or chain transfer to give polynorbornene with a narrow molecular weight distribution. The reaction is terminated by adding a ketone (typically benzophenone) or an aldehyde. However, there are some drawbacks associated with this initiator system. Titanacyclobutanes require a temperature of 50°C in order to ring-open even norbornene and they are very reactive towards functionalities owing to the highly electrophilic nature of the metal centre, this also makes them difficult to prepare and handle.

Kress and Osborn prepared the first well characterised tungsten alkylidene complexes of the type $W(CH\text{-}t\text{-}Bu)(OCH_2\text{-}t\text{-}Bu)_2X_2$, (X=halide).[13] Although these were inactive themselves, they formed highly active complexes on addition of a Lewis acid co-catalyst such as $GaBr_3$.

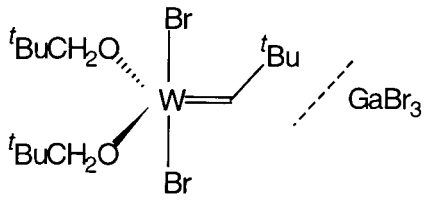

Figure 1.7 Osborn's well-defined tungsten initiator/co-catalyst.

Schrock and co-workers introduced well-defined tungsten and molybdenum initiators with bulky alkoxide and arylimido ligands of the type $M(CHR)(NAr)(OR')_2$.[14]

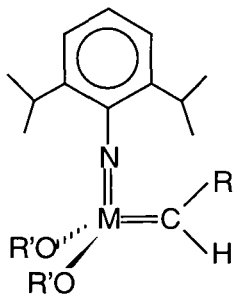

M = W or Mo
R = CMe_3 or CMe_2Ph
R' = CMe_3 , CMe_2CF_3 or $CMe(CF_3)_2$

Figure 1.8 Well-defined Schrock initiators.

Four co-ordination allows small substrates to attack the metal centre and give five co-ordinate intermediate metallacyclobutanes. The bulky alkoxide groups and the imido ligand prevent intermolecular reactions which could result in inactive complexes or decomposition of the catalyst. The bulky ligands also slow down bimolecular decomposition reactions. Substitution of the methyl groups on the alkoxides with the more electronegative trifluoromethyl groups makes the complex more active since the trifluoro groups draw electron density away from the metal centre. This makes the metal centre of the complex more electrophilic and a better acceptor for the incoming olefin which can be regarded as a π donor.[15] This effect is demonstrated by the observation that when OR is $O(C(CH_3)(CF_3)_2)$ the tungsten complex will readily metathesis acyclic olefins, whereas when OR is OBu^t it does not react with acyclic olefins. As a consequence of the high reactivity of tungsten, alkylidenes of this metal do not polymerise many functionalised monomers. Molybdenum catalysts, by contrast, tolerate a larger number of functionalities, including esters, amides, imides and ketones.

Ruthenium carbene initiators

Although molybdenum catalysts work in the presence of several functionalities the search for catalysts that tolerate more functional groups continued. The aim of this work was to develop a catalyst that was selective enough to complex and react with the soft C=C π-bond in the presence of hard carbonyls like ester groups, ketones and imides. It was found that as the metal centres in these complexes were chosen from further to the right in the Periodic Table, the resulting alkylidenes reacted more selectively with olefins in the presence of other functional groups, see Table 1.1.

Titanium	**Tungsten**	**Molybdenum**	**Ruthenium**
Alcohol, water	Alcohol, water	Alcohol, water	Olefins
Acids	Acids	Acids	Alcohol, water
Aldehydes	Aldehydes	Aldehydes	Acids
Ketones	Ketones	Olefins	Aldehydes
Esters, amides	Olefins	Ketones	Ketones
Olefins	Esters, amides	Esters, amides	Esters, amides

Table 1.1 As the central atom moves to the right in the Periodic Table of elements, it becomes softer and has more d-electrons. Complexation and reaction with the π-electrons of olefin is favoured over the complexation and reaction with the harder oxygen containing functionalities.

The remarkable tolerance towards heteroatoms and protic functionalities displayed by ruthenium-based initiators makes them attractive candidates for ROMP processes which are typically intolerant of the above conditions.[16] The first generation of ruthenium-based initiators were simple ruthenium salts and coordination complexes, e.g. $RuCl_3$ and $Ru(H_2O)_6(tos)_2$.[17] Although these compounds are highly active for the polymerisation of strained cyclic olefins, they constitute an ill-defined system. A propagating species, i.e. a rutheniumcarbene or rutheniumcyclobutane, has never been isolated from or detected during polymerisations with these initiators.

Reaction of 3,3-diphenylcyclopropene with either $RuCl_2(PPh_3)_3$ or $RuCl_2(PPh_3)_4$ produces the vinylcarbene complex $Ru(=CHCH=CPh_2)(Cl)_2(PPh_3)_2$ (compound **1a**, Figure 1.9), which was described by Grubbs and co-worker in 1992.[18] Norbornene and other highly strained cyclic olefins such as cyclobutene and cyclooctene are readily polymerised by this initiator in a living fashion. However, it is inactive for the polymerisation of less-strained cyclic olefins and acyclic metathesis.[19-21] Modification of compound **1a** by the exchange of the triphenylphosphine (PPh_3) ligands with tricyclohexylphophines (PCy_3) results in a much more active catalyst, compound **2a**, as a result of increased σ-donation from the phosphine ligands.[23] It catalyses the ROMP of both high- and low-strained cyclic olefins as well as the metathesis of acyclic olefins at room temperature. Although these complexes exhibit both high metathesis activity and remarkable stability toward functional groups, the multistep synthesis of the carbene precursor (diphenyl cyclopropene) and the low initiation rate of compounds **1a** and **2a** limits their use.

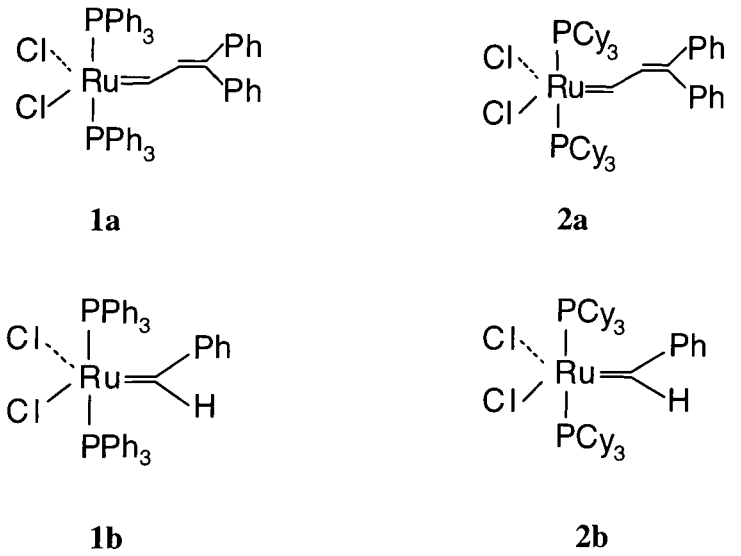

Figure 1.9 Well-defined Ruthenium initiators.

In 1995, Grubbs and co-workers reported the use of diazoalkanes as an alternative carbene source to provide air-stable alkylidene ruthenium complexes, compounds **1b** and **2b,** in high yield. These complexes are very efficient catalysts for the ROMP of norbornene and substituted cyclobutenes.[23-26]

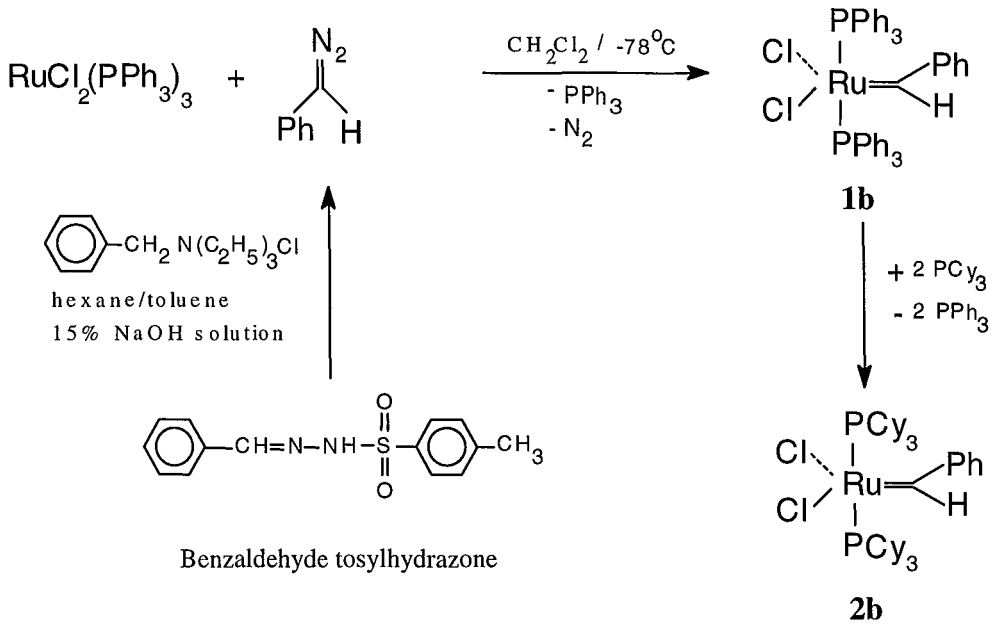

Figure 1.10 The synthesis of air-stable alkylidene ruthenium complexes.

An important advance in this work was the use of the alkylidene ruthenium complex, compound **2b**, as an initiator for our ROMP-processing system. This system has three advantages: first, the initiator is selective enough to react with olefin in the presence of imide groups in the monomer structures; secondly, it is soluble in the monomers and so no solvent is required in the processing system. Thirdly, the polymerisation rate is slow enough to allow the two components to be thoroughly mixed before they are introduced into the mould and neither inhibitors nor accelerators are required.

The Mechanism of Olefin Metathesis and Ring Opening Metathesis Polymerisation. [7]

According to the 'pair-wise' mechanism proposed by Bradshaw, it was thought that two double bonds came together in the vicinity of the transition metal site and that the orbitals of the transition metal overlapped with those of the double bonds in such a way as to allow exchange to occur via a weakly held cyclobutane type complex.[27] This pair-wise mechanism has now been abandoned in favour of one proposed by Hérrison and Chauvin in which a metal-carbene complex is the propagating species.[28]

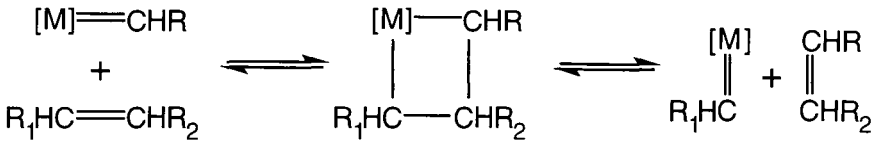

Figure 1.11 Hérrison and Chauvin's mechanism of olefin metathesis.

The process involves reversible [2+2] cycloaddition of the olefinic carbon-carbon double bond to a metal carbene species to form a metallocyclobutane which then ring opens either non-productively (degeneratively) to regenerate the original reaction mixture or productively to form a new olefin and a new metal carbene. In ring opening metathesis polymerisation, since the carbon-carbon double bond is enclosed within a ring, repetition of this cycle of productive metathesis results in an unsaturated polymer chain.

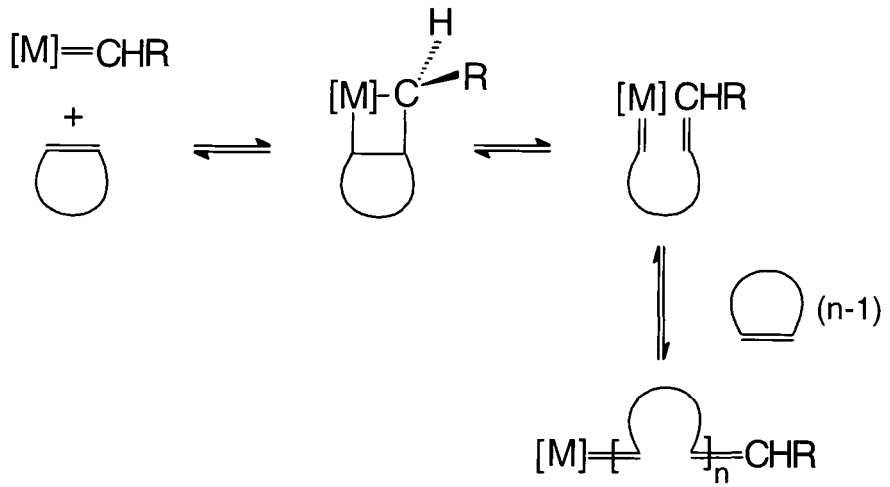

Figure 1.12 Mechanistic pathway for ring opening metathesis polymerisation.

All the above steps are reversible, so the outcome of the metathesis of acyclic alkenes and ring opening polymerisation depends on reaction conditions, such as temperature, concentration, reaction duration, the nature of the olefin and the nature of the propagating polymer chain end. Methathesis can be terminated by a reaction of the propagating metal carbene chain end with oxygen or oxygenated species (water, alcohol, etc.). Alternatively, well defined metathesis can be terminated by a 'Wittig type' reaction, typically with an oxygen containing molecule, usually a ketone or

aldehyde, which leads to the formation of unreactive organometallic compound (Figure 1.13).[15]

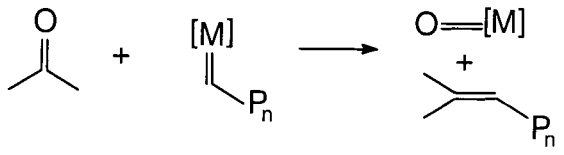

Figure 1.13 Termination of metathesis by a 'Wittig type' reaction.

Thermodynamic Aspects of Ring Opening Metathesis Polymerisation. [7]

For an addition polymerisation or any other reaction to occur the change in the Gibbs Free Energy (ΔG) must be ≤ 0. This change is expressed as a function of the enthalpy change (ΔH), the entropy change (ΔS) and the absolute temperature (Kelvin scale).

$$\Delta G = \Delta H - T\Delta S$$

For polymerisations the entropy (ΔS) is always negative since the monomers are combined with each other into macromolecules resulting in a reduction of their freedom. This makes the entropy term ($-T\Delta S$) positive, and for a favourable reaction, the change in enthalpy has to be larger than the $T\Delta S$ component. The temperature where $\Delta G = 0$, namely $T = \Delta H/\Delta S$, is called the *ceiling* temperature, and above this temperature, the polymerisation reaction does not take place.

In general the most favourable conditions for ring opening metathesis polymerisation of cycloalkenes are high monomer concentration, low temperature and high pressure. The enthalpy change (ΔH), is dependent on the ring strain. Therefore for highly strained 3, 4, 8 and higher membered monocyclic rings and for bicyclic rings, the enthalpy change is high (*i.e.* negative) and polymerisations go to completion at normal temperatures and monomer concentrations. For monomers with low ring strain, that is 5, 6 and 7 membered rings, the reaction entropy is a major determining factor, since the reaction enthalpy is low. The ΔG of polymerisation may also be sensitive to structural factors such as the nature of substituents and their position on the ring. Lower

temperatures and high monomer concentrations should favour polymerisation since this makes the entropy term -TΔS smaller.

A significant advantage of norbornene, bicyclo[2,2,1]hept-2-ene, derivatives as monomers for ROMP is that they have a greatly reduced tendency to undergo secondary metathesis (back biting) with the vinylene units in the polymer backbone due to the steric hindrance of approach to the olefinic moiety resulting from the branching at the α-carbons. In general, polymerisations with 5-*exo* substituted and 5,6-di-*exo* substituted-2-norbornene compounds have been more successful than with the corresponding *endo* isomers. This could be due to stabilising interaction between the endo substituent and the double bond or due to slightly larger ring strain of the *exo* isomer.

Microstructure of Polymer Chains

The way that the monomer unit is incorporated into the polymer chain determines the microstructure, that is the frequency and distribution of the isomeric repeat units, of the resulting polymer.[7,29] The microstructure of a polymer can be controlled in favourable cases by changing the catalyst system and the reaction conditions, so that it may be possible to synthesise a polymer with the required microstructure and associated physical properties for a specific application.

The three main factors which define the microstructure of polymers obtained by ring opening metathesis polymerisation are:-

1. *cis/trans* vinylene ratios and distribution,
2. tacticity effects, and
3. head/head, head/tail and tail/tail frequency and distribution.

1. *Cis/trans* vinylene ratios and distribution.

The backbone of polymers prepared by ROMP contains unsaturated bonds which can be either *cis* or *trans*, see Figure 1.14. The proportion of *cis* and *trans* in a particular polymer is primarily determined by the catalyst system, concentration, solvent and temperature. The nature of the monomer may also affect the outcome. In practice it

has proved possible to prepare polymers with *cis/trans* distributions varying from all *cis* to all *trans*.

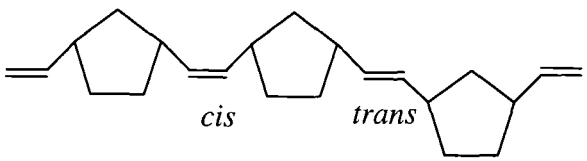

Figure 1.14 *Cis/Trans* double bonds in polynorbornene.

2. Tacticity effects.

Monomers such as symmetrically substituted bicyclo[2.2.1]hept-2-enes do not have chiral centres but give rise to polymer repeating units containing chiral centres. There is the possibility of two centres adjacent to the double bond having the same chiralities resulting in a racemic dyad or different chiralities, giving a meso dyad. Sequences of racemic dyads give syndiotactic polymers and sequences of meso dyads provide isotactic polymers. Polymers with a random distribution of meso and racemic dyads are known as atactic. As each C=C bond can have *cis* or *trans* geometry there are four possible regular microstructural arrangements as shown below.

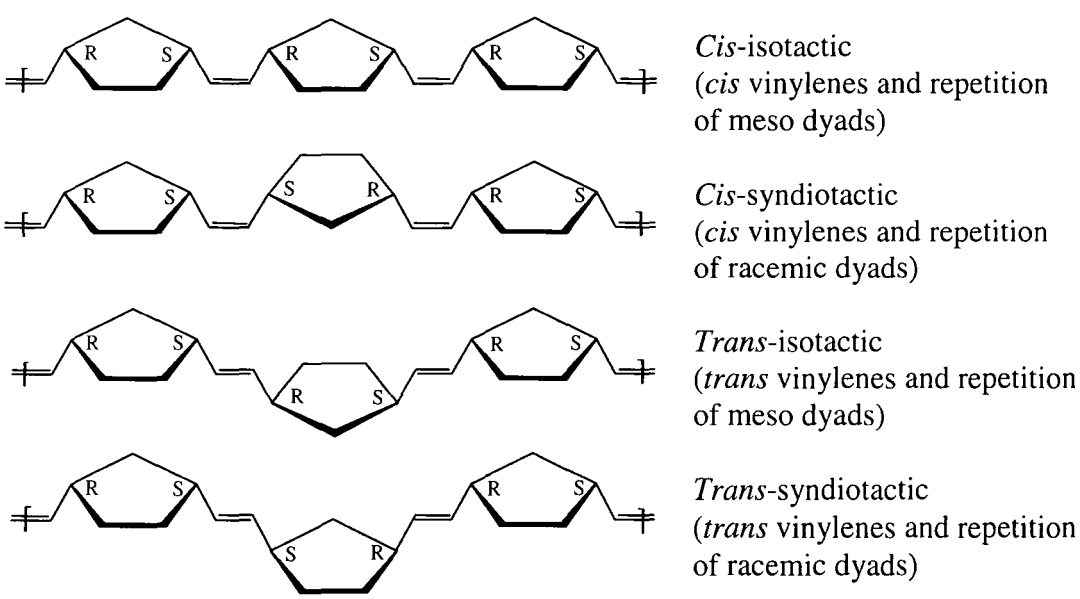

Figure 1.15 Tacticity effects in polynorbornene

3. Head/head, head/tail and tail/tail frequency and distribution

In the case of unsymmetrically substituted monomers such as a 5-substituted bicyclo[2.2.1]hept-2-ene, polymers can form with head-head (HH), head-tail (HT) or tail-tail (TT) structures, see Figure 1.16.

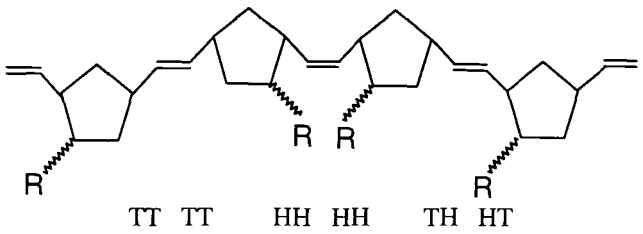

Figure 1.16 Head/Tail effects in the polymer of an unsymmetrically substituted monomer.

Furthermore, each of these structures can have meso or racemic dyads and cis/trans isomerism, so a large number of configurations becomes possible. The polymers prepared in this thesis are made from symmetrically substituted monomers. Symmetrical monomers, such as *exo*- and *endo*-N-alkylnorbornene-5,6-dicarboxyimide (*exo*- and *endo*-CnM), cannot give rise to HH, HT or TT addition.

1.3 Polymer processing

Polymer processing is an engineering speciality concerned with the operations carried out on polymeric materials or systems to make useful items. These operations produce one or more of the following effects: chemical reaction, flow, or a permanent change in a physical property. Typical polymer processing operations coming within this definition include injection moulding, calendering, dispersion of pigment in polymers, and surface modification of plastic film. Injection moulding is one of the most important operations of polymer processing; it involves flow but neither chemical reaction nor a permanent change in a physical property. A thermoplastic is melted and injected, in the liquid state and under high pressure, into a closed mould where it cools and solidifies. The mould is then opened, the moulded item ejected, and the sequence repeated.[30,31] The development of a number of very fast polymerisations to give urethane systems with a wide choice of final properties resulted in a new processing

method, reaction injection moulding, which has been said to have a high growth potential.[33]

1.3.1 Reaction Injection Moulding (RIM)

Reaction injection moulding (RIM) was developed early in the 1960s.[30-39] It is a process for the high-speed production of polymer parts directly from low viscosity reactants injected into a mould. In this process two or more low viscosity liquid streams, which react with each other when brought together, are mixed prior to being injected into large cavities. Some of the polymerisation reaction occurs during the filling stage. The bulk of the reaction takes place after filling and during the curing stage. Part shape is determined by fast polymerisation in the mould and subsequent chemical crosslinking or physical change such as domain formation and recrystallisation, not by cooling as in thermoplastic injection moulding. A Schematic diagram for the process is shown in Figure1.17.[33] The flow rate of the two highly reactive monomers or prepolymers must be accurately controlled to provide the correct stoichiometry. The two metered streams are forced to impinge at high velocity to achieve good mixing. From the mixhead they flow into the mould and react rapidly to produce a solid part.

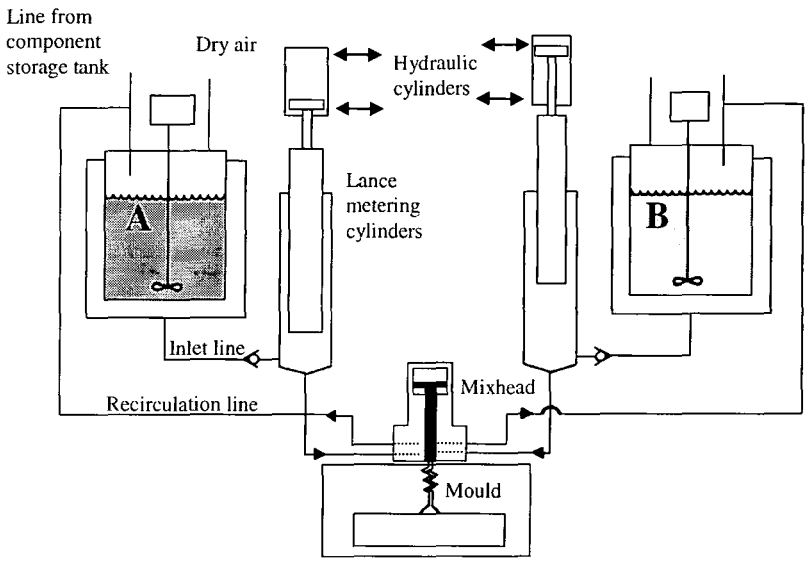

Figure 1.17 Schematic diagram of the reaction injection moulding process, after Kroschwitz.[33]

The advantages of the RIM process are clear. Polymer is formed after the reactants mix is in the desired shape and the low viscosity reactants can be mixed easily and the mould filled at low pressure. An important aspect of the RIM process as opposed to conventional thermoplastic injection moulding (TIM) is the big reduction in equipment costs resulting from the use of low viscosity monomer or prepolymer feeds. Injection pressures can be reduced from the 2000 atm typical in TIM to about 100 atm in the RIM mixhead and less than 10 atm in the mould. Thus, very large and complex shaped items can be formed using rather small clamping pressures and inexpensive moulds.[36,37] The key to the success of the RIM process is fast rates of polymerisation to ensure the demands of short cycle time from closing the mould, through the injection of reactants and the cure, to the ejection of the items. It can be seen that potentially RIM is an energy-saving process in the fabrication of polymeric products.

RIM Chemistry- Thermodynamic and Kinetic requirements

The most important step which must take place in RIM is the rapid transformation of a liquid, or a mixture of liquids, into a solid with some desirable physical properties. In order to produce a solid from a liquid, some form of molecular aggregation has to occur and polymerisation is probably the most likely route for making materials with useful solid state properties by this technique. Whatever the chemical route to a polymer, it is an essential thermodynamic requirement that the free energy change (ΔG), $\Delta G = \Delta H - T\Delta S$, for spontaneous reaction should be negative.[40] As mentioned in the previous section, the entropy change (ΔS) for the polymerisation is related to the molecular order in the system before and after reaction and ΔS must be negative. For ΔG to be negative, the enthalpy of reaction must also be negative and larger than $T\Delta S$, where T is the temperature of reaction on the Kelvin scale. Although this is a very simple summary of polymerisation thermodynamics, it does lead to the conclusion that heat should be evolved during polymerisation. The amount of heat evolved will depend on the type and the amount of bond rearrangements which take place in a particular reaction. It is possible to see that $\Delta G = 0$ when $\Delta H = T\Delta S$, i.e. a temperature sensitive thermodynamic equilibrium may exist between the forward and reverse reactions. These facts have important consequences in the overall RIM process. For example, since virtually all the heat of reaction is liberated within the mould, it is difficult to

regulate the sample temperature. A large temperature rise might take the system above the ceiling temperature and result in some depolymerisation. If this happened the product might contain undesirable residual low molecular weight material.

The requirement for fast polymerisation in the mould is related to the need for fast production rates in the manufacturing situation. The reactions used in RIM may involve either a step growth polymerisation, such as polyurethane, polyurea, or epoxy formation, or a chain growth polymerisation, as in DCPD RIM (see later). Chain growth polymerisations[41,42] involve initiation, propagation and termination steps. Polymerisation of vinyl and diene monomers usually conform to this scheme. The rate of conversion of monomer to polymer is generally governed by the propagation reaction rate which can be expressed by equation below.

$$\text{Rate of polymer formation} = k_p\,[M]\,[M_n^*] \qquad (1)$$

Where k_p is the propagation rate constant, and [M] and $[M_n^*]$ are the instantaneous monomer and active centre concentrations respectively. For the rate to be large k_p, [M] and $[M_n^*]$ should be as large as possible. Whereas the overall rate of step reactions[41,43] can be expressed as shown below.

$$\text{Rate of polymer formation} = k\,[\text{catalyst}]\,[A]\,[B] \qquad (2)$$

The reaction rate constant k is dependent on the reactivity of the functional groups [A] and [B] which are involved in the reaction. The overall rate is a function of k, the concentration of A and B and, where applicable, the catalyst.

Apart from the thermodynamic and kinetic requirements outlined above the reagents used in the RIM system must:

(a) be liquid at or near ambient temperature and have low viscosity, preferably in the range 0.01-1.0 Pa. s.,

(b) be as physically compatible as possible to assist the impingement mixing process when that is used,

(c) have a reasonable self-life even when loaded with catalysts or filler, and

(d) have low vapour pressure and low toxicity to minimise the handing problem in a production situation.

The reaction is complicated by the rheological changes that happen during polymerisation.[32,34] These changes include (1) domain formation, in which materials change from single phase to multiple phases because of the thermodynamic incompatibility of polymer segments or blocks; (2) gelation, in which materials change from a viscous fluid to a gelled network with chemical or physical crosslinking; and (3) phase separation or crystallisation, in which the reacting mixture changes from a rubbery material to a glassy polymer or from an amorphous material to a semicrystalline polymer with increasing degree of polymerisation and packing of the polymer segments. Generally, material and operational parameters determine the 'mouldability' of a specific polymer system in a particular mould. The mouldability diagrams established for thermoplastic injection moulding (TIM) can give a starting point for process optimisation and a rough guide for starting new materials in a RIM system.

In TIM, mouldability is usually tested in an empirical way. The mouldability area in the temperature/pressure diagram is bounded by four curves. Above the top curve the polymer degrades thermally, whereas below the bottom curve it will not flow. To the left of the 'short shot' curve, the polymer is too viscous to fill the mould completely at the applied pressure. To the right of the 'moulding area', injection pressure is high and viscosity low enough that flash (i.e. leakage from the mould) might be encountered. Moulding area diagrams like Figure 1.18 are well known to TIM and this approach has been extended to RIM. In practice, RIM operators can more easily vary injection time and demould time than either the material or the mould temperature.

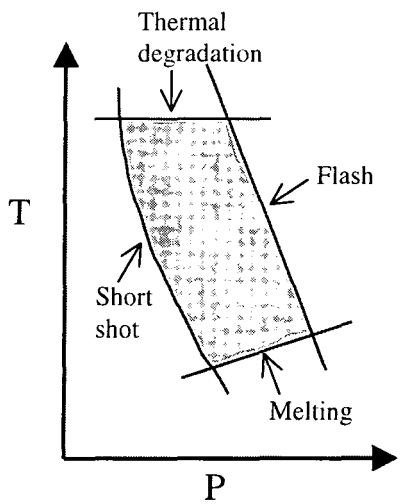

Figure 1.18 Schematic TIM 'moulding area' diagram.

RIM-process and system characterisation

For convenience of analysis, the RIM process can be divided into mixing, filling, and curing as outline by Broyer and Macosko.[44] In practise, mixing and filling can be treated together as the filling stage. Therefore, the basic steps of the process are filling and curing. In the RIM process, reaction can be activated by two different methods: mixing and heat transfer. For the mixing activated process, two highly reactive monomers or prepolymers are brought into intimate molecular contact by impingement mixing. From the mixing head they flow into the mould and react rapidly to form a solid part. The mould wall temperature (T_w) is not much different from the starting material temperature (T_o) since the monomers are highly reactive at T_o. For this system, the criterion of good impingement mixing has to be fulfilled. Urethanes are very reactive at 40-50 °C, the temperature at which they are mixed by impingement. Mould walls usually are controlled at 60-80 °C (close to the mixing temperature). In the thermally activated RIM process, the monomers do not react appreciably at T_o but are highly reactive at T_w. Reaction usually starts after the material comes in contact with the hot walls. The mould wall temperature (T_w) is much higher than the starting temperature (T_o). Thermally activated RIM systems include epoxies and polyesters. Epoxy RIM formulations are mixed at 40-70 °C but do not react appreciably until they are brought in contact with the hot mould (100-150 °C).

RIM-filling stage

The important parameters during the filling stage are initial material temperature (T_o), and filling time (T_f). As mentioned before, for the mix activated system the reactive monomers have to be brought into intimate molecular contact by impingement mixing. During filling, the viscosity of the flowing mixture increases due to chemical reaction and filling must be over before this rise becomes too large. Thus, it is important to find the guidelines to avoid premature gelling. Another limiting criterion for the filling stage is related to flow instabilities, which can result in the generation of large bubbles in the final product. Finally the material temperature should not exceed a pre-determined maximum, in order to prevent thermal degradation.

RIM-curing stage

When the mould is full, injection is stopped. The material is left in the mould, reacting until it is dimensionally stable. This stage of the RIM process is called curing. During this stage, the chemical reactions go to near completion and the structure of the final product is determined through crosslinking, phase separation, or crystallisation. The most relevant parameters during this stage are mould wall temperature (T_w) and demould time (T_d). Mould temperature is also found to be an important parameter affecting product properties and surface quality. Very high mould temperatures result in a very thin, peeling and coarse skin, while low temperatures cause the skin turn to thick and brittle. The duration of the curing step depends on how long it takes for the material to reach a conversion level at which it is dimensionally stable and can be removed from the mould. On the other hand, the temperature throughout the mould should never rise above the material degradation point.[45,46] For bulk polymerisation, in order to reach a high conversion, the reaction temperature should be higher than Tg and the product may need a postcure treatment after demoulding to reach ultimate conversion and physical properties.

Reinforced reaction injection moulding (RRIM) is an extension of RIM. Materials for RIM and RRIM are very similar, but the machinery is substantially dissimilar because of the differences in viscosity and abrasiveness of the materials being processed. The reinforcing materials like milled glass and short glass fibres can, in principle, be added to one or both components but some important change must be made to the equipment for RRIM; for example, circulation pumps must be able to handle viscous materials and keep fibres in suspension, consequently wear resistant materials are needed. In practice fibres are added in both liquid steams to allow balancing of viscosities and to attain good mixing. However, several limitations have been found in RRIM technology: (1) the process is only successful for milled glass of 0.8- 6 mm. size and other short fillers, e.g. mica flake, (2) Chopped glass fibre is difficult to handle in the machines, (3) fibre breakage during circulation and impingement mixing is serious, and (4) leakage of material lines because of abrasion by the reinforcing agent. Prelocating a glass mat inside the mould has also been tried. This technology is named structure RIM (SRIM) or composite RIM, which is similar to an existing technology called resin transfer moulding (RTM). These RIM variants are summarised in Figure 1.19.

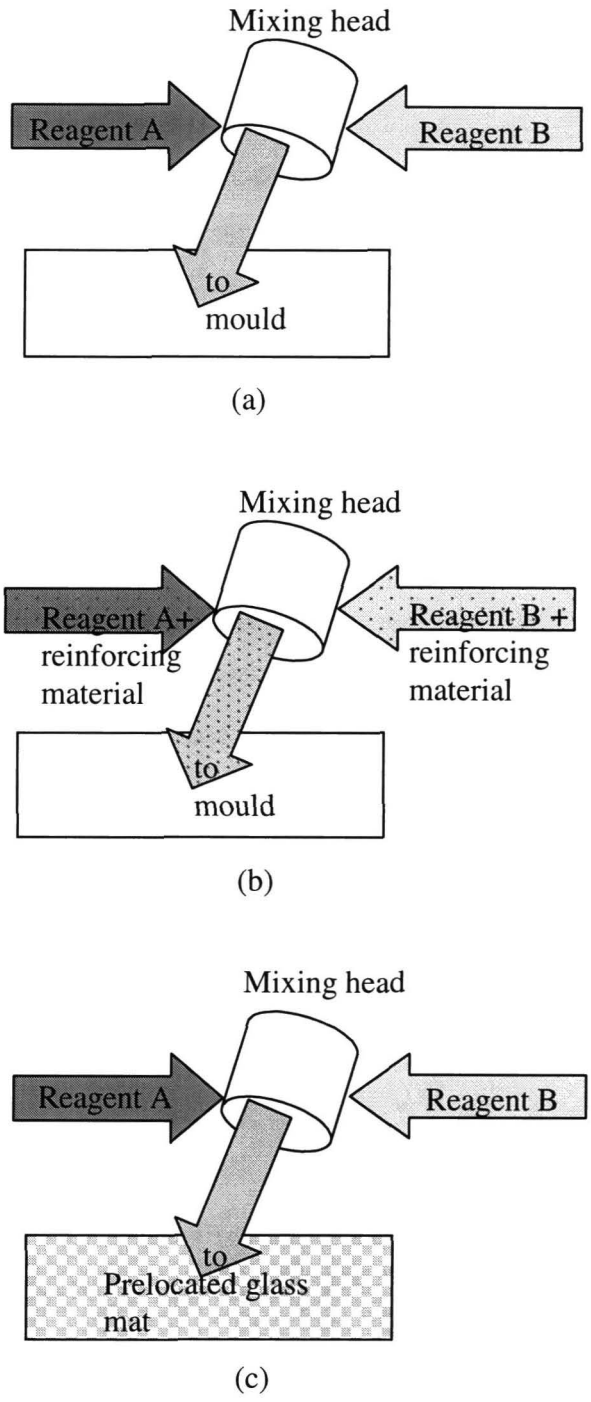

Figure 1.19 Basic principle of (a) RIM, (b) RRIM and (C) SRIM.

1.3.2 Resin Transfer Moulding (RTM)

Liquid composite moulding (LCM) has been well documented in recent years.[47-49] LCM is a term which includes RTM and SRIM.[47] The common feature is the introduction of a liquid resin or resins (usually thermosets) under a forcing pressure gradient into a closed mould which contains a fibre perform. These materials

are generally composed of high strength fibres dispersed in a polymer matrix and offer several attractive features to manufacturers and end-users. The performance advantages over metal equivalents include weight reduction, design flexibility, corrosion resistance and reduced noise transmission. With respect to optimum property performance in composites, very high conversion and controllable gel times are required to allow resins to permeate the reinforced shape completely.

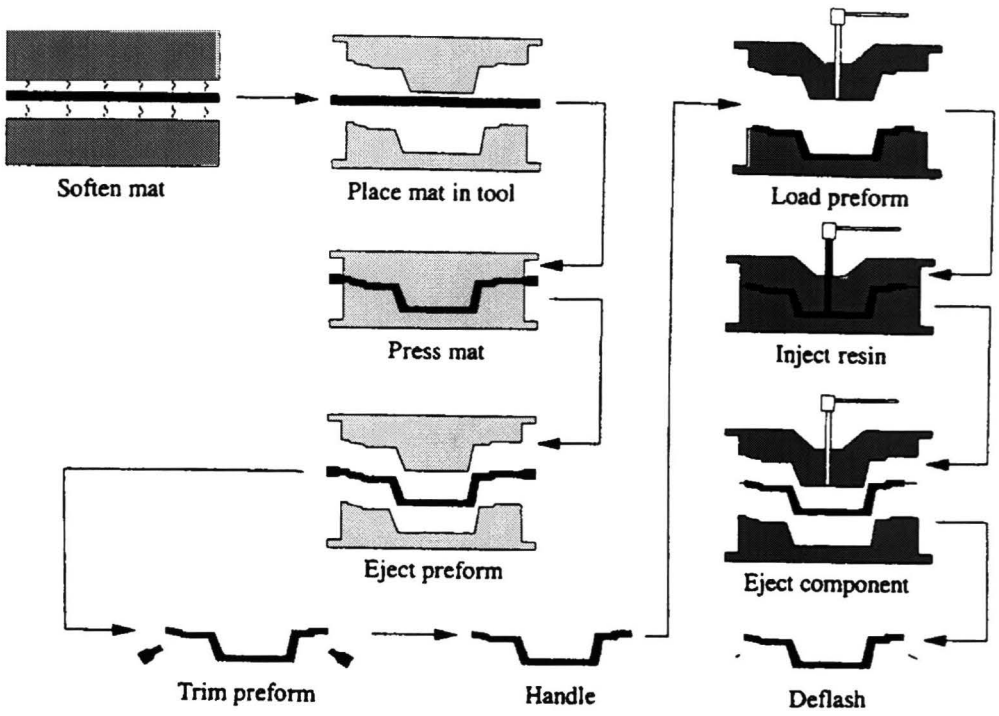

Figure 1.20 Schematic diagram of the resin transfer moulding process, after ref.[48]

Typically, SRIM will require higher pressure than RTM meaning more expensive moulds. However, highly reactive polyurethane and high flow rates will give faster production rates than RTM. Cycle times are of the order of seconds for SRIM and several minutes for RTM depending on part geometry. Currently, market development for RTM is inhibited by long moulding cycle times. The process can be considered as consisting of two essential phases which, depending upon process variables, may coincide to a greater or lesser degree:-

- impregnation (comprising resin flow, air displacement, fibre wetting, and heat transfer), and
- polymerisation (including heat transfer).

Several different processes are used in RTM. Some resins used in RTM (typically polyester and vinyl ester) are formed by free-radical polymerisation, in which the growing polystyrene chain reacts with the unsaturated polyester molecules to form a crosslinked structure. An advantage with this reaction is the versatility offered in processing and the wide range of material properties obtainable. Ambient temperature curing systems have been formulated but require prolonged periods for cure and can present processing difficulties owing to the high resin viscosity. Heat activated systems improve resin processability by reducing resin viscosity during impregnation and reducing mould cycle time. Epoxy resins are also used extensively in RTM and harden by addition polymerisation. A curing agent is mixed with the epoxy resin to crosslink the polymer and form a solid structure. As with polyester and vinyl ester resins, epoxy resins provide great versatility in both material and processing properties. Polyurethane resins, typically used in SRIM, form by addition polymerisation, followed by crosslinking. Resin viscosity remains low during urethane formation but builds rapidly during crosslinking. This is ideally suited to a high volume LCM process, in which low viscosity is desirable during mould filling to minimise impregnation pressure, while sufficient structure is required as early as possible to permit ejection of the moulded component.

1.4 The application of RIM and RTM

Polymerisation in the RIM process is more complicated than that in conventional polymerisation because, in order to combine polymerisation with the processing step, reaction has to occur in the bulk. Therefore the reaction should not give off any by-products, such as water of condensation, unless they can be quickly absorbed in the system by a filler or used for foaming to compensate for the polymerisation shrinkage. To date, the major commercial RIM process materials are polyurethanes, being more than 95% of the total processed. The reason for this is that polyurethane chemistry is able to provide both a fast, complete reaction with no side products and a wide range of

property variability through the introduction of crosslinking, foaming and fibre reinforcement. Development of similar desirable characteristics in polyurea, nylon, epoxy, polyester, silicone rubber and other polymers is currently an active field of research.[32,50-53]

Dicyclopentadiene (DCPD), which until recently was a low value component of the C_5 stream of petroleum refining, is one of the newest monomers used in commercial RIM systems.[7,54-61] It is cheap and can be polymerised by metathesis polymerisation, which yields a highly crosslinked olefinic polymer. The cyclic ring opening polymerisation results in an exothermic, fast reaction from the relief of ring strain energy. This polymerisation process can be tailored to have the characteristics which make it readily adaptable to either reaction injection moulding (RIM) or resin transfer moulding (RTM). Various polymers and copolymers with different structures such as linear and crosslinked homopolymers; random, graft and block copolymers; stereospecific polymers with all *cis* or *trans* double bonds on the main chains can be obtained by altering the catalytic systems.[62]

Oshika[63] and Dall'Asta[64] showed that DCPD could be polymerised by metathesis catalysts. It could be polymerised by $MoOCl_3$ to a gel at 35°C and then cured to a hard brown resin at 140°C, as described by Devlin.[65] Copolymers of DCPD with norbornene and its derivatives are easier to process than the homopolymers, and can be compounded with filler etc. to form rigid articles, such as hub caps, by injection moulding. Cyclopentadiene itself can be used as co-monomer with norbornene derivatives and yields products of high impact strength.[66]

An important advance in this area of technology was the use of organoammonium molybdates or tungstates of the type $(R'_4N)_{2y-6x}Mo_xO_y$ or $(R'_3NH)_{2y-6x}Mo_xO_y$ as catalyst in conjunction with an aluminium compound such as Et_2AlCl or (RO)RAlCl as cocatalyst.[67] These systems have two advantages: first, where R' is a long chain (e.g. C_{12}) the catalyst is soluble in the monomer and no solvent is required; secondly, the introduction of an alkoxy (or aryloxy) group in the co-catalyst reduces the reactivity to the point where the complete reaction mixture can be made up at room temperature, has a pot life of 1-8 hour, and can be injected into the mould at 60-200 °C under conditions such that reaction is complete in 2 minutes. Compounds of the type **a** and **b**

(see Figure 1.21), having two double bonds of essentially equal reactivity to ROMP are ideal as cross-linking agents to produce a thermosets product.[7,67]

(a) (b)

Figure 1.21 Crosslinking bifunctional metathesis monomer

It should be note that in DCPD it is the norbornene-type double bond that undergoes ROMP, the opening of the other double bond by metathesis is thermodynamically less favourable. With some metathesis catalysts crosslinking may also occur through vinyl addition processes of the cyclopentenyl group during or after ring opening metathesis polymerisation, which causes the product to be insoluble in organic solvents, as shown in Figure 1.22.[68]

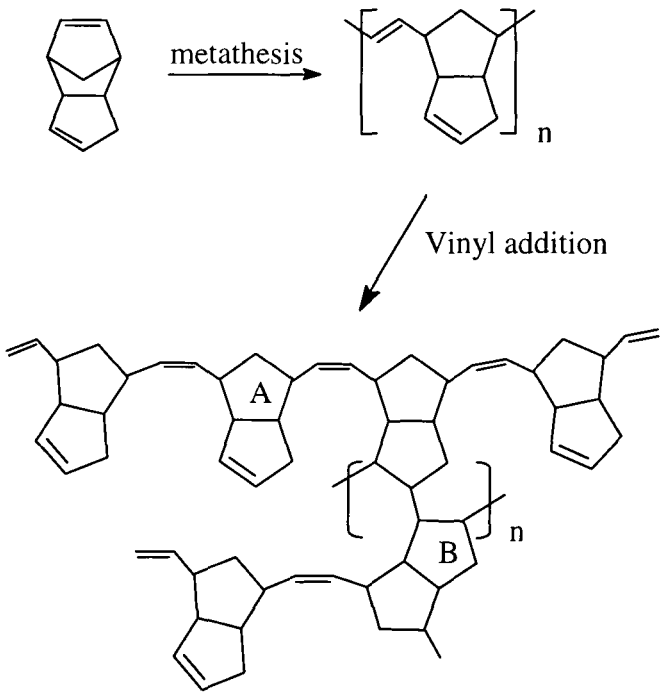

Figure 1.22 ROMP of DCPD : (unit A) polymerisation through the norbornene ring; (unit B) polymerisation through vinyl addition.

RIM of DCPD by ROMP using two streams rather than one has been extensively tested. A typical arrangement is to place the catalyst, e.g. WCl_6/ ROH, in one monomer stream and the cocatalyst (activator) e.g. Et_2AlCl, in the other. The two streams pass first into a mixing chamber and then into the mould where the heat of reaction raises the temperature within a minute to about 150°C.[69] The product is a tough, rigid, thermoset polymer of high modulus and excellent impact strength. An early example of a catalyst system for this process was developed at the Koninklijke/Shell Laboratorium in Amsterdam. It consists of WCl_6/2,6-diisopropylphenol (1/2) with R_3SnH as cocatalyst. Both components are soluble in DCPD and have long shelf-life.[70] Since that time many other systems have been investigated and a vast patent literature exists.

One of the chief problems of the two-stream method is the prevention of premature reaction leading to clogging in the region between the mixing chamber and the mould. This problem can be overcome either by the use of less active cocatalyst or by the inclusion of a Lewis base (moderator), such as benzonitrile, dibutyl ether, tetrahydrofuran, acetylacetone or an alkylacetonacetate, or by use of a comonomer having an ester substituent. In all cases the initial reaction is slowed down to the extent that there may be a short induction period allowing the reaction mixture to reach the mould before the period of rapid reaction. The functional of the Lewis base is to co-ordinate or chelate to the metal centre, so modifying the initiation and propagation rates.

For objects produced by RIM, it is desirable to have as high a conversion of monomer as possible, since the residual monomer will affect both the mechanical properties of the product and the extent of residual odour. With many catalyst systems the conversion is often only 90-95%. Another minor problem is that DCPD has a melting point of 32 °C, which necessitates heating the input stream if the monomer is very pure. This can be avoid by using a mixture of cyclopentadiene oligomers, which can be produced by heating DCPD to 125-250°C in a closed system. The production of large moulded objects (up to 300 kg) from DCPD-based feeds using RIM technology was developed mainly in the USA by BF Goodrich Co. under the trade name Telene.[71] In 1988 Hercules inaugurated a 13,600 ton capacity plant at Deer Park, Texas, to produce poly(dicyclopentadiene) under the trade name Metton. The catalyst used was a

combination of $WCl_6/WOCl_4$ and nonylphenol with Et_2AlCl.[72] In the Telene process the preferred catalyst is a trialkylammonium molybdate. Up to 10% trimer of cyclopentadiene is added to the monomers, not only to decrease the melting point of DCPD, but also to increase crosslinking in the polymer. BF Goodrich have licensed their process to the Japanese company Nippon Zeon, which manufactures the product under the name Pentem. The development of this area is still in progress.

An early RTM used in the early 1940s was known as the Macro method.[47-49] There were few applications though the 1950s and 1960s with some interest during the 1970s for fabrication of marine and recreational parts. Significant development work began during the 1980s with the introduction of structural and semi-structural parts for aircraft, defence applications, automotive structures and high performance sport goods. This process provides a useful fabrication route for structural components which are difficult to produce using alternative composite manufacturing processes. Liquid moulding is now in use for a growing number of applications in the aerospace and automotive industries. As the market continues to grow, new developments in materials and processes have emerged to meet the demands of specific industries. However, the ROMP system had not been widely used in RTM. For this work, we proposed to synthesis new polymeric materials via ROMP and to develop a process which might lend itself to RIM and/or RTM.

1.5 References for Chapter 1

[1] R. L. Banks and G. C. Bailey., *Ind. Eng. Chem. Prod. Res. Dev.*, **3**, 170, 1964.

[2] A. W. Anderson and N. G. Merckling., U.S. Patent 2721 189, *Chem. Abstr.*, **50**, 3008i, 1955.

[3] N. Calderon, *Chem. Eng. News*, **45**, 51, 1967.

[4] N. Calderon, H. Y. Chen and K. W. Scott, *Tetrahedron Lett.*, **23**, 3327, 1967.

[5] N. Calderon, E. A. Ofstead and W. A. Judy, *J. Polym. Sci. Part A*-1, **5**, 2209, 1967.

[6] N. Calderon, E. A. Ofstead, J. P. Ward, W. A. Judy and K. W. Scott, *J. Am. Chem. Soc.*, **90**, 4133, 1968.

[7] 'Olefin Metathesis and Metathesis Polymerisation', K. J. Ivin and J. C. Mol, Academic Press, 1997.

[8] E. O. Fischer and A. Maasbol, *Angew. Chem. Inter. Ed.*, **3**, 580, 1964.

[9] C. P. Casey and T. S. Burkhardt, *J. Am. Chem. Soc.*, **95**, 5833, 1973.

[10] T. R. Howard, J. B. Lee and R. H. Grubbs, *J. Am. Chem. Soc.*, **102**, 6876, 1980.

[11] P. A. Straus and R. H. Grubbs, *Organometallics*, **1**, 1658, 1982.

[12] L. R. Gilliom and R. H. Grubbs, *J. Am. Chem. Soc.*, **108**, 733, 1986

[13] J. Kress and J. A. Osborn, *J. Am. Chem. Soc.*, **105**, 6346, 1983.

[14] R. R. Schrock, J. S. Murdzek, G. C. Bazan, J. Robbins, M. Dimare and M. O'Regan, *J. Am. Chem. Soc.*, **112**, 3875, 1990.

[15] R. R. Schrock, *Acc. Chem. Res.*, **23**, 158, 1990.

[16] M. A. Hillmyer, A. D. Benedicto, S. T. Nguyen, Z. Wu and R. H. Grubbs, *Macromol. Symp.*, **89**, 411, 1995.

[17] M. A. Hillmyer, C. Lepetit, D. V. McGrath, B. M. Novak and R. H. Grubbs, *Macromolecules*, **25**, 3345, 1992.

[18] S. T. Nguyen, L. K. Johnson and R. H. Grubbs, *J. Am. Chem. Soc.*, **114**, 3974, 1992.

[19] Z. Wu, A. D. Beneticto and R. H. Grubbs, *Macromolecules*, **26**, 4975, 1993.

[20] S. T. Nguyen, R. H. Grubbs and J. W. Ziller, *J. Am. Chem. Soc.*, **115**, 9858, 1993.

[21] G. C. Fu, S. T. Nguyen, R. H. Grubbs, *J. Am. Chem. Soc.*, **115**, 9856, 1993.

[22] B. R. Maughon and R. H. Grubbs, *Macromolecules*, **29** (18), 5765, 1996.

[23] P. Schwab, M. B. France, J. W. Ziller and R. H. Grubbs, *Angew. Chem. Int. Ed. Engl*, **34** (18), 2039, 1995.

[24] P. Schwab, R. H. Grubbs and J. W. Ziller, *J. Am. Chem. Soc.*, **118**, 100, 1996.

[25] D. M. Lynn, S. Kanaoka, and R. H.Grubbs, , *J. Am. Chem. Soc.*, **118**, 784, 1996.

[26] E. L. Dias, S. T. Nguyen and R. H. Grubbs, *J. Am. Chem. Soc.*, **119**, 3887, 1997.

[27] C. P. C. Bradshaw, E. J. Howmann, and L. Turner, *J. Catal.*, **7**, 269, 1967.

[28] J. L. Herrison, and Y. Chauvin, , *Makromol. Chem.*, **141**, 161, 1971.

[29] 'Comprehensive Polymer science', V.4, Pergamon Press, 1989.

[30] 'Polymer Processing', J. M. McKelvey, John Wiley and Son Inc., New York, 1962.

[31] 'Polymer Processing', C. E. Schildknecht, Interscience Publishers, New York, 1956.

[32] 'Comprehensive Polymer Since', S. L. Aggarwal, 1st Edition, **7**, Pergamon Press, 1989.

[33] 'Concise Encyclopedia of Polymer Science and Engineering, J. I. Kroschwitz, John Wiley & Sons, New York, 1990.

[34] M. Zloczower and C. W. Macosko, *Polym. Process. Eng.*, **4**(2-4), 173, 1986.

[35] 'Reaction Injection Moulding', W.E. Becker, Van Nostrand Reinhold Co., Inc., New York, 1979.

[36] P. D. Coates and A.F. Johnson, *Plast. and Rubb. Process. Appl.*, **1**, 223, 1981.

[37] C. W. Macosko, *Soc. Plast. Eng.*, Tech. Pap., **29**, 525, 1983.

[38] S. H. Metzger and D.J. Prepelka, *J. Elast. Plast.*, **8**, 141, 1976.

[39] R. P. Titlebaum, *SPE Tech. Papers*, **21**, 233, 1975.

[40] K. J. Ivin, *Angew. Chem.*, Int Ed., **12** (6), 487, 1973.

[41] 'Textbook of Polymer Science', F. W. Billmeyer, Wiley Toppan, New York, 1971.

[42] 'The Kinetics of Vinyl Polymerisation by Radical Mechanism', C. H. Bampord, W. G. Barb, A. D. Jenkins and P. F. Onyon, Butterworth, London, 1958.

[43] 'Principle of Polymerisation', G. Odian, McGraw-Hill, New York, 1970.

[44] E. Broyer and C. W. Macosko, *AIChE J.*, **22**, 268, 1967.

[45] E. B. Richter and C.W. Macosko, *Polym. Eng. Sci.*, **20**, 921, 1980.

[46] P. W. Sibal, R. E. Camargo, and C.W. Macosko, *Int. J. Polym. Process.*, **1**(2), 147, 1983-1984.

[47] C. D. Rudd, E. V. Rice, L. J. Bulmer, and A. C. Long, *Plast., Rubb. and Compos. Process. Appl.*, **20**, 67, 1993.

[48] 'Liquid Moulding technologies' , C. D. Rudd, A. C. Long, K. N. Kendall, and C. G. E. Mangin, Woodhead Publishing Limited, London, 1997.

[49] K. N. Kendall and C. D. Rudd, *Polym. Compos.*, **15**(5), 334, 1994.

[50] 'Concise Encyclopaedia of Polymer Science and Engineering, J. I. Kroschwitz, John Wiley & Sons, New York, 1990.

[51] M. Zloczower and C. W. Macosko, *Polym. Process. Eng.*, **4**(2-4), 173, 1986.

[52] 'Reaction Injection Moulding', W.E. Becker, Van Nostrand Reinhold Co., Inc., New York, 1979.

[53] 'Polydicyclopentadiene: A new RIM thermoses', R. P. Geer, *SPENATEC(National Tecnical Conference)*, Detroil, 1983.

[54] L. Matejka, C. Houtman, and C. W. Macosko, *J Appl. Polym. Sci.*, **30**, 2787, 1985.

[55] D. S. Breslow, *Chemtech*, 540, 1990.

[56] J. A. Johnson, and M. F. Farona, *Polym. Bull.*, **25**, 625, 1991.

[57] V. Heroguez, A. Soum, and M. Fontanille, *Polymer*, **33**, 3302, 1992.

[58] H. Balcar, A. Dosedlova, and L. Petrusova, *J. Mol. Catal*, **77**, 289, 1992.

[59] A. Bell, *J. Mol. Catal.*, **76**, 165, 1992.

[60] H. NG, I. Manas-Zloczower, and M. Shmorhun, *Polym. Eng. Sci.* **34** (11), 921, 1994.

[61] A. Bell, *Polym. Preprints*, **35**, 694, 1994.

[62] H. Li, Z. Wang, Y. Wang, B. He, *Reactive & Functional Polymers*, **33**, 193, 1997.

[63] T. Oshika, and H. Tabuchi, *Bull. Chem. Soc. Jpn.* **41**, 211, 1968.

[64] G. Dall'Asta, G. Motroni, R. Manetti, C. Tosi, *Makromol. Chem.* **130**, 153, 1969.

[65] P. A. Devlin, E. F. Lutz, *US Pat.*, 3,627,739, 1970.

[66] R. J. Minchak, *US Pat.*, 4,138,448, 1979.

[67] R. J. Minchak, P. C. Lane, *US Pat.*, 4,701,510, 1987.

[68] T. A. Davidson, K. B. Wagener, and D. B. Priddy, *Macromolecules*, **29**, 786, 1996.

[69] L. Matejka, C. Houtman, and C. W. Macosko, *J. Appl. polym. Sci.* **30**, 2787, 1985.

[70] J. H. Van Deursen, W. Sjardijn, *Chem. Mag.*, 669, 1989.

[71] C. Kirkland, *Plastics world*, **50**, 1990.

[72] D. S. Breslow, *CHEMTECH*, **20**, 540, 1990.

Chapter 2

Monomer synthesis and characterisation

2.1 Introduction

2.1.1 General introduction

The objective of the work discussed in this chapter is the synthesis and characterisation of two series of mono- and difunctional imidonorbornene derivatives. The use of these compounds as the feed monomers for trial bulk polymerisations, solution polymerisations and for producing shaped articles by polymerisation in a mould are described in Chapter 3, 4 and 5, respectively. The synthetic route involves the formation of a polycyclic structure via a Diels-Alder cycloaddition reaction of maleic anhydride with dicyclopentadiene to produce *exo*-norbornene-5,6-dicarboxyanhydride and the reaction of this product with amines and diamines to give imides and diimides, respectively. This same general route was also used to provide the *endo*-adduct, but the starting materials in this case were maleic anhydride and cyclopentadiene and the reaction conditions were milder.

2.1.2 The Diels-Alder cycloaddition reaction

The first step for the synthesis of the mono- and difunctional monomers used in this work involved the Diels-Alder cycloaddition reaction. In a typical Diels-Alder reaction a compound containing a double or triple bond, the dienophile, adds 1,4 to a conjugated diene (a 2+4 cycloaddition) to form a product containing a six-membered ring as shown in Figure 2.1.[1-4]

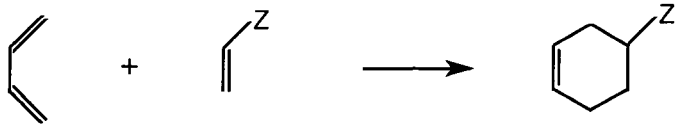

Figure 2.1 The Diels-Alder reaction between a conjugated diene and dienophile. Z = an electron withdrawing group.

In this reaction, two new σ-bonds are formed at the expense of two π-bonds in the starting materials. The reaction take place most rapidly and in the highest yield if the dienophile is substituted by an electron withdrawing group (conventional Diels-Alder)

or with electron donating groups on the olefin and electron withdrawing groups on the diene (Diels-Alder with inverse electron demand). The diene can react only in the *cis* conformation and therefore cyclic dienes react faster than acyclic dienes; five membered ring dienes are particularly favoured due to the coplanarity of the diene double bonds and the ideal distance between termini.

When the diene is cyclic, there are two possible ways in which addition can occur if the dienophile is not symmetrical. The larger side of the dienophile may be under the ring (*endo* addition), or it may be the smaller side (*exo* addition).[5]

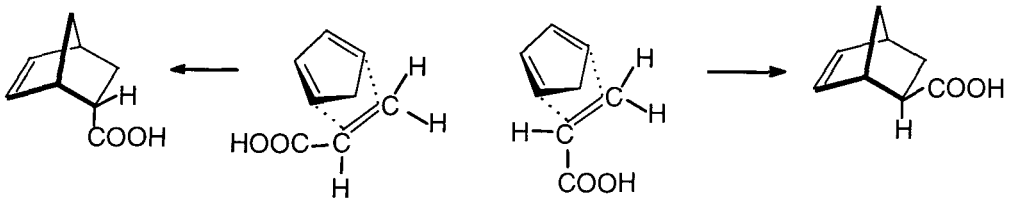

endo addition *exo* addition

In this work, the reaction of the substituted cyclic dienophile, maleic anhydride, and a cyclic diene, cyclopentadiene, produces either *exo*- or *endo*-addition depending upon the conditions. Under moderate temperature conditions the addition is predominantly *endo*, the kinetically favoured product. This is usually attributed to the fact that the dienophile is added so as to give a maximum of 'secondary overlap' of π-molecular orbitals in the transition state, as shown in Figure 2.2. The *endo*-adduct is invariably the kinetic product whether or not there is the possibility of 'secondary overlap' of π-molecular orbitals, for example, cyclopentene gives the *endo*-adduct as the kinetic product in reactions with cyclopentadiene. In order to obtain the more thermodynamically stable *exo*-adduct, severe temperature conditions, longer reaction times and repeated recrystallisation are usually necessary.[6] The pure 100% *exo*- or *endo*-isomer are not formed initially in the diene synthesis.

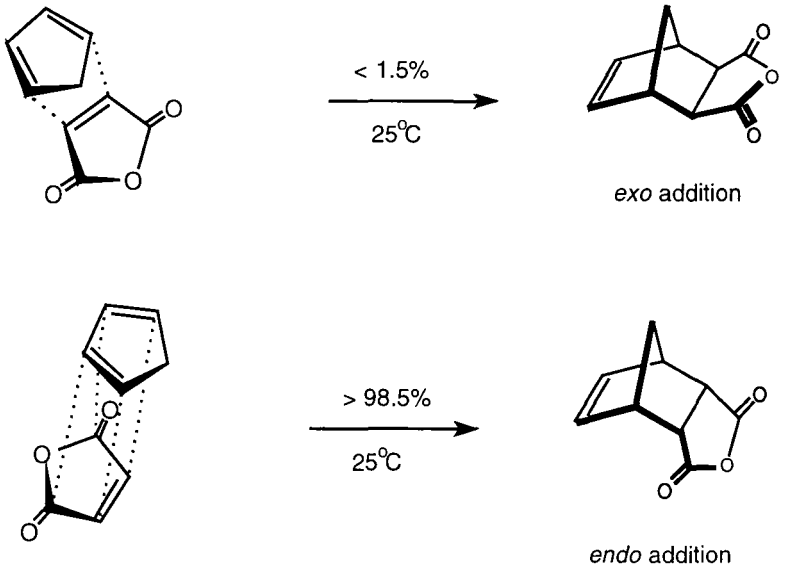

Figure 2.2 A schematic representation of the orientation of the reactants in the approach to the transition state and the products of the Diels-Alder cycloaddition between cyclopentadiene and maleic anhydride.

2.1.3 The formation of aliphatic carbon-nitrogen bonds [1,5]

In the second step of monomer synthesis, the mono- and difunctional monomers were prepared by forming bonds between carbons of norbornene dicarboxyanhydride and nitrogens of amines or diamines, respectively. With few exceptions the methods for forming bonds between nitrogen and carbon fall into two categories. In the first, nucleophilic nitrogen reacts with electrophilic carbon, and in the second, eletrophilic nitrogen reacts with nucleophilic carbon. Only the first category, which is by far the more important, will be discussed in this chapter since it is involved in the work to be described.

The commonest nitrogen nucleophiles are ammonia and its derivatives. These may be alkyl- or aryl-derivatives and, primary, secondary or tertiary amines are possible. The nitrogen atom possesses an unshared pair of electrons and is therefore nucleophilic. The nitrogen can react both with saturated carbon from which a group can be replaced with the covalent bonding-pair (S_N2 reaction),

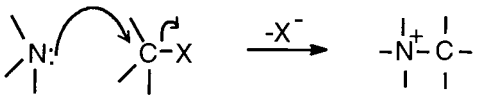

and with unsaturated carbon, leading the elimination of a proton and anion, e.g.

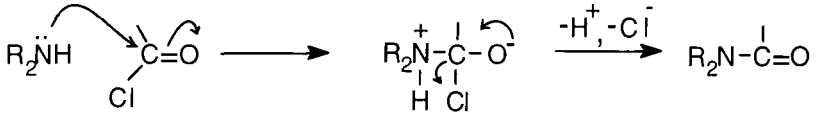

Intramolecular displacement can occur if a five- or six-membered ring is the product; e.g. succinimide can be obtained by heating the acyclic diamine of succinic acid:

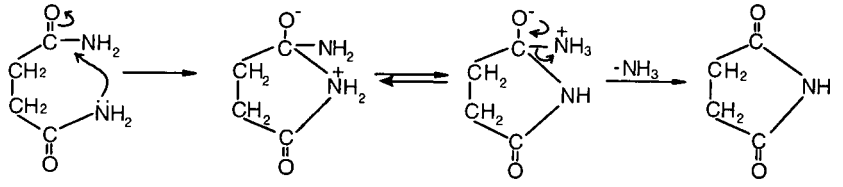

Succinimide

In practice, it is easier to obtain cyclic imides directly from the corresponding anhydrides by treatment with ammonia at high temperature. For example, heating phthalic anhydride with aqueous ammonia gives phthalimide in over 95% yield:

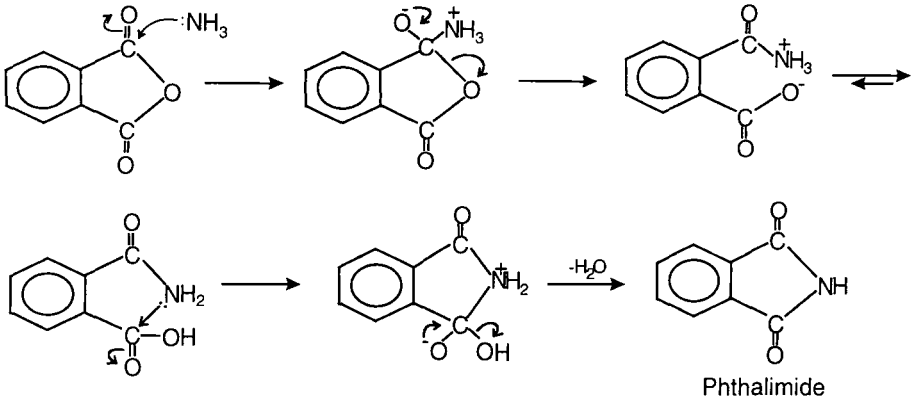

Phthalimide

For the monomers used in this study imides were prepared via an analogous reaction between anhydrides and amines.

2.2 Results and discussion

2.2.1 Synthesis and characterisation of *exo*-norbornene-5,6-dicarboxy anhydride: (*exo*-AN)[7-12]

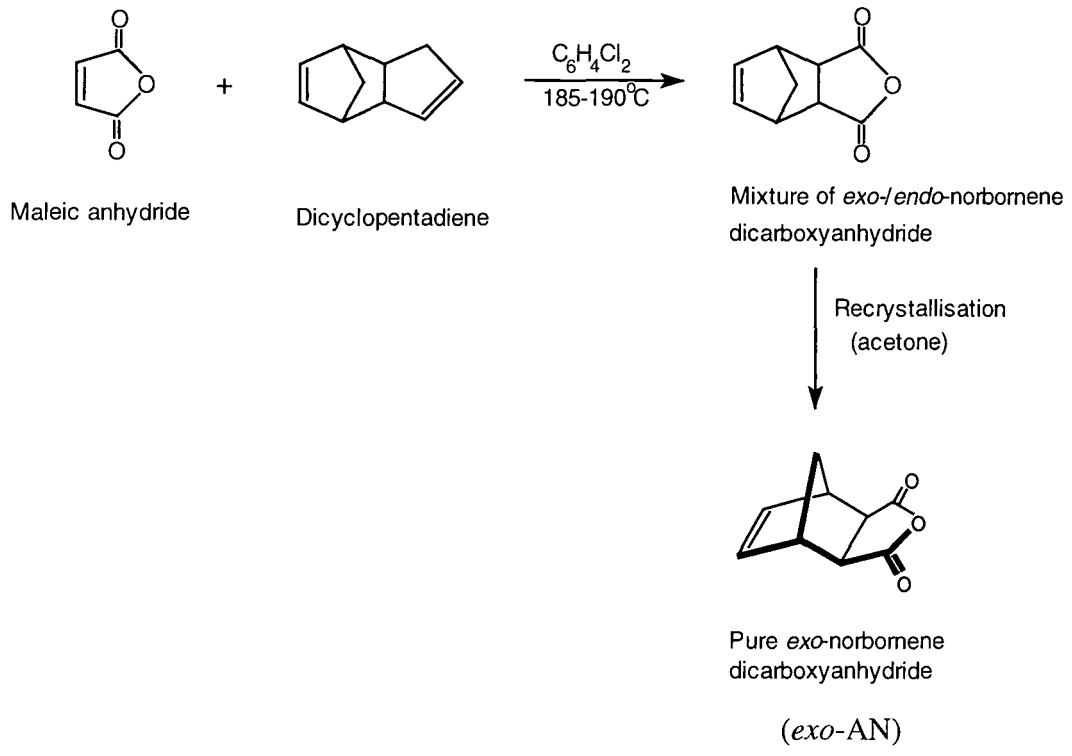

Figure 2.3 Outline of the synthesis route for *exo*-AN.

The Diels-Alder reaction between maleic anhydride and dicyclopentadiene was carried out at high temperature and gave an *exo*-/*endo*-norbornene anhydride mixture (*exo*-/*endo*-AN). A temperature above 180 °C was necessary for this reaction in order to obtain the more thermodynamically favoured *exo*-adduct. At elevated temperature, dicyclopentadiene was cracked *in situ* to yield the cyclopentadiene required. The amount of *exo*- and *endo*-adduct in the products obtained was determined by ^{1}H nmr spectroscopy. Figure 2.4 shows the ^{1}H nmr spectrum of the *exo*-/*endo*-AN mixture obtained from the Diels-Alder reaction, where both *exo* (6.37 ppm) and *endo* (6.29 ppm) olefin signals are clearly seen. As expected, it was found that longer reaction time was beneficial for the synthesis of the thermodynamically preferred, *exo*-isomer. The pure 100 % *exo*-AN was obtained by recrystallisation from acetone at least four times. The product was a transparent, colourless, crystalline solid with a m.pt. of 143

°C and was recovered in 35-44% yield. Evidence that the *exo*-AN has been purified successfully can be seen on comparison of ^{1}H nmr spectra of the *exo*-AN with the *endo*-AN, which was recovered from a reaction carried out under milder conditions, as shown in Figure 2.6

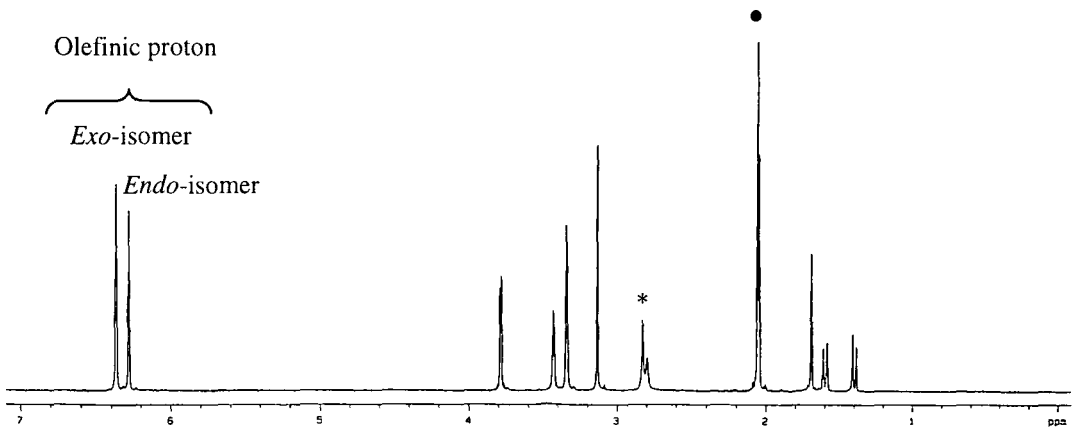

Figure 2.4 ^{1}H nmr spectrum of *exo*- and *endo*-AN mixture, product from Diels-Alder reaction, at 180 °C for 1hour.
• residual hydrogen in acetone-d_6
* water dissolved in acetone

2.2.2 Synthesis and characterisation of *endo*-norbornene-5,6-dicarboxy anhydride: (*endo*-AN)[7,9]

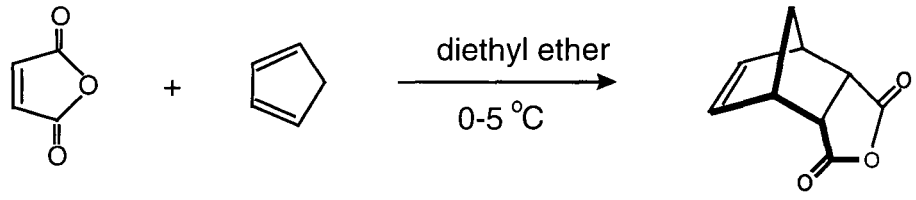

Maleic anhydride Cyclopentadiene *endo*-norbornene dicarboxyanhydride (*endo*-AN)

Figure 2.5 Outline of the synthesis route for *endo*-AN.

The same general route as the synthesis of *exo*-AN was used to provide the *endo*-adduct, but the starting materials in this case were maleic anhydride and cyclopentadiene and the reaction conditions, 0-5 °C, for the Diels-Alder cycloaddition were milder. As the reaction was carried out at low temperature, it was necessary to pre-crack dicyclopentadiene by pyrolysis (>180 °C) to yield the cyclopentadiene required. The advantage of synthesising *endo*-AN by this method is that it is fast and the *exo*-adduct content is low. The major drawback of this method is that it requires freshly distilled cyclopentadiene. Under these conditions the Diels-Alder cycloaddition of cyclopentadiene with maleic anhydride gave predominantly *endo* (~98%), the kinetically favoured product. Pure 100% *endo*-AN was obtained by one recrystallisation from acetone. The product was a transparent, colourless, crystalline solid with a m.pt. of 165°C and was recovered in 89% yield.

Comparison of the ^{1}H nmr spectra of the *exo*-AN and *endo*-AN revealed differences in chemical shifts and fine structures of the resolved signals, see Figure 2.6. In the spectrum of *exo*-AN the triplet arising from the olefinic $H_{2,3}$ hydrogens is found at 6.37 ppm, 0.08 ppm from that in *endo*-AN which occurs at 6.29 ppm. The difference between chemical shifts for $H_{5,6}$ in *exo*- and *endo*-AN is greater than the difference between $H_{1,4}$ of both structures. The peak corresponding to $H_{5,6}$ of *exo*-AN is found at 3.13 ppm, 0.65 ppm from that in the *endo*-adduct which occurs at 3.78 ppm, whereas the peak corresponding to $H_{1,4}$ in both *exo*- and *endo*-AN are almost at the same position, 3.35 ppm and 3.43 ppm, respectively. This is expected as $H_{5,6}$ are next to the anhydride functionality and more influenced by the change in position of this group than are $H_{1,4}$.

The difference between chemical shifts for H_7 and $H_{7'}$ is greater in the *exo*-AN than in the corresponding *endo*-AN. This difference is expected as $H_{7'}$ is closer to the anhydride functionality. The peak corresponding to $H_{7'}$ of *exo*-AN is found at 1.38 ppm, whereas the peak corresponding to H_7 of *exo*-AN and $H_{7,7'}$ of *endo*-AN are almost at the same position, 1.58 ppm and 1.68 ppm, respectively. The ^{1}H and ^{13}C nmr assignment, elemental analysis, mass spectrum and infrared spectrum of the monomers obtained are recorded in the experimental section of this chapter.

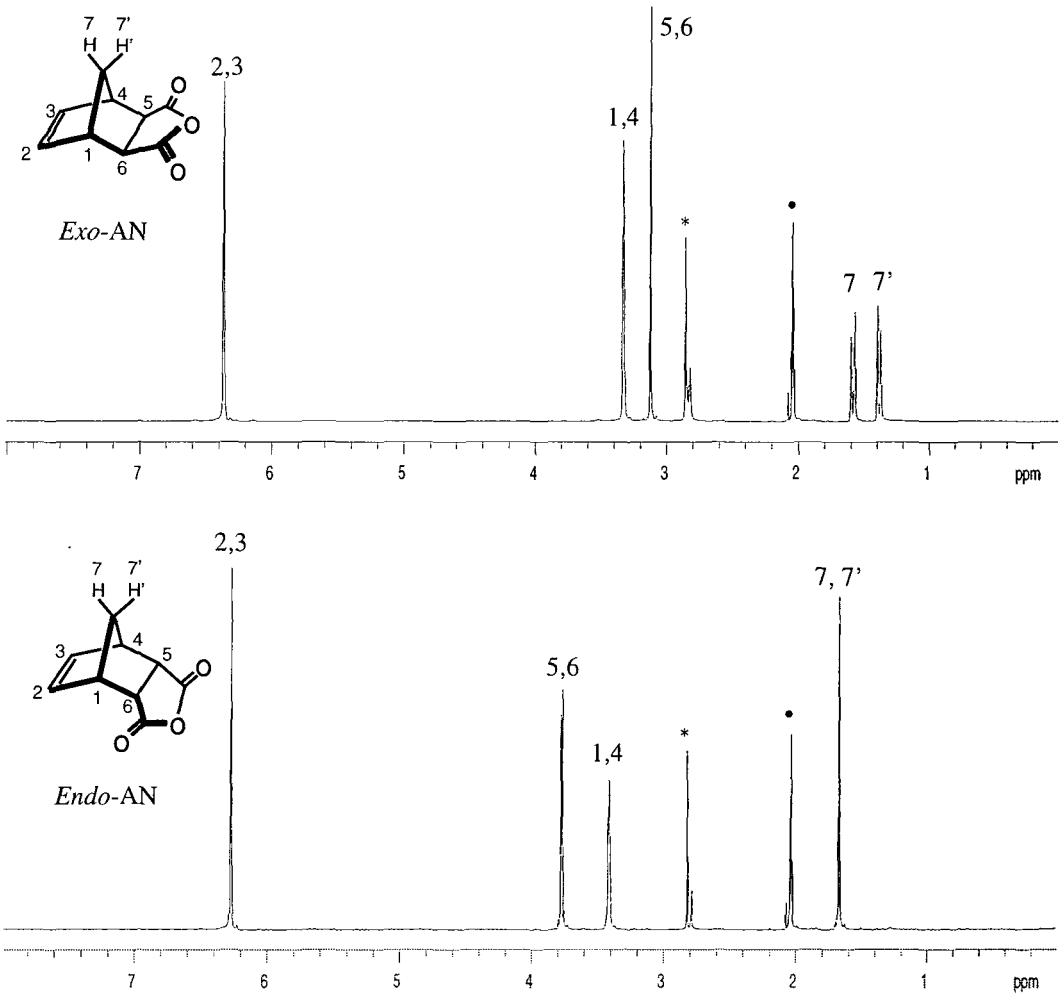

Figure 2.6 ^{1}H nmr spectra of pure *exo*-AN and *endo*-AN.

• residual hydrogen in acetone-d_6.

* water dissolved in acetone.

2.2.3 Synthesis and characterisation a series of *exo*-monofunctional monomers: *exo*-N-alkylnorbornene-5,6-dicarboxyimide (*exo*-CnM)[13]

A series of *exo*-N-alkylnorbornene-5,6-dicarboxyimide (*exo*-CnM) were synthesised according to the route shown in Figure 2.7. The reaction of *exo*-AN with n-alkylamine in refluxing glacial acetic acid for 2 hours at 120 °C gave the imide monomers. The monomers were recovered as colourless liquids in high yields (85-90%) with respect to *exo*-AN. For example, the reaction of *exo*-AN with n-hexylamine in glacial acetic acid gave *exo*-C6M monomer in 90% yield. The ^{1}H nmr spectrum of this compound was recorded in $CDCl_3$ solution and is consistent with the assigned structure, as shown in

Figure2.9a. The ^{1}H and ^{13}C nmr assignment, elemental analysis, mass spectrum and infrared spectrum of all monomers obtained are recorded in the experimental section of this chapter.

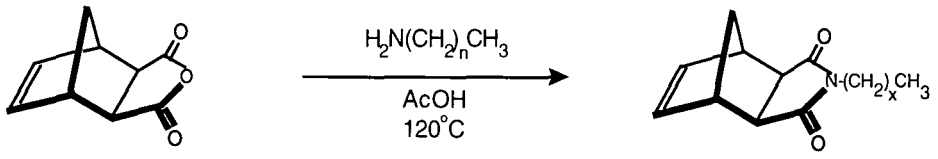

Pure *exo*-norbomene dicarboxyanhydride

exo-N-alkyl norbornene dicarboxyimide; *exo*-CnM

exo-C3M x = 2 (87% yield)

exo-C4M x = 3 (89% yield)

exo-C5M x = 4 (89% yield)

exo-C6M x = 5 (90% yield)

exo-C8M x = 7 (85% yield)

Figure 2.7 Outline of the synthetic route for *exo*-monofunctional monomers: *exo*-CnM, where n = the number of carbon atoms in the alkyl group.

2.2.4 Synthesis and characterisation of *endo*-N-hexylnorbornene-5,6-dicarboxyimide: (*endo*-C6M)

Endo-N-hexylnorbornene-5,6-dicarboxyimide (*endo*-C6M) was prepared as shown in Figure 2.8.

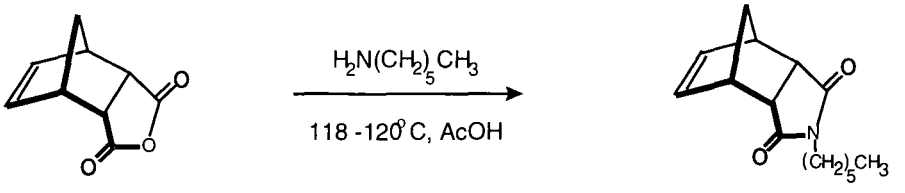

endo-norbornene dicarboxyanhydride

endo-N-hexylnorbornene-5,6-dicarboxyimide

endo-C6M (91 %yield)

Figure 2.8 Outline of the synthetic route for *endo*-N-hexylnorbornene-5,6-dicarboxyimide: (*endo*-C6M).

The reaction of *endo*-AN with n-hexylamine in refluxing glacial acetic for 2 hours at 120°C gave *endo*-C6M. The monomer was recovered as a colourless liquid in 91% yield with respect to *endo*-AN. Comparison of the ^{1}H nmr spectra of *exo*- and *endo*-C6M revealed differences in chemical shifts and fine structures of the resolved signals as shown in Figure 2.9a and b. The detailed assignment of ^{1}H and ^{13}C nmr, elemental analysis, mass spectrum and infrared spectrum of all monofunctional monomers obtained are recorded in the experimental section of this chapter.

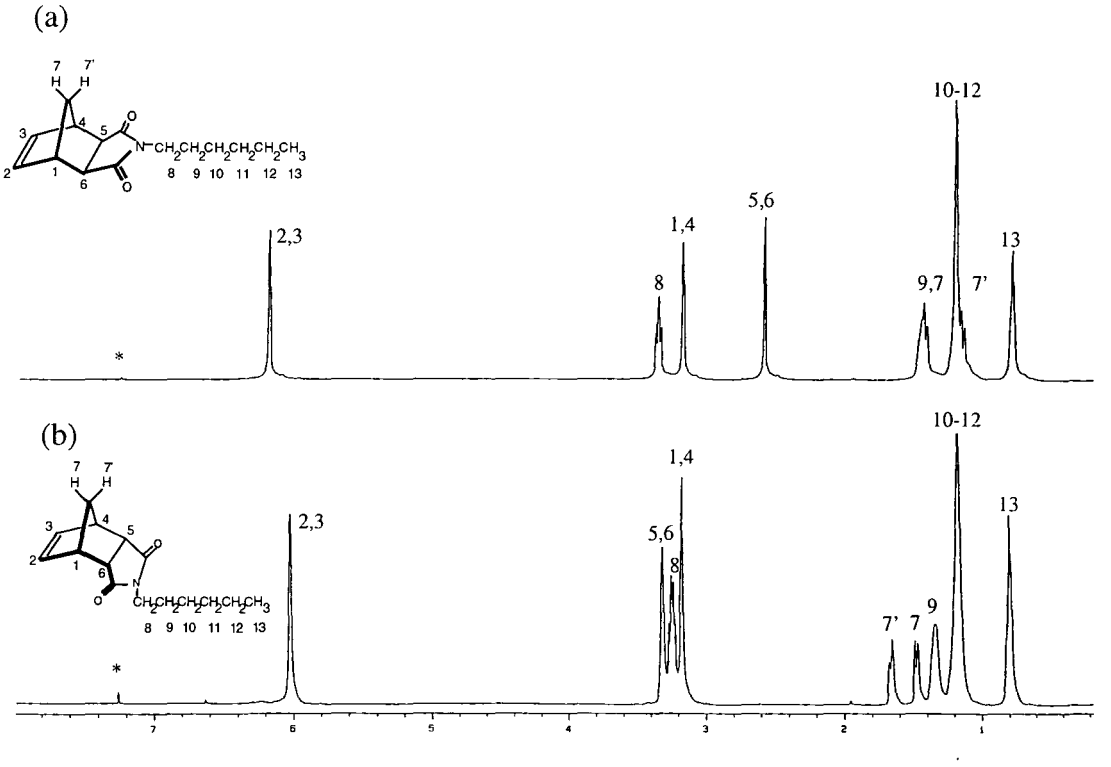

Figure 2.9 ^{1}H nmr spectra of (a) *exo*-C6M and (b) *endo*-C6M.
* residual hydrogen in $CDCl_3$

2.2.5 Synthesis and characterisation a series of *exo,exo*-difunctional monomers: *exo,exo*-N,N'-alkylene-di-(norbornene-5,6-dicarboxyimides): (*exo*-CnD)

A series of *exo,exo*-N,N'-alkylene-di-(norbornene-5,6-dicarboxyimides), difunctional monomers, were synthesised according to the route shown Figure 2.10.

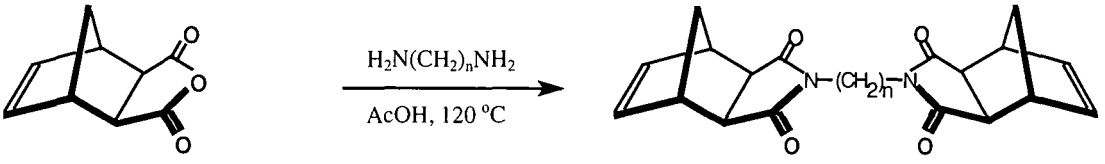

Exo-norbornene dicarboxyanhydride (*exo*-AN)

Difunctional monomer *Exo*-CnD

exo-C3D (91 %yield)
exo-C5D (90 %yield)
exo-C6D (92 %yield)
exo-C9D (83 %yield)
exo-C12D (80 %yield)

Figure 2.10 Outline of the synthetic route for *exo*-difunctional monomer: (*exo*-CnD), where n = the number of methylene units separating the reactive imidonorbornene units.

The *exo*-AN was reacted with diamines in refluxing glacial acetic for 2 hours at 120°C to give difunctional monomers, *exo*-CnD. The difunctional monomers were recovered as white solids in high yield (~80-92%) with respect to *exo*-AN. For example, the reaction of *exo*-AN with 1,6-hexanediamine in glacial acetic acid gave *exo*-C6D as a white crystalline solid in 92% yield. The ^{1}H and ^{13}C nmr spectra of the this compound were recorded in solution in $CDCl_3$. Both spectra are consistent with the assigned structure as shown in Figure 2.11. The assignment of ^{1}H and ^{13}C nmr, elemental analysis, mass spectrum and infrared spectrum of all difunctional monomers obtained are recorded in the experimental section of this chapter.

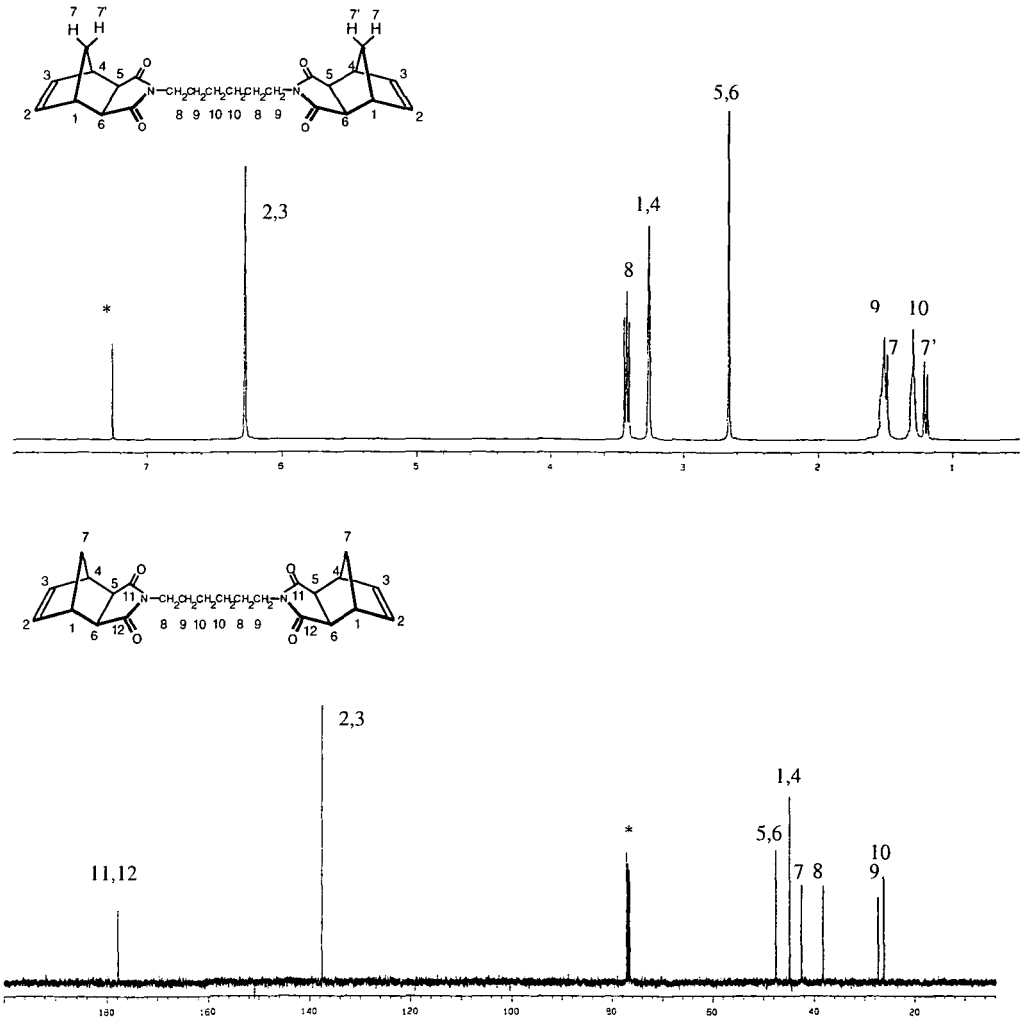

Figure 2.11 ^{1}H and ^{13}C nmr spectra of *exo*-C6D.

* residual hydrogen in $CDCl_3$

2.3 Experimental

Reagents

Maleic anhydride, dicyclopentadiene, 1,2-dichlorobenzene, n-alkylamine and dialkylamine were purchased from Aldrich Company Ltd, acetic acid, anhydrous diethyl ether, acetone were purchased from BDH Chemical Company Ltd. All reagents and solvents were used without further purification.

2.3.1 Synthesis and characterisation of *exo*- and *endo*-norbornene-5,6-dicarboxy anhydride: (*exo*- and *endo*-AN)

Synthesis and characterisation of *exo*-norbornene-5,6-dicarboxy anhydride: (*exo*-AN)

Maleic anhydride (490.0 g, 5.0 mol) and 1,2-dichlorobenzene (500 ml) were place in a 4-necked, round bottomed flange flask (3,000 ml) fitted with a condenser, thermometer, dropping funnel, and mechanical stirrer. The mixture was stirred and heated to 180 - 185 °C. Dicyclopentadiene (335.0 ml, 330.0 g, 2.5 mol) was added to the flask via the dropping funnel over a period of 2 hours to give a clear, yellow solution. The mixture was heated to reflux for further 6 hours, giving a brown solution, which was allowed to cool overnight. The resulting light yellow crystals, a mixture of 71% *exo*- and 29% *endo*-isomer, were recovered by filtration from the brown solution and recrystallised several times from acetone to give 100% pure *exo*-isomer (*exo*-AN) as a transparent, colourless crystal (360.0 g, 2.2 mol, 44.0% yield).

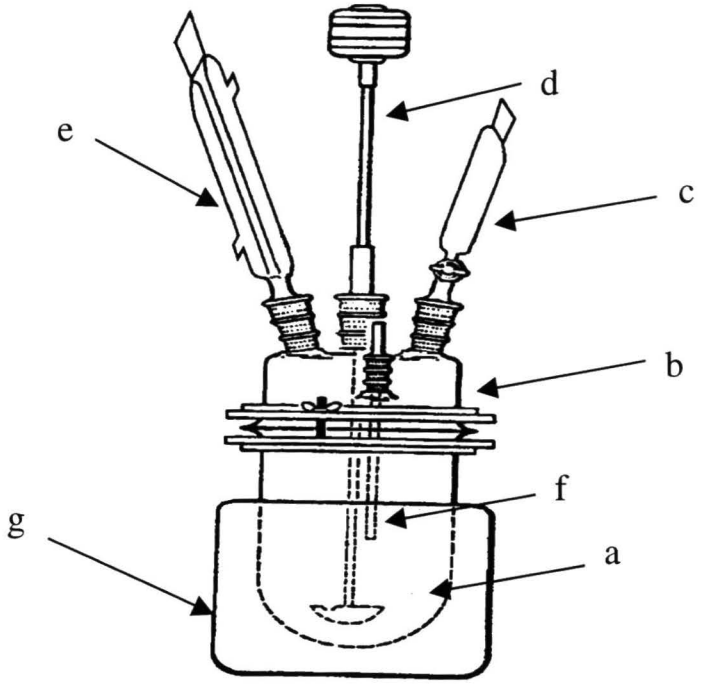

Figure 2.12 The apparatus for the synthesis of *exo*-AN. (a) flange flask bottom, (b) flange flask top, (c) dropping funnel, (d) mechanical stirrer, (e) condenser, (f) thermometer, (g) heating mantle.

• **Mpt**: 143 °C (Lit[7] 142.5-143.5 °C) .

• **Elemental analysis**- Found C, 65.65%, H,4.83%; calculated for $C_9H_8O_3$: C, 65.85%, H 4.91%.

• **^{1}H nmr**- (see Appendix 2.1), (d_6-acetone, 400 MHz), δ (ppm)): 6.37 (t, 2H, $H_{2,3}$), 3.35 (p, 2H, $H_{1,4}$), 3.13 (d, 2H, $H_{5,6}$), 1.58 (m, 1H, H_7), 1.38 (m, 1H, $H_{7'}$).

• **^{13}C nmr**- (see Appendix 2.2), (d_6-acetone, 100 MHz, δ (ppm)): 173.00 ($C_{8,9}$), 138.68 ($C_{2,3}$), 49.77 ($C_{5,6}$), 47.38 ($C_{1,4}$), 44.59 (C_7).

• **Mass spectrum-** (see Appendix 2.3), (EI^+): 164 ($C_9H_8O_3$, M^+), 120 (M^+-CO_2), 66 (M^+-$C_4H_2O_3$).

• **IR-** (see Appendix 2.4), (KBr disc, cm^{-1}): 3090 (olefinic C-H stretching), 2997-2884 (saturated C-H stretching), 1859, 1776 (Asymmetric and symmetric C=O stretching, respectively), 1040 (cyclic anhydride C-O-C stretching).

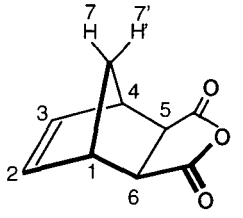

Assignment of H atoms in compound *exo*-AN

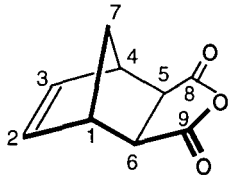

Assignment of C atoms in compound *exo*-AN

Synthesis and characterisation of *endo*-norbornene-5,6-dicarboxyanhydride: (*endo*-AN)

Maleic anhydride (98.0 g, 1.0mole) and anhydrous diethyl ether (600 cm^3) were place in a 1 litre 3-necked round bottom flask fitted with a condenser, thermometer, dropping funnel and magnetic bar. The mixture was stirred to dissolve the maleic anhydride at room temperature and then was cooled down in an ice/salt bath and maintained between 0-5°C. Cyclopentadiene (66 g, 1.0 mole) was added dropwise via a dropping funnel over a period of 2 hours. The temperature of the solution was not allowed to rise above 5 °C during the addition. The mixture was stirred with cooling for a further 2 hours, after which the ice bath was removed and a white powder precipitated. Diethyl ether was decanted off and the product dried in vacuum to give a white crystalline solid, a mixture of 2% *exo*- and 98% *endo*-isomer. The mixture was

recrystallised once from acetone to give 100% pure *endo*-isomer (*endo*-AN) as transparent, colourless crystals (145.0 g, 0.9 mol, 89% yield).

- **Mpt**: 164 °C (Lit[7] 165 °C).
- **Elemental analysis**- Found C, 65.65%, H,4.83%; calculated for $C_9H_8O_3$: C, 65.85%, H 4.91%.
- **^{1}H nmr**- (see Appendix 2.5), (d_6-acetone, 400 MHz, δ (ppm)): 6.29 (t, 2H, $H_{2,3}$), 3.78 (m, 2H, $H_{5,6}$), 3.43 (m, 2H, $H_{1,4}$), 1.69 (m, 2H, $H_{7,7'}$).
- **^{13}C nmr**- (see Appendix 2.6), (d_6-acetone, 100 MHz, δ (ppm)): 172.54 ($C_{8,9}$), 135.33 ($C_{2,3}$), 53.03 ($C_{5,6}$), 47.79 ($C_{1,4}$), 46.03 (C_7).
- **Mass spectrum**- (see Appendix 2.7), (EI^+): 164 ($C_9H_8O_3$, M^+), 120 (M^+-CO_2), 66 (M^+-$C_4H_2O_3$).
- **IR**- (see Appendix 2.8), (KBr disc, cm^{-1}): 3070 (olefinic C-H stretching), 2997-2890 (saturated C-H stretching), 1825, 1770 (Asymmetric and symmetric C=O stretching, respectively), 1044 (cyclic anhydride C-O-C stretching).

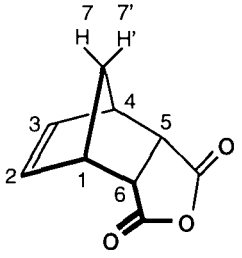

Assignment of H atoms in compound *endo*-AN

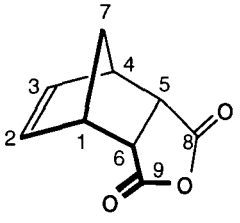

Assignment of C atoms in compound *endo*-AN

2.3.2 Synthesis and characterisation of monofunctional monomers

General procedure for the synthesis of monofunctional monomers (*exo*- and *endo*-norbornene-5,6-dicarboxyimide): *exo*-CnM (n =3, 4, 5, 6 and 8) and *endo*-C6M

A known weight of *endo*- or *exo*-AN was dissolved in glacial acetic acid at 118-120°C in a round bottom flask equipped with a condenser, dropping funnel, thermometer and magnetic stirrer bar. The required amount of n-alkyl amine was added slowly. The reaction mixture was heated to reflux for 2 hours at 120°C using a silicone oil bath. The reaction mixture was poured into cold distilled water which was then extracted

with dichloromethane. The organic layer was washed twice with distilled water and dried over anhydrous magnesium sulphate. The solvent was then removed under reduce pressure to give the clear, pale yellow liquid. The crude products were distilled under vacuum to give the clear liquid products, *exo*-CnM if n = 5, 6, and 8, whereas n = 3 and 4 solidified at room temperature.

Synthesis and characterisation of *exo*-N-hexylnorbornene–5,6-dicarboxyimide: (*exo*-C6M)

Exo-AN (82.0 g, 0.5 mol) was dissolved in glacial acetic acid (500 ml) at 118-120°C in a 3-necked round bottom flask equipped with a condenser, dropping funnel, thermometer and magnetic stirrer bar. N-hexylamine (50.6 g, 66.0 ml, 0.5 mol) was added slowly via the dropping funnel over the period of 1.5– 2 hours. The reaction mixture was heat to reflux for 2 hrs at 120 °C, giving a clear, pale yellow solution. The reaction mixture was poured into cold distilled water which was then extracted with dichloromethane. The organic layer was washed twice with distilled water and dried over anhydrous magnesium sulphate. The solvent was then removed under reduce pressure to give a clear, pale yellow liquid. The crude product was distilled under vacuum to give the clear liquid, *exo*-C6M (111.1g, 0.45 mol, 90% yield).

- **Bpt**: 134°C @ 3mmbar.
- **Elemental analysis**- Found C, 72.68%, H, 8.63%, N, 5.65%; calculated for $C_{15}H_{21}NO_2$: C, 72.84%, H, 8.56%, N, 5.66% .
- **^{1}H nmr**- (see Appendix 2.9), ($CDCl_3$, 400 MHz, δ (ppm)): 6.19 (t, 2H, $H_{2,3}$), 3.35 (t, 2H, H_8), 3.17 (p, 2H, $H_{1,4}$), 2.58 (d, 2H, $H_{5,6}$), 1.43 (m, 3H, H_9 and H_7), 1.18 (m, 6H, $H_{10\text{-}12}$), 1.13 (m, 1H, $H_{7'}$), 0.76 (t, 3H, H_{13}).
- **^{13}C nmr**- (see Appendix 2.10), ($CDCl_3$, 100 MHz, δ (ppm)): 177.53 ($C_{14,15}$), 137.44 ($C_{2,3}$), 47.40 ($C_{5,6}$), 44.78 ($C_{1,4}$), 42.34 (C_7), 38.30 (C_8), 30.93 (C_9), 27.44 (C_{10}), 26.23 (C_{11}), 22.09 (C_{12}), 13.69 (C_{13}).
- **Mass spectrum**- (see Appendix 2.11), (EI^+): 247 ($C_{15}H_{21}NO_2$, M^+), 182 (MH^+-C_5H_6), 66 (M^+-$C_{10}H_{15}NO_2$).
- **IR-** (see Appendix 2.12), (KBr disc, cm^{-1}): 3080 (olefinic C-H stretching), 2980-2867 (saturated C-H stretching), 1768, 1700 (Asymmetric and symmetric C=O stretching, respectively), 1395 (C-N stretching).

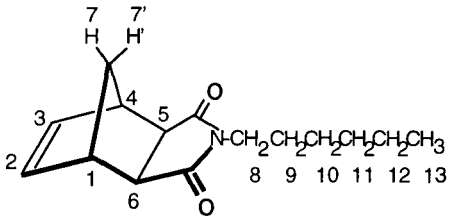

Assignment of H atoms in compound *exo*-C6M

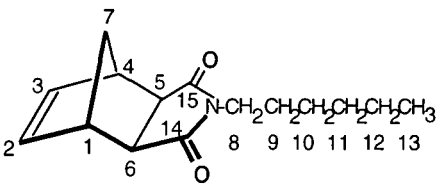

Assignment of C atoms in compound *exo*-C6M

Synthesis and characterisation of *exo*-N-propylnorbornene-5,6-dicarboxyimide: (*exo*-C3M)

The same procedure as for the synthesis of *exo*-C6M was used to synthesise *exo*-C3M, but the starting material in this case was n-propylamine (24.5 g, 34.0 ml, 0.5 mol). *Exo*-C3M (89.2 g, 0.41 mol, 87% yield) was obtained as a clear liquid which solidified at room temperature after the distillation of crude product under vacuum.

- **Bpt**: *105 °C @2mmbar.*
- **Mpt**: 45.5-46 °C.
- **Elemental analysis**- Found C, 70.12%, H, 7.54%, N, 6.91%; calculated for $C_{12}H_{15}NO_2$: C, 70.22%, H, 7.37%, N, 6.83%.
- **^{1}H nmr**- (see Appendix 2.13), ($CDCl_3$, 400 MHz, δ (ppm)): 6.18 (t, 2H, $H_{2,3}$), 3.30 (t, 2H, H_8), 3.17 (p, 2H, $H_{1,4}$), 2.56 (d, 2H, $H_{5,6}$), 1.44 (m, 2H, H_9), 1.41 (m, 1H, H_7), 1.12 (d, 1H, $H_{7'}$), 0.81 (t, 3H, H_{10}).
- **^{13}C nmr**- (see Appendix 2.14), ($CDCl_3$, 100 MHz, δ (ppm)): 178.24 ($C_{11,12}$), 137.93 ($C_{2,3}$), 47.40 ($C_{5,6}$), 45.24 ($C_{1,4}$), 42.82 (C_7), 40.37 (C_8), 21.23 (C_9), 11.55 (C_{10}).
- **Mass spectrum**- (see Appendix 2.15), (EI^+): 205 ($C_{12}H_{15}NO_2$, M^+), 140 (MH^+-C_5H_6), 66 (M^+-$C_7H_9NO_2$).
- **IR**-(see Appendix 2.16), (KBr disc, cm^{-1}): 3055 (olefinic C-H stretching), 3000-2881 (saturated C-H stretching), 1762, 1687 (Asymmetric and symmetric C=O stretching, respectively), 1384 (C-N stretching).

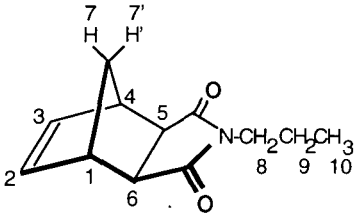

Assignment of H atoms in compound *exo*-C3M

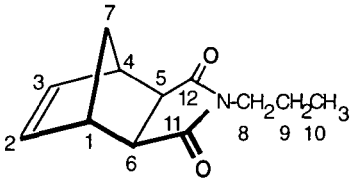

Assignment of C atoms in compound *exo*-C3M

Synthesis and characterisation of *exo*-N-butylnorbornene-5,6-dicarboxyimide: (*exo*-C4M)

The same procedure as for the synthesis of *exo*-C6M was used to synthesise *exo*-C4M, but the starting material in this case was n-butylamine (36.7 g, 49.4 ml, 0.5 mol). *Exo*-C4M (97.5 g, 0.45 mol, 89% yield) was obtained as a clear liquid which solidified at room temperature after the distillation of crude product under vacuum.

- **Bpt**: 113 °C @2mmbar.
- **Mpt**: 32 °C.
- **Elemental analysis**- Found C, 71.23%, H, 7.79%, N, 6.30%; calculated for $C_{13}H_{17}NO_2$: C, 71.21%, H, 7.81%, N, 6.39%.
- **^{1}H nmr**- (see Appendix 2.17), ($CDCl_3$, 400 MHz, δ (ppm)): 6.18 (t, 2H, $H_{2,3}$), 3.32 (t, 2H, H_8), 3.13 (p, 2H, $H_{1,4}$), 2.54 (d, 2H, $H_{5,6}$), 1.39 (m, 3H, H_9, and H_7), 1.18 (m, 2H, H_{10}), 1.09 (d, 1H, $H_{7'}$), 0.79 (t, 3H, H_{11}).
- **^{13}C nmr**- (see Appendix 2.18), ($CDCl_3$, 100 MHz, δ (ppm)): 177.98 ($C_{12,13}$), 137.71 ($C_{2,3}$), 47.68 ($C_{5,6}$), 45.05 ($C_{1,4}$), 42.60 (C_7), 38.38 (C_8), 29.72 (C_9), 20.12 (C_{10}), 13.54 (C_{11}).
- **Mass spectrum**- (see Appendix 2.19), (EI^+): 219 ($C_{13}H_{17}NO_2$, M^+), 154 (MH^+-C_5H_6), 66 (M^+-$C_7H_9NO_2$).
- **IR**- (see Appendix 2.20), (KBr disc, cm^{-1}): 3050 (olefinic C-H stretching), 3000-2875 (saturated C-H stretching), 1750, 1688 (Asymmetric and symmetric C=O stretching, respectively), 1380 (C-N stretching).

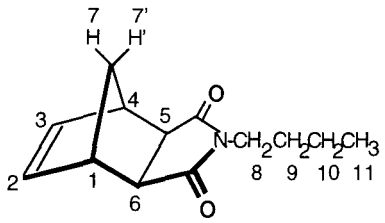

Assignment of H atoms in compound *exo*-C4M

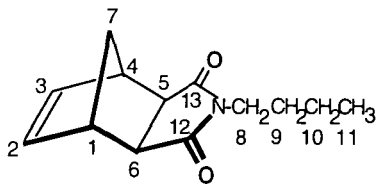

Assignment of C atoms in compound *exo*-C4M

Synthesis and characterisation of *exo*-N-pentylnorbornene-5,6-dicarboxyimide: (*exo*-C5M)

The same procedure as for the synthesis of *exo*-C6M was used to synthesise *exo*-C5M, but the starting material in this case was n-amylamine (43.6 g, 56 ml, 0.5 mol). *Exo*-C5M (103.7 g, 0.44 mol, 89% yield) was obtained as a clear liquid by the distillation the crude product under vacuum.

- **Bpt**: 150 °C @1.2 mmbar.
- **Elemental analysis**- Found C, 72.25%, H,8.16%, N, 6.07%; calculated for $C_{14}H_{19}O_2N$: C, 72.07%, H, 8.21, N, 6.00%.
- **^{1}H nmr**- (see Appendix 2.21), ($CDCl_3$, 400 MHz, δ (ppm)): 6.20 (t, 2H, $H_{2,3}$), 3.37 (t, 2H, H_8), 3.19 (p, 2H, $H_{1,4}$), 2.58 (d, 2H, $H_{5,6}$), 1.45 (m, 3H, H_9, and H_7), 1.22 (m, 4H, $H_{10,11}$), 1.16 (d, 1H, $H_{7'}$), 0.79 (t, 3H, H_{12}).
- **^{13}C nmr**- (see Appendix 2.22), ($CDCl_3$, 100 MHz, δ (ppm)): 178.92 ($C_{13,14}$), 137.64 ($C_{2,3}$), 47.59 ($C_{5,6}$), 45.96 ($C_{1,4}$), 42.51 (C_7), 38.51 (C_8), 28.87 (C_9), 27.24 (C_{10}), 22.02 (C_{11}), 13.84 (C_{12}).
- **Mass spectrum**- (see Appendix 2.23), (EI^+): 233 ($C_{13}H_{17}NO_2$, M^+), 168 (MH^+-C_5H_6), 66 (M^+-$C_9H_{13}NO_2$).
- **IR**- (see Appendix 2.24), (KBr disc, cm^{-1}): 3062 (olefinic C-H stretching), 2995-2877 (saturated C-H stretching), 1762, 1694 (Asymmetric and symmetric C=O stretching, respectively), 1394 (C-N stretching).

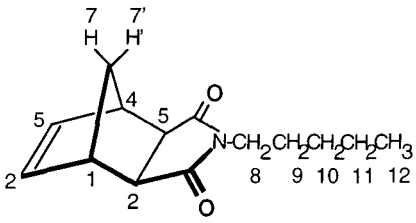

Assignment of H atoms in compound *exo*-C5M

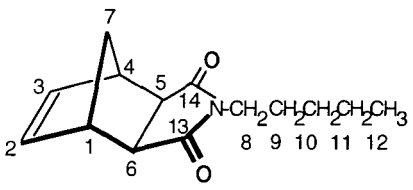

Assignment of C atoms in compound *exo*-C5M

Synthesis and characterisation of *exo*-N-octylnorbornene-5,6-dicarboxyimide: (*exo*-C8M)

The same procedure as for the synthesis of *exo*-C6M was used to synthesise *exo*-C8M, but the starting material in this case was n-octylamine (64.6 g, 83ml, 0.5 mol). *Exo*-C8M (116.9 g, 0.43 mol, 85% yield) was obtained as a clear liquid by the distillation the crude product under vacuum.

- **Bpt**: 144 °C @1 mmbar.
- **Elemental analysis**- Found C, 74.13%, H, 9.02%, N, 5.23%; calculated for $C_{17}H_{25}NO_2$: C, 74.15%, H, 9.15%, N, 5.09%.
- **^{1}H nmr**- (see Appendix 2.25), ($CDCl_3$, 400 MHz, δ (ppm)): 6.19 (t, 2H, $H_{2,3}$), 3.34 (t, 2H, H_8), 3.14 (p, 2H, $H_{1,4}$), 2.55 (d, 2H, $H_{5,6}$), 1.42 (m, 3H, H_9 and H_7), 1.16 (m, 11H, $H_{10\text{-}14}$ and $H_{7'}$), 0.75 (t, 3H, H_{15}).
- **^{13}C nmr**- (see Appendix 2.26), ($CDCl_3$, 100 MHz, δ (ppm)): 177.84 ($C_{16,17}$), 137.65 ($C_{2,3}$), 47.61 ($C_{5,6}$), 44.98 ($C_{1,4}$), 42.54 (C_7), 38.55 (C_8), 31.56 (C_9), 28.92 ($C_{10,11}$), 27.59 (C_{12}), 26.78 (C_{13}), 22.43 (C_{14}), 13.92 (C_{15}).
- **Mass spectrum**- (see Appendix 2.27), (EI^+): 275 ($C_{17}H_{25}NO_2$, M^+), 110 (MH^+-C_5H_6), 66 (M^+-$C_7H_9NO_2$).
- **IR**- (see Appendix 2.28), (KBr disc, cm^{-1}): 3062 (olefinic C-H stretching), 2998-2875 (saturated C-H stretching), 1756, 1688 (Asymmetric and symmetric C=O stretching, respectively), 1400 (C-N stretching).

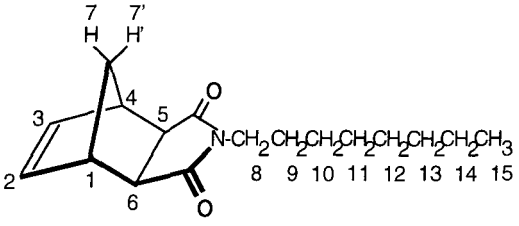

Assignment of H atoms in compound *exo*-C8M

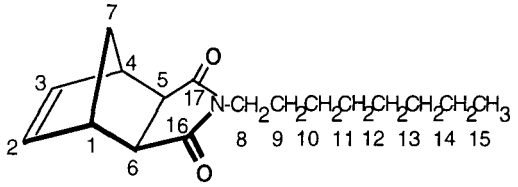

Assignment of C atoms in compound *exo*-C8M

Synthesis and characterisation of *endo*-N-hexylnorbornene-5,6-dicarboxyimide: (*endo*-C6M)

The same procedure as for the synthesis of *exo*-C6M was used to synthesise *endo*-C6M, but the starting material in this case were *endo*-AN (82.0 g, 0.5 mol) and n-amylamine (43.6 g, 56 ml, 0.5 mol). *Endo*-C6M (112.4 g, 0.46 mol, 91% yield) was obtained as a clear liquid by the distillation the crude product under vacuum.

- **Bpt**: 137 °C @3 mmbar.
- **Elemental analysis**- Found C, 72.69%, H, 8.53%, N, 5.61%; calculated for $C_{15}H_{21}NO_2$: C, 72.84%, H, 8.56%, N, 5.66%.
- **^{1}H nmr**- (see Appendix 2.29), ($CDCl_3$, 400 MHz, δ (ppm)): 6.05 (t, 2H, $H_{2,3}$), 3.34 (d, 2H, $H_{5,6}$), 3.28 (t, 2H, H_8), 3.20 (p, 2H, $H_{1,4}$), 1.69 (m, 1H, $H_{7'}$), 1.50 (m, 1H, H_7), 1.38 (m, 2H, H_9), 1.22 (m, 6H, $H_{10\text{-}12}$), 0.83 (t, 3H, H_{13}).
- **^{13}C nmr**- (see Appendix 2.30), ($CDCl_3$, 100 MHz, δ (ppm)): 177.59 ($C_{14,15}$), 134.02 ($C_{2,3}$), 52.06 (C_7), 45.56 ($C_{5,6}$), 44.74 ($C_{1,4}$), 38.29 (C_8), 31.18 (C_9), 27.61 (C_{10}), 26.39 (C_{11}), 22.35 (C_{12}), 13.87 (C_{13}).
- **Mass spectrum**- (see Appendix 2.31), (EI^+): 247 ($C_{15}H_{21}NO_2$, M^+), 182 (MH^+-C_5H_6), 66 (M^+-$C_{10}H_{15}NO_2$).
- **IR-** (see Appendix 2.32), (KBr disc, cm^{-1}): 3061 (olefinic C-H stretching), 2997-2868 (saturated C-H stretching), 1769, 1688 (Asymmetric and symmetric C=O stretching, respectively), 1400 (C-N stretching).

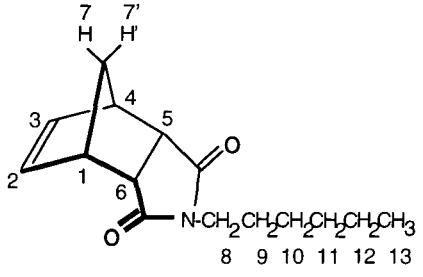

Assignment of H atoms in compound *endo*-C6M

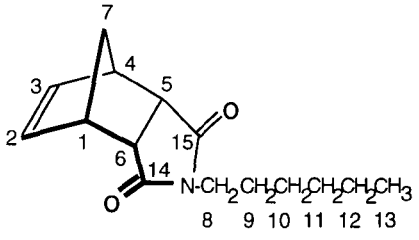

Assignment of C atoms in compound *endo*-C6M

2.3.3 Synthesis and characterisation of difunctional monomers

General procedure for the synthesis of *exo,exo*-difunctional monomers: *exo*-CnD

A known weight of *exo*-AN was dissolved in glacial acetic acid at 118-120°C in a round bottom flask equipped with a condenser, a solids addition tube (for solid diamines) or addition funnel (for liquid diamines), a thermometer and a magnetic stirrer bar. The required amount of n-alkyl diamine was added slowly. The reaction mixture was refluxed for 2 hours at 120 °C using a silicone oil bath. The reaction mixture was poured into cold distilled water which was then extracted with dichloromethane. The organic layer was washed twice with distilled water, dried over anhydrous magnesium sulphate, filtered and the solvent was removed under vacuum to give the difunctional monomers as white powders. Analytical samples were obtained by further recrystallisation from acetone.

Synthesis and characterisation of *exo,exo*-N,N'-propylene-di-(norbornene-5,6-dicarboxyimides): (*exo*-C3D)

exo-AN (20.0 g, 0.12 mol) was dissolved in glacial acetic acid (130 ml) at 118-120°C in a 3-necked round bottom flask equipped with a condenser, addition funnel, a thermometer and a magnetic stirrer bar. 1,3-Diaminopropane (4.4 g, 5 ml, 0.06 mol) was added to the flask via the dropping funnel over a period of 1 hour. The reaction mixture was heat to reflux for 2 hours, giving a pale yellow solution. The solution was poured into cold distilled water which was then extracted with dichloromethane. The organic layer was washed twice with distilled water, dried over anhydrous magnesium sulphate, filtered and the solvent was removed under vacuum. The final product was obtained by further recrystallisation from acetone to give the white powder, *exo*-C3D (40.0 g, 0.11 mol, 91% yield).

- **Mpt**: 131.6 °C
- **Elemental analysis**- Found C, 68.78%, H, 5.98%, N, 7.73%; calculated for $C_{21}H_{22}N_2O_4$: C, 68.84%, H, 6.05%, N, 7.64%.
- **^{1}H nmr**- (see Appendix 2.33), ($CDCl_3$, 400 MHz), δ (ppm)): 6.28 (t, 4H, $H_{2,3}$), 3.46 (t, 4H, H_8), 3.25 (p, 4H, $H_{1,4}$), 2.66 (d, 4H, $H_{5,6}$), 1.86 (p, 2H, H_9), 1.52 (m, 2H, H_7), 1.29 (m, 2H, $H_{7'}$).

• **^{13}C nmr**- (see Appendix 2.34), ($CDCl_3$, 100 MHz), δ (ppm)): 177.94 ($C_{10,11}$), 137.82 ($C_{2,3}$), 47.84 ($C_{5,6}$), 45.55 ($C_{1,4}$), 43.20 (C_7), 36.20 (C_8), 26.32 (C_9).

• **Mass spectrum**- (see Apendix 2.35), (EI^+): 366 ($C_{21}H_{22}N_4O_2$, M^+), 301 (MH^+-C_5H_6), 235 (MH^+-$C_{10}H_{12}$), 66 (M^+-$C_{16}H_{16}N_4O_2$).

• **IR-** (see Appendix 2.36), (KBr disc, cm^{-1}): 3048 (olefinic C-H stretching), 2996-2881 (saturated C-H stretching), 1859, 1776 (Asymmetric and symmetric C=O stretching, respectively), 1425 (C-N stretching).

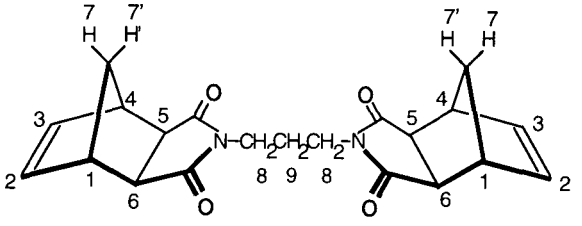

Assignment of H atoms in compound *exo*-C3D

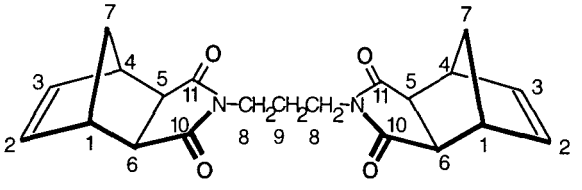

Assignment of C atoms in compound *exo*-C3D

Synthesis and characterisation of *exo,exo*-N,N'-pentylene-di-(norbornene-5,6-dicarboxyimides): (*exo*-C5D)

The same procedure as for the synthesis of exo-C3D was used to synthesise exo-C5D, but the starting material in this case was 1,5-diaminopentane (6.1 g, 0.06 mol) to yield exo-C5D as a white powder (42.5 g, 0.11 mol, 90% yield).

• **Mpt**: 185.1 °C

• **Elemental analysis**- Found C, 69.96%, H, 6.56%, N, 7.20%; calculated for $C_{23}H_{26}N_2O_4$: C, 70.03%, H, 6.64%, N, 7.10%.

• **^{1}H nmr**- (see Appendix 2.37), ($CDCl_3$, 400 MHz, δ (ppm)): 6.28 (t, 4H, $H_{2,3}$), 3.44 (t, 4H, H_8), 3.26 (p, 4H, $H_{1,4}$), 2.67 (d, 4H, $H_{5,6}$), 1.57 (m, 4H, H_9), 1.51(m, 2H, H_7), 1.31 (p, 2H, H_{10}), 1.21 (m, 2H, $H_{7'}$).

• **^{13}C nmr**- (see Appendix 2.38), ($CDCl_3$, 100 MHz), δ (ppm)): 178.05 ($C_{11,12}$), 137.80 ($C_{2,3}$), 47.79 ($C_{5,6}$), 45.13 ($C_{1,4}$), 42.75 (C_7), 38.35 (C_8), 27.26 (C_9), 24.30 (C_{10}).

• **Mass spectrum**- (see Appendix 2.39), (EI^+): 394 ($C_{23}H_{26}N_4O_2$, M^+), 329 (MH^+-C_5H_6), 263 (MH^+-$C_{10}H_{12}$), 66 (M^+-$C_{18}H_{20}N_4O_2$).

• **IR**- (see Appendix 2.40), (KBr disc, cm^{-1}): 3050 (olefinic C-H stretching), 2999-2847 (saturated C-H stretching), 1858, 1777 (Asymmetric and symmetric C=O stretching, respectively), 1420 (C-N stretching).

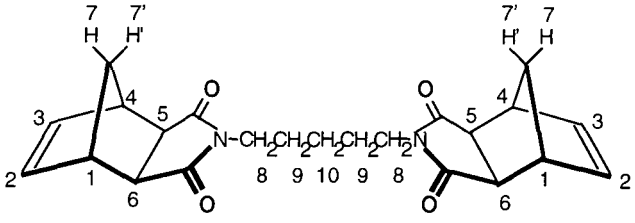

Assignment of H atoms in compound *exo*-C5D

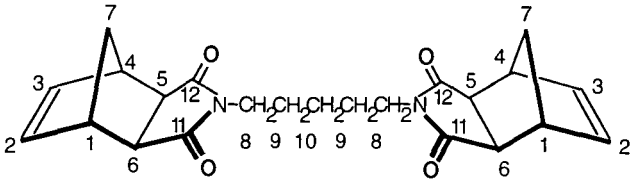

Assignment of C atoms in compound *exo*-C5D

Synthesis and characterisation of *exo,exo*-N,N'-hexylene-di-(norbornene-5,6-dicarboxyimides): (*exo*-C6D)

The same procedure as for the synthesis of exo-C3D was used to synthesise exo-C6D, but the starting material in this case was 1,6-diaminohexane (7.0 g, 0.06 mol) to yield exo-C6D as a white powder (45.3 g, 0.11 mol, 92% yield).

• **Mpt**: 154 °C

•**Elemental analysis**- Found C, 70.13%, H, 6.84%, N, 6.84%; calculated for $C_{24}H_{28}N_2O_4$: C, 70.57%, H, 6.91%, N, 6.86%.

• **^{1}H nmr**- (see Appendix 2.41), ($CDCl_3$, 400 MHz, δ (ppm)): 6.27 (t, 4H, $H_{2,3}$), 3.43 (t, 4H, H_8), 3.26 (p, 4H, $H_{1,4}$), 2.66 (d, 4H, $H_{5,6}$), 1.52 (m, 6H, H_9, and H_7), 1.31 (m, 4H, H_{10}), 1.20 (m, 2H, $H_{7'}$).

• **^{13}C nmr**- (see Appendix 2.42), ($CDCl_3$, 100 MHz, δ (ppm)): 177.94 ($C_{11,12}$), 137.67 ($C_{2,3}$), 47.66 ($C_{5,6}$), 45.01 ($C_{1,4}$), 42.62 (C_7), 38.40 (C_8), 27.45 (C_9), 26.33 (C_{10}).

• **Mass spectrum**- (see Apendix 2.43), (EI$^+$): 408 ($C_{24}H_{28}N_4O_2$, M^+), 343 (MH^+-C_5H_6), 277 (MH^+-$C_{10}H_{12}$), 66 (M^+-$C_{19}H_{22}N_4O_2$).

• **IR-** (see Appendix 2.44), (KBr disc, cm^{-1}): 3050 (olefinic C-H stretching), 2999-2889 (saturated C-H stretching), 1860, 1777 (Asymmetric and symmetric C=O stretching, respectively), 1420 (C-N stretching).

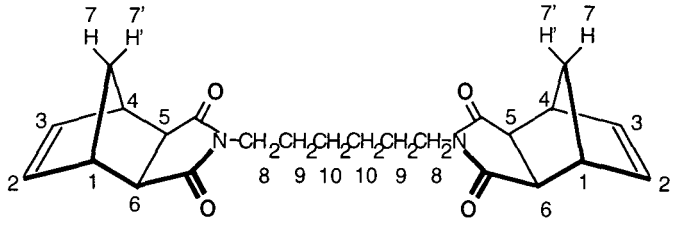

Assignment of C atoms in compound *exo*-C6D

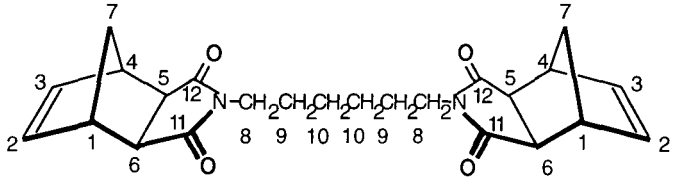

Assignment of C atoms in compound *exo*-C6D

Synthesis and characterisation of *exo,exo*-N,N'-nonylene-di-(norbornene-5,6-dicarboxyimides): (*exo*-C9D)

The same procedure as for the synthesis of exo-C3D was used to synthesise exo-C9D, but the starting material in this case was 1,9-diaminononane (9.5 g, 0.06 mol) to yield exo-C9D as a white powder (44.7g, 0.10 mol, 83% yield).

• **Mpt**: 68 °C

•**Elemental analysis**- Found C, 71.82%, H, 7.99%, N, 6.23%; calculated for $C_{27}H_{34}N_2O_4$: C, 71.97%, H, 7.61%, N, 6.22%.

• **^{1}H nmr**- (see Appendix 2.45), ($CDCl_3$, 400 MHz, δ (ppm)): 6.28 (t, 4H, $H_{2,3}$), 3.43 (t, 4H, H_8), 3.26 (p, 4H, $H_{1,4}$), 2.66 (d, 4H, $H_{5,6}$), 1.52 (m, 6H, H_9 and H_7), 1.25 (m, 12H, $H_{10\text{-}12}$ and $H_{7'}$).

• **^{13}C nmr**- (see Appendix 2.46), ($CDCl_3$, 100 MHz, δ (ppm)): 178.07 ($C_{13,14}$), 137.78 ($C_{2,3}$), 47.75 ($C_{5,6}$), 45.11 ($C_{1,4}$), 42.68 (C_7), 38.67 (C_8), 29.19 (C_9), 27.00 (C_{10}), 27.69 (C_{11}), 26.84 (C_{12}).

• **Mass spectrum-** (see Appendix 2.47), (EI^+): 450 ($C_{27}H_{34}N_4O_2$, M^+), 385 (MH^+-C_5H_6), 319 (MH^+-$C_{10}H_{12}$), 66 (M^+-$C_{22}H_{28}N_4O_2$).

• **IR-** (see Appendix 2.48), (KBr disc, cm^{-1}): 3050 (olefinic C-H stretching), 2997-2880 (saturated C-H stretching), 1860, 1779 (Asymmetric and symmetric C=O stretching, respectively), 1427 (C-N stretching).

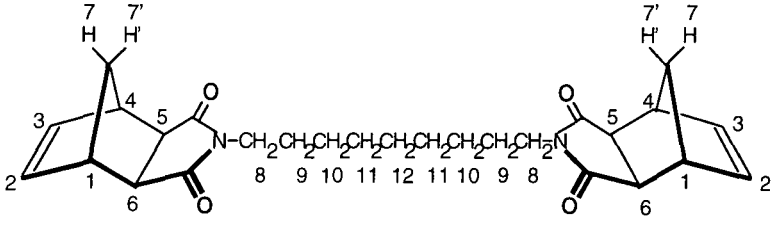

Assignment of H atoms in compound *exo*-C9D

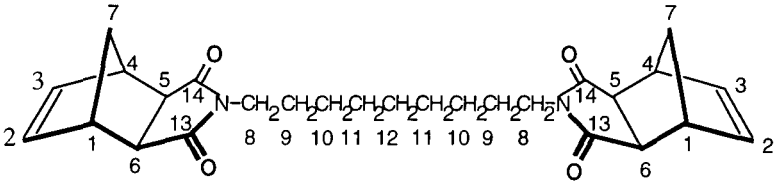

Assignment of C atoms in compound *exo*-C9D

Synthesis and characterisation of *exo,exo*-N,N'-dodecylene-di-(norbornene-5,6-dicarboxyimides): (*exo*-C12D)

The same procedure as for the synthesis of exo-C3D was used to synthesise exo-C12D, but the starting material in this case was 1,12-diaminododecane (12.0 g, 0.06 mol) to yield exo-C12D as a white powder (47.1 g, 0.10 mol, 80% yield).

• **Mpt**: 64 °C

•**Elemental analysis**- Found C, 73.29%, H, 8.51%, N, 5.79%; calculated for $C_{30}H_{40}N_2O_4$: C, 73.14%, H, 8.18%, N, 5.69%.

• **^{1}H nmr**- (see Appendix 2.49), ($CDCl_3$, 400 MHz, δ (ppm)): 6.28 (t, 4H, $H_{2,3}$), 3.46 (t, 4H, H_8), 3.27 (p, 4H, $H_{1,4}$), 2.66 (d, 4H, $H_{5,6}$), 1.44 (m, 6H, H_9 and H_7), 1.24 (m, 18H, $H_{10\text{-}13}$ and $H_{7'}$).

• **^{13}C nmr**- (see Appendix 2.50), ($CDCl_3$, 100 MHz, δ (ppm)): 178.35 ($C_{14,15}$), 138.06 ($C_{2,3}$), 48.02 ($C_{5,6}$), 45.39 $C_{1,4}$), 42.94 (C_7), 38.99 (C_8), 29.70 (C_9), 29.66 (C_{10}), 29.37 (C_{11}), 28.01 (C_{12}), 27.19 (C_{13}).

• **Mass spectrum**- (see Appendix 2.51), (EI$^+$): 492 ($C_{30}H_{40}N_4O_2$, M^+), 427 (MH^+-C_5H_6), 361 (MH^+-$C_{10}H_{12}$), 66 (M^+-$C_{25}H_{34}N_4O_2$).

• **IR-** (see Appendix 2.52), (KBr disc, cm^{-1}): 3045 (olefinic C-H stretching), 2997-2879 (saturated C-H stretching), 1860, 1779 (Asymmetric and symmetric C=O stretching, respectively), 1424 (C-N stretching).

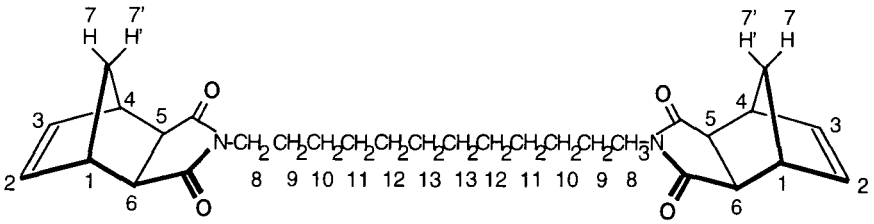

Assignment of H atoms in compound *exo*-C12D

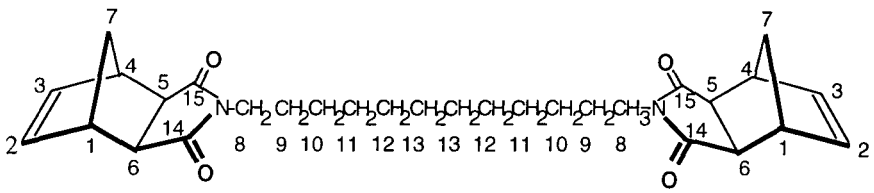

Assignment of C atoms in compound *exo*-C12D

2.4 References for Chapter 2

[1] 'Principles of Organic Synthesis', 2nd Ed., R. O. C. Norman, Chapman and Hall Ltd., New York, 1978.

[2] 'Introduction to Organic Chemistry', 3 rd Ed., A. Streitweser and C. H. Heathcock, Macmillan Publishing Company, New York, 1985.

[3] 'Organic Chemistry', 2nd Ed., J. Mc.Murray, Brooks & Coles, New York, 1988.

[4] 'Vogel's Textbook of Practical Organic Chemistry', 5th Ed., B. S. Furniss, A. J. Hannaford, P. W. G. Smith, and A. R. Tatchell, John Wiley and Sons, New York, 1989.

[5] 'Advanced Organic Chemistry: Reaction, Mechanisms and Structure', 4th Ed., J. March, John Wiley and Sons, New York, 1992.

[6] J. Sauer, *Angew. Chem. Internat. Edit.*, **6** (1), 16, 1967.

[7] D. Craig, *J. Am. Chem. Soc.*, **73**, 4889, 1951.

[8] K. F. Kastner and N. Calderon, *J. Mol. Catal.*, **15**, 47, 1982.

[9] P. Canonne, D. Belanger, G. Lemay, *J. Org. Chem.*, **47**, 3953, 1982.

[10] W. Berning, S. Hunig, F. Prokschy, *Chem. Ber.*, 117, 1455, 1984.

[11] S. C. G. Biagini, and et all., *Tatrahedron*, **51**, 7247, 1995.

[12] S. Kurosawa, T. Uasmma, Y. Tanka, and S. Kobayashi, *US Pat.* 4,022,954, 1997.

[13] A. A. Al-Hajaji, PhD Thesis, University of Durham, 1995.

Chapter 3

Trial bulk polymerisations of imidonorbornene derivatives

3.1 Introduction

3.1.1 General introduction

Metathesis polymerisation is a very versatile reaction. Materials ranging in properties from soft elastomers, through tough thermoplastics to highly crosslinked hard thermosets can be prepared by this chemistry.[1-12] Metathesis polymerisation, depending on the ring strain of the cycloolefin monomer, is fast and can be carried out to high conversion in the bulk without any major by-products. These characteristics lead to the possibility of producing polymeric materials from monomers in one step without using solvents and without the requirement to remove unpolymerised monomers. Fast polymerisation of dicyclopentadiene, for example, has been used in the commercial manufacture of reaction injection moulded parts by B. F. Goodrich Co., Nippon Xeon, Hercules Inc., and others.[13-17]

The work described in this chapter is concerned with making new polymeric materials via ROMP using a well-defined ruthenium carbene initiator, $Cl_2[(C_6H_{11})_3P]_2Ru{=}CHC_6H_5$. The object of the work was to study the possibility of this system for the RIM and/or RTM-processes. Small scale bulk polymerisations in glass tubes were used to test the polymerisability of mono- and difunctional imido norbornene derivatives with the ruthenium carbene initiator. The synthesis of all monomers used in this work was described in the previous chapter. The ruthenium carbene initiator was synthesised as described in the literature.[18-20] The experiments were carried out using neat monomer mixed with the initiator. This set of experiments represented a first scan of reaction conditions and, as will be described, the conversions obtained are not ideal for transfer to a RIM or RTM process in which the reactive mixture is usually injected or poured into a mould. It was expected that these first trials would provide guidance as to appropriate conditions and an indication of the problem to be solved before larger scale in-mould polymerisation was attempted.

This chapter is divided into three sections. The first section presents a brief introduction to crosslinked polymers. In general only information relevant to the work described in this thesis is discussed in detail, information on related topics can be found in the literature cited. The ROMP of *exo*- and *endo*-N-hexylnorbornene-5,6-

dicarboxyimide (*exo*- and *endo*-C6M) initiated by a well-defined ruthenium carbene in bulk is discussed in section 3.2. Subsequently the synthesis of the crosslinked polymers using difunctional monomer, *exo*-C6D, as a crosslinking reagent is described along with the polymer characterisation in section 3.3. The relative reactivity of *exo*- and *endo*-monomers via ROMP in solution was studied using the nmr technique and the results are discussed in Chapter 4. Optimised reaction conditions for RIM and/or RTM were developed subsequently to these preliminary studies and are discussed in Chapter 5.

3.1.2 Crosslinked polymers[21-24]

Crosslinking polymerisations lead to the formation of insoluble and infusible polymers in which chains are joined together to form a network structure. If a mixture mono- and difunctional monomers are polymerised then the latter becomes a constituent of two polymer chains, effectively crosslinking the chains together. When all the polymer chains are mutually connected an 'infinite network' is formed as shown in Figure 3.1.

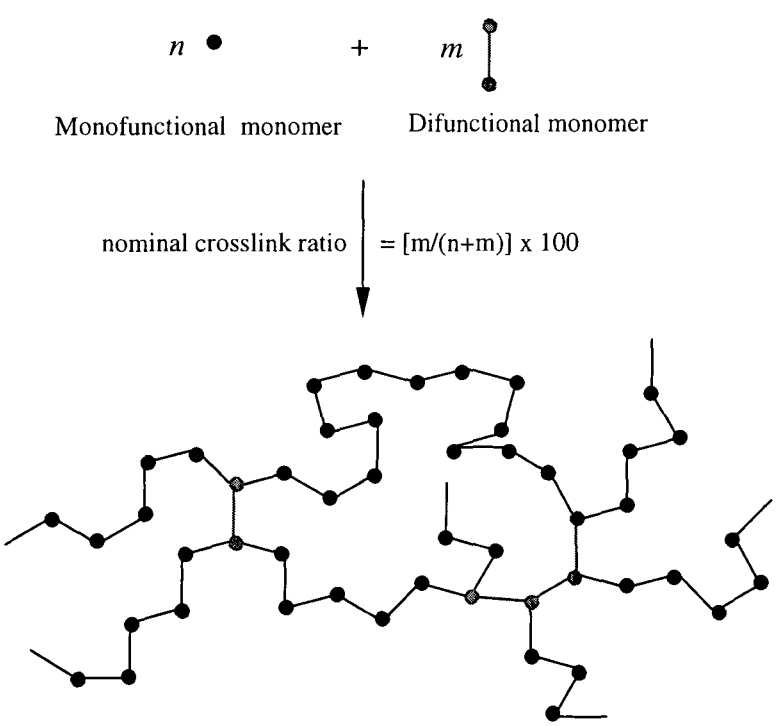

Figure 3.1 Structure of crosslinked polymer.

The content of difunctional monomer in a crosslinked polymer can be quoted as a percentage of difunctional monomer in the feed stock or the content of *actual* difunctional monomer present in the polymer network. There are other complications which make determination of *actual* difunctional monomer active in the polymer network difficult. Firstly, although a defined level of crosslinker can be used to synthesise the crosslinked polymer it is not certain that both functional groups in every difunctional monomer will react. Secondly, it is possible to produce 'entanglement crosslinks' by spurious entanglements, as shown in Figure 3.2. Generally 'entanglement crosslinks' increase when the rate of polymerisation is increased. It is also high in a non-agitated polymerisation systems, whereas vigorous agitation tends to minimise entanglements. There is no simple and rapid method for determining the effective difunctional monomer content in a polymer network. For convenience, the nominal figure based on the actual difunctional monomer feed was used in this work and is referred to the nominal crosslink ratio in Figure 3.1.

Figure 3.2 Permanent entanglement crosslink.

The usual way to characterise the degree of swelling of crosslinked polymers is through the volumetric swelling ratio, $q = v_f/v_i$ where v_f is the final volume, when the gel cannot absorb any more solvent and v_i is the initial volume before any solvent has been absorbed. Alternative measures of swelling are: (1) the polymer volume fraction $\phi = 1/q = v_i/v_f$; and (2) mass swelling ratio, $q_m = m_f/m_i$ where m_f and m_i are the final (swollen) and initial (dry) mass. In this work, q_m was used to determine the degree of swelling of the crosslinked polymers.

A theoretical prediction for Mc (the average molecular weight between crosslinks) can be determined from the ratio of mono- to difunctional monomers, assuming perfect incorporation of difunctional monomers. We can calculate a theoretical value for Mc, the average molecular weight between crosslinks using the following expression:

$$\text{Mc(theory)} = \frac{\text{Moles of monofunctional monomer}}{2 \times \text{Moles of difunctional monomer}} \times \text{Molecular weight of repeat unit.}$$

Thus for a 5% loading of difunctional monomer we expect a theoretical value for Mc of the repeat unit mass $\times \frac{100}{5} \times \frac{1}{2}$, i.e. 10 units. In general we can express the theoretical Mc as $\frac{\text{repeat unit mass} \times 50}{\text{mole\% of difunctional crosslinker}}$. An experimental value for Mc can be determined from shear modulus measurments using rubber elasticity theory.[25] The equation used is :- $\text{Mc(expt.)} = \frac{\rho R T}{G}$; where G = shear modulus 50 °C above Tg determined by Dynamic Mechanical Thermal Analysis using parallel plate geometry, ρ = density, determined using a density column, R = 8.31 $JK^{-1}mol^{-1}$ and T = temperature (Kelvin). When Mc(theory) ≈ Mc(expt.) perfect crosslinking has occurred.

In this work, the crosslinking was accomplished by polymerising a polyfunctional cycloolefin crosslinker containing two norbornene groups (*exo*-CnD) with cycloolefins containing a norbornene group (*exo*- and *endo*-CnM) in a manner where the crosslinker functions as a comonomer. If the polymerisation was carried out in the absence of the crosslinking agent, *exo*-CnD, a polymer which had a high degree of solubility in hydrocarbon solvents was obtained. In cases where the crosslinkers were used, the resulting polymers were solvent resistant and varied in properties from soft elastomers to brittle materials depending on their Tgs and crosslink density.

3.2 Trial bulk polymerisations of *exo*- and *endo*-monofunctional monomer mixtures: (*exo*- and *endo*-C6M)

In this section, *exo*- and *endo*-N-hexylnorbornene-5,6-dicarboxyimide (*exo*- and *endo*-C6M) were used as feed monomers and ROMP was initiated by using the ruthenium carbene, see Figure 3.3. Linear polymeric materials with unsaturated backbones and imido pendant groups were obtained as shown in Figure 3.4.

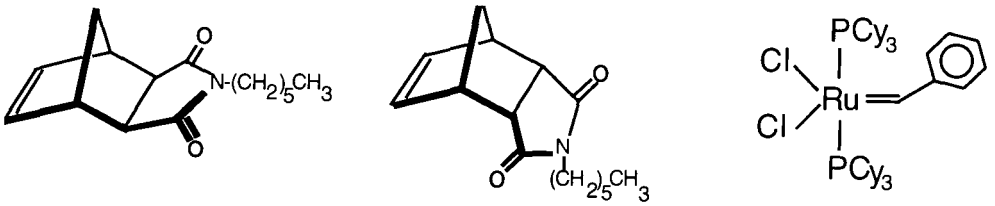

Exo-C6M *Endo*-C6M Ruthenium carbene initiator

Figure 3.3 Chemical structures of *exo*- and *endo*-C6M and the ruthenium carbene initiator.

3.2.1 Results and discussion

The polymer synthesis could be followed by the changes in colour and viscosity of the reaction mixture. The rate at which this occurred depending upon the amount of the *exo*- and *endo*-monomer used in the feed. The greater the amount of *exo*-monomer in the monomer feed the quicker the change in colour, from pink (initiator) to yellow (propagating species) and the increase in viscosity. Whereas using the *endo*-monomer at concentrations between 88 and 100% in the feed showed the colour change but did not show the change in viscosity under these conditions, indicating initiation but very slow propagation. Increased viscosity may be used as a qualitative indication of the polymerisation, but it can not be used for determining the conversion since the viscosity/molecular weight relationship is unknown for this system. The extent of the polymerisation can be studied by withdrawing and analysing small samples during the course of polymerisation or by terminating polymerisation at different stages in a series of reactions which have identical initial compositions. These methods had been used and will be discussed in Chapter 5.

3.2.1.1 Synthesis of linear polymeric materials

The *exo*-C6M (10 g) and the ruthenium carbene initiator (10 mg) were added to a test tube. The mixture was stirred at room temperature for 5 minutes before heating at 30-35°C for 10 minutes in an oil bath. After 10 minutes, the solution became highly viscous, and the temperature was raised to 110-120 °C for 30 minutes. After this time, the test tube was removed from the oil bath and the resulting polymer was isolated by

breaking away the glass. To study the effect of the *endo*-isomer in the polymerisation, *endo*-C6M and *exo*-C6M were mixed in different proportions and then polymerised under the same reaction conditions as above.

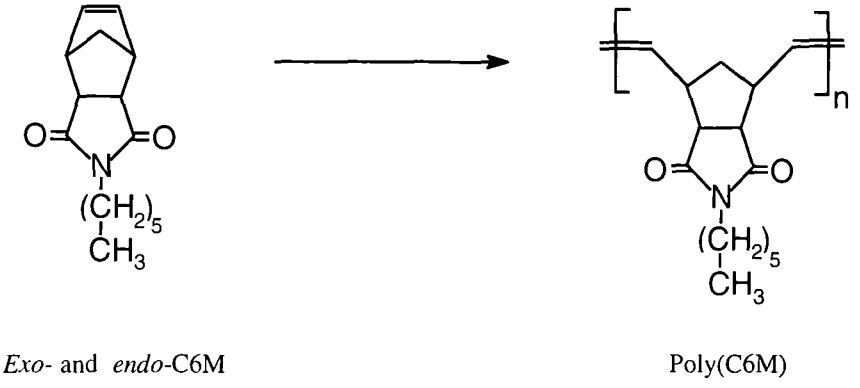

Exo- and *endo*-C6M Poly(C6M)

Figure 3.4 A schematic representation of the linear polymer synthesis.

3.2.1.2 Characterisation of polymeric materials obtained

This section describes the characterisation of the linear polymeric materials whose synthesis was described in section 3.3.1.1. The characterisation was carried out using ^{1}H nmr, GPC, DSC and TGA. All polymeric materials obtained in this section dissolved in toluene, tetrahydrofuran, chloroform, and dichloromethane. The pure linear polymers were isolated by precipitation of the crude polymeric materials from chloroform into excess methanol and dried under vacuum at 40°C for 2 days.

Polymer characterisation using ^{1}H nmr spectroscopy

The amount of unreacted monomer and the *cis/trans* content in the crude polymeric materials can be determined directly from the ^{1}H nmr spectra, as the olefinic hydrogen signals of the unreacted monomers and the polymer obtained are clearly distinguished. The resonances attributable to the *cis* and *trans* vinylene hydrogens of the polymer are well separated and can be seen in the range δ 5-6 ppm, whereas the resonances attributable to the olefinic hydrogen of *exo*- and *endo*-monomers are well separated and can be seen in the range δ 6-7 ppm. The ^{1}H nmr spectra of a 80% *exo*/20% *endo*-C6M monomer mixture, the crude polymeric material and the pure polymer obtained are shown in figure 3.5a, b and c, as a typical example of this analysis.

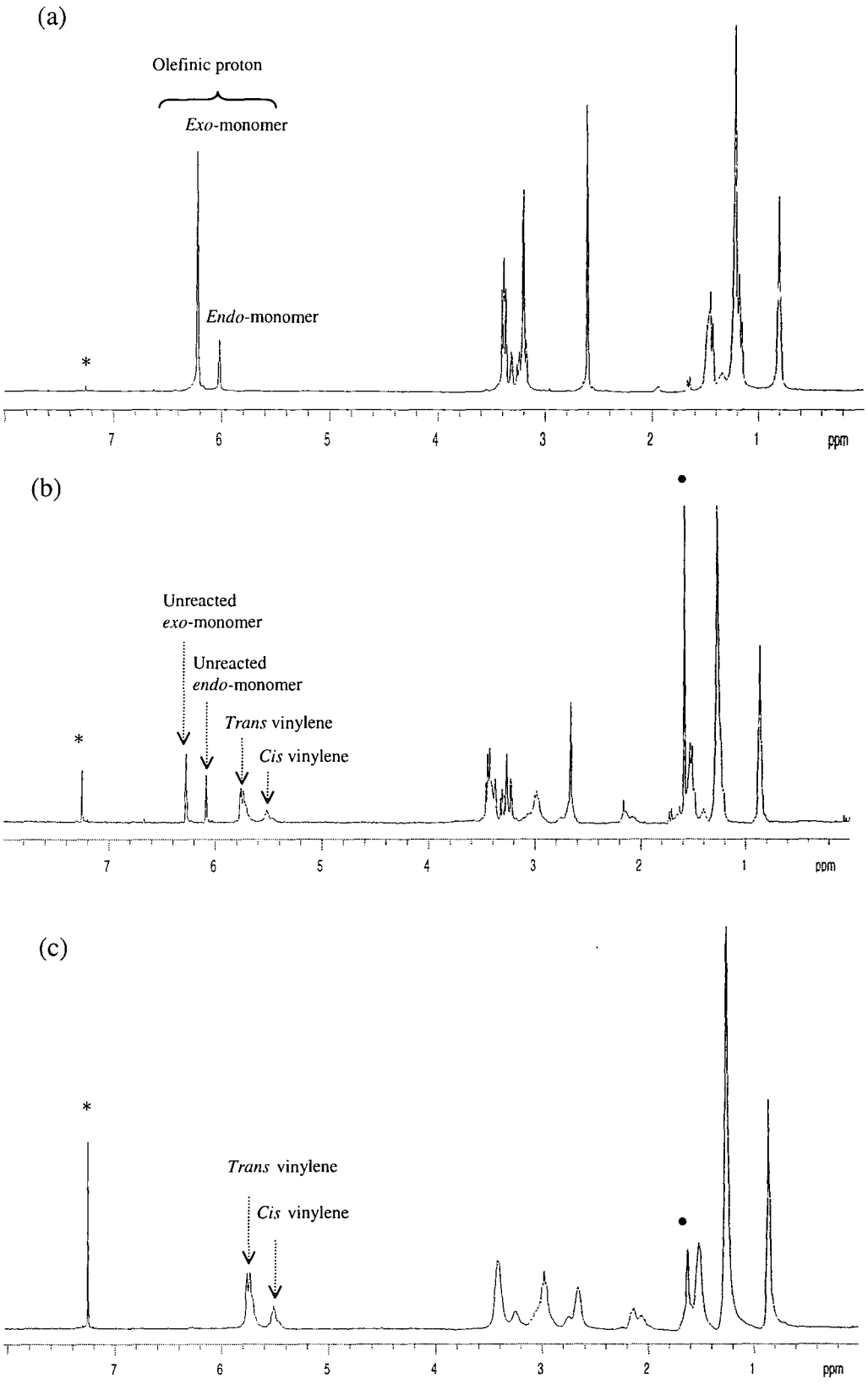

Figure 3.5 ^{1}H nmr spectra of (a) 80% *exo*-/20% *endo*-monomer mixture, (b) crude polymeric material and (c) pure linear polymer. * residual hydrogens in $CDCl_3$, • water dissolved in $CDCl_3$.

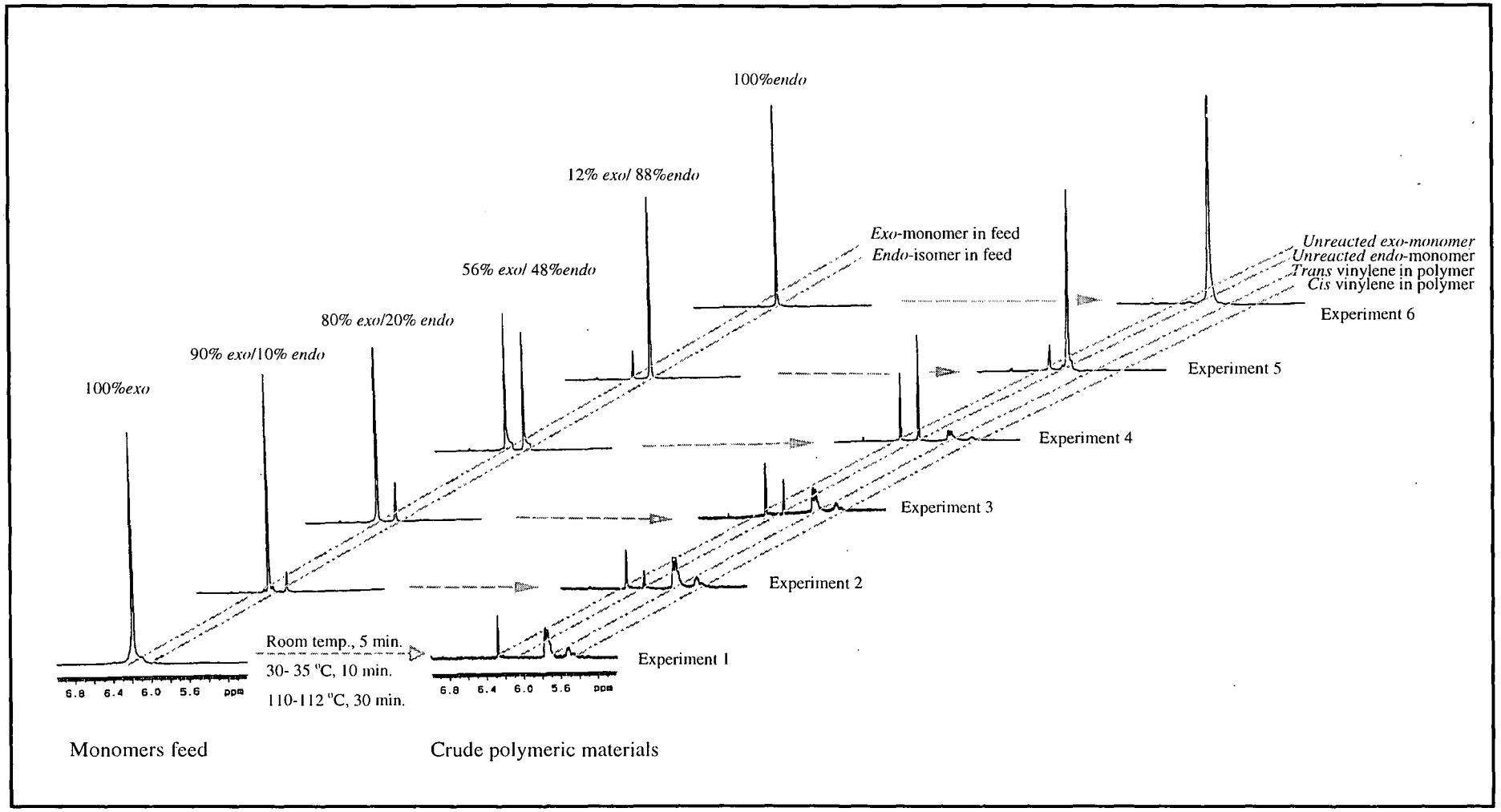

Figure 3.6 ^{1}H nmr spectra of the monomer feeds and polymers obtained from ROMP in bulk of *exo-/endo*-monomer mixtures.

Experiment	[M]/[I] ratio	% monomers in feed		Crude polymeric materails							Sample appearance
		Exo-C6M	*Endo*-C6M	% *Exo*-C6M		% *Endo*-C6M		% Polymer			
				unreacted	consumed A (B%)*	unreacted	consumed C (D%)**	Obtained	*Trans*	*Cis*	
1	4,600	100	0	11	89 (89%)	0	0	89	75	25	hard
2	5,500	90	10	13	77 (86%)	5	5 (50%)	82	74	26	hard
3	4,400	80	20	21	59 (74%)	12	8 (40%)	67	79	21	rubbery
4	4,700	56	44	26	30 (54%)	41	3 (7%)	33	77	23	rubbery
5	4,200	12	88	12	0	88	0	0	0	0	liquid mixture***
6	4,400	0	100	0	0	100	0	0	0	0	liquid mixture***

Table 3.1 ^{1}H nmr analysis of the crude polymeric materials obtained from ROMP in bulk of *exo*-/*endo*-monomer mixtures.

* Consumed A = *exo*-monomer in feed – unreacted *exo*-monomer in crude product Consumed B = (A x 100)/*exo*-monomer in feed
** Consumed C = *endo*-monomer in feed – unreacted *endo*-monomer in crude product Consumed D = (C x 100)/*endo*-monomer in feed
*** No polymer was obtained under the condition studied, and unreacted monomers were observed after the reaction.

The ^{1}H nmr spectra and the associated parameters for this set of experiments were determined and are recorded in Figures 3.6 and Table 3.1, respectively. The details of the ^{1}H and ^{13}C nmr assignment of the monomers and the polymers are described in section 2.3 and 4.3.1.2, respectively. ^{1}H nmr analysis indicated that there were residual *exo*- and *endo*-monomers in all crude samples, as shown in Figure 3.6. Even in the case of pure *exo*-monomer, experiment 1, ^{1}H nmr analysis revealed that there was residual *exo*-monomer present. It is apparent that the *exo*-isomer polymerised preferentially as the proportion of *endo*-monomer in the monomer mixture is increased the overall extent of polymerisation decreases until, at 88 and 100% *endo*-monomer content in the feed, experiment 5 and 6, polymerisation is entirely suppressed. However, the data also show that at 10% *endo*-monomer content in the feed, experiment 2, half is consumed in the polymerisation whereas when there is 44% *endo*-monomer in the feed, experiment 4, only 7% of it is consumed.

Polymer characterisation by GPC

Experiment	% monomer in feed		GPC*		
	Exo-C6M	*Endo*-C6M	$\overline{M}n$	PDI	No. of peaks
1	100	0	1,413,000	1.3	1
2	90	10	843,000	1.6	1
3	80	20	454,000	1.7	1
4	56	44	345,000	1.8	1

Table 3.2 GPC analysis of the polymeric materials obtained from ROMP in bulk of *exo*- and *endo*-C6M.

* Waters differential diffractometer detector, three Polymer Laboratories gel columns (exclusion limits 100, 10^{3}, 10^{5} A), chloroform eluent, polystyrene calibration.

The number average molecular weight ($\bar{M}n$) and polydispersity index, $\bar{M}w/\bar{M}n$ (PDI) of all polymeric materials obtained in this section are recorded in Table 3.2 and the original traces are shown in Appendix 3.1-3.4. It was found that the product 'polystyrene equivalent' molecular weights decrease and the polydispersities increase as the proportion of *endo*-monomer in the feed increases. The highest molecular weight polymer, $\bar{M}n = 1.4x10^6$, was obtained from experiment 1 in a reaction proceeding to 89% conversion when there was no *endo*-monomer included in the feed.

Polymer characterisation by DSC and TGA

The crude polymeric materials obtained from experiments 1 to 4 were purified by precipitation from chloroform into excess methanol. The aim was to compare the Tg of the crude products and pure linear polymers. All the pure linear polymers were obtained as white solids. The glass transition temperature and the temperature for 2% weight loss of crude polymeric materials and pure polymers are recorded along with the conversion and the number average molecular weights in Table 3.3. All DSC traces are shown in Appendix 3.5-3.12.

Experiment	% unreacted monomers*	$\bar{M}n$	DSC Tg (°C)		TGA 2% weight loss(°C)	
			Crude polymer	Pure polymer	Crude Polymer	Pure polymer
1	11	1,413,000	82	86	295	>300
2	18	843,000	30	82	169	>300
3	33	454,000	-41	81	157	>300
4	67	345,000	-59	81	157	>300

Table 3.3 Thermal analysis of the polymers obtained from ROMP in bulk of *exo-*/ *endo*-C6M monomer mixtures.

* % unreacted *exo-* and *endo*-monomers in the crude products.

It is clear that as the amount of unreacted monomers trapped in the polymer matrix increases the observed glass transition temperature (Tg) and temperature for 2% weight loss of the crude products decrease. The glass transition temperatures of crude polymers decrease dramatically from 82 to –59°C, as the amount of the unreacted monomers trapped in the polymer matrixes increase from 11 to 67%.

The Tg values for pure linear polymers were in the range 81-86°C which are higher than those of the crude products. This clearly indicates that the glass transition of the products is related to the amount of the residual monomers which act as plasticisers. Thermogravimetric analysis (TGA) on all crude samples shows a substantial weight loss increased from 157 to 295 °C as the amount of the unreacted monomer decreases and the molecular weight of the polymer increases, whereas pure polymers show a substantial weight loss above 300 °C.

3.3 Trial bulk polymerisations of mono- and difunctional monomer mixtures: (*exo*-and *endo*-C6M and *exo*-C6D)

In this section *exo,exo*-N,N'-hexylene-di-(norbornene-5,6-dicarboxyimides), *exo*-C6D, was used as a crosslinking reagent. A relatively high mixing temperature, 50 °C, was necessary for these experiments because of the limited solubility of *exo*-C6D in *exo*-C6M at room temperature. The trial bulk polymerisations were carried out in the test tubes which also served as moulds. The solid difunctional monomer was dissolved in liquid monofunctional monomer prior to addition of the initiator. The final products were isolated by breaking away the glass.

3.3.1 Results and discussion

ROMP in bulk of *exo*-C6M and *exo*-C6D initiated by the ruthenium carbene yielded crosslinked polymeric materials with unsaturated backbones and imido pendant group as shown in Figure 3.7.

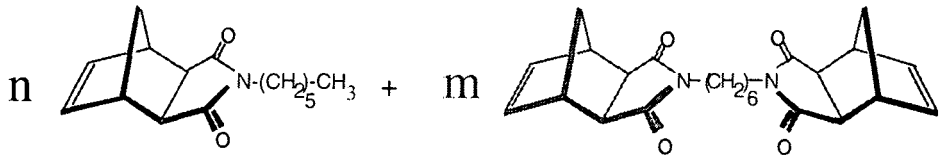

Exo-C6M
Monofunctional monomer

Exo-C6D
Difunctional monomer

$$\text{nominal crosslink ratio} = \left(\frac{m}{n+m}\right) \times 100$$

Ru carbene initiator

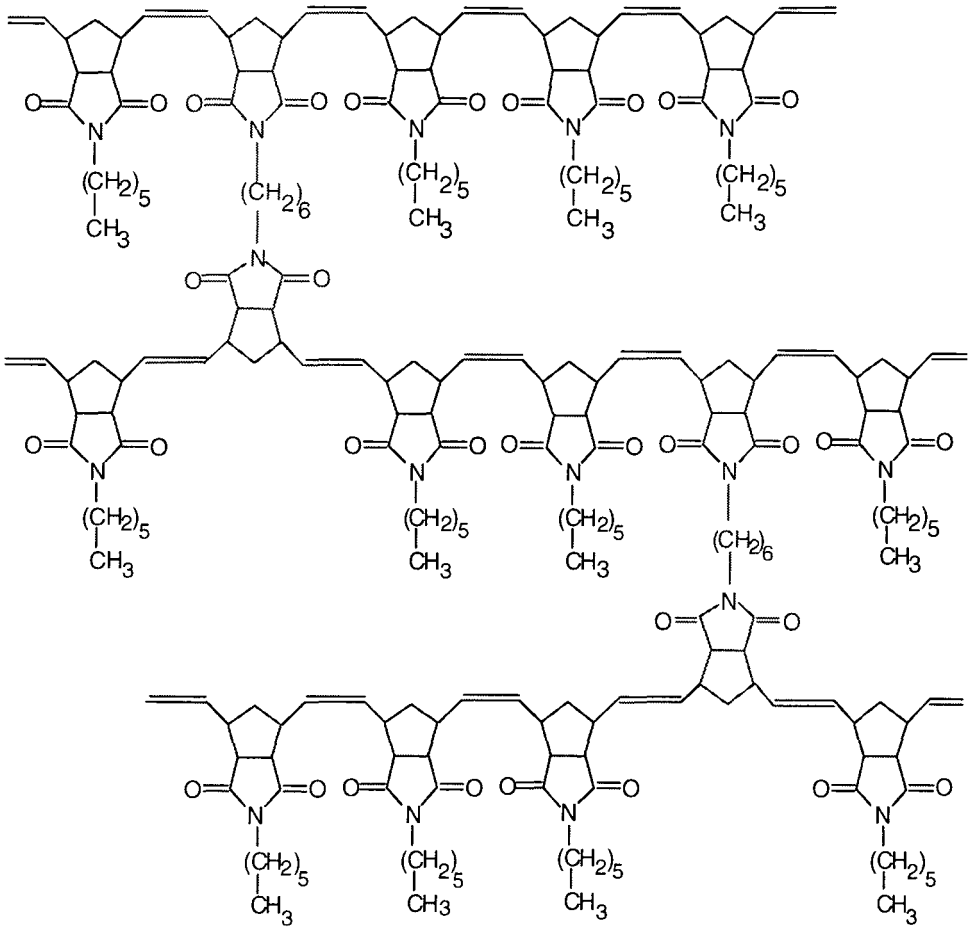

Crosslinked polymer

Figure 3.7 A schematic representation of the crosslinked polymer synthesis.

3.3.1.1 Synthesis of crosslinked polymeric materials

The same procedure as was used for the synthesis of linear polymeric materials was repeated except that in these experiments the difunctional monomer, *exo*-C6D, was dissolved completely, by heating and stirring at 50°C, in the monofunctional monomer, *exo*-C6M, prior to the addition of the initiator. A few minutes after the addition of the initiator at 50°C, the solution became highly viscous, and the temperature was raised to 100-120°C for 30 minutes. The polymer was obtained as clear yellow hard material which was insoluble giving a gel in chloroform, dichloromethane and tetrahydrofuran which is consistent with the formation of crosslinked polymer.

To study the effect of the *endo*-isomer in the polymerisation, an *exo-/endo*-monomer mixture was mixed with *exo*-C6D prior to the addition of the initiator. The monomer mixture was stirred at 50 °C until *exo*-C6D dissolved completely and then polymerised under the same reaction conditions as above.

3.3.1.2 Characterisation of polymeric materials obtained

This section describes the characterisation of the crosslinked polymeric materials whose synthesis was described in section 3.3.1.1. The characterisation of the crude polymeric materials was carried out using DSC and TGA. The crude products were subjected to sol/gel extraction using chloroform in a Soxhlet apparatus. The gel fractions were examined using DSC and TGA and the sol fractions were examined by GPC and ^{1}H nmr spectroscopy.

Characterisation of crude polymeric materials and gel fractions by DSC and TGA

The thermal analysis data for these preliminary crosslinking experiments are recorded in Table 3.4, in comparison with data for analogous experiments in the absence of crosslinker. DSC traces are shown in Appendix 3.13 -3.16. The main interest in these crosslinked polymer properties lies in the values of the glass transition temperature (Tg) and the temperature for 2% weight loss (TGA). The crosslinked polymeric material which was obtained from pure *exo*-monomer crosslinked with a 3 mole% loading of the difunctional reagent, experiment 7, exhibited a lowering of Tg of about 3 °C, in comparison with that of a sample prepared in an experiment carried out in the absence of crosslinking agent in the monomer feed, which is consistent with a slightly

lower monomer conversion. When 19% *endo*-monomer was included in the feed stock the raw product, experiment 8, exhibited a very low Tg at –38 °C, which is consistent with heavy plasticisation by unreacted monomer. When *exo*-C6D is incorporated in the monomer feed the gelation time of the polymerisation system was shorter than that without *exo*-C6D. This might be because the rate of the reaction increased and/or the crosslinked polymer formed was insoluble in the liquid monomer. If gelation occurred too early, the polymerisation reaction would not go to completion and the residual monomer would act as plasticiser. In practice the gelation appears quite suddenly in the reacting mass, the stirrer stops and at this point it may be that access to the active chain ends by monomer is inhibited.

Experiment	1	7	3	8
Exo-C6M (% by mole)	100	97	80	78
Endo-C6M (% by mole)	0	0	20	19
Exo-C6D (% by mole)	-	3	-	3
Ratio of monomer/ initiator	4,600	3,700	4,400	3,800
Mixing temperature (°C)	room	50	Room	50
Gel fraction (W_g, % by weight)	-	86	-	51
Sol fraction (Ws, % by weight)	-	14	-	49
Temp. for 2% weight loss for crude product (°C)	295	281	157	157
Tg of crude product (°C)	82	79	-41	-38
Tg of gel fraction(°C)	-	88	-	88
Degree of swelling (q, by weight (g))	-	4	-	7.5
Polymer appearance	hard	hard	rubbery	rubbery

Table 3.4 The characterisation of crosslinked polymeric materials compared with linear polymeric materials.

The sol/gel content of the crosslinked samples was determined by extraction of the sol fractions. About 4 g (W_i) of crude products were subject to sol/gel extraction using chloroform in a Soxhlet apparatus for 3 days. The gel fractions were dried under vacuum at 40 °C for 2 days and weighed (W_g). The weight difference between W_g and W_i was taken as the weight of sol (W_s). The values of W_g, W_s and Tg of the gel fractions were determined and are recorded in Table 3.4. It was found that the gel fractions decrease, from 86 to 51% (by weight) when *endo*-monomer is included in the monomer feed, experiment 8, in comparison with experiment in the absence of *endo*-monomer in the monomer feed, experiment 7. The Tg values for the pure crosslinked materials were about 88 °C which are higher than those of the crude products. The Tg of the gel fraction from experiment 7 was much higher than that of the crude product, from –38 to 88 °C. A substantial decrease in the temperature for 2% weight loss (TGA) for the crude samples, from 281 to 157 °C, is observed as the amount of sol increased from 14 to 49%. This indicates that Tg and temperature for 2% weight loss of the products are affected by the amount of residual monomer, sol fractions, which act as plasticisers.

Characterisation of gel fractions by swelling

Swelling measurement of the gel fractions were carried out in toluene at room temperature. Small pieces of gels, weighing about 1 g, were immersed in toluene for 2 days, the swollen gels were removed from the solvent, quickly dried with filter paper and weighed. The values of the degrees of swelling (q_m) were determined and the results are recorded in Table 3.4. It is apparent that the degree of swelling (q_m) of the gel fraction increased when the *endo*-monomer was included in the monomer feed, experiment 8, in comparison with data for an analogous experiment in the absence of *endo*-monomer in the monomer feed, experiment 7. This indicates that the polymer which was obtained from experiment 8 has a high swelling capacity which is the property of a lightly crosslinked polymer, since the degree of swelling invariably decreases with increasing degree of crosslinking. Whereas in experiment 7, a highly crosslinked product with a lower extractable content showed a lower swelling capacity. It can be concluded that both the crosslink density and the content of unreacted monomer are effected by the *endo*-monomer in the monomer feed.

Characterisation of sol fraction by GPC

In the first attempt to determine the amount of the unreacted crosslinking agent (*exo*-C6D), the sol fractions were submitted to GPC. The traces indicated a mixture consisting of low molecular weight linear and branch polymers, broad peak a, unreacted mono- and difunctional monomers, peaks c and b respectively. These were confirmed by the GPC elution times and by enrichment, see Figure 3.8. It is apparent that there was a very low amount of residual *exo*-C6D in the sol fractions, indeed too low to be calculated reliably from the area under peaks in the GPC traces.

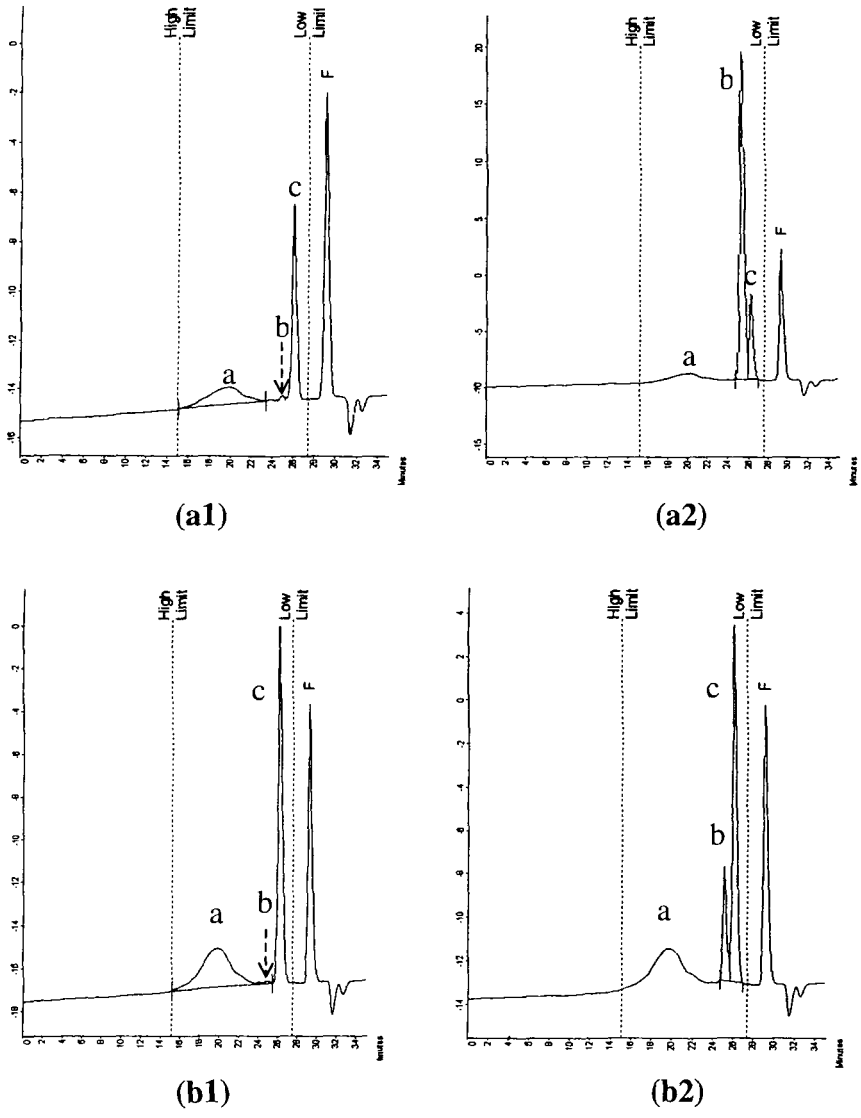

Figure 3.8 GPC trace of (a1) sol fraction from experiment 7, (a2) sol fraction from experiment 7 after the addition of *exo*-C6D, (b1) sol fraction from experiment 8, (b2) sol fraction from experiment 8 after the addition of *exo*-C6D.

Characterisation of sol fractions by ^{1}H nmr spectroscopy

In practice, the amounts of the unreacted monofunctional monomers (*exo*- and *endo*-C6M), unreacted difunctional monomer (*exo*-C6D) and polymers (linear and branch) in the sol fractions could be determined from the ^{1}H nmr spectra. The resonances attributable to the *cis* and *trans* vinylene hydrogens of the polymer are well separated and can be seen in the range δ 5-6 ppm. The peak corresponding to the olefinic hydrogens of the unreacted *endo*-monomer is found at 6.09 ppm, 0.19 ppm from those in *exo*-C6M and *exo*-C6D which overlap at 6.28 ppm. The methyl groups of alkyl pendant groups of the monomers (*exo*- and *endo*-isomer) and the polymers overlap at 0.87 ppm. The ^{1}H nmr spectra and associated parameters of the sol fractions from experiments 7 and 8 are shown in Figure 3.9 and Table 3.5, respectively.

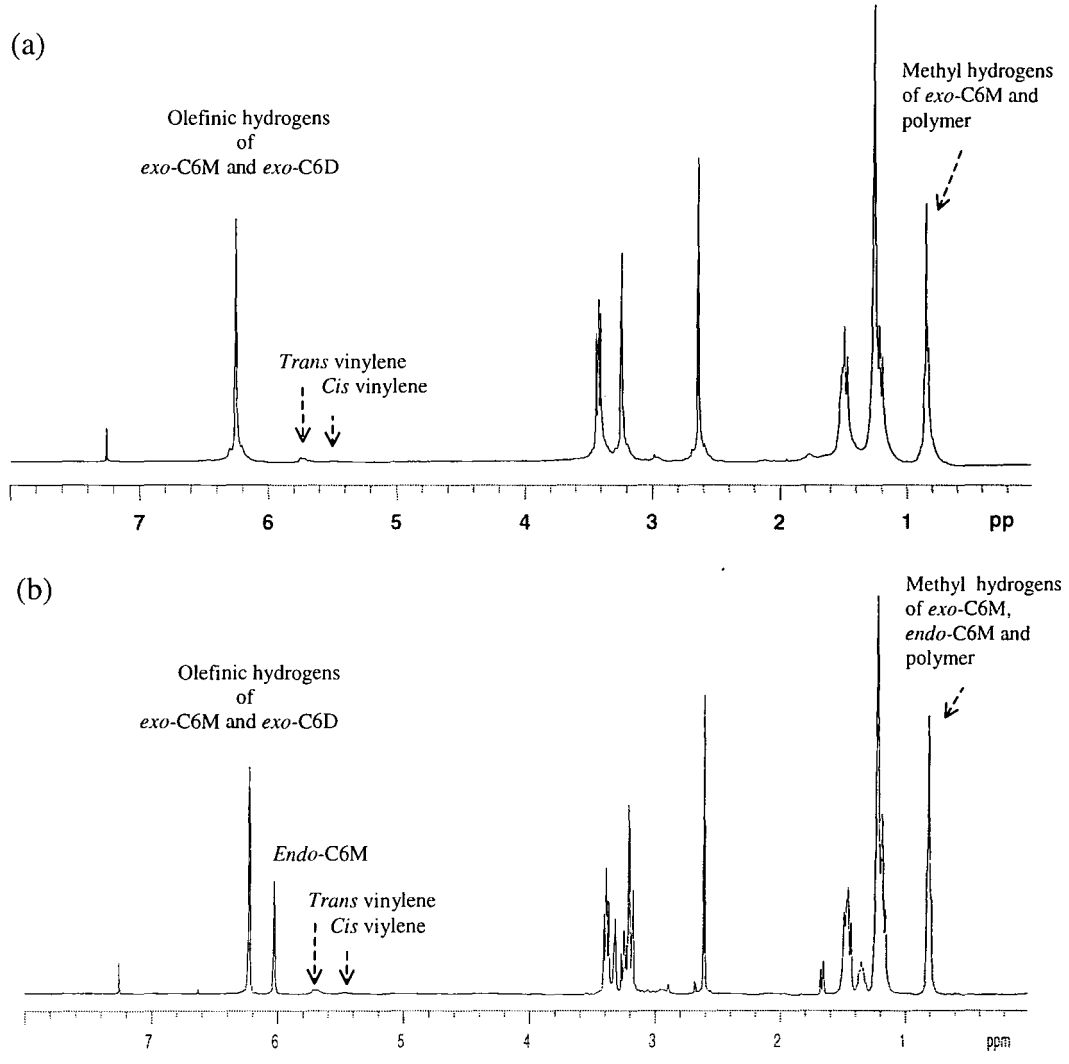

Figure 3.9 ^{1}H nmr spectra of (a) the sol fraction from experiment 7 and (b) the sol fraction from experiment 8.

experiment	% sol fraction in crude product	^{1}H nmr					
		% extractable polymer obtained*		% unreacted *exo*-C6M		% unreacted *endo*-C6M	
		in sol	in crude	in sol	in crude	in sol	in crude
7	14	7	1	93	13	-	-
8	49	8	4	62	30	30	15

Table 3.5 ^{1}H nmr analysis of the sol fractions obtained from sol/gel extraction of crosslinked polymeric materials. * linear and branch polymers.

Analysis of the sol fractions by ^{1}H nmr spectroscopy clearly indicated that there was only a small amount of the linear and branch polymers in the sol fractions. It is apparent that most of the product obtained in the crude polymeric materials was crosslinked polymer, indicating effectiveness of *exo*-C6D as a crosslinker. However, it was found that the amount of the unreacted difunctional monomer in the extracts was too low to be determined by ^{1}H nmr spectroscopy, indicating relatively high reactivity of the difunctional monomer. The limited solubility of *exo*-C6D in *exo*-C6M prevented a detailed examination of mono:difunctional monomer ratios on the course of this polymerisation. This problem has been solved by using crosslinking agents, *exo*-CnD, with the different sequence lengths of methylene units between the reactive imidonorbornene functional groups which will be discussed in Chapter 5.

It is apparent that the *endo*-isomer is much less reactive than the corresponding *exo*-isomer in both linear and crosslinked polymerisations and largely fails to undergo ring-opening polymerisation in bulk under the condition studied. In conjunction with the observation that pure *endo*-isomer is unpolymerisable, one may conclude that consecutive *endo*-units along the polymer chain are excluded. The data to hand are insufficient to conclude whether the barrier to *endo-endo* linking is in the carbene-to-metallacycle transition state, or is due to steric restrictions in the polymer chain itself. An *endo* repeating unit in the chain has four carbons of the five-membered ring *cis*-substituted, which may be sterically less favourable than an *exo*-derived unit where the two pairs of substituents are in a *trans* relationship. However, some of *endo*-monomer

was found to be consumed in these polymerisations. It may be that the *endo*-monomer terminates chain growth or that once an *endo* residue is incorporated at the chain end the new *endo*-derived chain end is less reactive than an *exo*-derived chain end and, indeed, can only initiate polymerisation of a more reactive *exo*-monomer. These possibilities have been investigated using ^{1}H nmr technique and are discussed in Chapter 4.2.

3.4 References for Chapter 3

[1] 'Olefin Metathesis and Metathesis Polymerisation', K. J. Ivin and J. C. Mol, Acadamic Press, 1997.

[2] L. Matejka, C. Houtman, and C. W. Macosko, *J Appl. Polym. Sci.*, **30**, 2787, 1985.

[3] D. S. Breslow, *Chemtech*, 540, 1990.

[4] J. A. Johnson, and M. F. Farona, *Polym. Bull.*, **25**, 625, 1991.

[5] V. Heroguez, A. Soum, and M. Fontanille, *Polymer*, **33**, 3302, 1992.

[6] H. Balcar, A. Dosedlova, and L. Petrusova, *J. Mol. Catal*, **77**, 289, 1992.

[7] A. Bell, *J. Mol. Catal.*, **76**, 165, 1992.

[8] H. NG, I. Manas-Zloczower, and M. Shmorhun, *Polym. Eng. Sci.* **34** (11), 921, 1994.

[9] A. Bell, *Polym. Preprints*, **35**, 694, 1994.

[10] T. Oshika, and H. Tabuchi, *Bull. Chem. Soc. Jpn.* **41**, 211, 1968.

[11] G. Dall'Asta, G. Motroni, R. Manetti, C. Tosi, *Makromol. Chem.* **130**, 153, 1969.

[12] J. Asrar, *Macromoleclues*, **25**, 5150, 1992.

[13] G. M. Tom (Hercules, Inc.), *US Patent*, 4,507,453, 1985.

[14] D. W. Kloslewise (Hercules, Inc.), *US Patent*, 4,400,340, 1983.

[15] E. J. Dewitt (B. F. Goodrich), *US Patent*, 4,418,178, 1986.

[16] T. P. Linwood (B. F. Goodrich), *European Patent Application,* 8,811,299.2, 1989.

[17] C. Kirkland, *Plastic World*, **50**, 1990.

[18] P. Schwab, M. B. France, J. W. Ziller, R. H. Grubbs, *Angew. Chem.*, Int. Ed. Engl., **34**, 2039, 1995.

[19] P. Schwab, R. H. Grubbs, J. W. Ziller, *J. Am. Chem. Soc.*, 118, 100, 1996.

[20] E. L. Diaas and R. H. Grubbs, *Organometallics*, 17, 2758, 1998.

[21] 'Concise Encyclopaedia of Polymer Science and Engineering', J. I. Kroschwitz, John Wiley & Sons, New York, 1990.

[22] 'Principles of Polymerisation', 2nd ed., G. Odian, John Wiley & Sons, New York, 1981.

[23] 'Polymers: Chemistry & Physics of Modern Materials', 2nd ed., J. M. G. Cowie, Chapman and Hall, New York, 1991.

[24] D. C. Sherrington, *Chem. Commun.*, 2275, 1998.

[25] 'The Physics of Rubber Elasticity', J. R. G. Treloar, Oxford University Press, 1958, P. 80 et seq.

Chapter 4

Solution polymerisation of imidonorbornene derivatives

4.1 Introduction

The aim of the work described in this chapter was the synthesis of both linear and highly crosslinked polymers via ROMP using a well-defined ruthenium carbene initiator, $Cl_2[(C_6H_{11})_3P]_2Ru{=}CHC_6H_5$. The polymerisation reactions were carried out in, or in the presence of, a solvent which overcomes many of the disadvantages of the bulk polymerisations described in the previous Chapter. The solvent allows easier stirring, at least in the early stages of reaction, since the viscosity of the reaction mixture is decreased, and consequently good thermal control is achieved. Whereas, the highly exothermic nature and tendency towards gelling combined to make the bulk polymerisation reaction difficult to control.[1] Also for ROMP of this system in solution, initiation and propagation can be probed directly by ^1H nmr spectroscopy. Consequently, the relative reactivity of the monomers with the ruthenium carbene initiator can be investigated. Polymers of controlled molecular weight can be obtained without unreacted monomer and initiator. A wide range of polymers can be prepared from solution polymerisation as compared to bulk polymerisation. The polymers derived from solid monomers, those are *exo*-C3M and all difunctional monomers, could be prepared more easily in solution than in bulk polymerisation. The monomers *endo*-C6M and *exo*-C8M show very low reactivity and were not suitable for ROMP in bulk but underwent solution polymerisation.

The description of work in this chapter is divided into four parts. The study of the reactivity of *exo*- and *endo*-monomers is the first topic discussed. The investigation of the homo and copolymerisation of *exo*- and *endo*-N-hexylnorbornene-5,6-dicarboxyimide (*exo*- and *endo*-C6M) initiated by a well-defined ruthenium carbene in a deuterated solvent using the nmr technique is discussed in section 4.2. Subsequently the synthesis of homo and copolymers of *exo*- and *endo*-isomers on a preparative scale was undertaken in order to understand more about the factors determining polymer structure and assembly mechanism in these polymerisation systems, this work is discussed in section 4.3.

A study of the effect of the length of the pendant N-alkyl group on the physical and thermal properties was undertaken. *Exo*-monomers with different length N-alkyl groups, *exo*-C3M, C4M, C5M, C6M and C8M, were polymerised on the preparative

scale; these syntheses are described in section 4.4 along with the characterisation of the products.

Finally, ROMP in solution of *exo*-difunctional monomers to produce the highly crossliked polymers with different numbers of methylene unit separating the reactive imidonorbornene units, *exo*-C3D, C5D, C6D, C9D, C12D, was investigated. The aim was to study the reactivity of these difunctional monomers. The effect of the methylene spacer sequences between the reactive imidonorbornene units on the thermal property of the polymers obtained is described in section 4.5.

4.2 Nmr scale polymerisations of *exo*- and *endo*-monofunctional monomers: (*exo*- and *endo*-C6M)

Introduction

The nmr scale homo- and copolymerisations of the highly reactive *exo*-monomer and the less reactive *endo*-monomer were investigated using the well-defined ruthenium carbene initiator in a deuterated solvent. For ROMP in solution, initiation and propagation can be probed directly by ^{1}H nmr spectroscopy, as the carbene signals for the initiating and propagating species are clearly distinguished. The polymerisations were performed in a small sample vial with a micro magnetic stirrer. Reactions were carried out in the Glove Box at room temperature. In order to record ^{1}H nmr spectra the reaction mixture was transferred into a screw capped nmr tube and taken out of the Glove Box. The extent of initiation can be judged by the appearance of the signal for the new propagating species which is shown as a multiplet peak in the nmr spectrum at 19.48 ppm for the *exo*-propagating species and at 18.65 ppm for the *endo*-propagating species. The alkylidene hydrogen of the ruthenium carbene initiating species gives a singlet in the nmr spectrum at 20.68 ppm in d_6-benzene or at 20.03 ppm in d_2-dichloromethane[2], as shown in Figure 4.1a. The initiator signal decreases in intensity simultaneously with the appearance of the propagating carbene signals. The reaction mixture was monitored by ^{1}H nmr repeatedly until the reaction stopped as indicated by the complete disappearance of signal due to olefinic hydrogens of the monomers, 6.19 ppm (*exo*) and 6.03 ppm (*endo*), as shown in Figure 4.1b and c, respectively. This indicated that the monomer had been consumed completely before the addition of the next aliquot of monomer.

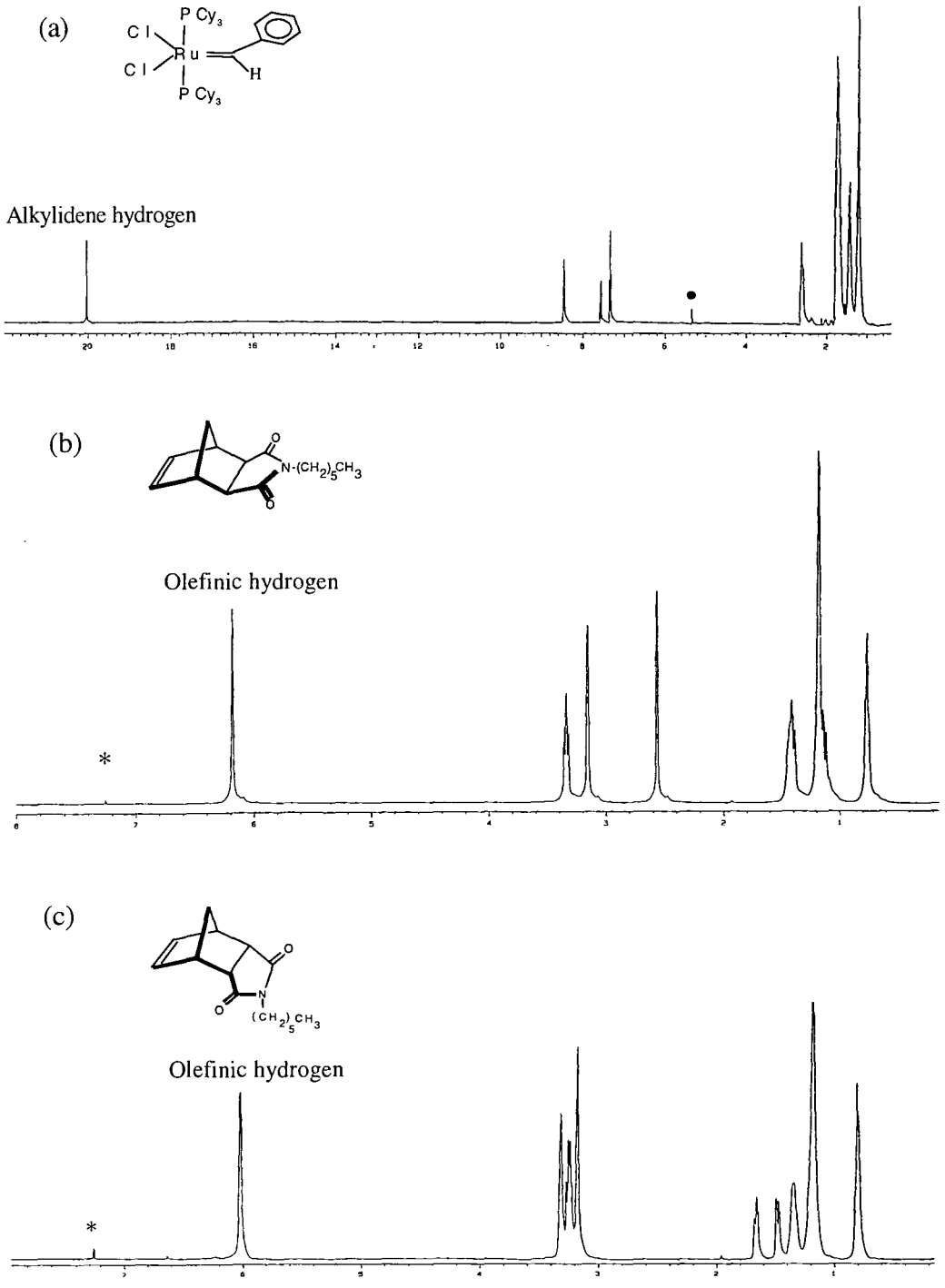

Figure 4.1 ^{1}H nmr spectra of (a) the ruthenium carbene initiator, (b) *exo*-C6M, (c) *endo*-C6M.

• residual hydrogens in d_2-dichloromethane

* residual hydrogens in $CDCl_3$

4.2.1 Results and discussion

4.2.1.1 Polymerisation of *exo*-monomer

The polymerisation of *exo*-monomer was investigated using the ruthenium carbene initiator in the Glove Box at room temperature. The initiator (~10 mg) and *exo*-monomer (30 mg, 10 equivalents) were dissolved in d_2-dichloromethane in separate sample vials. The initiator solution was transferred into the monomer solution and stirred for 10 minutes. The reaction mixture was transferred into a screw capped nmr tube, removed from the Glove Box and cooled in ice for transport to the spectroscopy laboratory (5 minutes) where it was analysed by ^{1}H nmr spectroscopy immediately. The reaction mixture was monitored by ^{1}H nmr until the polymer growth stopped as indicated by the disappearance of the singlet signal of the olefinic hydrogen of *exo*-monomer, at 6.19 ppm. The polymerisation reaction solution was returned to the Glove Box and allowed to stand for a few hours before a second aliquot of the *exo*-monomer (10 equivalents) was added to the reaction mixture. The reactions which are expected to occur are shown below.

Initiation

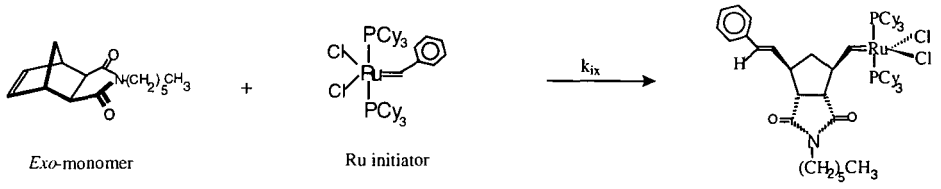

Propagation

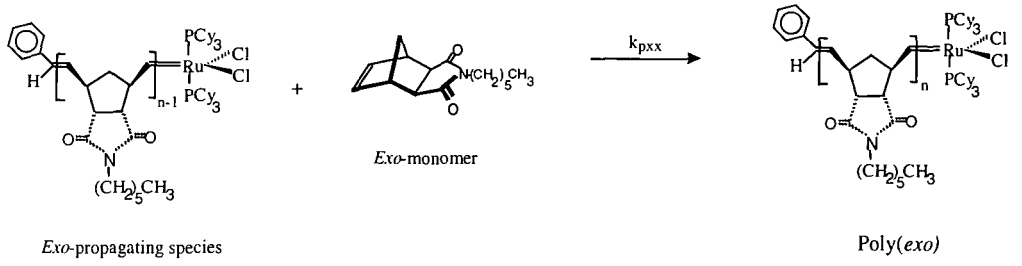

Figure 4.2 Reactions in the polymerisation of *exo*-monomer by the well-defined ruthenium carbene initiator.

The homopolymerisation of the *exo*-monomer was very fast, being complete in 10 minutes at room temperature in both steps. The appearance of the multiplet peak at 19.48 ppm due to the propagating alkylidene hydrogen of the *exo*-derived chain end is clearly distinguished from the singlet peak of the alkylidene hydrogen of the ruthenium carbene initiator at 20.03 ppm, as shown in Figure 4.3a and b. In both cases all the monomer was consumed rapidly as evidenced by the disappearance of the olefin signal at 6.19 ppm. The polymerisation of the *exo*-monomer was shown to be consistent with living polymerisation since the *exo*-propagating species was found to be stable over the lifetime of the polymerisation and addition of a second aliquot monomer resulted in continuation of the polymerisation.

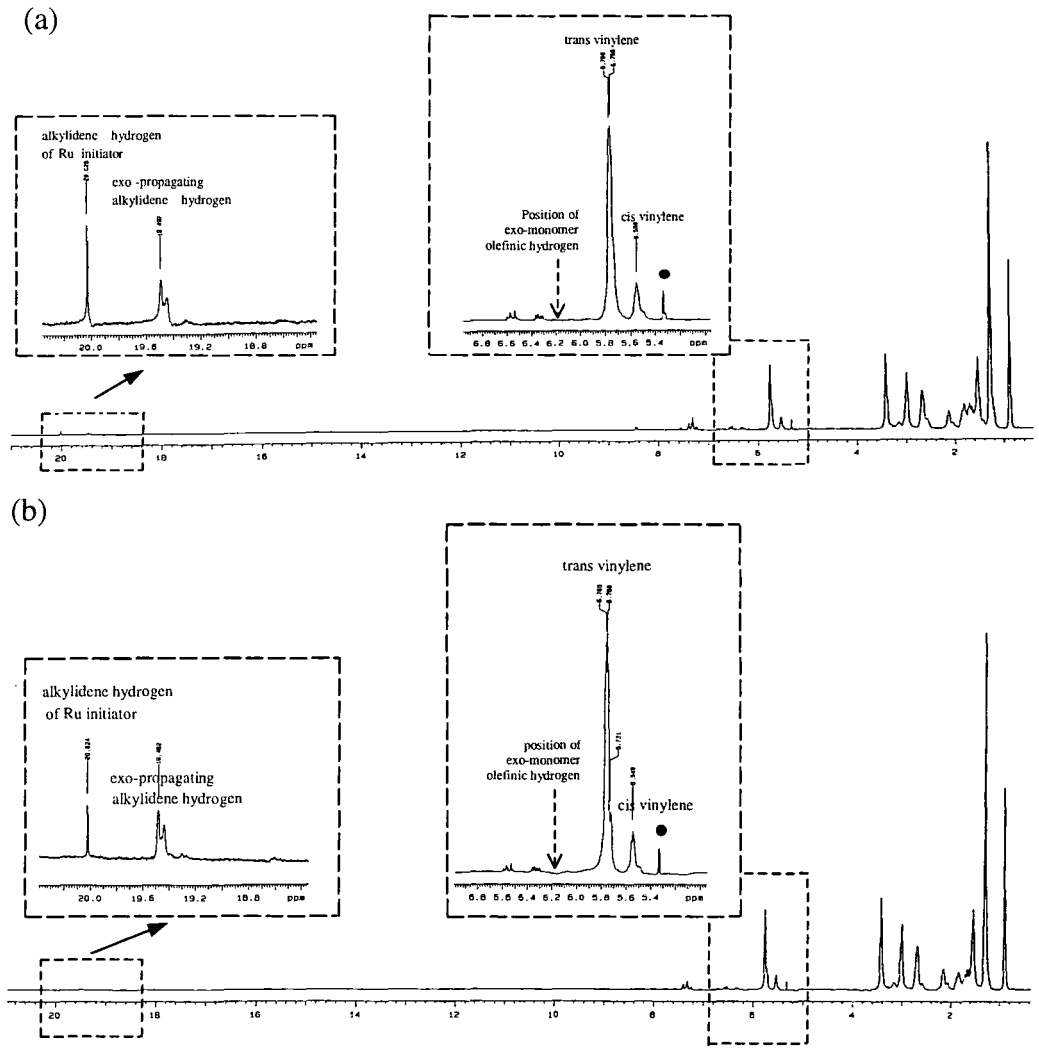

Figure 4.3 ^{1}H nmr spectra from a sequential polymerisation of *exo*-monomer.

(a) 10 min after the first 10 eq of *exo*-monomer was added

(b) 10 min after the second 10 eq of *exo*-monomer was added.

• residual hydrogens in CD_2Cl_2

The observation of a singlet signal at 20.03 ppm due to unconsumed initiator is a common feature of all these reactions. Even in the case of high monomer concentration where two successive 30 equivalent aliquots of the *exo*-monomer were added, ^{1}H nmr analysis revealed that there was still residual unconsumed initiator in the reaction mixture, as shown in Figure 4.4a and b.

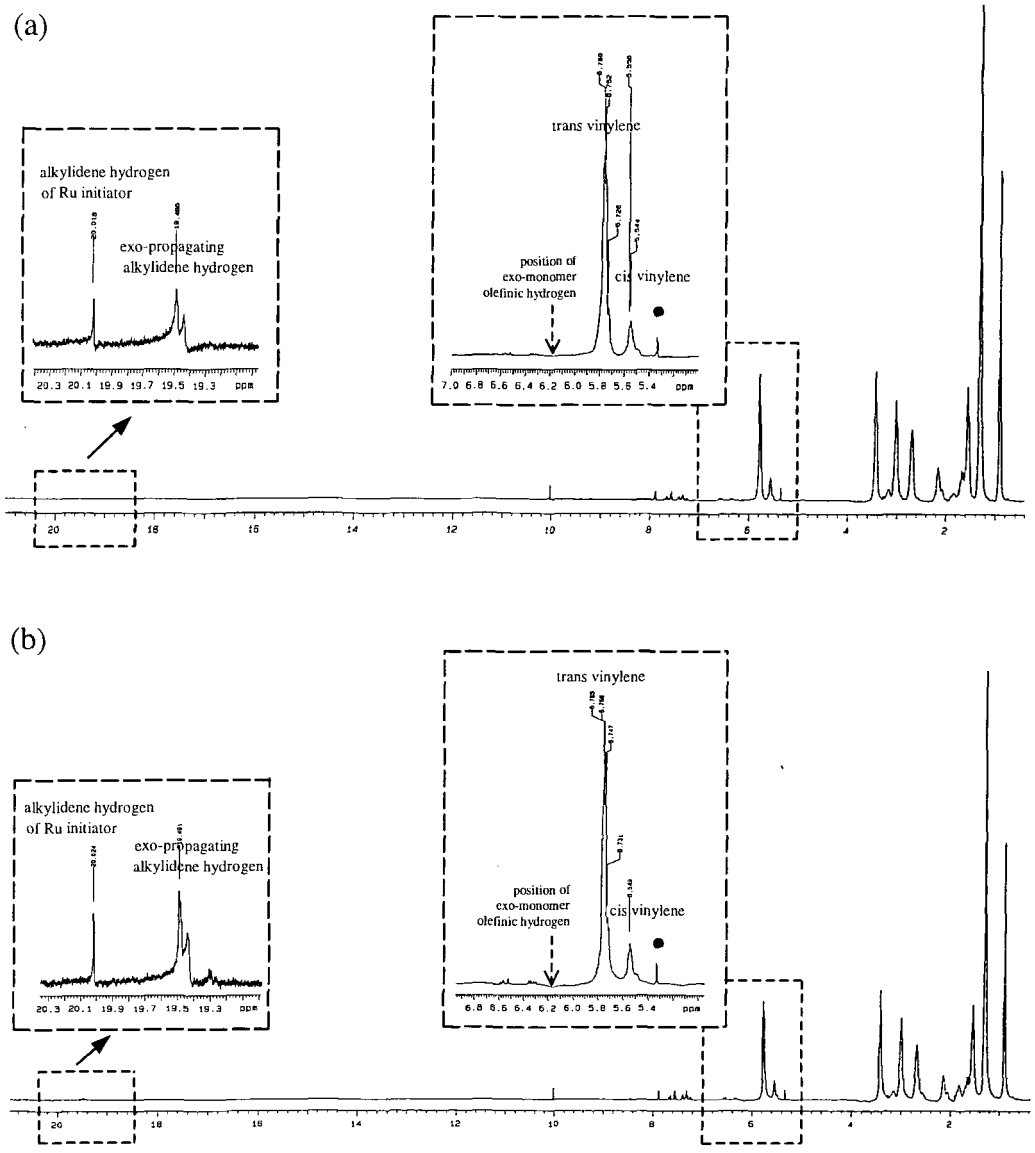

Figure 4.4 ^{1}H nmr spectra from a sequential polymerisation of *exo*-monomer at higher concentration.

(a) 10 min after the first 30 eq of *exo*-monomer was added.

(b) 10 min after the second 30 eq of *exo*-monomer was added.

- residual hydrogens in CD_2Cl_2

This indicates that $k_{pxx} >> k_{ix}$, where k_{pxx} is the rate constant for the propagation of the *exo*-monomer by the *exo*-propagating species and k_{ix} is the rate constant for the initiation of *exo*-monomer by the ruthenium carbene initiator. It is clear that the *exo*-propagating species derived from the initiator is more reactive than the original initiating carbene species for reaction with the *exo*-monomer, i.e. $k_{ix}/k_{pxx}<1$.

4.2.1.2 Polymerisation of *endo*-monomer

Polymerisation of the *endo*-monomer was investigated using the ruthenium carbene initiator according to the above procedure. The reaction mixture was monitored by ^1H nmr until the polymer growth stopped as indicated by the disappearance of the singlet signal of the olefinic hydrogen of *endo*-monomer, at 6.03 ppm. The polymerisation reaction solution was allowed to stand for a few days before a second amount of *endo*-monomer (30 mg, 10 equivalents) was added to the reaction. The reactions which are expected to occur are shown below.

Initiation

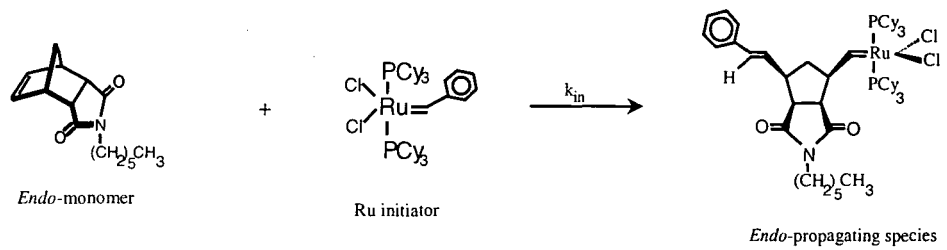

Propagation

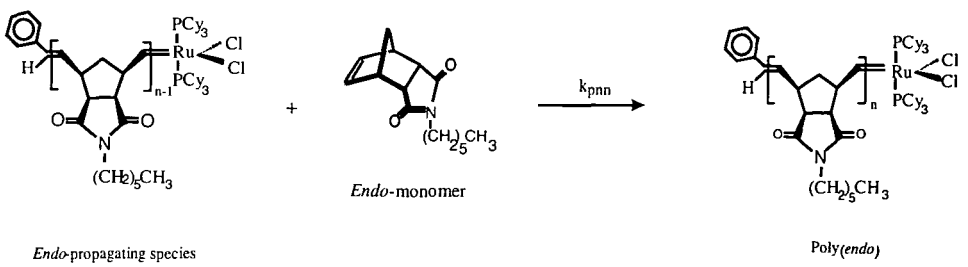

Figure 4.5 Reactions in the polymerisation of *endo*-monomer by the well-defined ruthenium carbene initiator.

The homopolymerisation of the *endo*-monomer by the ruthenium carbene initiator is appreciably slower than the homopolymerisation of the *exo*-monomer under the same conditions. The appearance of a multiplet peak at 18.65 ppm due to the propagating alkylidene hydrogen of the *endo*-derived chain end is clearly distinguished from the singlet peak of the initiating alkylidene hydrogen of the initiator at 20.03 ppm. In this case, full initiation was observed since the singlet signal of the alkylidene hydrogen of the initiator had disappeared completely, after several days under the same conditions used for the *exo*-reaction, as shown in Figure 4.6a and b.

(a)

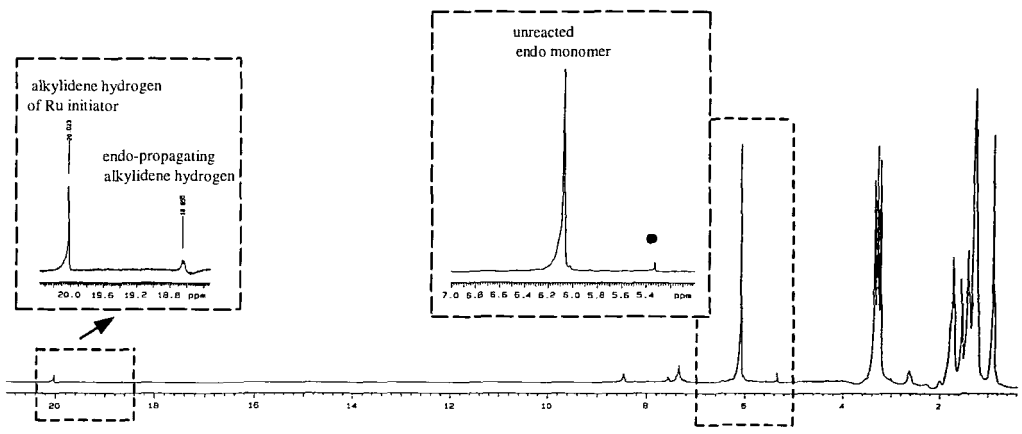

(b)

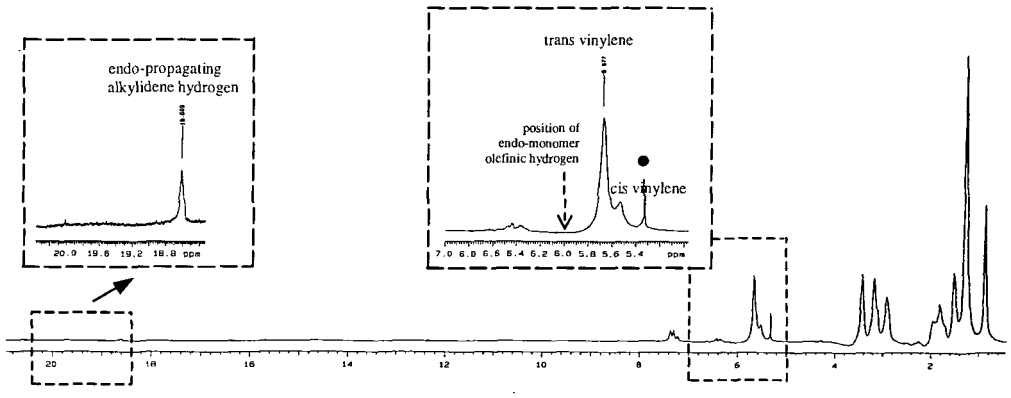

Figure 4.6 ^{1}H nmr spectra from a sequential polymerisation of *endo*-monomer.

(a) 1h after the first 10 eq of *endo*-monomer was added.

(b) 10 days after the first 10 eq of *endo*-monomer was added.

• residual hydrogens in CD_2Cl_2

This indicates that k_{in} and k_{pnn}, where k_{in} is the rate constant for the initiation of the *endo*-monomer and k_{pnn} is the rate constant for the propagation of the *endo*-monomer, are much smaller than k_{ix} and k_{pxx} for the *exo*-reaction, and that k_{in}/k_{pnn} is large, i.e. $k_{in}/k_{pnn} \geq 1$. However, the polymerisation was shown to proceed in a living fashion since the *endo*-propagating species was found to be stable over the lifetime of the polymerisation, i.e. several days, and the second addition of *endo*-monomer resulted in continuation of the polymerisation, as shown in Figure 4.7a and b.

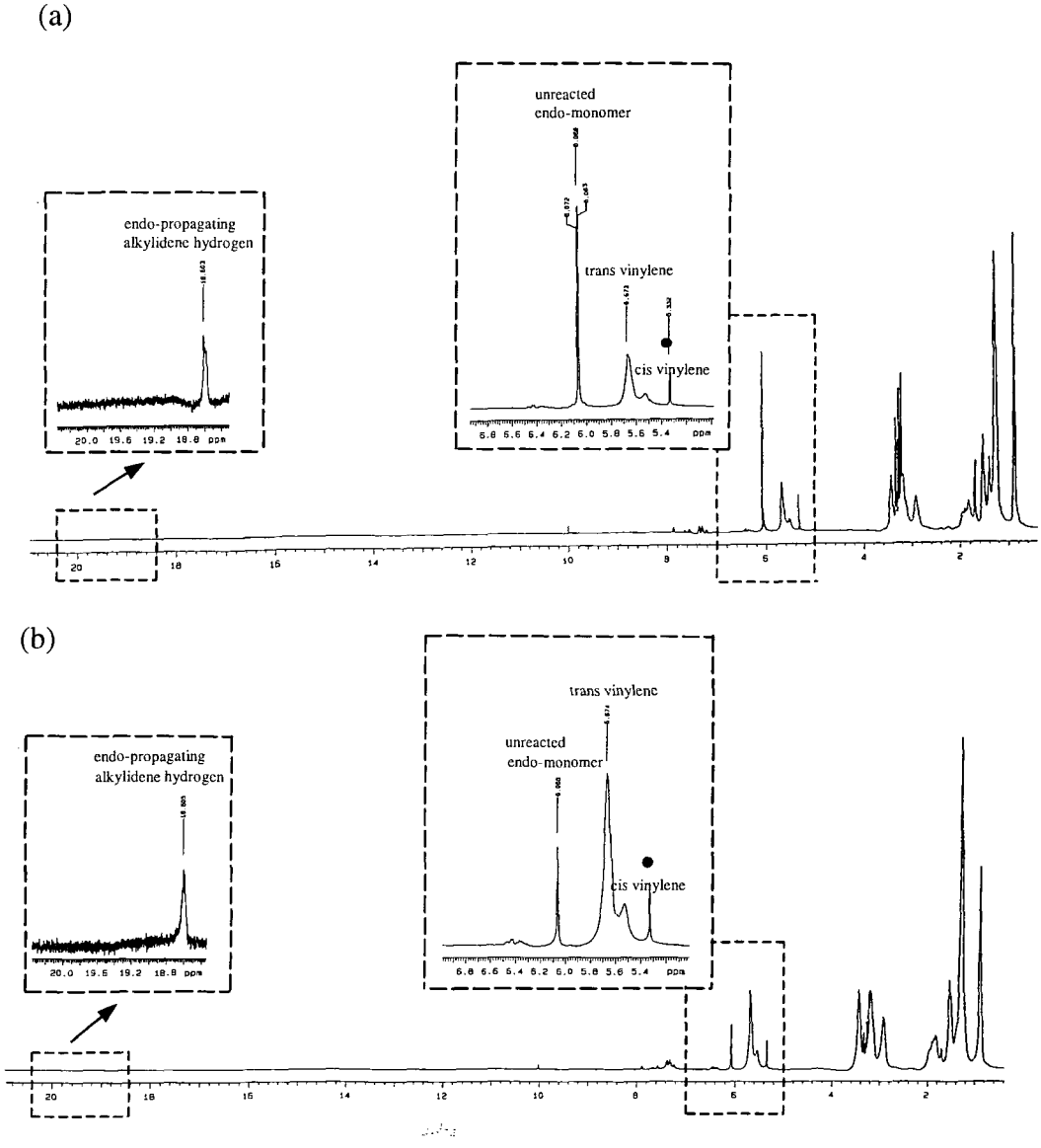

Figure 4.7 ^{1}H nmr spectra from a sequential polymerisation of a second aliquot of *endo*-monomer, (a) 1 day after the second 10 eq of *endo*-monomer was added, (b) 4 days after the second 10 eq of *endo*-monomer was added.

- residual hydrogens in CD_2Cl_2

4.2.1.3 Synthesis of a triblock (*exo-endo-exo*) copolymer

Having established the living polymerisation of *exo*- and *endo*-monomers, a multi-step block copolymerisation of the *exo*-monomer and the *endo*-monomer was carried out using the ruthenium carbene initiator according to the above procedure. The first two steps of the polymerisation were carried out using the same stepwise manner as before (see Figures 4.3 and 4.4). The polymerisation solution was allowed to stand for a few hours before *endo*-monomer (21 mg, 7 equivalents) was added to the reaction mixture. The mixture was monitored by ^{1}H nmr until all the *endo*-monomer was consumed. The ^{1}H nmr spectra obtained during this process are shown in Figure 4.8a, b and c. The reaction mixture was allowed to stand for a few hours before two successive aliquots of the *exo*-monomer (15 mg, 5 equivalent and 90 mg, 30 equivalent, respectively) were added. The mixture was monitored by ^{1}H nmr until all the *exo*-monomer was consumed. The ^{1}H nmr spectra measured during this process are shown in Figure 4.10a and b. The multi-step block copolymerisation of the *exo*- and *endo*-monomers was shown to proceed in a living fashion since the *exo*-propagating species was found to be stable over the lifetime of the polymerisation and the addition of the *endo*-monomer results in continuation of the polymerisation and vice versa.

(a)

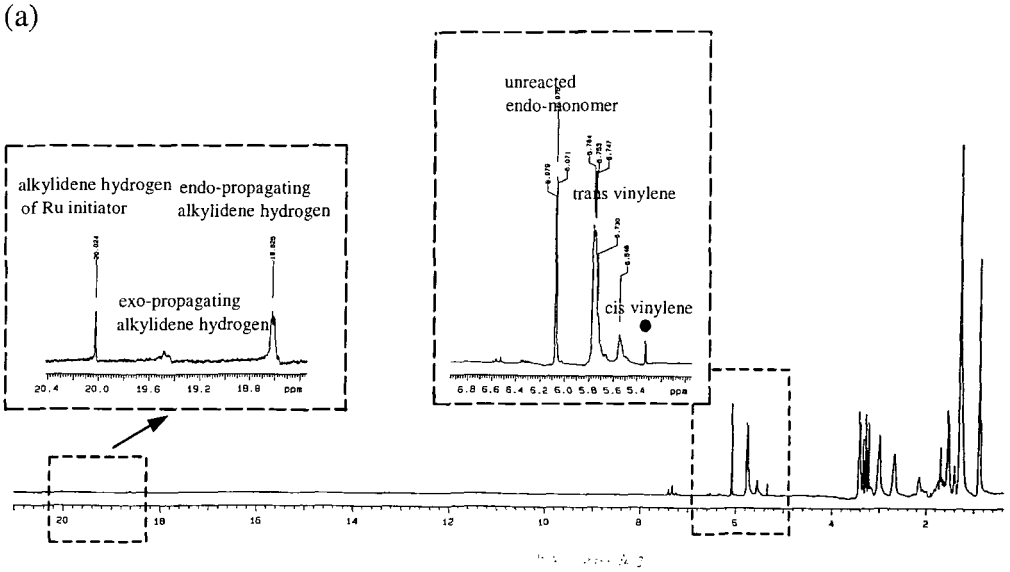

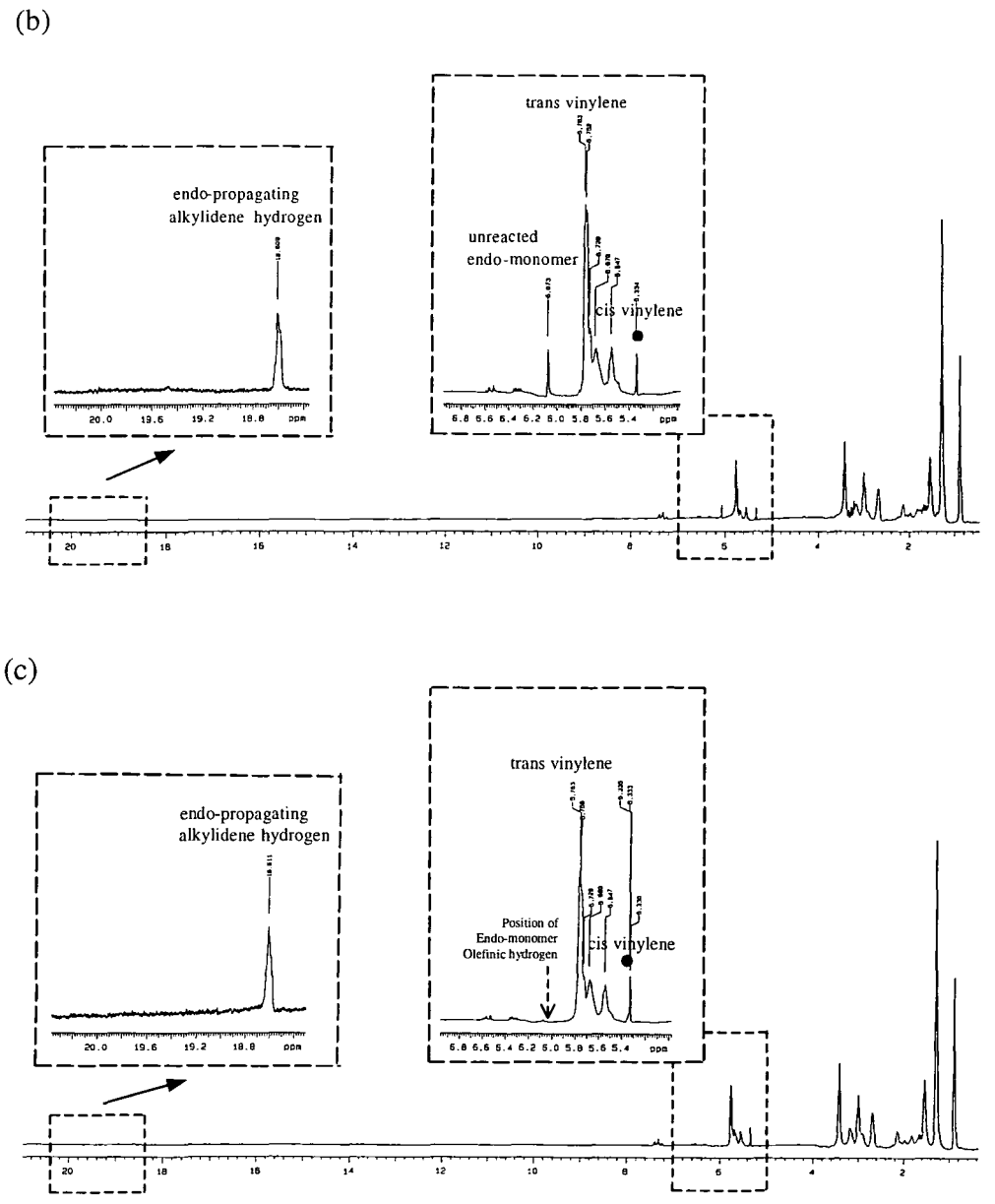

Figure 4.8 ^{1}H nmr spectra from the addition of *endo*-monomer to a mixture of living *exo*-derived chain end with residual ruthenium initiator present.

(a) 2h after added 7 eq of *endo*-monomer.

(b) 3 days after added 7 eq of *endo*-monomer.

(c) 10 days after added 7 eq of *endo*-monomer.

- residual hydrogens in CD_2Cl_2

When 7 equivalents of *endo*-monomer was added to the reaction mixture, see Figure 4.4b, the monomer was consumed slowly over several days, as shown in Figure 4.8a, b, and c. The appearance of the new *endo*-propagating species signal at 18.65 ppm is

clearly seen and accompanies the reduction of the *exo*-propagating species signal at 19.48 ppm, whereas no reduction of the original initiating ruthenium carbene signal at 20.03 ppm was observed (see Figure 4.4b and 4.8a). This means the *endo*-monomer propagates slowly and initially only on the *exo*-propagating chain end, indicating that the *exo*-propagating species is more reactive than the initiating ruthenium carbene species with the *endo*-monomer, or $k_{pxn} >> k_{in}$, where k_{pxn} is the rate constant for the propagation of the *endo*-monomer by the *exo*-propagating species and k_{in} is the rate constant for the initiation of the *endo*-monomer. Also it is apparent that the *endo*-monomer propagated slowly and reacted slowly with the original initiating carbene species after all the *exo*-propagating species was consumed, as shown in Figure 4.8b. It can be concluded that the original initiating carbene species is more reactive than the *endo*-propagating species or $k_{in} > k_{pnn}$, where k_{pnn} is the rate constant for the propagation of the *endo*-monomer by the *endo*-propagating species. The reactions which are expected to occur in this sequence can be summarised as shown below.

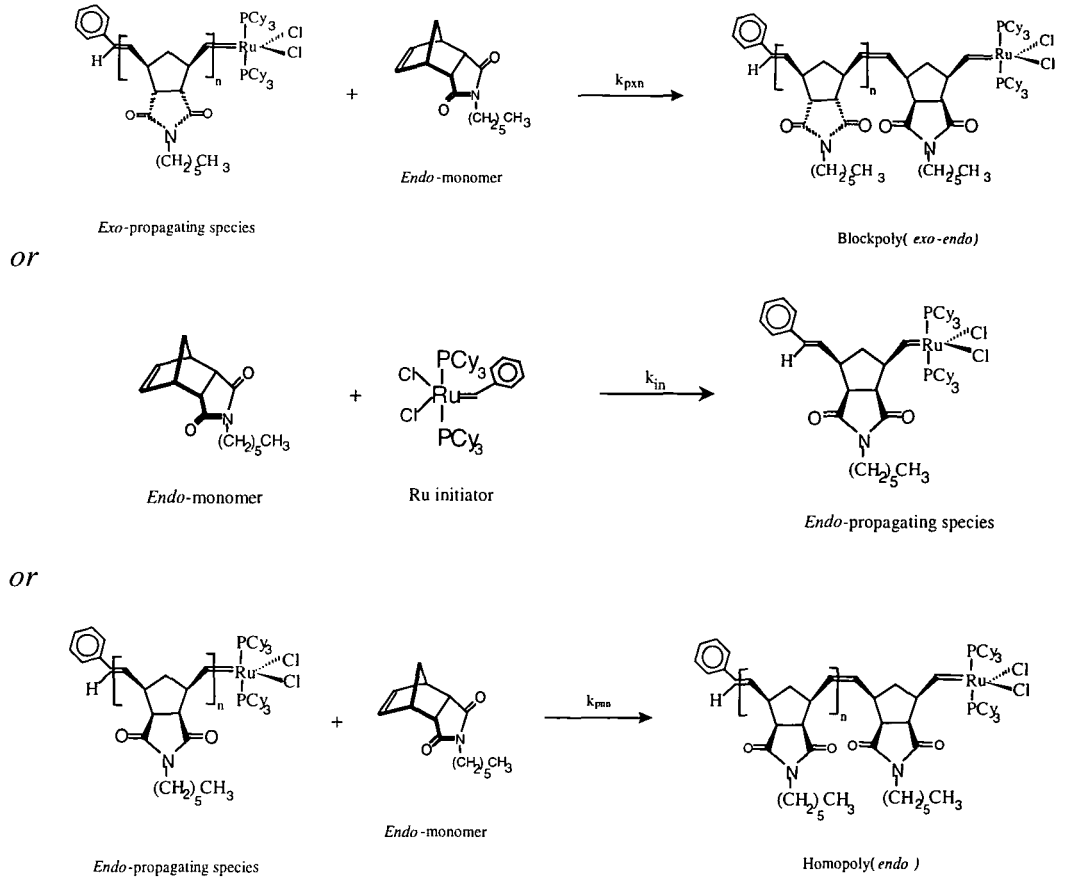

Figure 4.9 Reactions occurring on addition of *endo*-monomer to a mixture of living *exo*-derived chain end with residual ruthenium initiator present.

When 5 equivalents of the *exo*-monomer were added to the reaction mixture whose spectrum was given in figure 4.8c, the appearance of the *exo*-propagating signal at 19.48 ppm simultaneously with the reduction of the *endo*-propagating signal at 18.65 ppm would be expected if the propagation of *exo*-monomer on the *endo*-propagating chain end occurred readily. However, the ^{1}H nmr taken 10 minutes after the addition of *exo*-monomer shows no signals which can be attributed to either the *exo*-monomer or the *exo*-propagating species as shown in Figure 4.10a. This can be explained only if the *exo*-derived chain end, formed when the *exo*-monomer reacts with the *endo*-propagating chain ends, are very highly reactive *exo*-propagating species and the remaining *exo*-monomer is incorporated at these chain ends which are present in very low, indeed undetectable, concentration. Meanwhile the majority of the propagating species, which are *endo*-units, remain essentially dormant. This indicates that the *exo*-propagating species is more highly reactive than the *endo*-propagating species for *exo*-monomer or $k_{pxx} >> k_{pnx}$, where k_{pxx} is the rate constant for the propagation of *exo*-monomer by *exo*-propagating species and k_{pnx} is the rate constant for the propagation of *exo*-monomer by *endo*-propagating species. Another 30 equivalents of the *exo*-monomer was added to the reaction to ensure that the *exo*-monomer propagated, indeed, on the *exo*-propagating chain end rather than on the *endo*-propagating chain end. Again the result from ^{1}H nmr taken 10 minutes after the addition of monomer shows the absence of the *exo*-monomer while no signal of *exo*-propagating species was observed since they are in too low a concentration to be visible in the ^{1}H nmr, as shown in Figure 4.10b.

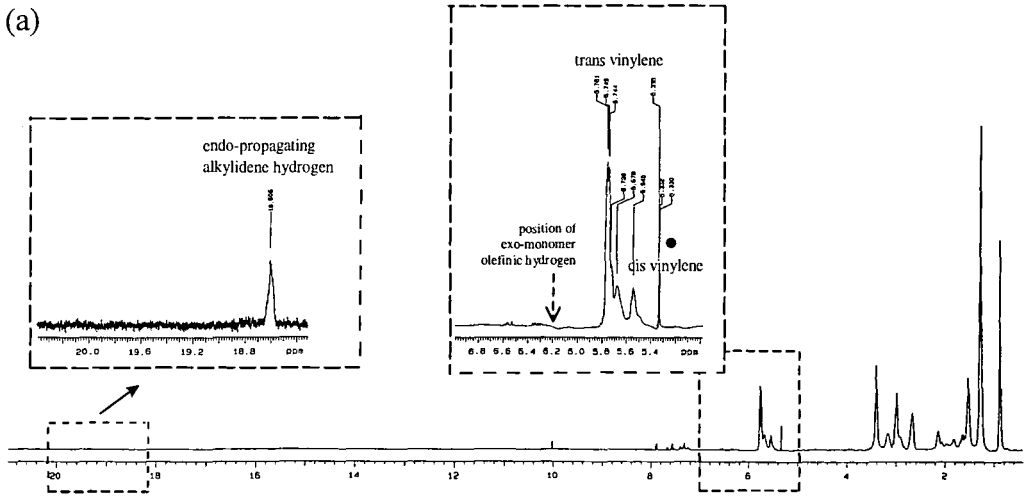

(b)

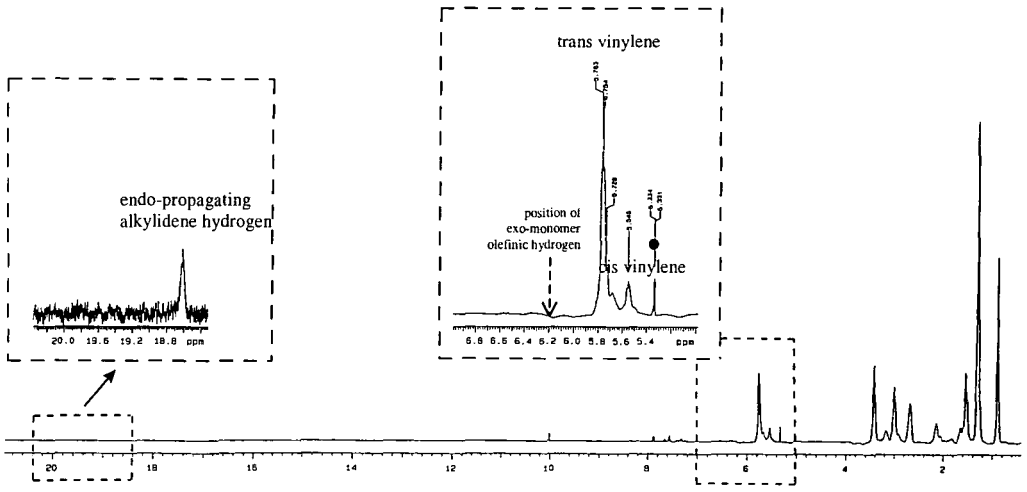

Figure 4.10 ^{1}H nmr spectra from a sequential addition of *exo*-monomer to the mixture of living *endo*-derived chain end.

(a) 10 min after 5 eq of *exo*-monomer was added.

(b) 10 min after 30 eq of *exo*-monomer was added .

- residual hydrogens in CD_2Cl_2

The conclusion of this study is therefore that the attempt to produce a triblock copolymer results mostly in a diblock copolymer with a small proportion of triblock material having one long *exo* sequence.

4.2.1.4 Polymerisation of *exo*-and *endo*-monomer mixture

The living polymerisation of *exo*- and *endo*-monomers was established in section 4.2.1.1 and 4.2.1.2, respectively. Triblock (*exo-endo-exo*) copolymer was synthesised by sequential addition of the monomers and described in section 4.2.1.3, although this process was not well controlled and was only partially successful, the product being mostly diblock material. In this section the copolymerisation of a 72*exo*/28*endo*-monomer mixture was investigated. The aim of the work was to understand the behaviour of these two isomers and calculate the composition of the copolymer being formed at any one time in the reaction. The initiator (10 mg) and the *exo/endo*-monomer mixture (30 mg, 10 equivalents) were dissolved in d_2-dichloromethane in separate vials. The initiator solution was transferred into the monomer solution and

stirred for 5 minutes. The reaction mixture was transferred into a screw capped nmr tube and analysed by ^{1}H nmr spectroscopy. The reaction mixture was monitored by ^{1}H nmr until all *exo*-and *endo*-monomer were consumed. The ^{1}H nmr spectra during this process are shown below, Figure 4.11a, b, c, d, e and f. The ^{1}H nmr parameters from this set of spectra were determined and recorded in Table 4.1.

(a)

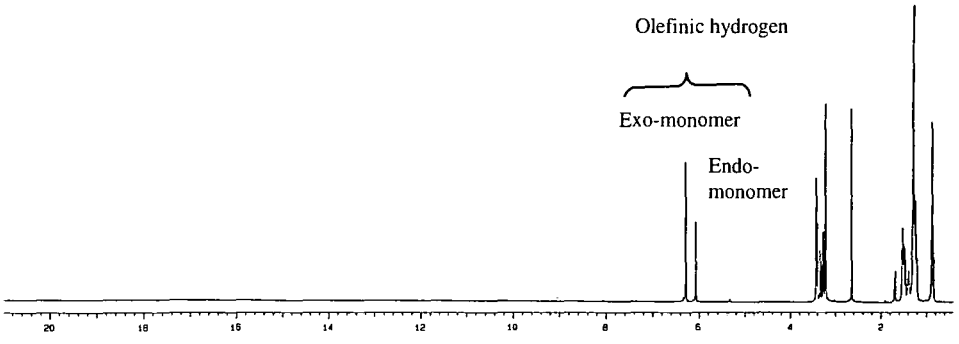

(b)

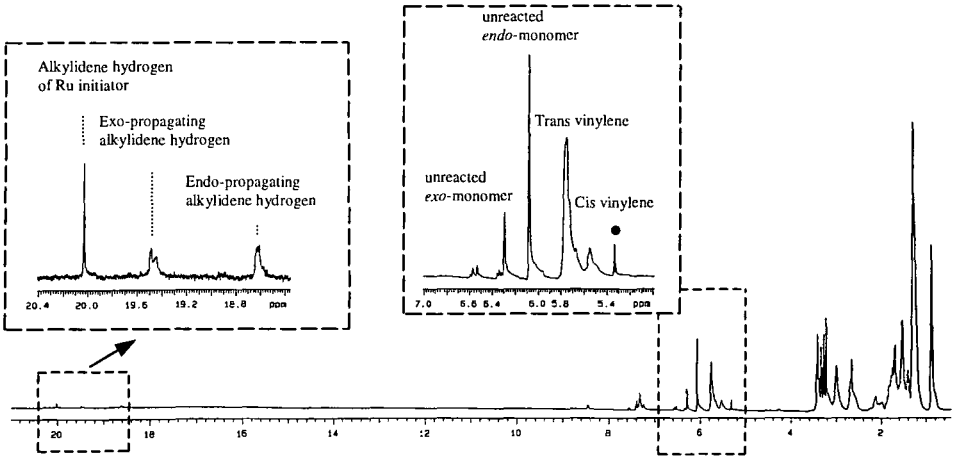

(c)

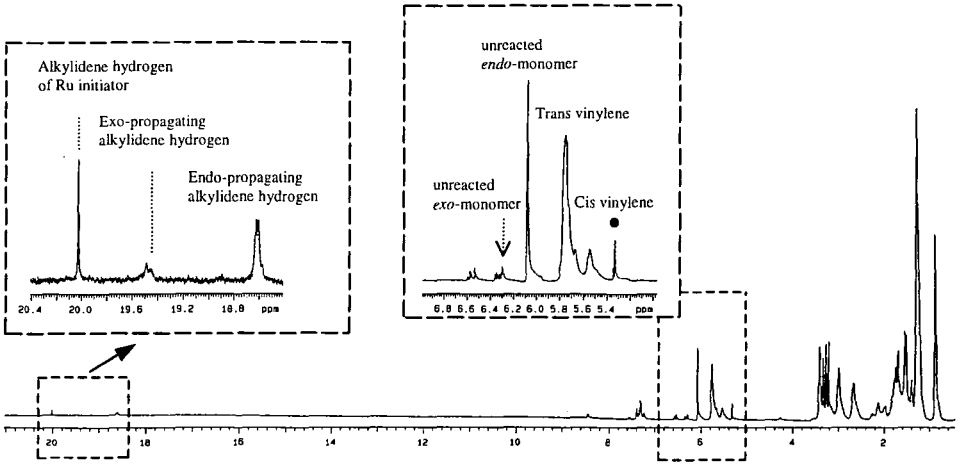

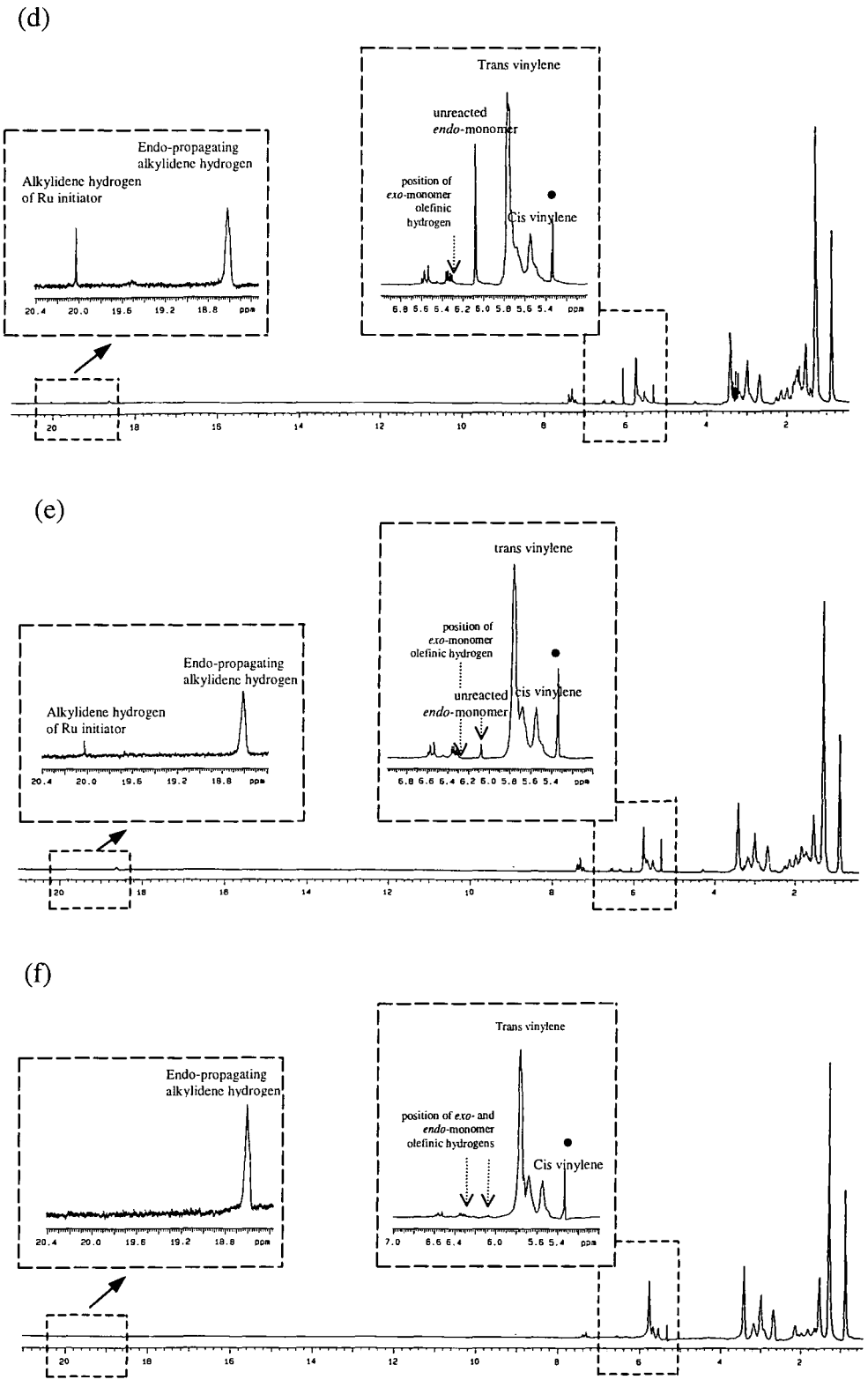

Figure 4.11 ^{1}H nmr spectra from the polymerisation of *exo*-and *endo*-monomer mixture; (a) 72*exo*/28*endo*-monomer mixture, (b) 5 minutes, (c) 1 hour , (d) 2 days , (e) 8 days, and (f) 10 days after the polymerisation reaction started.

• residual hydrogens in CD_2Cl_2

Reaction Time (hours)	% Alkylidene hydrogen (δ 18.5–20.5 ppm)			% Olefinic hydrogen (δ 5.4-6.4 ppm)						
				Exo-monomer (6.29 ppm)		*Endo*-monomer (6.03 ppm)		Polymer (5.5 – 5.8 ppm)		
	Ru (20.03 ppm.)	*Exo* (19.48 ppm)	*Endo* (18.65 ppm)	unreacted	consumed A (B)*	unreacted	consumed C (D)**	Obtained	*Trans*	*Cis*
0	100	0	0	72	0	28	0	0	0	0
1/12	30	37	33	1	71 (99%)	26	2 (7%)	73	84	16
1	30	23	47	< 0.05	72(>99.95%)	22	6 (21%)	78	83	17
48	23	14	63	0	72 (100%)	21	7 (25%)	77	83	17
192	15	0	85	0	72 (100%)	9	19 (68%)	91	80	20
240	0	0	100	0	72(100%)	3	25 (89%)	97	81	19

Table 4.1 ^{1}H nmr analysis of the nmr scale polymerisation of a 72*exo*/28*endo*-monomer mixture with the ruthenium carbene initiator.

* consumed A = 72 – unreacted *exo*-monomer consumed B = (consumed A x 100)/ 72

** consumed C = 28 – unreacted *endo*-monomer consumed D = (consumed C x 100)/ 28

It was found that 99% of *exo*-monomer was consumed, whereas only 7% of *endo*-monomer was consumed within 5 minutes, as shown in Figure 4.11b and Table 4.1. The multiplet peak at 19.48 ppm, due to the propagating alkylidene hydrogen of the *exo*-derived chain end, accounted for 37% of the total alkylidene hydrogen intensity; the multiplet at 18.65 ppm, due to the propagating alkylidene hydrogen of the *endo*-derived chain end, accounted for 33% of the alkylidene signal, and both are clearly distinguished from the singlet peak, 30% in intensity, due to the original ruthenium carbene initiator at 20.03 ppm. This indicates that 70% of the ruthenium carbene initiator was used to initiate the polymerisation of 99% of *exo*-monomer and 7% of *endo*-monomer. However, it is interesting to note that the *exo*-derived chain end propagating species only exceeds the concentration of the *endo* chain end propagating species by 4% even at this early stage of reaction. This is consistent with the results from the previous section where it was established that the order of reactivity of chain end propagating and initiating alkylidene species was: *exo* derived alkylidene more reactive than initiator, which was more reactive than *endo* chain end species and that the *exo*-monomer was more reactive than the *endo*-monomer. Thus this observation is explained if the *exo*-monomer is rapidly consumed and then the reactive *exo*-propagating chain ends are capped by *endo*-monomer.

Within one hour, less than 0.05% of the *exo*-monomer was left in the mixture and 21% of *endo*-monomer was already consumed. It is apparent that at this stage the *endo*-monomer propagated and reacted slowly with the *exo*-propagating chain end, as the increase in intensity of the *endo*-propagating signal at 18.65 ppm accompanies the reduction of *exo*-propagating species signal at 19.48, whereas no reduction of the original initiating ruthenium carbene signal at 20.03 ppm was observed, as shown in Figure 4.11c. After 2 days, 67% of *endo*-monomer was already consumed and none of the *exo*-monomer was left in the reaction mixture. At this stage, after the *exo*-propagating chain ends are completed capped the initiator is consumed slowly by *endo*-monomer as shown in Figure 4.11d and e. All *endo*-monomer was consumed completely and the full consumption of initiator was observed within 10 days, as shown in Figure 4.11f. The propagation reactions which are expected to occur in this reaction can be summarised as shown below.

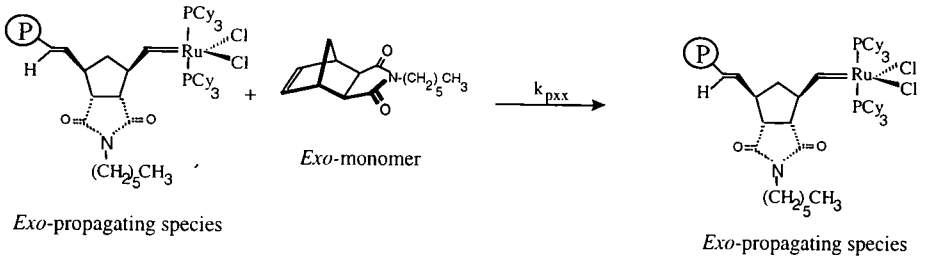

Exo-propagating species

Exo-monomer

Exo-propagating species

or

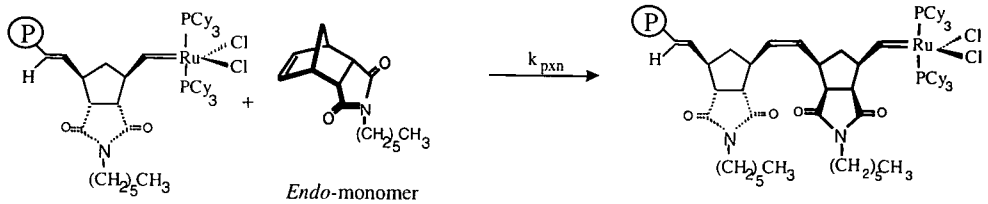

Exo-propagating species

Endo-monomer

Endo-propagating species

or

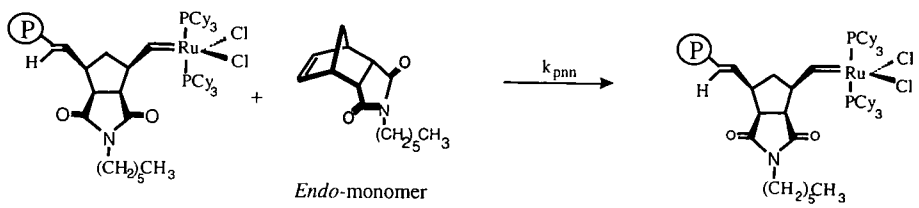

Endo-propagating species

Endo-monomer

Endo-propagating species

or

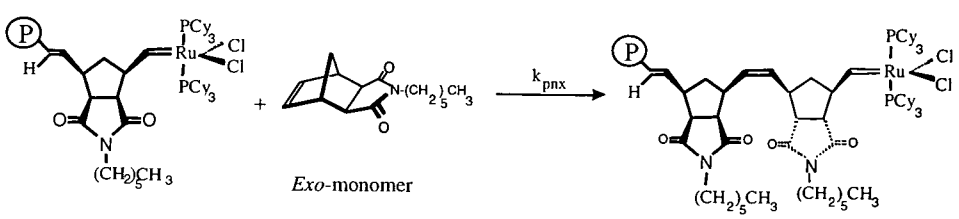

Endo-propagating species

Exo-monomer

Exo-propagating species

Figure 4.12 The propagation reactions in the polymerisation of *exo*- and *endo*-monomer mixture by the well-defined ruthenium carbene initiator; P = polymer chain.

The results from this and the previous sections show that the ratio (r) of the reactivity[3] of the *exo*-propagating species with *exo*-monomer to the reactivity of the *exo*-propagating species with *endo*-monomer >>1, or $r_x = k_{pxx}/k_{pxn}$ >>1 and the ratio of the reactivity of the *endo*-propagating species with *endo*-monomer to the reactivity of the *endo*-propagating species with *exo*-monomer <<1, or $r_n = k_{pnn}/k_{pnx}$ <<1. In this solution polymerisation all the monomers and initiating species are eventually consumed but as a consequence of the relative reactivities established in this work, it is clear that the products must be block or blocky copolymers rather than the statistical copolymers and it is highly probable that there will be some homopolymer of the *endo*-isomer present.

4.3 Preparative scale polymerisations of *exo*- and *endo*-monofunctional monomers

Introduction

In section 4.2 the homo and copolymerisation of the highly reactive *exo*-monomer and less reactive *endo*-isomer were investigated using the well-defined ruthenium initiator. The polymerisation of the *endo*-monomer is appreciably slower than the *exo*-monomer under the same conditions. However, the polymerisation of both *exo*- and *endo*-monomers were shown to proceed in a living fashion. In this section, homo and diblock copolymers of *exo*-and *endo*-monomers were obtained on a preparative scale. The aim of work described in this section was to understand more about the mechanism and the structure of the polymers obtained from these polymerisation systems. In order to get larger quantities of polymeric materials, the solution copolymerisation of *exo*- and *endo*-C6M were carried out on a 1.5 g scale. All solution polymerisations were carried in the Glove Box at room temperature. The *cis/trans* vinylene content, the molecular weight ($\overline{M}n$), PDI and the glass transition temperature (Tg) of the polymers were obtained using nmr, GPC and DSC techniques.

4.3.1 Results and discussion

The ROMP of *exo*- and *endo*-monofunctional monomers yields linear polymers with unsaturated backbones and imido pendant groups. Polymer synthesis could be

followed by the colour change of the solution from purple-pink (initiator) to yellow or orange (propagating species). The polymerisations were terminated by addition of ethyl vinyl ether which cleaved the polymers from the metal centre leaving a chain end methylene and a methoxycarbene on the metal.

4.3.1.1 Syntheses of homo and diblock copolymers

The homo and block copolymerisations of *exo*- and *endo*-monomers were carried out on a 1.5 g scale in the Glove Box at room temperature. The initiator (10 mg) and *exo*-C6M (1.5 g) were dissolved in dichloromethane (5 ml and 25 ml, respectively) in separate ampules. The initiator solution was transferred into the *exo*-monomer solution and stirred for 7 days. The solution of living polymer and residual initiator was divided to three portions using a measuring cylinder. The first portion (hereinafter called experiment 1) was terminated by adding ethyl vinyl ether and precipitated into excess methanol. *Exo*-C6M (0.7 g) and *endo*-C6M (0.7g) were added to the second and the third portions, hereinafter called experiment 2 and 3 respectively. The solutions were stirred for 7 days before being terminated by adding ethyl vinyl ether. The polymers were precipitated by pouring the solutions into an excess of methanol.

The same procedure, as described above, was used to synthesise diblock (*endo-exo*-C6M) copolymer, but the starting monomer in this case was *endo*-C6M (1.5 g). The initiator solution (10 mg) was transferred into the *endo*-monomer solution (1.5 g) and stirred for 7 days. The resulting solution was divided to three portions. The first portion (hereinafter called experiment 4) was terminated by adding ethyl vinyl ether and precipitated into excess methanol. *Exo*-C6M (0.7 g) and *endo*-C6M (0.7g) were added to the second and the third portions, hereinafter called experiment 5 and 6 respectively. The solutions were stirred for 7 days before being terminated by adding ethyl vinyl ether and precipitating into excess methanol.

All the polymers obtained in this section were further purified by reprecipitation from chloroform into methanol. The polymers were obtained as white solids and dried under vacuum at 30 °C for 2-3 days. All of the linear polymers made were soluble in toluene, tetrahydrofuran, dichloromethane and chloroform.

4.3.1.2 Characterisation of polymers obtained

This section describes the characterisation of the polymers whose synthesis was described in section 4.3.1.1. The characterisation was carried out using ^{1}H and ^{13}C nmr, GPC, DSC and TGA.

Polymer characterisation using ^{1}H and ^{13}C nmr spectroscopy

The most useful probes of polymer structure and mechanism for these polymerisations are ^{1}H and ^{13}C nmr spectroscopy. All nmr spectra of the polymers obtained in the section were recorded as solutions in $CDCl_3$. Full assignment of the spectra was carried out with the aid of COSY and HETCOR spectra. All signals in the ^{1}H nmr spectra are broad, this is a characteristic of many polymer spectra. The observed broading is due to the fact that a specific type of hydrogen atom in the basic repeat unit within the polymer chain is found in many slightly different chemical environments, this leads to a certain type of hydrogen atom resonating over a range of frequencies.

ROMP of *exo*- and *endo*-monomers gives linear polymers containing unsaturated carbon-carbon double bonds and imido pendant groups. The double bonds along the polymer chain show *cis/trans* isomerism which affects the chemical shift of hydrogens and carbons in the backbone. The ^{1}H and ^{13}C nmr spectra of poly(*exo*-C6M) obtained from experiment 1 were similar to those obtained from experiment 2. Poly(*exo*-C6M) samples from both experiments were recovered as white solids in high conversion (>90%). The ^{1}H and ^{13}C nmr spectra of diblock copolymer obtained from experiment 3 were similar to those obtained from experiment 5. Diblock copolymers from both reactions 3 and 5 were recovered as white solids in moderate conversion (~65-75%). The ^{1}H and ^{13}C nmr spectra of poly(*endo*-C6M) obtained from experiment 4 were similar to those obtained from experiment 6. Poly(*endo*-C6M) samples from both reactions were recovered as white solids in low conversion (<20%). It seems reasonable to propose that the orientation of the imide group toward double bond in the case of *endo*-monomer results in poor reactivity and low conversion. There are a number of papers which have described a similar difference in the polymerisation behaviour of *exo*- and *endo*-isomers.[4-8]

The ^{13}C nmr spectra of poly(*exo*-C6M) [experiment 1], diblock (*endo-exo*-C6M) [experiment 5] and poly(*endo*-C6M) [experiment 4] are shown in Figure 4.13a, b, and c respectively, as typical examples. The chemical shifts and assignments of ^{13}C nmr for the homo and block copolymers of *exo*- and *endo*-monomers are recorded in Table 4.2. The allylic carbons adjacent to a *cis* double bond (α-*cis* carbons) always appear about 5 ppm upfield from the analogous carbons adjacent to a *trans* unit (α-*trans* carbons)[9]: this rule provides the starting point for making assignments in the spectra of all the polymers obtained in this work. In poly(*exo*-C6M), the low frequency region showed signals at 46.05 ppm which originate from α-*trans* carbons, C1 and C4, and at 50.85 ppm which originate from β-*trans* carbons, C5 and C6, see table 4.2 for notations. Whereas the α-*cis* carbons, C1 and C4, showed a signal as a small peak at *ca.* 41.02 ppm (about 5 ppm upfield from the α-*trans* carbons) and the β-*cis* carbons, C5 and C6, showed a small peak at 52.80 ppm. These two small peaks at 41.02 ppm for the α-*cis* carbons and 52.80 ppm for the β-*cis* carbon disappear in the spectrum of poly(*endo*-C6M) which has all *trans* vinylenes.

The relative intensities of the *trans* and *cis* olefinic resonances in the range δ 129-135 ppm can be used to confirm the *cis/trans* content in these polymers. The multiplet peaks at 134.01 ppm and 132.00 ppm due respectively to *cis* and *trans* vinylene signals of poly(*exo*-C6M) are clearly distinguished from the multiplet peaks for the *trans* vinylene signal of poly(*endo*-C6M) at 129.33 ppm. These results shown that using the ruthenium carbene as an initiator, ROMP of either *exo*- or *endo*-monomer gives a high *trans* content and pure *endo*-monomer produces exclusively *trans*-polymer. This is consistent with literature reports which record that the ruthenium carbene initiator provides predominantly *trans* double bonds in the metathesis of other norbornenes.[10]

The ^{1}H nmr spectra of poly(*exo*-C6M) [experiment 1], diblock (*endo-exo*-C6M) [experiment 5] and poly(*endo*-C6M) [experiment 4] are shown in Figure 4.14a, b, and c respectively, as typical examples. The chemical shifts and assignments of ^{1}H nmr spectra for the homo and block copolymers of *exo*- and *endo*-monomers are recorded in Table 4.3.

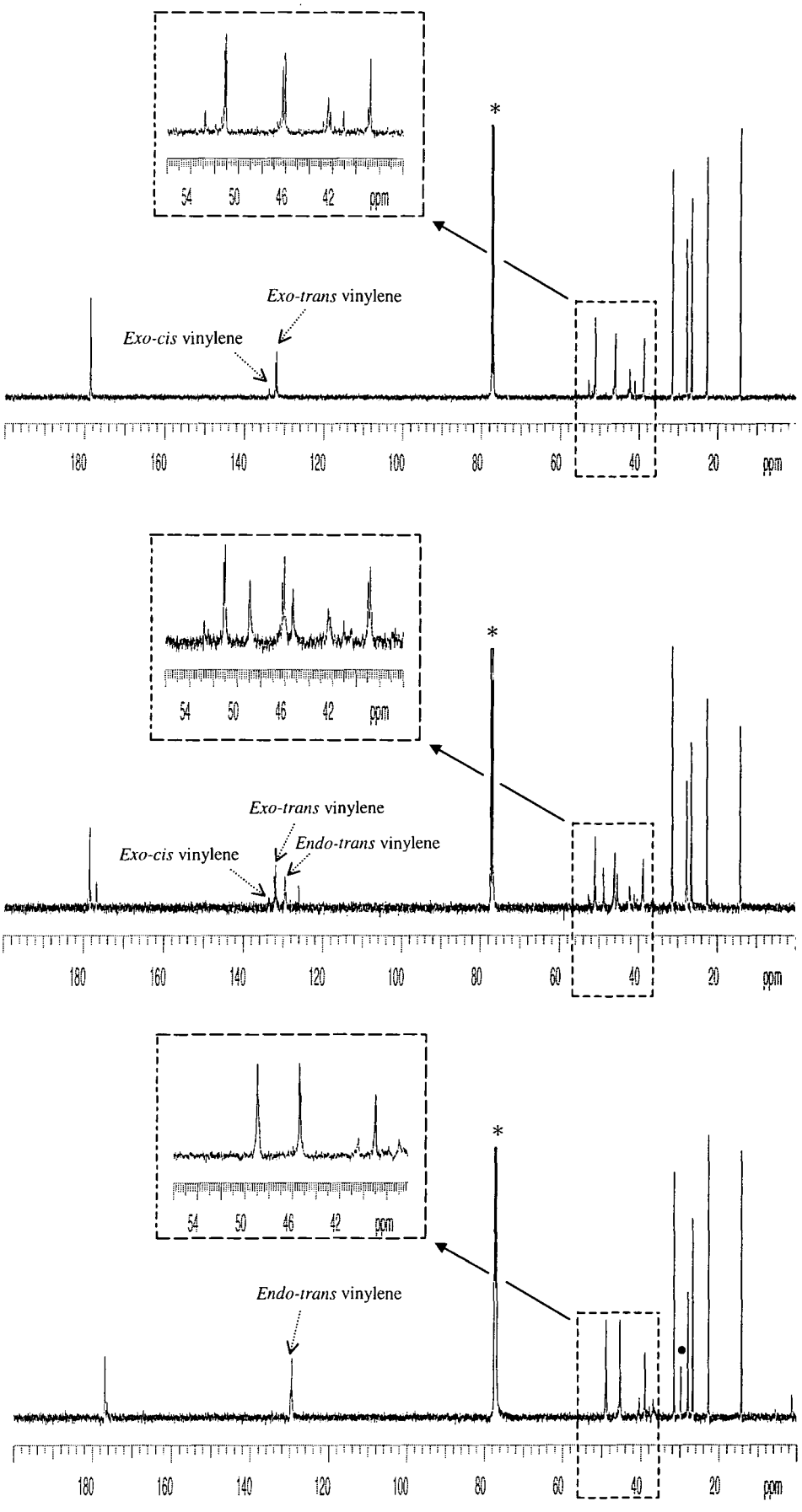

Figure 4.13 ^{13}C nmr spectra of (a) poly(*exo*-C6M), (b) diblock(*endo,exo*-C6M) and (c) poly(*endo*-C6M). * residual carbons in $CDCl_3$. • acetone dissolved in $CDCl_3$.

Experimental No.	^{13}C nmr	
	Carbon	Position (ppm) and assignment
1 and 2 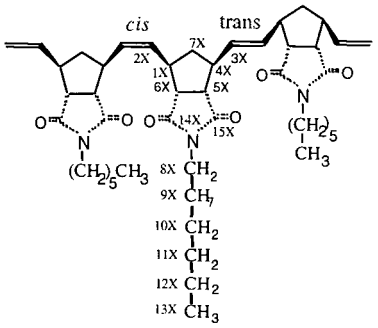 Poly(*exo*-C6M)	C-14,15X	178.28
	C-2,3X	134.01(*cis*), 132.00(*trans*)
	C-5,6X	52.80 (*cis*), 50.85 (*trans*)
	C-1,4X	46.05 (*trans*), 41.02(*cis*)
	C-7X	42.21
	C-8X/ C-9X	38.81/ 31.45
	C-10X/ C-11X	27.63/ 26.60
	C-12X/ C-13X	22.49/ 13.99
3 and 5 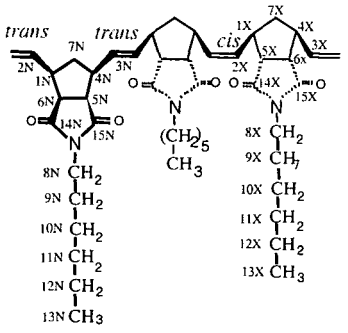 Block(*endo-exo*-C6M)	C-14,15X	178.28
	C-14,15N	176.25
	C-2,3X	134.01 (*cis*), 132.00 (*trans*)
	C-2,3N	129.33 (*trans*)
	C-5,6X	52.80 (*cis*), 50.85(*trans*)
	C5,6N	48.76 (*trans*)
	C-1,4X	46.05 (*trans*), 41.02 (*cis*)
	C1,4N	45.36 (*trans*)
	C-7X	42.21
	C-7N	36.43
	C-8X and N	38.81
	C-9X and N	31.45
	C-10X and N	27.63
	C-11Xand N	26.60
	C-12X and N	22.49
	C-13X and N	13.99
4 and 6 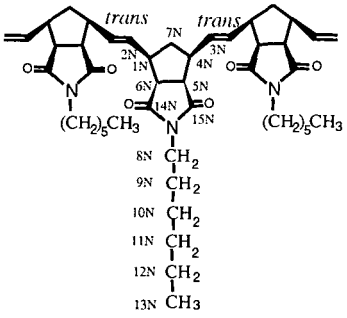 Poly(*endo*-C6M)	C-14,15N	176.68
	C-2,3N	129.33 (*trans*)
	C-5,6N	48.76 (*trans*)
	C-1,4N	45.36 (*trans*)
	C-7N	36.43
	C-8N/ C-9N	38.91/ 31.45
	C-10N/ C-11N	27.63/ 26.60
	C-12N/ C-13N	22.49/ 13.99

Table 4.2 Summary of ^{13}C nmr assignment of poly(*exo*-C6M), block(*endo-exo*-C6M) and poly(*endo*-C6M); X = *exo*-isomer and N = *endo*-isomer.

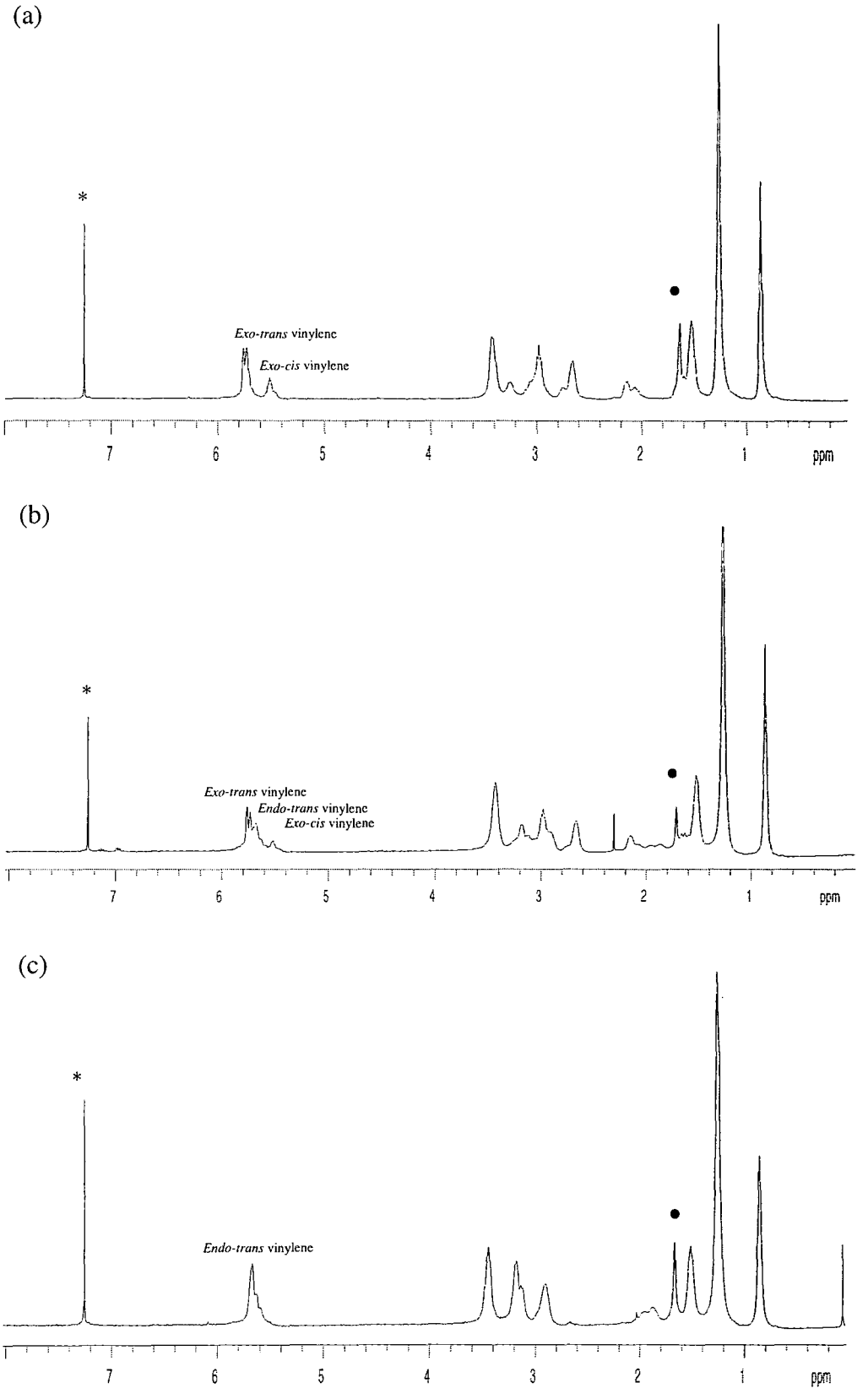

Figure 4.14 ^{1}H nmr spectra of (a) poly(*exo*-C6M), (b) diblock(*endo,exo*-C6M) and (c) poly(*endo*-C6M); * residual hydrogens in $CDCl_3$. • water dissolved in $CDCl_3$.

Experimental No.	^{1}H nmr	
	Proton	Position (ppm) and assignment
1 and2 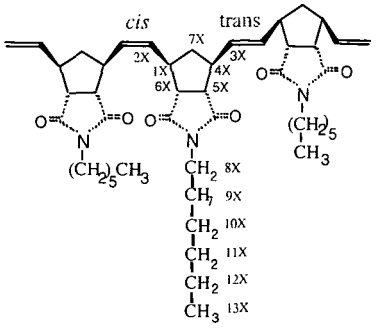 Pol(*exo*-C6M)	H-2,3X	5.75 (*trans*), 5.55 (*cis*)
	H-8X	3.44
	H-1,4X	3.25 (*cis*), 2.98 (*trans*)
	H-5,6X	2.74 (*cis*), 2.68 (*trans*)
	H-7X	2.12
	H-7X'	1.62
	H-9X	1.54
	H-10,11,12X	1.27
	H-13X	0.87
3 and 5 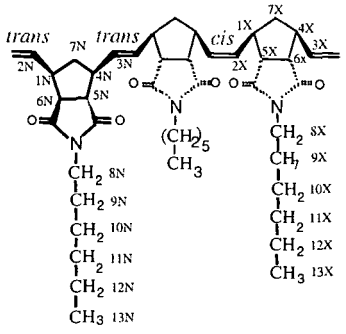 Block(*endo-exo*-C6M)	H-2,3X	5.75 (*trans*), 5.55 (*cis*)
	H-2,3N	5.67 (*trans*)
	H-8X and N	3.43
	H-5,6N	3.17
	H-1,4X	2.97
	H-1,4N	2.91
	H-5,6X	2.65
	H-7X	2.12
	H-7'N	1.92
	H-7'X	1.62
	H-9X and N	1.54
	H-10,11,12X and N and H-7'N	1.27
	H-13X and N	0.87
4 and 6 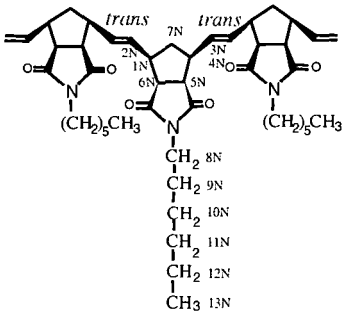 Poly(*endo*-C6M)	H-2,3N	5.67 (*trans*)
	H-8N	3.45
	H-5,6N	3.16 (*trans*)
	H-1,4N	2.91 (*trans*)
	H-7N	1.92
	H-9N	1.45
	H-10,11,12N and H-7'N	1.27
	H-13N	0.87

Table 4.3 Summary of ^{1}H nmr assignment of poly(*exo*-C6M), block(*endo-exo*-C6M) And poly(*endo*-C6M); X = *exo*-isomer and N = *endo*-isomer.

Comparison of ^{1}H nmr spectra of poly(*exo*-C6M), diblock(*endo-exo*-C6M) and poly(*endo*-C6M) revealed differences in chemical shifts and *cis/trans* content of the polymers. The *cis* and *trans* contents of the polymers are readily determined from ^{1}H nmr spectra, in which the resonances attributable to the *cis* and *trans* olefinic hydrogens are well separated and can be seen in the range δ 5-6ppm. The multiplet peaks at 5.75 ppm due to *trans* vinylene signal of poly(*exo*-C6M) and the multiplet peaks at 5.55 ppm due to *cis* vinylene signal of poly(*exo*-C6M) are clearly distinguished from the multiplet peaks of *trans* vinylene signal of poly(*endo*-C6M) at 5.67 ppm. The percentage conversion and *cis/trans* content of the polymers obtained in this section were determined and the results are recorded in Table 4.4.

Experiment	% conversion	^{1}H nmr	
		% trans vinylene	*% cis* vinylene
1 (*exo*)	91.3%*	80	20
2 (*exo+exo*)	95.6%**	81	19
3 (*exo+endo*)	66.6%**	94	6
4 (*endo*)	18.7%*	100	0
5 (*endo+exo*)	75.6%**	90	10
6 (*endo+endo*)	23.7%**	100	0

Table 4.4 ^{1}H nmr analysis of polymers produced in preparative scale polymerisation of *exo*- and *endo*-monomer with the ruthenium carbene initiator.

* The calculations were with respect to M_1 (g)/3

** The calculations were with respect to [(M_1 (g)/3) +M_2 (g)]

Where M_1 = mass of the first monomer and M_2 = mass of the second monomer.

It is clear that the *cis/trans* content of the resulting polymers depends upon the amount of each monomer isomer incorporated into the polymer chain. ROMP of the *exo*-isomer with the ruthenium carbene initiator, gives some double bonds having the *cis* configuration in the linear polymer generally about 20%. Block copolymers showed *cis* vinylene configurations of between 5-10%. Whereas, in the similar condition with *endo*-isomer only *trans* stereochemistry is observed. These results can be compared with earlier studies of closely related monomers were Mo(CH-*t*-Bu)(NAr)$(OCMe_3)_2$ initiation gave 98% and 93% *trans* vinylene content with *exo*- and *endo*-C8M respectively and the initiator Mo(CH-*t*-Bu)(NAr)$(OCMe(CF_3)_2)_2$ gave 32% and 57% *trans* vinylene for the same monomers.[12, 13]

The possible propagation steps for *exo*- and *endo*-monomers are shown in Figure 4.15. The two possible propagation steps for the *exo*-monomer are shown as step 1 and 2, and for the *endo*-monomer are shown as step 3 and 4. Steps 1 and 3 would lead to *cis*-polymer, while step 2 and 4 lead to *trans*-polymer. The *endo*-C6M is much less reactive than the corresponding *exo*-isomer and the polymer can be obtained only in very low conversion. The explanation for this may arise from differences in steric interactions of the substitutents on the monomer and the ligands on the metal (not shown). It may be that the carbonyl groups in the *endo*-position play a key role in retarding the polymerisation by interacting with the metal and slowing down the polymerisation. Steps 2 and 4, leading to *trans* vinylene, may be favoured if the intermediates have less steric hindrance than those in steps 1 and 3; however, it is difficult to visualise these interactions and at this stage in the development of our understanding of mechanism in these ROMP process it is not certain that all the ligands remain bonded to the metal centre though out the reaction.

The possible structures for polymers from the ROMP of *exo*- and *endo*-monomers with the ruthenium carbene initiator are shown in Figures 4.16 and 4.17, respectively. An *endo* repeating unit in the polymer chain has four carbons of the five-member ring carrying *cis*-substitutents, as shown in Figure 4.17, which is sterically less favourable than the situation in the *exo*-derived units, where the two pairs of substituents are in a *trans* relationship, as shown in Figure 4.16.

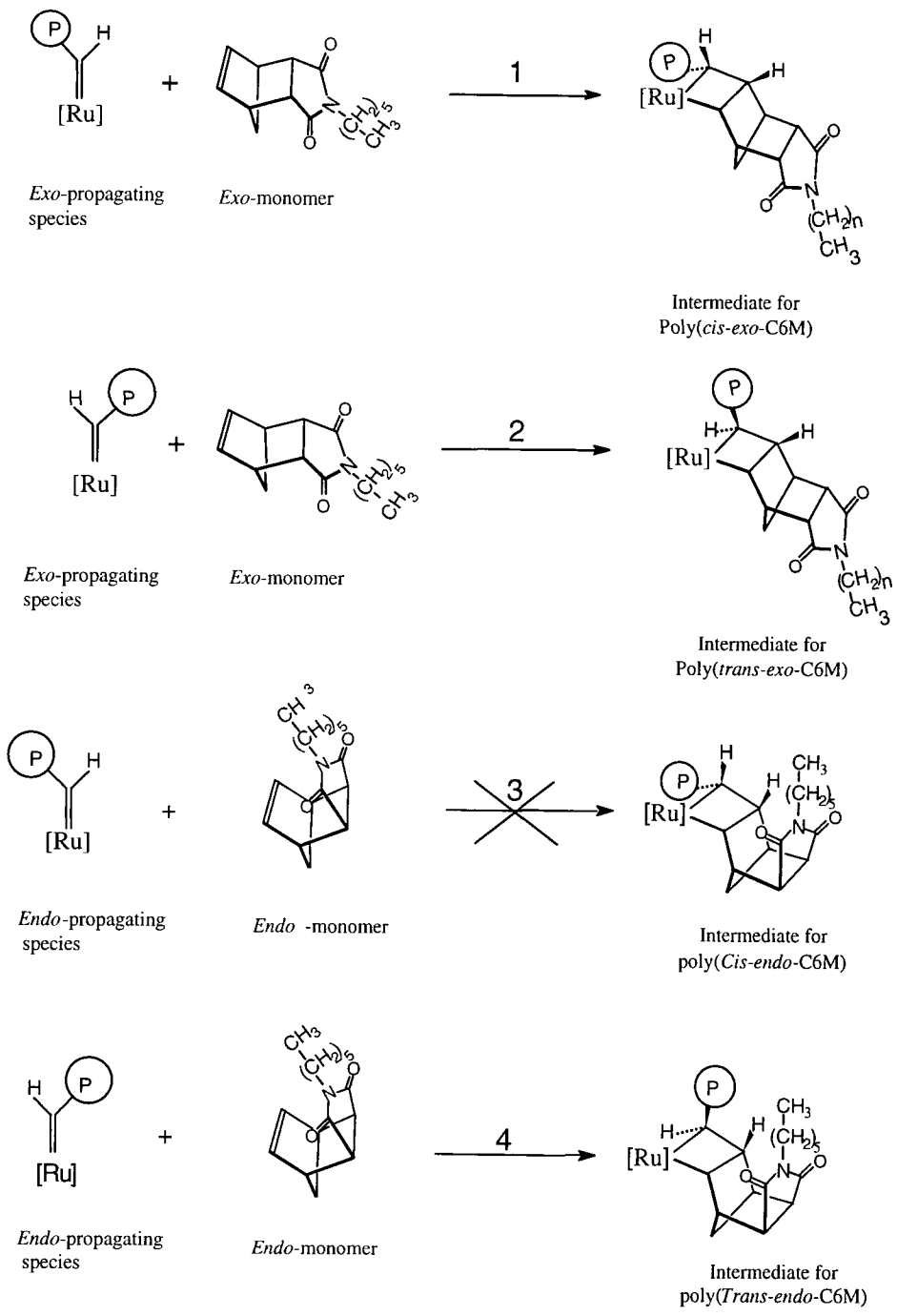

Figure 4.15 The possible propagation step of *exo*- and *endo*-monomers; P = Polymer.

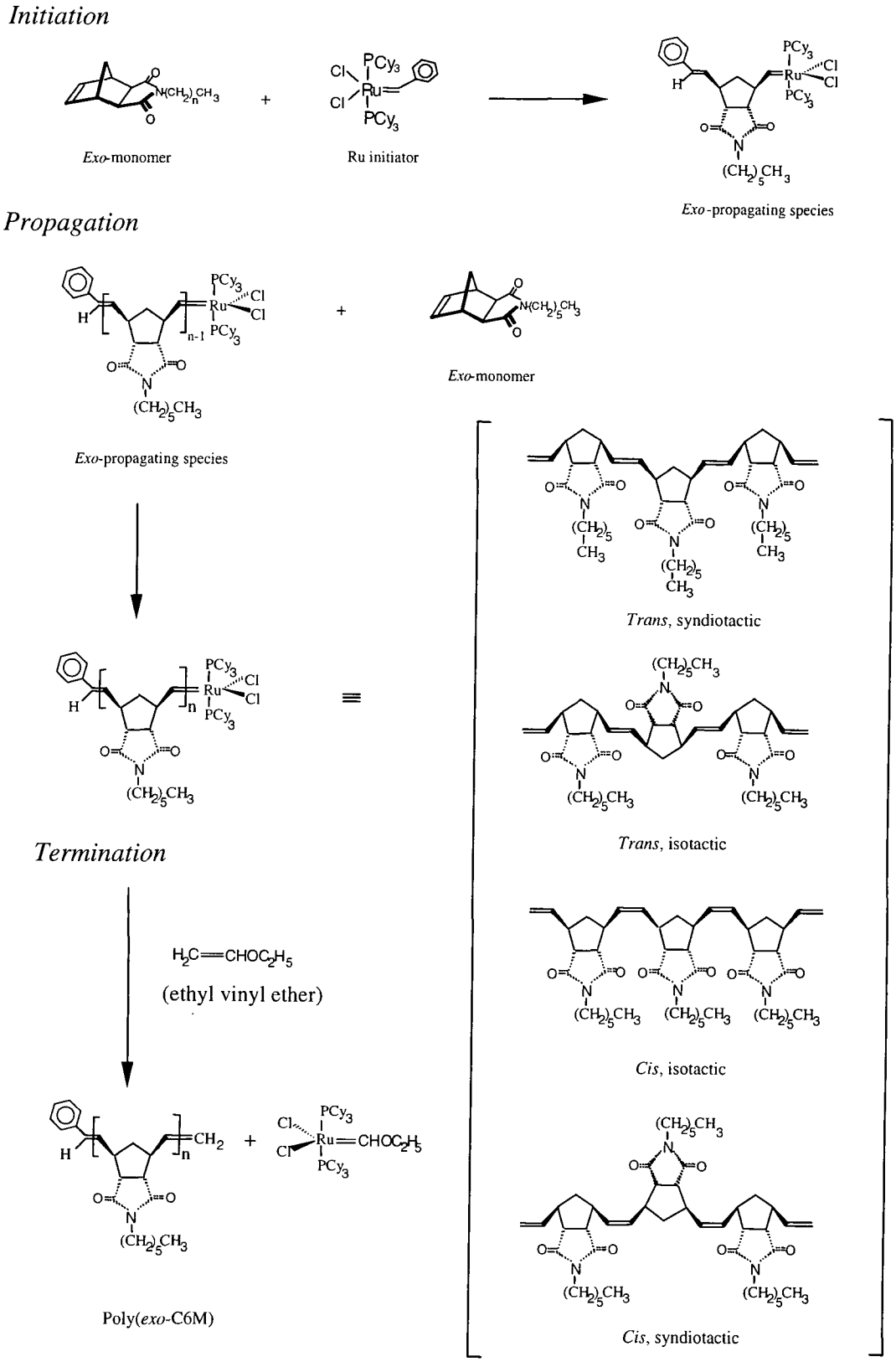

Figure 4.16 Possible structure of polymer derived from *exo*-monomer.

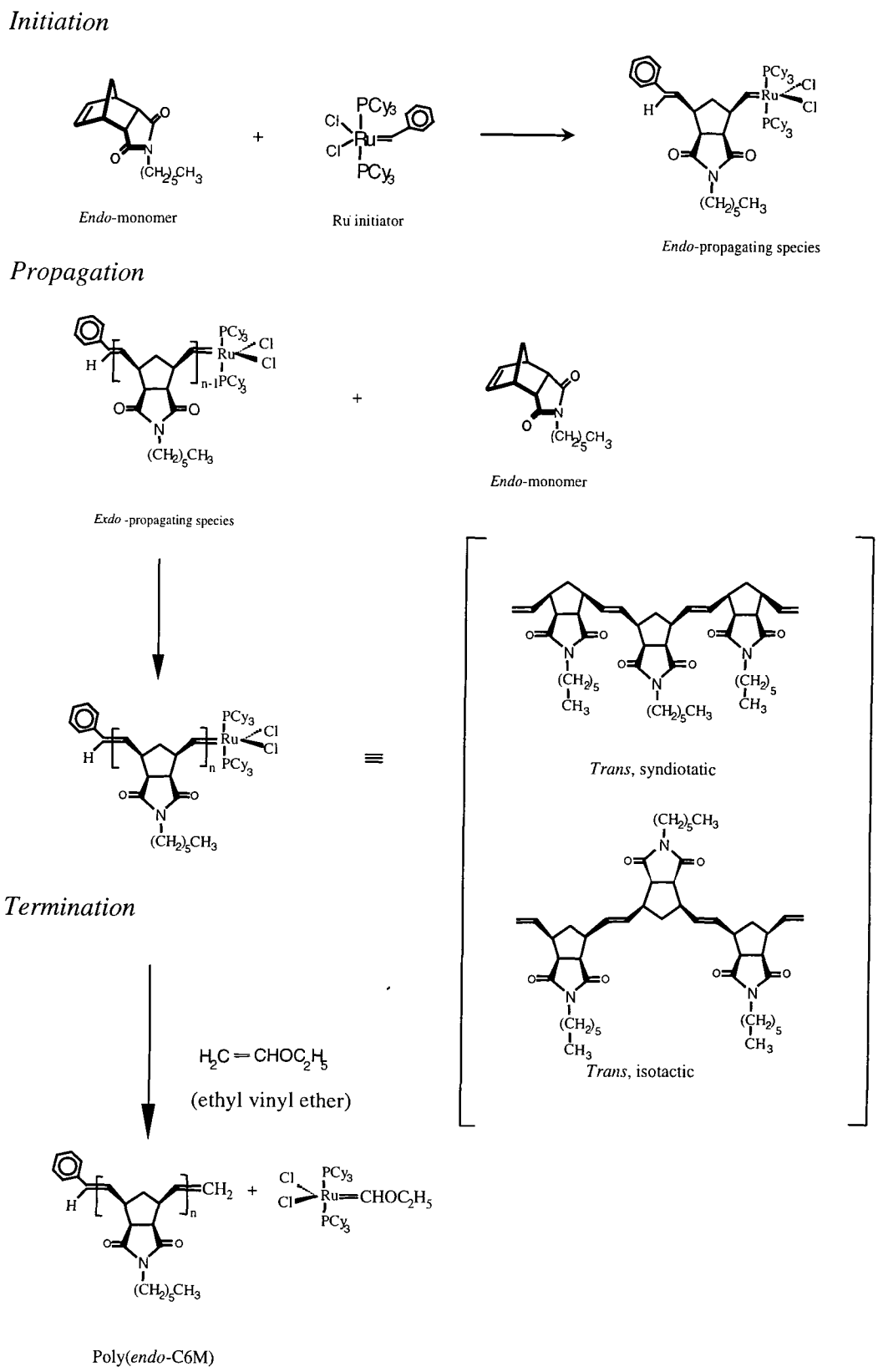

Figure 4.17 Possible structure of polymer derived from *endo*-monomer.

Characterisation by GPC

The number average molecular weight ($\bar{M}n$) and polydispersity index, $\bar{M}w/\bar{M}n$ (PDI), of all polymers obtained in this section are recorded along with the conversions in Table 4.5.

Experiment	% conversion	GPC*		
		$\bar{M}n$	PDI	No. Of peaks
1 (*exo*)	91.3%	125,000	1.2	2
2 (*exo+exo*)	95.6%	291,000	1.4	1
3 (*exo+endo*)	66.6%	132,000	1.2	1
4 (*endo*)	18.7%	50,000	1.4	1
5 (*endo+exo*)	75.6%	116,000	2.9	2
6 (*endo*+endo)	23.7%	32,000	1.9	1

Table 4.5 GPC analysis of polymers produced in preparative scale polymerisations of *exo*- and *endo*-monomers with the ruthenium carbene initiator.

* Waters differential diffractometer detector, three Polymer Laboratories gel columns (exclusion limits 100, 10^3, 10^5 °A), chloroform eluent, polystyrene calibration.

The results from the GPC indicate that the homo and block copolymerisation of *exo*- and *endo*-monomers occurs in a living fashion. The addition of the second monomer resulted in continuation of the polymerisation and the number average molecular weight ($\bar{M}n$) is increased, except for the experiment 6 which will be discussed later in this section. Both the conversion and $\bar{M}n$ for the polymerisations of *endo*-monomer, experiment 4 and 6, were lower than those obtained from the polymerisation of *exo*-monomer, experiment 1 and 2, under the similar conditions. Molecular weight

distributions were bimodal in some cases. When *exo*-monomer was used in the polymerisation, the PDI was generally narrower than those obtained from the polymerisation of *endo*-monomer which is probably due to the inherent differences in k_i and k_p for these polymerisation system as discussed in section 4.2. The relatively narrow PDI of poly(*exo*-C6M) is due to slow initiation relative to the propagation, $k_{ix} < k_{pxx}$. The molecular weight distribution was bimodal in the case of poly(*exo*-C6M), experiment 1, with a small higher molecular weight peak at about twice the mass of the main peak. This observation is consistent with a small amount of coupling between two growing carbenes. This kind of observation has been made before in relation to the Schrock molybdenum initiators when dioxygen impurity terminates one chain and the resulting chain end aldehyde couples with a living carbene chain.[15] However this seems unlikely in this case as ruthenium carbenes are inert to aldehydes, we are unable to offer a rationalisation for this occasional observation of bimodal product.

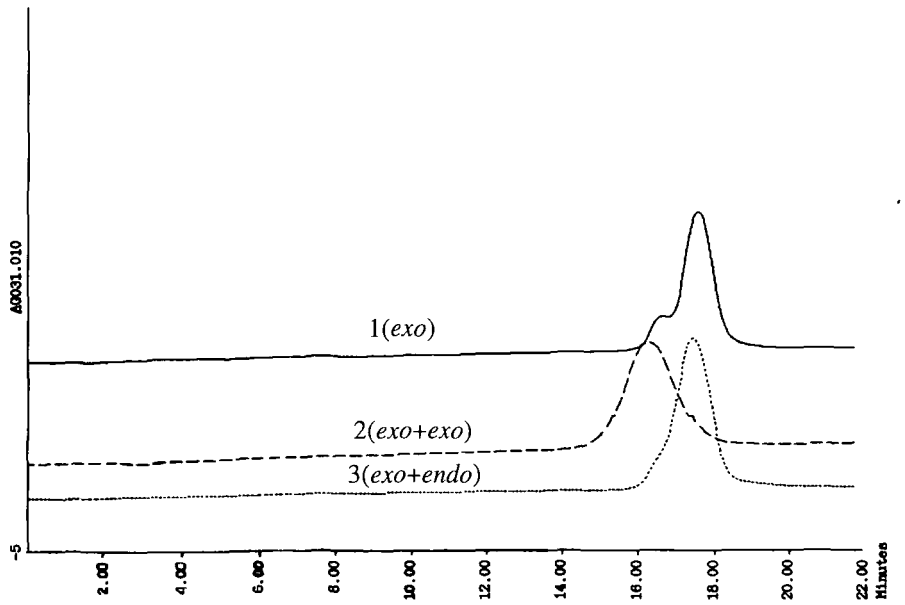

Figure 4.18 GPC traces for the polymers obtained from monomer initiated by the ruthenium initiator. (1) polymer of *exo*-monomer for 7 days, (2) polymer 1 after continued polymerisation of additional *exo*-monomer, (3) polymer 1 after continued polymerisation of additional *endo*-monomer. Molecular weights are reported versus polystyrene calibration.

As determined by GPC, the $\overline{M}n$ increased from 125,000 for the first block of poly(*exo*-C6M), experiment 1, to 291,000 for the polymer obtained from the second addition of *exo*-monomer and 132,000 for the diblock(*exo-endo*) copolymer, experiment 2 and 3 respectively. The $\overline{M}n$ shifted dramatically for polymer obtained from experiment 2 relative to the initial block, experiment 1. This indicates the relative absence of chain transfer and termination reactions. The PDI is slightly increased from 1.2 to 1.4 which is probably due to a part of second aliquot of *exo*-monomer being initiated by the remaining unreacted initiator. As mentioned in the section 4.2.1.1, unconsumed initiator is a common feature for the polymerisation of *exo*-monomer. The PDI remained the same and the $\overline{M}n$ slightly increased for the diblock(*exo-endo*) copolymer, experiment 3, relative to the first block, experiment 1. This diblock copolymer was obtained in only moderate conversion. The results indicate that *endo*-monomer propagated slowly on the reactive chain end of *exo*-polymer.

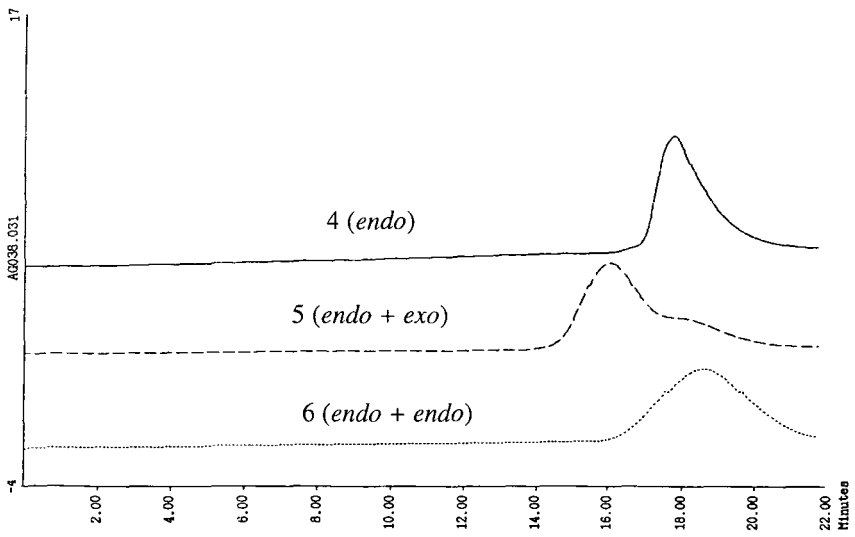

Figure 4.19 GPC traces for the polymers obtained from monomer initiated by the ruthenium initiator. (4) polymer of *endo*-monomer for 7 days, (5) polymer 4 after continued polymerisation of additional *exo*-monomer, (6) polymer 4 after continued polymerisation of additional *endo*-monomer. Molecular weights are reported versus polystyrene calibration.

The molecular weight of the resulting diblock(*endo-exo*) copolymer, experiment 5, is clearly higher than the initial block, experiment 4. The $\overline{M}n$ increased dramatically from 50,000 to 116,000 for the diblock copolymer obtained from second addition of *exo*-monomer to the initial block, *endo*-polymer. The molecular weight distribution was bimodal in this case and showed an additional peak in the higher molecular weight region compared to the peak observed for the first block. This results can be explained by using the information established in sections 4.2.1.2 and 4.2.1.3. Complete initiation was expected in the polymerisation of the first block, *endo*-polymer, since $k_{in}/k_{pnn} >> 1$. This means there was no initiator left in the reaction before adding the second monomer. After the addition of the second aliquot of *exo*-monomer, the *exo*-monomer propagated on the reactive chain ends of the living *endo*-polymer and the first *exo*-propagating chain ends formed became very reactive and the remaining *exo*-monomer was incorporated at these chain ends resulting in the increased molecular weight and bimodal distribution. The decrease in the $\overline{M}n$ and the increase in DPI of the poly(*endo*-C6M) obtained from experiment 6 suggests that a slow back-biting reaction occurred in this case. This is reasonably consistent with the fact that the backbone of all *trans endo*-polymer is subject to high steric strain, although it might also be expected to be sterically hindered to attack.

Characterisation by thermal analysis

The thermal analysis of all polymers obtained in this section are recorded along with the *% trans* content and $\overline{M}n$ in Table 4.6. All DSC traces are shown in Appendix 4.1–4.6. The effect of the polymer structures upon their physical properties in highlighted by the glass transition temperatures (Tg) measured by differential scanning calorimetry (DSC). The *exo*-homopolymer and copolymers exhibit glass transitions in the range 85-88 °C, reflecting their similar structures, namely predominantly polymers from *exo*-monomer with similar *cis/trans* contents. The Tg increases slightly with increase in *trans* content. The *endo*-polymers, which are all *trans* at the vinylenes, exhibited the highest Tg at about 115-118 °C. A similar trend in Tg with *cis/trans* content has been observed for poly(bis(trifluoromethyl)norbornadiene)[15,16] and amino ester functionalised norbornenes[17].

Experiment	*% trans* vinylene	$\bar{M}n$	DSC Tg (°C)	TGA Temp. (°C) for 2% weight loss
1 (*exo*)	82	125,000	85	425
2 (*exo+exo*)	81	291,000	84	414
3 (*exo+endo*)	94	132,000	88	350
4 (*endo*)	100	50,000	118	330
5 (*endo+exo*)	90	116,000	86	300
6 (*endo+endo*)	100	32,000	116	350

Table 4.6 Thermal analysis of polymers produced in preparative scale polymerisations of *exo*- and *endo*-monomer with the ruthenium carbene initiator.

It is clear that the low molecular weight polymer of the *endo*-monomer exhibited a higher glass transition temperature than the high molecular weight polymer of *exo*-monomer. It might be concluded that the *cis* substitution of the four carbon atoms of the cyclopentane ring in poly(*trans-endo*-C6M) gives rise to strong steric hindrance and make the chain stiffer and motion more difficult, which is evident in the high glass transition temperature of this relatively low molecular weight material. Thermogravimetric analysis (TGA) on all polymer samples shown a substantial weight loss in the temperature range 300-425°C. This might result from the elimination of the maleimide group but the chemistry of the thermal degradation process was not examined due to lack of time, clearly the polymers derived from the *endo*-monomer were less thermally stable which may be a consequence of the increased steric strain in these materials.

4.4 Preparative scale syntheses of linear polymers: Poly(*exo*-CnM)

Introduction

From the work described in sections 4.2 and 4.3 it can be concluded that the *endo*-monomer (*endo*-C6M) has very low reactivity with the ruthenium carbene initiator. In this section, the ROMP of the *exo*-monofunctional monomers with different length N-alkyl groups, *exo*-C3M, C4M, C5M, C6M, C8M, was investigated. The aims of the work described in this section were to study the effect of the length of the pendant N-alkyl group and the molecular weight on the thermal properties of the polymers. With these monomers a wider range of polymers can be prepared via solution polymerisation than by bulk polymerisation. In order to obtain polymers without residual unreacted monomer in the sample, solution polymerisations of a series of *exo*-monomers with different length N-alkyl groups were carried out. Polymerisation of *exo*-C3M, mpt. 45.5 °C, can not be carried out easily in the melt due to the relatively high melting point of the monomer and the rapid reaction at higher temperature; whereas the *exo*-C8M, which is a liquid at room temperature, shows very low reactivity for ROMP using the ruthenium carbene as an initiator in bulk. The bulk polymerisation of all these *exo*-monofunctional monomers will be discussed in detail in Chapter 5.

4.4.1 Results and discussion

The ROMP of *exo*-monofunctional monomers, *exo*-C3M, C4M, C5M, C6M, C8M, yields linear polymers with unsaturated backbones and different length pendant N-alkyl groups, as shown in Figure 4.20.

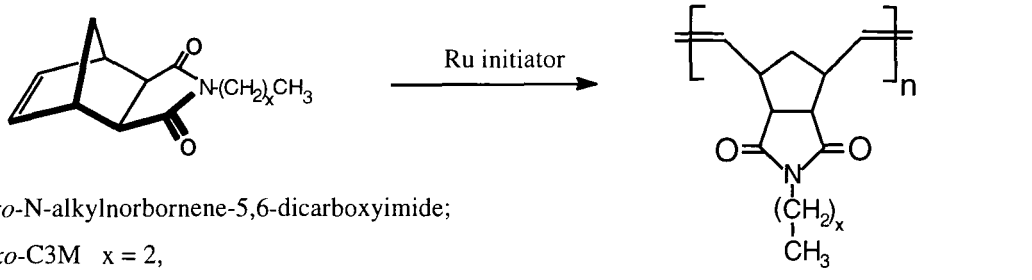

Exo-N-alkylnorbornene-5,6-dicarboxyimide;
exo-C3M x = 2,
exo-C4M x = 3,
exo-C5M x = 4,
exo-C6M x = 5,
and *exo*-C8M x = 7

Poly(*exo*-N-alkylnorbornene-5,6-dicarboxyimide)
x = 2, 3, 4, 5, and 7

Figure 4.20 A schematic representation of the linear polymer syntheses.

4.4.1.1 Syntheses of linear polymers

The polymerisations of *exo*-monofunctional monomers were carried out on a 10 g scale in the Glove Box at room temperature. The ruthenium carbene initiator (10 mg) and *exo*-monomer (10 g) were dissolved in dichloromethane (5 ml and 100 ml, respectively) in separated ampules. The initiator solution was transferred into the monomer solution and the mixture stirred for 2 days. The polymerisations were terminated by adding ethyl vinyl ether and the products recovered as white solids by precipitation into excess methanol. The polymers were further purified by reprecipitation from chloroform into methanol and dried under vacuum at 30 °C for 2-3 days. The same procedure as above was also used to provide poly(*exo*-C4M) with different molecular weights by varying the [M]/[I] ratio. All of the linear polymers made were soluble in toluene, tetrahydrofuran, dichloromethane and chloroform.

4.4.1.2 Characterisation of polymers obtained

This section describes the characterisation of the polymers whose synthesis was described in section 4.4.1.1. The characterisation was carried out using ^{1}H and ^{13}C nmr, GPC, DSC and TGA. All linear polymer gave clear transparent films from solution.

Polymer characterisation using ^{1}H and ^{13}C nmr spectroscopy

The *exo*-monomers used to make the linear polymers described in this section, all give polymers showing *cis/trans* vinylene isomerism. The *cis/trans* contents were calculated directly from the ^{1}H nmr spectra. All nmr spectra of the polymers were recorded for solutions in $CDCl_3$ and are shown in Appendix 4.7 – 4.16. The ^{1}H and ^{13}C nmr spectra of poly(*exo*-C3M) are shown in Figure 4.21a and b respectively, as typical examples. The chemical shifts, *cis/trans* vinylene contents and assignments of ^{1}H and ^{13}C nmr spectra for all polymers obtained are recorded in Table 4.7. ROMP of all *exo*-monomers in solution proceeded in high conversion (~85-96%) and gave products with *cis* vinylene contents generally of about 15-19%. These results are consistent

with the results from section 4.3 where it was established that the *cis/trans* content depends upon the relative amount of *exo-* and *endo*-monomers incorporated into the polymer chain; ROMP of *exo*-monomers gave about 20% *cis* content, whereas only *trans* stereochemistry was observed for the *endo*-monomer. The *cis*/trans contents of the polymers show relatively little or no dependence upon the [M]/[I] ratio and length of the N-alkyl pendant groups.

Polymer	[M]/[I]	% conversion	^{1}H nmr	
			% trans vinylene	*% cis* vinylene
Poly(*exo*-C3M)	4,000	95.9	85	15
Poly(*exo*-C4M)-H*	10,700	96.0	85	15
Poly(*exo*-C4M)-M*	6,700	94.0	83	17
Poly(*exo*-C4M)-L*	3,700	91.6	81	19
Poly(*exo*-C5M)	3,600	90.6	83	17
Poly(*exo*-C6M)	3,200	90.9	83	17
Poly(*exo*-C8M)	3,700	85.0	83	17

Table 4.7 ^{1}H nmr analysis of polymers produced in preparative scale polymerisations of *exo*-monomers with the ruthenium carbene initiator.

* H, M and L = high, medium and low average molecular weight, respectively.

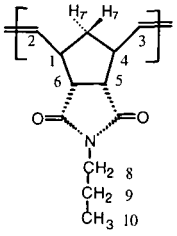

Assignment of H atoms in poly(*exo*-C3M)

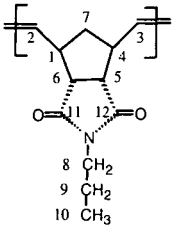

Assignment of C atoms in poly(*exo*-C3M)

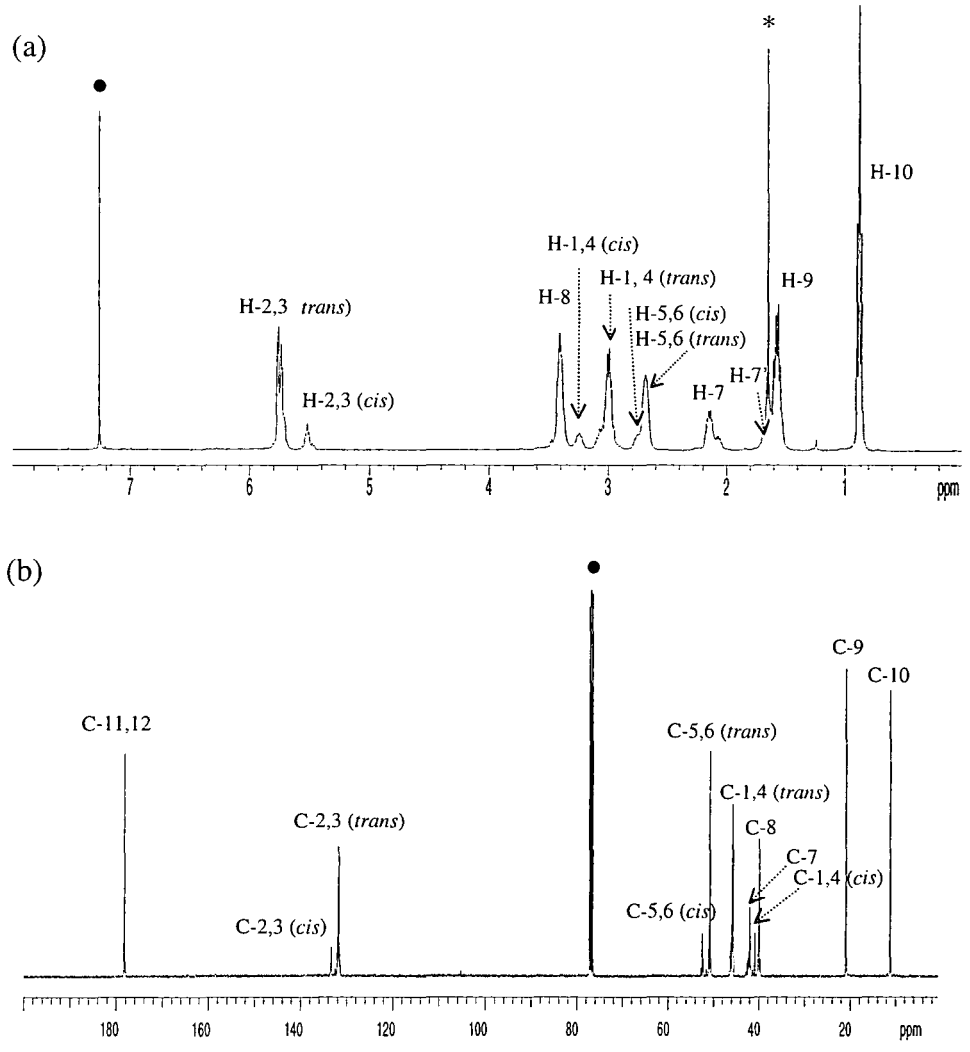

Figure 4.21 ^{1}H and ^{13}C nmr spectra of poly(*exo*-C3M).

- residual hydrogens in $CDCl_3$

* water dissolved in $CDCl_3$

Polymer	^{1}H nmr		^{13}C nmr	
	Hydrogen	Chemical shift (ppm)	Carbon	Chemical shift (ppm)
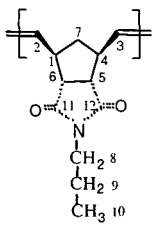	H-2,3	5.75 (*trans*), 5.56 (*cis*)	C-11,12	178.29
	H-8	3.40	C-2,3	133.70 (*cis*), 131.79 (*trans*)
	H-1,4	3.25 (*cis*), 3.00 (*trans*)	C-5,6	52.50 (*cis*),50.90 (*trans*)
	H-5,6	2.75 (*cis*), 2.70 (*trans*)	C-1,4	45.98 (*trans*),41.01 (*cis*)
	H-7	2.10	C-7	42.03
	H-7'	1.69	C-8	40.00
Poly(*exo*-C3M)	H-9	1.57	C-9	20.97
	H-10	0.88	C-10	11.21
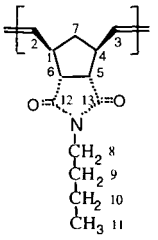	H-2,3	5.76 (*trans*), 5.51 (*cis*)	C-11,12	178.29
	H-8	3.43	C-2,3	133.60(*cis*), 131.77 (*trans*)
	H-1,4	3.22 (*cis*), 2.99 (*trans*)	C-5,6	52.21 (*cis*), 50.90 (*trans*)
	H-5,6	2.74 (*cis*), 2.67 (*trans*)	C-1,4	45.78 (*trans*), 40.82 (*cis*)
	H-7	2.11	C-7	42.02
	H-7'	1.62	C-8	38.01
	H-9	1.53	C-9	29.70
Poly(*exo*-C4M)	H-10	1.28	C-10	20.01
	H-11	0.92	C-11	13.61
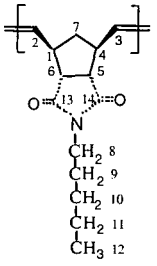	H-2,3	5.76 (*trans*), 5.52 (*cis*)	C-13,14	178.29
	H-8	3.44	C-2,3	133.50 (*cis*), 132.00(*trans*)
	H-1,4	3.25 (*cis*), 3.00 (*trans*)	C-5,6	52.45 (*cis*), 50.29 (*trans*)
	H-5,6	2.75 (*cis*), 2.64 (trans)	C-1,4	45.97 (trans), 40.78 (*cis*)
	H-7	2.10	C-7	42.04
	H-7'	1.64	C-8	38.50
	H-9	1.51	C-9	28.97
Poly(*exo*-C5M)	H-10,11	1.28	C-10	27.34
	H-12	0.92	C-11	22.20
			C-12	13.95

Table 4.8 Summary of ^{1}H nmr assignment of poly(*exo*-CnM); where n = 3, 4, 5, 6, and 8.

Polymer	^{1}H nmr		^{13}C nmr	
	Hydrogen	Chemical shift (ppm)	Carbon	Chemical shift (ppm)
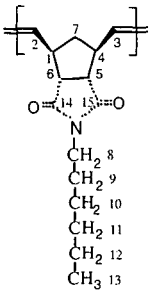 Poly(*exo*-C6M)	H-2,3	5.75 (*trans*), 5.55 (*cis*)	C-14,15	178.28
	H-8	3.43	C-2,3	133.45 (*cis*), 131.97(*trans*)
	H-1,4	3.24 (*cis*), 3.00 (*trans*)	C-5,6	52.56 (*cis*), 50.87 (*trans*)
	H-5,6	2.75 (*cis*), 2.67 (*trans*)	C-1,4	45.84 (*trans*), 41.02 (*cis*)
	H-7	2.10	C-7	42.21
	H-7'	1.64	C-8	38.61
	H-9	1.54	C-9	31.45
	H-10,11,12	1.27	C-10	27.61
	H-13	0.87	C-11	26.60
			C-12	22.49
			C-13	13.99
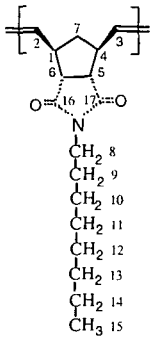 Poly(*exo*-C8M)	H-2,3	5.75 (*trans*), 5.56 (*cis*)	C-15,16	178.27
	H-8	3.43	C-2,3	133.56 (*cis*), 131.85 (*trans*)
	H-1,4	3.25 (*cis*), 3.00 (*trans*)	C-5,6	52.20 (*cis*), 50.93 (*trans*)
	H-5,6	2.74 (*cis*), 2.67 (*trans*)	C-1,4	46.00 (*trans*), 40.43 (*cis*)
	H-7	2.15	C-7	42.04
	H-7'	1.62	C-8	38.56
	H-9	1.53	C-9	31.78
	H-10,11,		C-10,11	29.18
	12,13,14	1.26	C-12	27.67
	H-15	0.86	C-13	26.78
			C-14	22.61
			C-15	14.10

Table 4.8 (continued) Summary of ^{1}H nmr assignment of poly(*exo*-CnM); where n = 3, 4, 5, 6 and 8.

Characterisation by GPC

The number average molecular weight ($\bar{M}n$) and PDI of all linear polymers obtained in this section are recorded along with the [M]/[I] ratio in Table 4.9. The GPC traces and the full details of the molecular weight analysis for all polymers obtained are shown in Appendix 4.17-4.23.

Polymer	[M]/[I]	GPC**		
		$\bar{M}n$	PDI	No. of peaks
Poly(*exo*-C3M)	4,000	453,000	1.9	1
Poly(*exo*-C4M)-H*	10,700	1,033,000	1.6	1
Poly(*exo*-C4M)-M*	6,400	736,000	1.8	1
Poly(*exo*-C4M)-L*	3,700	462,000	1.8	1
Poly(*exo*-C5M)	3,600	498,000	1.8	1
Poly(*exo*-C6M)	3,200	820,000	1.7	1
Poly(*exo*-C8M)	3,700	492,000	1.9	1

Table 4.9 GPC analysis of polymers produced in preparative scale polymerisations of *exo*-monomers with the ruthenium carbene initiator.

* H, M and L = high, medium and low average molecular weight, respectively.

** Water differential diffractometer detector, three Polymer Laboratories gel columns (exclusion limits 100, 10^3, 10^5 °A), chloroform eluent, polystyrene calibration.

In the majority of cases, the *exo*-monomers were polymerised with [M]/[I] ratios about 4,000 to yield linear polymers with $\bar{M}n$ values of approximately 500,000 versus polystyrene calibration. Poly(*exo*-C6M), which was prepared using the same [M]/[I] ratio, exhibited approximately twice the molecular weight of the other polymers; this observation is consistent with termination by coupling. All the polymers obtained in this section show relatively broad and monomodal molecular weight distribution. As discussed previously propagation is much faster than initiation in all these *exo*-system. The relatively high value of the PDIs are probably due to the fact that the solution became very viscous resulting in less efficient mixing during the course of the reaction. Poly(*exo*-C4M) samples with different molecular weights were successfully prepared by varying the [M]/[I] ratio. It was found that the molecular weight of the polymers obtained can be controlled and shown a very roughly linear relationship with the [M]/[I] ratio, as shown in Figure 4.22.

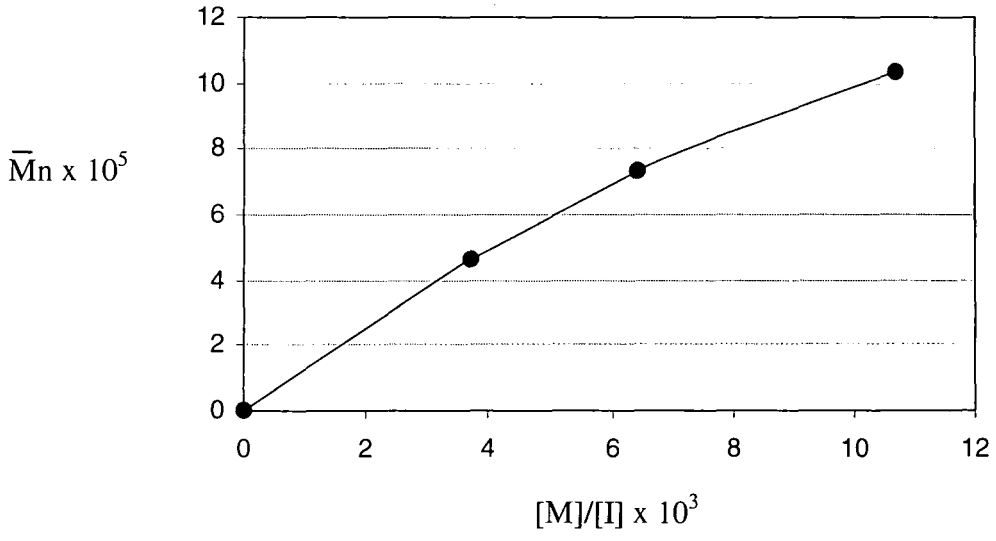

Figure 4.22 Plot of number average molecular weight ($\bar{M}n$) versus monomer/initiator ratio ([M]/[I]) of poly(*exo*-C4M).

Polymer characterisation by thermal analysis

The glass transition temperature (Tg) and temperature for 2% weight loss of all linear polymers obtained in this section are recorded along with their number average molecular weights in Table 4.10. The DSC traces of all polymers obtained are shown in Appendix 4.24-4.30. It was found that the glass transitions of these linear polymers

depended upon the length of the side groups. In a series of linear polymers with different length of N-alkyl pendant group, the Tg decreases as the side group gets longer. However, Tg did not depend much upon the number average molecular weight of the polymers in the range of Mn investigated; thus, poly(*exo*-C4M)s with the number average molecular weights in the range 462,000 to 1,033,000 showed only a slight increased in Tg from 126 to 129 °C. This is consistent with the results from section 3.2.1.2 where it was established that the products from bulk experiments showed Tg which related to the amount of the residual monomers which act as plasticiser rather than the molecular weight. Thermogravimetric analysis (TGA) on all linear polymer samples show a substantial weight loss in the temperature range 400-421 °C. This might result from the elimination of the maleimide group although this has not been proved.

Polymer	$\overline{M}n$	DSC Tg (°C)	TGA Temp. (°C) for 2% weight loss
Poly(*exo*-C3M)	453,000	140	403
Poly(*exo*-C4M)-H*	1,033,000	129	400
Poly(*exo*-C4M)-M*	736,000	127	403
Poly(*exo*-C4M)-L*	462,000	126	414
Poly(*exo*-C5M)	500,000	100	400
Poly(*exo*-C6M)	820,000	84	421
Poly(*exo*-C8M)	492,000	59	403

Table 4.10 Thermal analysis of polymers produced in preparative scale polymerisations of *exo*-monomers with the ruthenium carbene initiator.

* H, M and L = high, medium and low average molecular weight, respectively.

4.5 Preparative scale syntheses of highly crosslinked polymers: Poly(*exo*-CnD)

Introduction

As the results from section 4.4 show the polymerisation *exo*-monofunctional monomers with different length N-alkyl groups yields linear polymers in high conversion (85-96%) and having *cis* vinylene contents generally in the range 15-20%. It was found that the molecular weight of the linear polymers obtained can be controlled to some extent and showed a roughly linear relationship with the [M]/[I] ratio. The glass transition temperatures of the polymers are affected by the length of the pendant N-alkyl group but not by the number average molecular weight in the range studied. In this section, the solution polymerisation of *exo*-difunctional monomers with different numbers of methylene unit separating the reactive imidonorbornene units, *exo*-C3D, C5D, C6D, C9D and C12D, was investigated on a 1.5 g scale. The aim of the work was to study the reactivity of these difunctional monomers.

4.5.1 Results and discussion

The ROMP of *exo*-difunctional monomers, *exo*-C3D, C5D, C6D, C9D and C12D, yielded highly crosslinked polymers with different methylene spacer sequences between the polymer chains. The solid *exo*-difunctional monomers were dissolved in dichloromethane before the addition of initiator solution. The difunctional monomers show very different rates of dissolving. The monomers (1.5 g) with shorter methylene chain between the reactive imidonorbornene units dissolved completely in the solvent (20 ml, dichloromethane) quicker than the longer ones. The polymer synthesis could be followed by the colour change of the solution mixture from purple-pink (initiator) to yellow (propagating species). The reactions which are expected to occur are shown below, Figure 4.23. All crosslinked polymers were obtained as hard brown solids. The polymer samples were subjected to sol-gel extraction using chloroform in a Soxhlet apparatus to yield hard white solids.

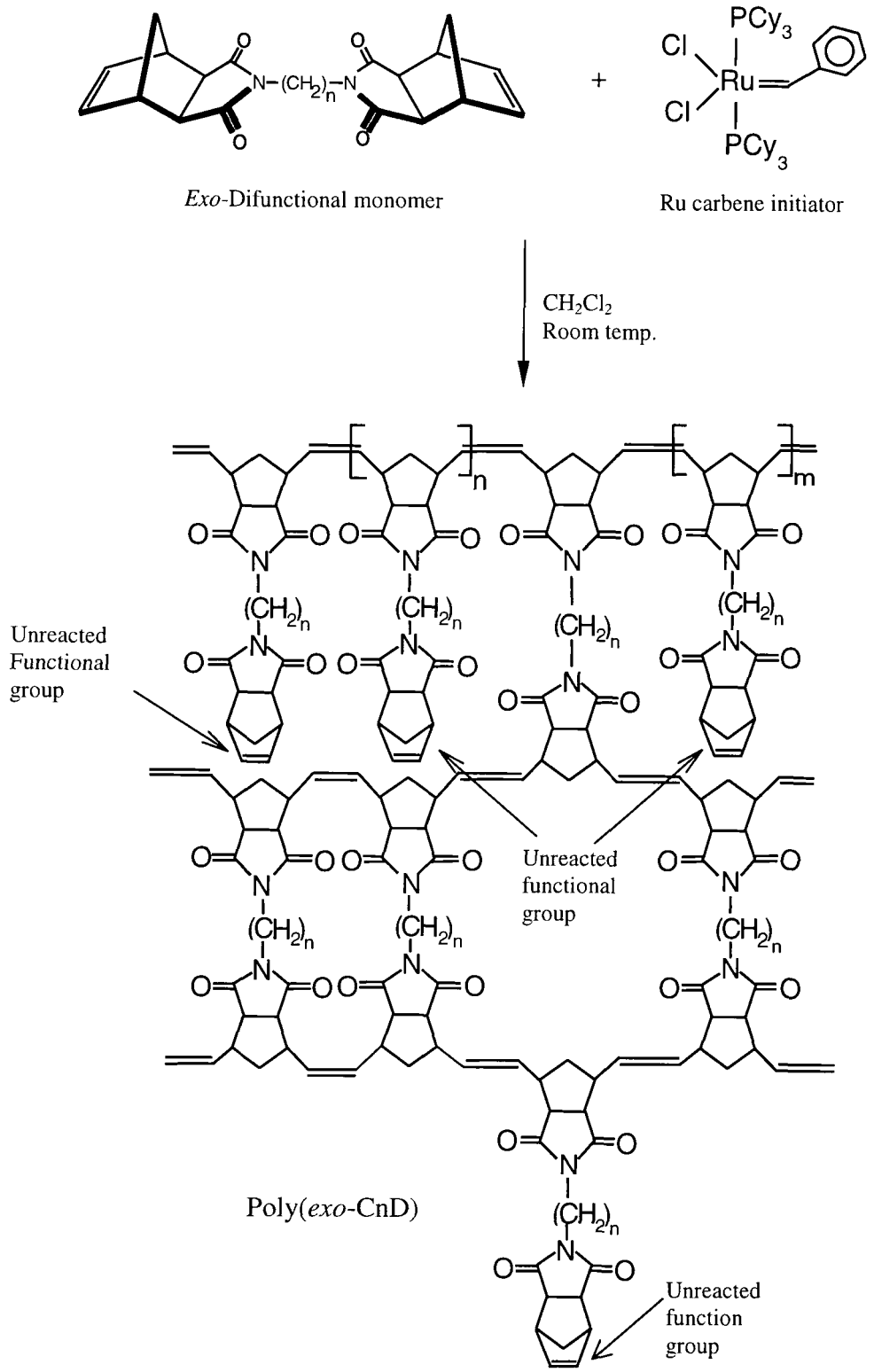

Figure 4.23 The polymerisation of *exo*-difunctional monomers with the Ru carbene initiator; where n = number of methylene unit separating the reactivity imidonorbornene units (n = 3, 5, 6, 9 and 12).

4.5.1.1 Syntheses of highly crosslinked polymers

The polymerisations of *exo*-difunctional monomers were carried out on a 1.5 g scale at room temperature. The initiator (10 mg) and the *exo*-difunctional monomer (1.5 g) were dissolved in dichloromethane (5 ml and 20 ml, respectively) separately. The initiator solution was transferred into the monomer solution and stirred until the mixture gelled, as judged visually and by the fact that the stirrer stopped. The gel mixture was allowed to stand at room temperature for an hour before addition of a solution of ethyl vinyl ether (0.5 ml) in dichloromethane (25 ml) to terminate all propagation. The gels were stirred in dichloromethane for a few hours before being recovered by filtration and dried under vacuum at 30 °C for 2-3 days. All the highly crosslinked polymers obtained in this section were subjected to sol/gel extraction with chloroform for 2 days. The polymers were obtained as coarse white hard powders and dried under vacuum at 40^0C for 3 days. All gels obtained were insoluble in toluene, chloroform, dichloromethane and tetrahydrofuran.

4.5.1.2 Characterisation of polymers obtained

Polymer	Gel time* (min)	% conversion	Degree of swelling (by weight)
Poly(*exo*-C3D)	1	96.5	3.0
Poly(*exo*-C5D)	2	93.4	3.2
Poly(*exo*-C6D)	5	94.4	3.0
Poly(*exo*-C9D)	7	91.6	2.1
Poly(*exo*-C12D)	8	92.1	2.3

Table 4.11 The analysis of highly crosslinked polymers.

* determined when the stirrer had stopped

The solution ROMP of all *exo*-difunctional monomers proceeded very rapidly. The colour of the reaction solutions changed from purple-pink (initiator) to yellow (propagating species) in less than one minute. The solutions gelled within 8 minutes, the exact time depending upon the reactivity of the monomers used. The gel times which were determined when the stirrer had stopped and the polymerising mixture formed a gel-like product are recorded in Table 4.11. The reaction mixture using monomers with shorter methylene sequences between the reactive imidonorbornene units gelled much quicker than those with longer sequences. Comparison of the reaction times and conversions for reaction in the previous, 4.3 and 4.4, and this section showed that the *exo*-difunctional monomers are very reactive and highly crosslinked polymers were obtained in high conversion (~91-96 %) in a few hours, whereas the linear polymers derived from *exo*-C6M were obtained in slightly lower conversion (~85-95%) within 2 days. It seems reasonable to suggest that the *exo*-CnD are somewhat more reactive than *exo*-CnM, which might result from the fact that there are more reactive sites on *exo*-CnD than on *exo*-CnM (2:1).

The crude crosslinked polymers were subjected to sol-gel extraction and the cross-linked residues dried and then swollen in toluene for 2 days. The degrees of swelling were determined and the results are also given in Table 4.11. It is apparent that the degree of swelling (q_m) of the gel fraction for the polymers with short methylene spacers between the polymer chains, poly(*exo*-CnD) where n = 3, 5 and 6, are higher than those of the polymers with longer spacers, poly(*exo*-CnD) where n = 9 and 12. This probably indicates that poly(*exo*-C9D) and poly(*exo*-C12D) have higher crosslink-densities than the other polymers. It seems reasonable to suggest that both functional groups of the longer difunctional monomers, *exo*-C9D and *exo*-C12D, reacted to a greater extent than those of *exo*-C3D, *exo*-C5D and *exo*-C6D probably as a result of reduced steric hindrance. However, the data to hand are insufficient to determine the amount of the *exo*-CnD which has both functional groups reacted.

4.6 Reference for Chapter 4

[1] 'Principles of Polymerisation', G. Odian, John Wiley & Sons, Inc., New York, 1981.

[2] P. Schwab, R. H. Grubbs and J.W. Ziller, *J. Am. Chem. Soc.*, **118**, 100, 1996.

[3] 'Principles of polymerisation' 3rd ed; G. Odian, Wiley: New York, 1999.

[4] K. F. Kastner, N. Calderon, *J. Mol. Catal.*, **15**, 47, 1982.

[5] 'Olefin Matathesis and Ring Opening Polymerisation of Cyclo-olefins', 2nd ed., V. Dragutan, A. T. Balaban, and M. Dimonie, Wiley-Interscience, New York, 1985.

[6] J. Asrar, US. Patent 4,965,330, 1990.

[7] S. Kanaoka and R. H. Grubbs, *Macromolecules*, **28**, 4707, 1995.

[8] J. Gratt and R. E. Cohen, *Macromolecules*, **30**, 3137, 1997.

[9] 'Olefin Metathesis and Metathesis Polymerisation', K. J. Ivin, J. C. Mol, Academic Press, London, 1997.

[10] J. G. Hamilton, K. J. Ivin, J. J. Rooney, *Br. Polym. J.* , 16, 20, 1994.

[11] A. A. Al-Hajaji, PhD Thesis, University of Durham, 1995.

[12] E. Khosravi and A. A. Al-Hajaji, *Eur. Polm. J.*, **34(2)**, 153, 1998.

[13] E. Khosravi and A. A. Al-Hajaji, *Polymer*, **39(23)**, 5619, 1998.

[14] D. V. McGrath, G. H. Grubbs and J. W. Ziller, *J. Am. Chem. Soc.*, 113, 3611, 1991.

[15] W. J. Feast, V. C. Gibson, E. Khosravi, E. L. Marshall and J. P. Mitchell, *Polymer*, 33 (4), 873, 1992.

[16] J. H. Oskam and R. R. Schrock, *J. Am. Chem. Soc.*, **115**, 11831, 1993.

[17] C. G. Biagini, M. P. Coles, V. C. Gibson, M. R. Giles, E. L. Marshall and M. North, *Polymer*, **39** (5), 1007, 1998.

Chapter 5

ROMP-processing of imidonorbornene derivatives

5.1 Introduction

Trial bulk and solution polymerisations of *exo*- and *endo*-monofunctional monomers and *exo*-difunctional monomers initiated by the Grubbs' ruthenium carbene have been described previously in Chapter 3 and 4 respectively. It was observed that *endo*-monomer is much less reactive than the *exo*-monomers both in bulk and solution. For ROMP in solution, the *exo*-monomer is rapidly consumed and once an *endo*-monomer is incorporated at the chain end the new *endo*-derived chain end is less reactive than *exo*-derived chain end. It is apparent that this new *endo*-derived chain end prefers to initiate polymerisation of the more reactive *exo*-monomer rather than the less reactive *endo*-monomer. For ROMP in bulk, where shorter reaction times and efficient mixing are required, the *endo*-monomer was found to terminate the chain growth and therefore was unsuitable for use as a monomer feed for in-mould processing.

The work described in this chapter is concerned with making linear and crosslinked polymeric materials via ROMP using *exo*-isomers as monomers in the feed. The aim of the work was to develop a process for producing shaped articles by introducing a reactive liquid mixture into a mould in which the reacting liquid mixture undergoes ROMP in the bulk to produce the moulded article. The experiments were carried out by mixing neat monomer with the initiator, varying the monomer/initiator ratio, initial mixing time, initial mixing temperature, the time and the temperature during which the filled mould was placed in an oven (hereinafter called curing time and curing temperature), the length of the pendant N-alkyl groups of the monofunctional monomers, and the spacer length between the reactive imidonorbornene units of difunctional monomers. The moulded articles were obtained by introducing the reaction mixture into a glass mould or a small sample vial depending on the amount of the monomer used and the size of the product required. In this work, a glass mould, which formed plaque samples, 50mm x 50 mm x 3 mm thick, was made from a silicone pattern sandwiched between two glass plates. A smooth surface finish was obtained by covering the glass plate walls with a fibre glass reinforced Teflon sheet. After the mould was filled, it was closed and polymerisation was completed by placing the mould in an oven. The final product was removed easily from the glass mould immediately while hot or after cooling. A short time after removal from the oven, heat removal was not complete and the product was hot and flexible. The plaque became a

rigid solid after cooling to room temperature. In the case where a small glass vial served as the mould, the final product was obtained as a disc of 20 mm diameter and approximately 5-7 mm thick by breaking away the glass.

After demoulding, general observations of the sample were recorded. The general criteria used to judge a 'hard' part include the following; (1) the moulded part must come out of the mould as one piece and the part must be rigid not rubbery. (2) The surface quality on the both sides must be smooth. The unreacted monomer content, the glass transition temperature (Tg), and the gel fraction were used to characterise the crude products. The unreacted monomer content in the linear polymeric materials was determined using ^{1}H nmr spectroscopy and selected samples were characterised using TGA, DSC and DMTA techniques. The glass transition temperature and the mechanical properties of the crosslinked polymeric materials were determined using the DMTA technique and selected samples were submitted to sol-gel analysis.

5.2 ROMP-processing of *exo*-monofunctional monomers

The *exo*-C6M was used as a standard monomer in the first attempt to find the optimum reaction conditions for providing polymeric materials which have as high a conversion of monomer as possible, since incomplete reaction and particularly residual monomer will affect the physical and thermal properties of the product. The effect of monomer/initiator ratio, initial mixing time, initial mixing temperature, and curing time and curing temperature on conversion and product properties were investigated. The details of the synthesis and characterisation of the moulded articles from these experiments are described in sections 5.2.1-5.2.4. Subsequently the effect of the length of the pendant N-alkyl groups of the *exo*-monomers on thermal and physical properties were investigated and are described in section 5.2.5.

5.2.1 Effect of monomer/initiator ratio on conversion and product properties

The *exo*-C6M (20 g, 0.08 mol) and variable amounts of the ruthenium carbene initiator were mixed in a small reaction vessel and stirred at room temperature for 15 minutes. The reacting mixture was transferred into a glass mould using a syringe. After the mould was filled it was closed and placed in an oven at 100 °C for an hour. The mould

then was removed from the oven and the final product was removed from the mould and allowed to cool to room temperature. Small pieces of all moulded articles were cut from the plaque and characterised using ^{1}H nmr spectroscopy, TGA, and DSC. The relevant parameters were determined and are recorded in Table 5.1. The ^{1}H nmr spectrum and DSC trace for a sample prepared using a monomer/initiator ratio of 3,700/1, experiment 1, are shown in Figure 5.1 as a typical example.

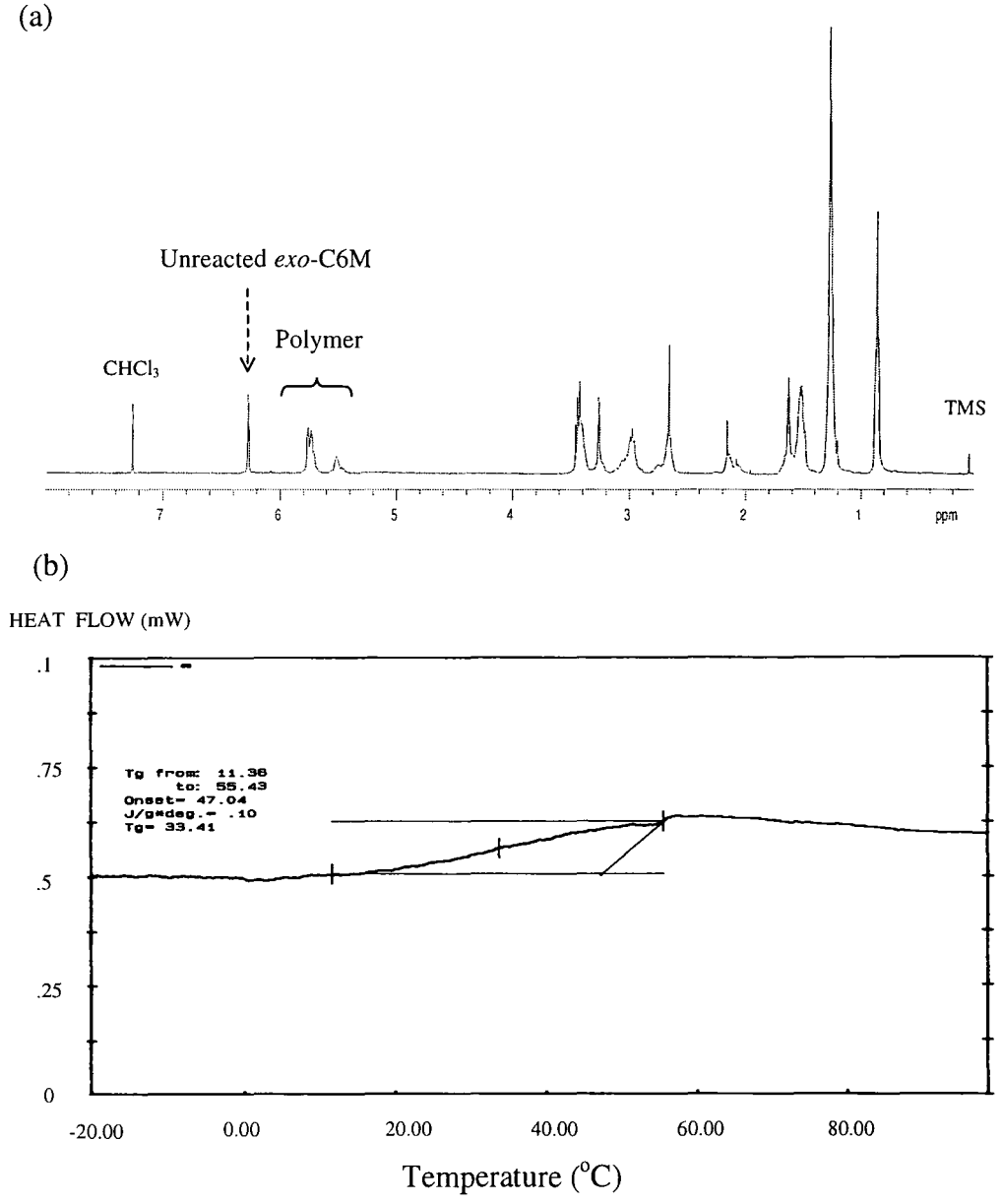

Figure 5.1 (a) ^{1}H nmr spectrum and (b) DSC trace of a sample prepared using a monomer/initiator ratio of 3,700/1.

Sample no.	1	2	3	4
Exo-C6M (g)	20	20	20	20
(mole)	0.08	0.08	0.08	0.08
Ru initiator (mg)	18	14	11	6
(mole x 10^{-5})	2.1	1.7	1.5	0.7
Ratio (by mole) Monomer/initiator	3,700	4,800	5,500	11,100
^{1}H nmr				
(% unreacted monomer)	21	26	37	50
(% polymer)	79	74	63	50
% trans vinylene				
(in crude product)	59	55	48	40
(in polymer matrix)	75	75	76	79
% cis vinylene				
(in crude product)	20	19	15	10
(in polymer matrix)	25	25	24	21
DSC (Tg , °C)	33	31	-2	-43
TGA (Temp. for 2% weight loss, °C)	181	181	169	151
Sample appearance	hard	hard	rubbery	soft rubbery

Table 5.1 The analysis of moulded articles produced by varying the monomer/initiator ratio.

One-step in-mould processing of *exo*-C6M with varying amount of the ruthenium carbene initiator yield moulded articles ranging in property from soft rubbery to hard materials. During stirring the monomer and the initiator for 15 minutes, the viscosity of the liquid mixtures increase slightly. This indicates that the chemical reaction had started. However, during this time the colour of the liquid mixtures changed slowly, which indicates slow initiation. The colour of the reacting mixtures changed from

purple-pink (initiator) to yellow (propagating species) during the period when the filled moulds were in the oven.

^{1}H Nmr analysis of the moulded articles obtained in this way clearly indicated that there was residual *exo*-C6M in all the materials. It is apparent that the overall extent of the polymerisation decreases as the ratio of monomer/initiator is increased. At low initiator concentrations, experiments 3 and 4, the products displayed low monomer conversion and were obtained as rubbery shaped articles. The glass transition temperatures of the moulded articles decrease from 33 to -43 °C, as the amount of the unreacted monomer trapped in the polymer matrix increased from 21 to 50%. All the crude products showed a *cis* vinylene contents generally of about 21-26%. Thermogravimetric analysis (TGA) on all products obtained showed a substantial weight loss in the temperature range 151-181 °C. This might result from the elimination of the unreacted monomer and/or low molecular weight species although this has not been proved. It is clear that the appearance and thermal properties of the final products related to the extent of monomer conversion. It can be concluded that the unreacted monomer is a very effective plasticiser and permanently plasticised the final products.

5.2.2 Effect of initial mixing time on conversion and product properties

The *exo*-C6M monomer (15 g, 0.06 mol) and the ruthenium carbene initiator (12 mg, 1.5 x10^{-5} mol, monomer/initiator ratio 4,100/1) were mixed in a small reaction vessel at room temperature. About 2-3 g of the reacting mixture was transferred into a small glass vial using a syringe after stirring for 5, 10, 20 and 30 minutes, respectively. The filled vials were placed immediately in an oven at 100 °C for an hour. After removal from the oven, the vials were allowed to cool to room temperature. The final products were removed as rigid clear yellow solids by breaking away the glass. The crude products were cut up and characterised using ^{1}H nmr spectroscopy and DSC. All the relevant parameters were determined and are recorded in Table 5.2. The ^{1}H nmr spectrum and DSC trace of a sample produced in an experiment using an initial mixing time of 30 minutes, experiment 4, are shown in Figure 5.2 as a typical example.

It was found that the viscosity of the reaction mixture increases slowly during stirring at room temperature. A longer initial mixing time lead to an increase of the viscosity of the reaction mixture. After stirring the reaction mixture for 30 minutes, it became highly viscous and made the mould filling difficult. After stirring the mixture for 40 minutes under the condition studied the viscosity became too large for the mixture to be transferred into a mould using a syringe . The colour of the mixture change slowly from purple to yellow during 40 minutes stirring, indicating slow initiation.

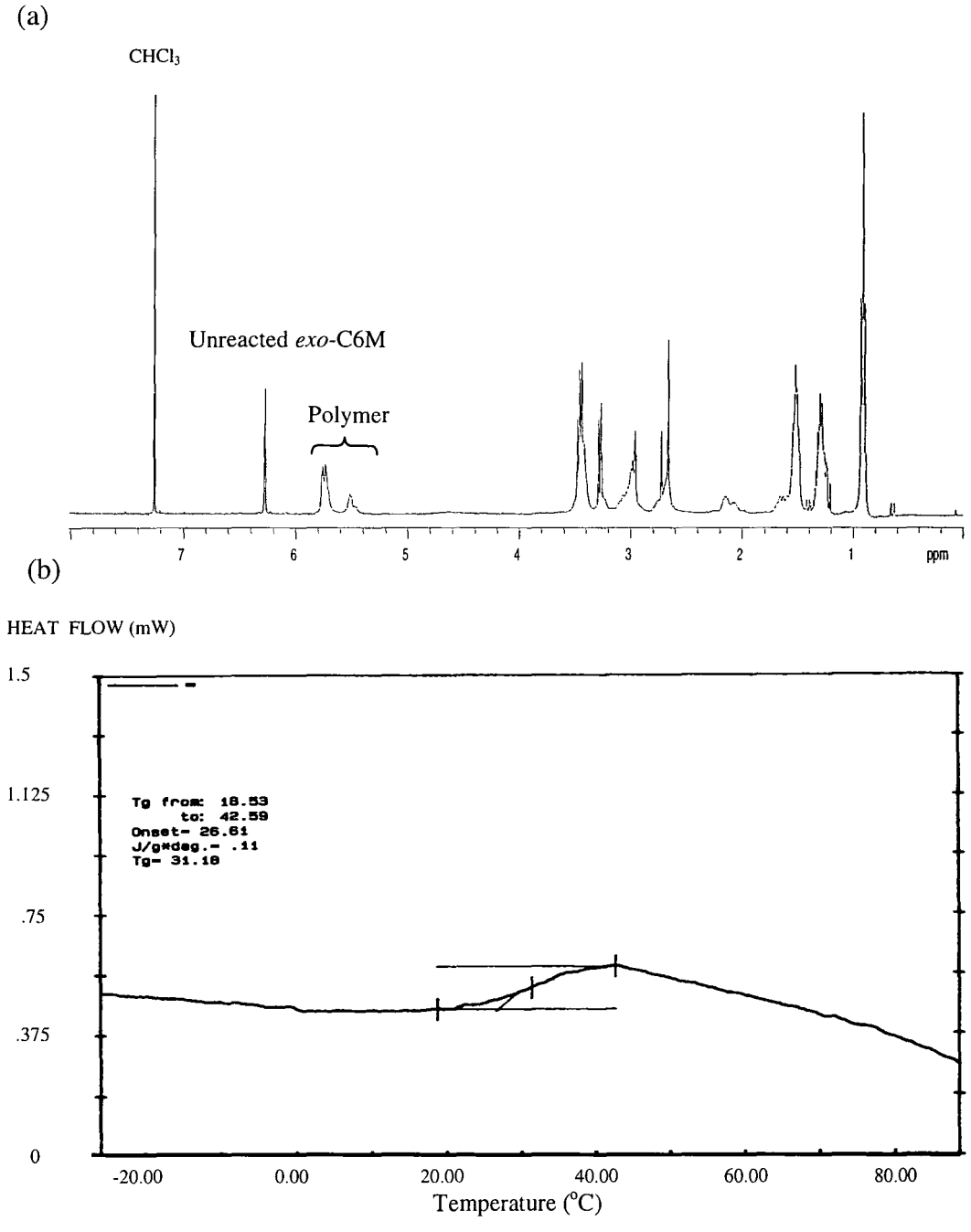

Figure 5.2 (a) ^1H nmr spectrum and (b) DSC trace for a sample prepared using initial mixing time 30 minutes.

Sample no.	1	2	3	4
Initial mixing time (min)	5	10	20	30
^{1}H nmr				
(% unreacted monomer)	30	26	25	23
(% polymer)	70	74	75	77
% trans vinylene				
(in crude product)	52	55	54	58
(in polymer matrix)	75	74	74	75
% cis vinylene				
(in crude product)	17	19	19	19
(in polymer matrix)	25	26	26	25
DSC (Tg, °C)	28	30	31	31
TGA (Temp. for 2% weight loss, °C)	169	177	177	181
Sample appearance	hard	hard	hard	hard

Table 5.2 The analysis of moulded articles produced by varying the initial mixing time.

^{1}H Nmr analysis of the final products obtained from the work described in this section indicated that there was residual *exo*-C6M in all the materials. It was found that the overall extent of the polymerisation did not depend much on the initial mixing time under the conditions studied, as the final products showed the same appearance and only slightly different conversions and Tgs. The conversion increases slightly from 74 to 77%, as the initial mixing time is increased from 10 to 30 minutes, experiment 2, 3 and 4 respectively. However, too short an initial mixing time, experiment 1, results in the lowest conversion in the final product. This might be because the mixture was not well mixed before it was introduced into a glass vial. All the final products showed *cis* vinylene contents of about 25%. Thermogravimetric analysis (TGA) on all products obtained show a substantial weight loss in the temperature range 169-181 °C. This might result from the elimination of the unreacted monomer and/or low molecular weight species although this has not been proved.

5.2.3 Effect of initial mixing temperature on conversion

The *exo*-C6M monomer and the ruthenium carbene initiator were mixed and stirred at room temperature in a small reaction vessel. The reacting mixture was transferred into a glass mould using a syringe before the mixture became too viscous. After the mould was filled it was closed and placed in an oven at 100 °C for an hour. Then the mould was removed from the oven and the final product was removed from mould as a rigid solid after cooling to room temperature. In order to study the effect of the initial mixing temperature, the monomer and the initiator were mixed and stirred at 40, 60 and 80 °C by placing the reaction vessel in an oil bath before introducing the reacting mixture to the glass mould. The final products were cut up and characterised using ^{1}H nmr spectroscopy in $CDCl_3$ solution. All the relevant parameters were determined and are recorded in Table 5.3.

It was found that the reaction rate and the viscosity of the reaction mixture increased as the initial mixing temperature was increased. After stirring the reaction mixtures at room temperature, experiment 1, and at 40 °C in an oil bath, experiment 2, the mixtures became only slightly viscous due to the relatively slow polymerisation reaction. The moulded articles were obtained by introducing the liquid mixture into a glass mould. However, very rapid reaction took place when the mixtures were stirred at 60 and 80 °C, experiment 3 and 4 respectively and the mixtures were very viscous within 5 minutes. The attempt to transfer the mixtures from these reactions failed because the viscosities were too high. The final products were obtained, as low conversion rubbery materials, by placing the reactors directly in an oven at 100 °C for an hour.

^{1}H Nmr analysis of the crude products obtained indicated that when the initial mixing temperature is increased from room temperature to 40°C, the conversion remained constant at about 80%. At higher initial temperature the conversion dropped off quite rapidly, e.g. at 60 °C the conversion dropped to 60% and at 80 °C the conversion was only 52%. As the reactions were too rapid at high temperature, the mixtures were poorly mixed and in the resulting viscous mixture access of the monomer to the active chain end was restricted. It can be concluded that it is important to retard the

polymerisation long enough to mix together the initiator and monomer by using a low initial mixing temperature.

Sample no.	1	2	3	4
Exo-C6M (g)	20	15	15	15
(mol)	0.08	0.06	0.06	0.06
Ratio (by mole) Monomer/initiator	3,700	4,000	3,800	4,000
Initial mixing temperature (°C)	room	40	60	80
Initial mixing time (min)	15	15	5	2-3
^{1}H nmr				
(% unreacted monomer)	21	20	40	48
(% polymer)	79	80	60	52
% trans vinylene				
(in crude product)	59	60	44	38
(in polymer matrix)	75	75	73	74
% cis vinylene				
(in crude product)	20	20	16	14
(in polymer matrix)	25	25	27	26
Sample appearance	hard	hard	rubbery	rubbery

Table 5.3 The analysis of moulded articles produced by varying the initial mixing temperature.

5.2.4 Effect of curing time and curing temperature on conversion and product properties

Experiment 1

The *exo*-C6M monomer and the ruthenium carbene initiator were mixed in a small reaction vessel and stirred at room temperature for 15 minutes. The reacting mixture was transferred into a glass mould using a syringe. The filled mould was placed in an

oven at 100 °C or 160°C for 30 or 60 minutes. The moulded articles were cut up and characterised using ^{1}H nmr spectroscopy, TGA, DSC and GPC. All the parameters determined are recorded in Table 5.4. The ^{1}H nmr spectrum and DSC trace of the product of the experiment using a curing temperature of 160 °C and curing time of 60 minutes, experiment 2, are shown in Figure 5.3 as a typical example.

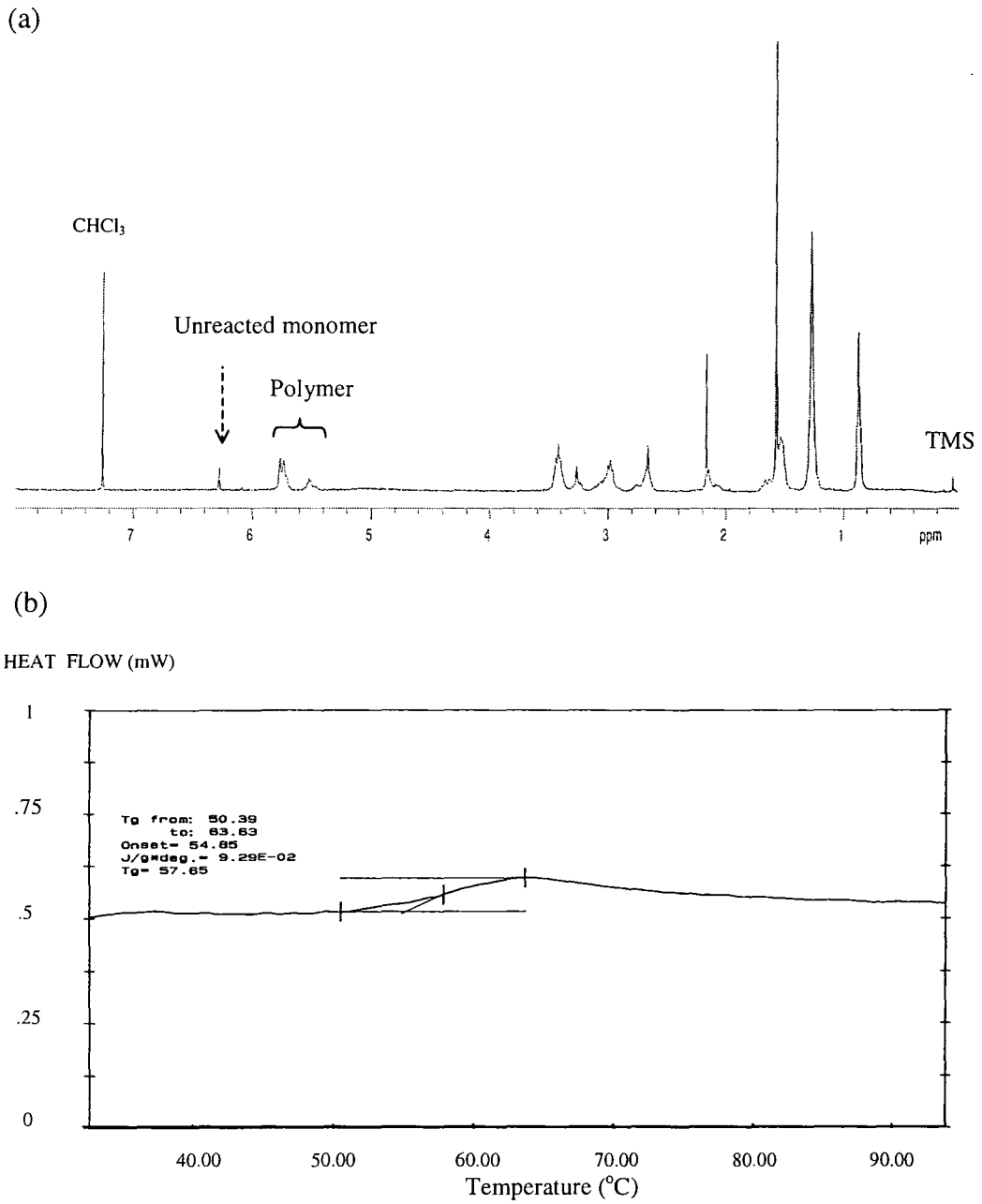

Figure 5.3 (a) ^{1}H nmr spectrum and (b) DSC trace of the moulded article from an experiment using curing temperature 160 °C and curing time 60 minutes.

Sample no.	1	2	3	4
Exo-C6M (g)	20	20	15	20
(mole)	0.08	0.08	0.06	0.08
Ratio (by mole) Monomer/initiator	3,700	3,800	5,200	5,500
Curing temperature (°C)	100	160	160	100
Curing time	60	60	60	60
^{1}H nmr				
(% unreacted monomer)	21	9	26	37
(% polymer)	79	91	74	63
% trans vinylene				
(in crude product)	59	70	56	48
(in polymer matrix)	75	77	76	76
% cis vinylene				
(in crude product)	20	21	18	15
(in polymer matrix)	25	23	24	24
GPC (Mn)	1,387,000	38,200	136,000	402,000
PDI (Mw/Mn)	1.2	2.7	5.8	2.1
DSC (Tg , °C)	33	58	25	-2
TGA (Temp. for 2% weight loss, °C)	181	207	169	169
Sample appearance	hard	hard	hard	rubbery

Table 5.4 The analysis of moulded articles produced at different curing temperatures.

The experimental results showed that the higher curing temperature seemed to be beneficial. It is clearly seen that the conversion, the thermal properties and the appearance of the moulded articles were improved by using higher curing temperature.

The appearance and the thermal properties of the moulded articles seem more closely related to the conversion than to the molecular weight, which is consistent with the result from section 4.4. All the final products showed *cis* vinylene contents generally of about 23-25% and showed a substantial weight loss in the temperature range 169-207 °C.

Experiment 2

The *exo*-C6M monomer (20 g, 0.08 mol) and the ruthenium carbene initiator (16 mg, 1.9 $x10^{-5}$ mol, monomer/initiator ratio 4,100/1) were mixed in a small reaction vessel and stirred at room temperature. A small amount of the reacting mixture was transferred into the nmr tubes after stirring the liquid mixture for 5 and 20 minutes. The initial reactions during 5 and 20 minutes were then analysed immediately by using ^{1}H nmr spectroscopy. After 20 minutes stirring, the reacting mixture was divided and introduced into 6 vials using a syringe. All the vials were placed in an oven at 160 °C and one was removed from the oven every 10 minutes. The moulded articles were obtained as clear yellow solids after cooling to room temperature by breaking away the glass. The final products were cut up and characterised using the ^{1}H nmr spectroscopy. The experimental results are shown in Table 5.5 and Figure 5.4.

^{1}H Nmr analysis of the samples taken from the reaction mixture after stirring the liquid mixture for 5 and 20 minutes, sample number 1 and 2 respectively, showed that a slow reaction took place after the monomer was mixed with the initiator. Longer initial mixing times lead to higher conversion and the viscosity of the mixture increased as the conversion increased. However, only 11% conversion was observed after the neat monomer was mixed with the initiator for 20 minutes at room temperature. This indicates that the monomer did not react appreciably in bulk at room temperature.

The conversion increased dramatically from 11% to 60% after the reactive mixture was introduced into a mould and the filled mould was kept in the oven at 160°C for 10 minutes, sample number 3. This indicates that the rate of this polymerisation can be activated by higher temperatures. It was found that the overall extent of the polymerisation increased and showed a roughly linear relationship with the curing time at 160°C, as shown in Figure 5.4.

Sample no.	Initial mixing time at room temp. (min)	Curing time at 160°C (min)	^{1}H nmr (% polymer in crude product)	Sample appearance
1	5	-	6	liquid
2	20	-	11	viscous liquid
3	20	10	62	rubbery
4	20	20	68	hard
5	20	30	75	hard
6	20	40	80	hard
7	20	50	87	hard
8	20	60	90	hard

Table 5.5 ^{1}H nmr analysis of moulded articles produced by varying the curing time.

Experiment 3

The *exo*-C6M monomer (20 g, 0.08 mol) and the ruthenium carbene initiator (17 mg, 2.1×10^{-5} mol, monomer/initiator ratio 3,900/1) were mixed in a small reaction vessel and stirred at room temperature for 20 minutes. After 20 minutes, reacting mixture was divided and introduced into 8 vials using a syringe. The vials were then placed in a hot oil bath at 60 °C. The first vial was removed from the hot oil bath after 10 minutes and was allowed to cool to room temperature. After 20 minutes, all remaining vials were moved from the oil bath. One of them was allowed to cool to room temperature and the other 6 vials were placed in an oven at 160 °C. At every 10 minutes, one vial was removed from the oven and was allowed to cool to room temperature. All moulded articles obtained were cut up and characterised using ^{1}H nmr spectroscopy. The experimental results are shown in Table 5.6 and Figure 5.4.

^{1}H Nmr analysis of the moulded articles showed that the rate of the polymerisation and the conversion are increased as the curing temperature increases. It was found that the improved process of experiment 3 provides the samples which contain a reduced amount of unreacted monomer in comparison with the data for the analogous experiment 2, see Figure 5.4. This might be because the reactive mixtures were allowed to polymerise at the moderated polymerisation rates, at 60 °C, before rapid reaction took place at 160°C. If the rapid reaction took place too early, the liquid mixture became highly viscous. At this stage, it may be that access to the active chain ends by the monomer is inhibited.

Sample no.	Initial mixing time at room temp. (min)	Curing time at 60 °C (min)	Curing time at 160 °C (min)	^{1} H nmr (% polymer in crude product)	Sample appearance
1	20	10	-	25	highly viscous liquid
2	20	20	-	32	soft rubbery
3	20	20	10	79	hard
4	20	20	20	83	hard
5	20	20	30	86	hard
6	20	20	40	94	hard
7	20	20	50	96	hard
8	20	20	60	96	hard

Table 5.6 The analysis of crude samples produced by varying the curing time and temperature.

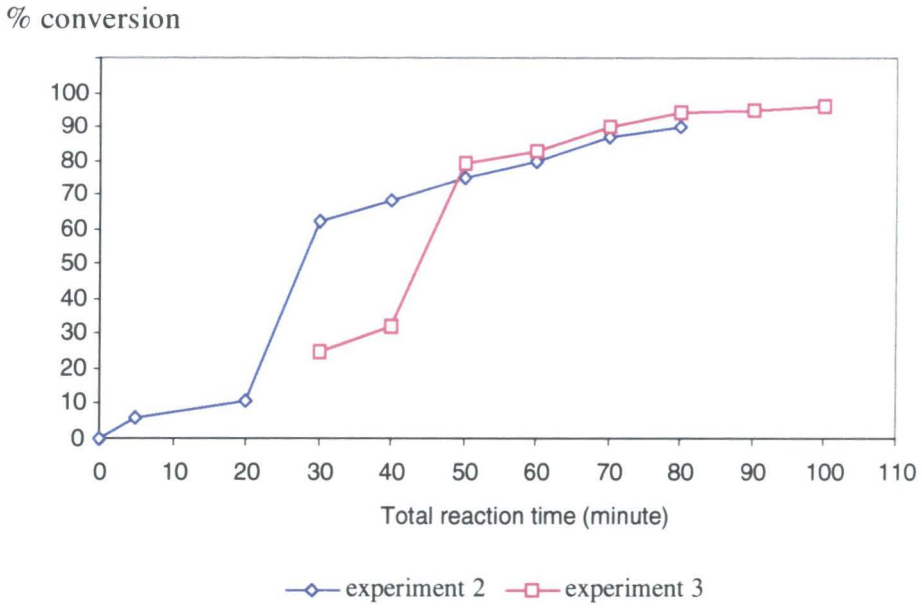

Figure 5.4 The extent of polymerisation of *exo*-C6M as a function of curing time and temperature profile (see experiments 2 and 3 for details).

5.2.5 Effect of the length of the pendant N-alkyl groups on conversion and product properties

Monomer	[M]/[I]	Initial mixing temperature (°C)	Initial mixing time (min)	Curing time at 60 °C (min)	Curing time at 160 °C (min)
exo-C3M	3,900	50	3	-	-
exo-C4M	3,800	35	20	20	60
exo-C5M	4,000	20	20	20	60
exo-C6M	3,700	20	20	20	60
exo-C8M	3,900	20	20	20	60

Table 5.7 Reaction condition for producing moulded articles from *exo*-CnM, where n = 3, 4, 5, 6, and 8.

In this section, the preparation of moulded articles derived from *exo*-monofunctional monomers (*exo*-C3M, *exo*-C4M, *exo*-C5M, *exo*-C6M and *exo*-C8M) using the reaction conditions shown in Table 5.7 is described. Polymerisation of *exo*-C3M, mpt. 45.5 °C, could not be carried out in the melt due to the high melting point of the monomer and the rapid reaction at this mixing temperature. Very rapid reaction took place within a few minutes when the melted monomer and the initiator were mixed and stirred at 50 °C. An attempt to transfer the reacting mixture from this reaction into the mould failed because the viscosity of the mixture was too high. The initial step of the polymerisation of *exo*-C4M, mpt. 32 °C, was carried out in the melt at an initial mixing temperature of 35 °C in an oil bath. The temperature of the oil bath was not allowed to rise above 40 °C in order to melt the monomer and slow the rate of the reaction down as much as possible. The mixture was well mixed for 20 minutes before being transferred to a glass mould. The moulded article was obtained as a clear yellow rigid solid. Polymerisation of *exo*-C5M, *exo*-C6M and *exo*-C8M, were carried out by stirring the monomer and initiator mixtures at room temperature for 20 minutes before being transferred to a glass mould. The moulded articles derived from *exo*-C5M and *exo*-C6M were obtained as clear yellow rigid solids. Whereas the moulded sample derived from *exo*-C8M was obtained as a very soft rubbery material, indicating low conversion. The conversion, the *cis/trans* content, the glass transition temperature of the moulded articles were determined by ^{1}H nmr spectroscopy and DSC. The ^{1}H nmr spectrum, and DSC trace of the moulded article derived from *exo*-C6M are shown in Figure 5.5, as a typical example. The conversion, *cis/trans* content, glass transition temperature of the moulded articles derived from *exo*-CnM, where n = 4, 5, 6 and 8, are recorded in Table 5.8.

(a)

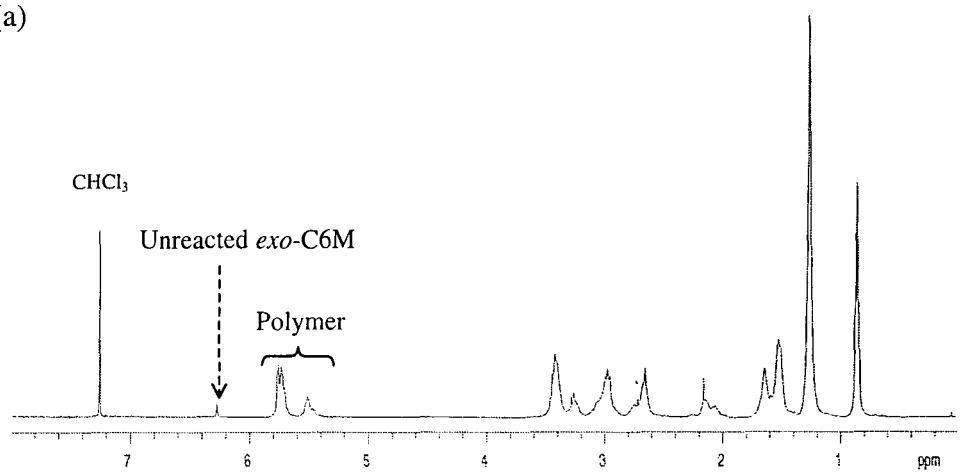

(b)

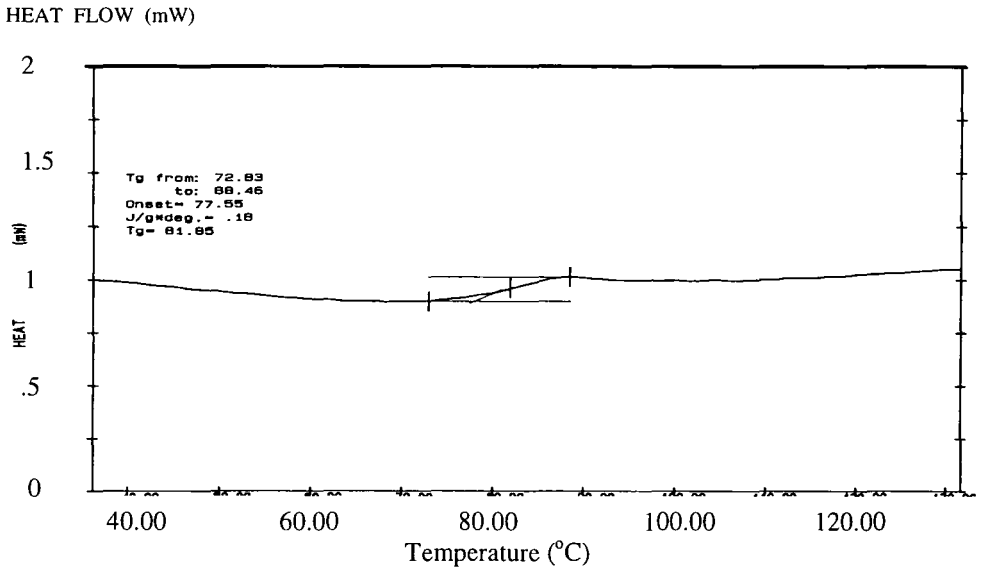

Figure 5.5 (a) ^{1}H nmr spectrum and (b) DSC trace of crude poly(*exo*-C6M).

Sample no.	^{1}H nmr			Tg (°C)		Sample appearance
	% conversion	% *Trans*	% *Cis*	DSC	DMTA	
1 *exo*-C4M	94	75	25	113	136	hard
2 *exo*-C5M	96	75	25	95	106	hard
3 *exo*-C6M	98	74	26	82	93	hard
4 *exo*-C8M	52	76	24	-55	-	soft rubbery

Table 5.8 The analysis of moulded articles produced with varying length of pendant N-alkyl groups.

^{1}H Nmr analysis of the products obtained indicated that moulded samples with a high conversion (94 to 98%) can be obtained under the conditions studied except for the product derived from *exo*-C8M. The data to hand is insufficient to construct an unambiguous explanation. However, it may be that the long pendant N-alkyl group in

the *exo*-C8M structure retards the polymerisation by steric inhibition of the propagating chain end from the monomer. Alternatively, the monomer might form micelles since the molecule has a relatively long nonpolar hydrocarbon chain and a polar head group, the ruthenium carbene initiator might dissolve in the hydrocarbon interior of the micelles and become ineffective. All the crude samples showed *cis* vinylene contents generally of about 24 to 26%. This indicates that the *cis/trans* content of the polymers is not affected by the length of the N-alkyl pendant groups.

Pieces of the plaques were cut for the DMTA analysis[1-3] (see Appendix 1 for the analysis details). The thermal and the mechanical properties of the materials derived from *exo*-CnM, where n = 4, 5, and 6, were determined, whereas the material derived from *exo*-C8M was too fluid to measure. The dynamic modulus curve and damping (tan δ) curve as a function of temperature for the material derived from *exo*-C6M are shown in Figure 5.6, as a typical example.

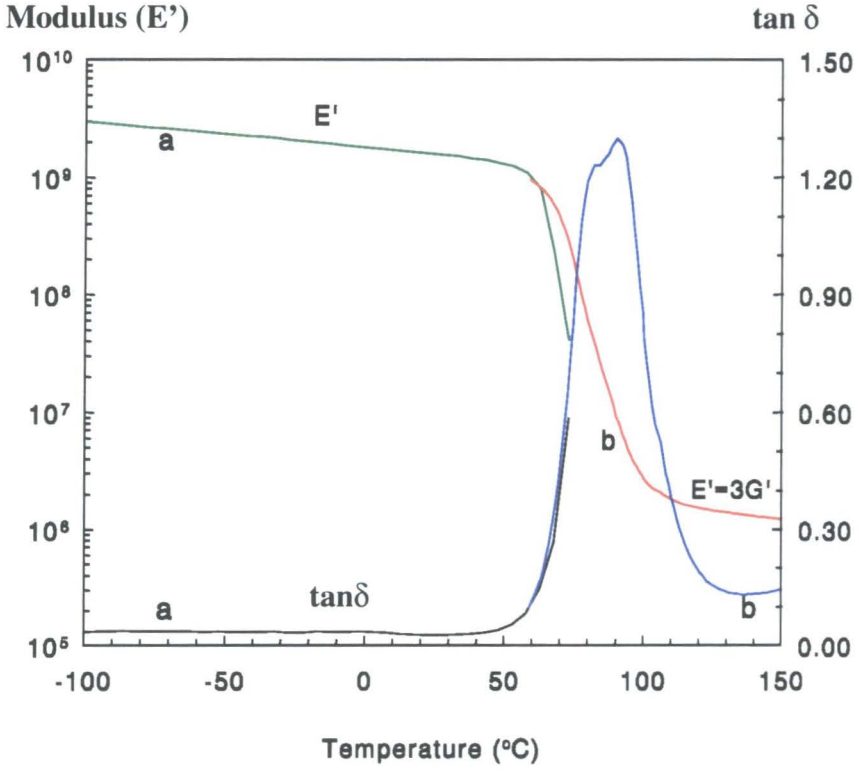

Figure 5.6 Modulus and damping curves for a material derived from *exo*-C6M using a dual cantilever beam geometry (RSAII dynamic analyser), curve **a** and a parallel plate geometry (RDAII dynamic analyser), curve **b**.

The data in figure 5.6 were obtained on a Rheometrics Dynamical Spectrometer. The behaviour of the materials at temperature below their glass transition temperature (Tg) was studied using a dual cantilever beam geometry (RSAII dynamic analyser) while near and above Tg a parallel plate geometry (RDAII dynamic analyser) was used. Curve **a** of figure 5.6 shows that at low temperature the modulus (E') of material derived from *exo*-C6M is high, about $3x10^9$ Pa (N/m^2), indicating low molecular motion of the polymer chain.[2] Whereas the damping or tanδ is low, which indicates that material has nearly perfect elastic behaviour at low temperature. The modulus decreases slowly as the temperature increases. At the glass transition region, curve **b**, the modulus decreases and the damping increases very rapidly. The damping peak or $\tan\delta_{max}$ occurs when part of the frozen-in segments become free to move and part of the energy is dissipated as heat. The comparative dynamic mechanical and damping (tanδ) curves as a function of temperature for moulded articles derived from *exo*-CnM, where n = 4, 5 and 6 are shown in Figure 5.7a and b.

As can be seen clearly in Figure 5.7a, the temperature at which the drop in the dynamic modulus occurred for materials derived from *exo*-CnM, where n = 4, 5 and 6, increased when monomers with the shorter N-alkyl groups were used. The damping peak or tan δ_{max} also shifts to higher temperature as the length of the pendant group gets shorter, as shown in Figure 5.7b. The increase in tan δ_{max} was in the same direction as the increase in Tg measured by DSC, see Table 5.8. However, it was observed that Tg values obtained from the DSC technique were about 10 °C lower than the those obtained from the DMTA. The glass transition decreases as the flexibility of the side group of the polymer chains increases when monomers with longer N-alkyl groups were used. These results are consistent with the results from section 4.4 where the pure linear polymers were obtained from solution polymerisation. It is interesting to note that the pure linear polymers obtained from section 4.4 showed higher Tg than the linear materials obtained in this section since there was no residual monomer in those samples to act as plasticiser.

(a)

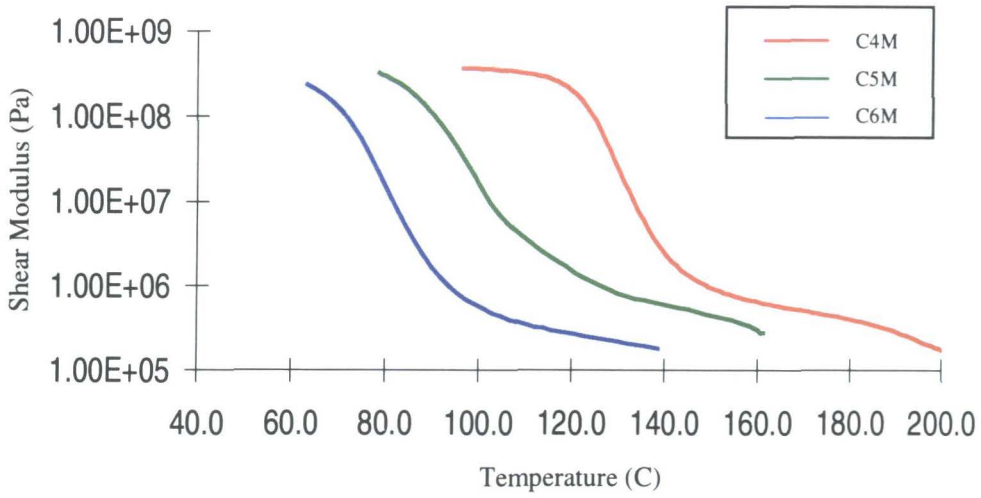

(b)

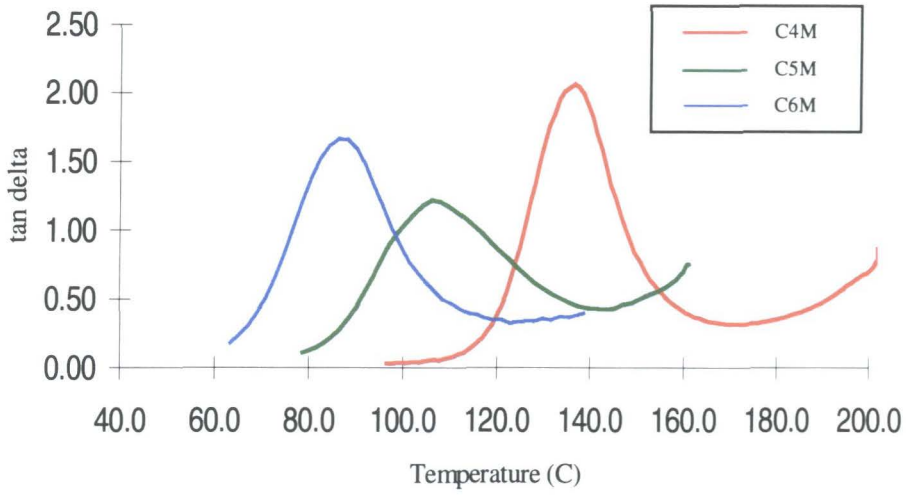

Figure 5.7 (a) the modulus curves and (b) damping or tanδ curved as a function of temperature for mould articles derived from *exo*-CnM, where n = 4, 5 and 6.

The mechanical properties of the materials derived from *exo*-CnM, where n = 4, 5 and 6, were determined using three point bending and parallel plate geometry (see Appendix 1 for the analysis details) and the relevant parameters are recorded in Table 5.9.

Sample no.	Meachanical Analysis			
	Three point bending			Parallel plate geometry
	Flexural modulus (GPa) at 20°C	Flexural strength (MPa) at 20°C	Mode of failure at 20°C	Shear Modulus (MPa) at Tg + 50°C
1 *exo*-C4M	2.36	85.3	brittle	0.33
2 *exo*-C5M	1.53	84.2	yield	0.37
3 *exo*-C6M	1.46	60.4	Yield	0.19

Table 5.9 Mechanical properties of moulded articles derived from *exo*-CnM, where n = 4, 5 and 6.

It was found that the flexural modulus, flexural strength and shear modulus decreased as the length of the pendant group increased. It is apparent that the materials with the shorter pendant groups are more rigid than those with the longer pendant group as the materials derived from *exo*-C4M showed a brittle failure at 20 ^{0}C, whereas materials derived from *exo*-C5M and *exo*-C6M showed a yield failure mode. This indicates that the mechanical properties of the materials are affected by the length of the pendant N-alkyl groups on the main chain of the linear polymers.

5.3 ROMP-processing of *exo*-mono and difunctional monomers

Trial bulk copolymerisation of *exo*-C6M and *exo*-C6D have been described previously in section 3.3. It was found that high initial mixing temperature at 50 °C was necessary in this reaction, since *exo*-C6D has a very limited solubility in *exo*-C6M. The rate of this reaction was very rapid and the mixture became highly viscous within a few minutes of addition of the initiator. This result suggests that *exo*-C6D is not suitable for using as a crosslinker for in-mould processing in which the reactive mixture is injected into a mould. In this section difunctional monomers with different sequences of methylene units separating the reactive imidonorbornene units, were used as

crosslinkers. It was expected that the difference in the spacer length between reactive norbornene units of the difunctional monomers would lead to different solubilities in the monomer and hence to different crosslinked materials and different properties. The determination of solubility of *exo*-C3D, C5D, C6D, C9D and C12D in *exo*-C6M was carried out at room temperature in a small test tube. *Exo*-C6M (3 g) was placed in the test tube with a stirrer. Small portions of known weight (about 0.1-0.25 g each time) of a solid difunctional monomer was added into the test tube. The mixture was stirred vigorously after each addition until the solid appeared to be insoluble. The amount of the solid difunctional monomers which can be dissolved in *exo*-C6M was recorded and the data are summarised in Figure 5.8.

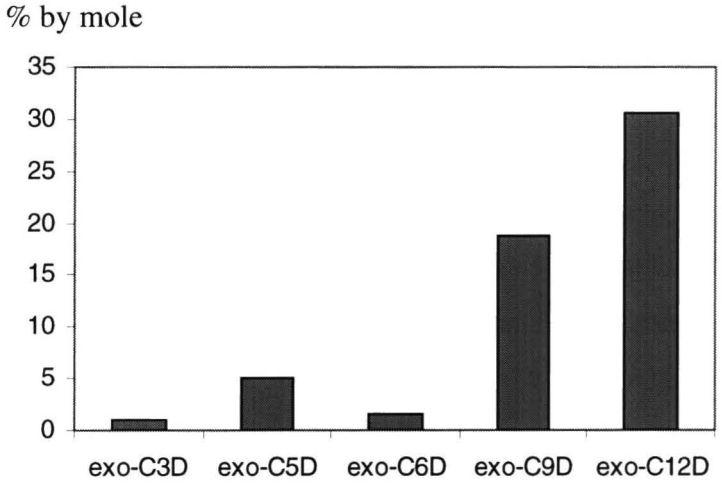

Figure 5.8 The solubility of the difunctional monomers in *exo*-C6M.

It was found that the solubility of the difunctional monomers increased as the spacer length between the reactive imidonorbornene units of the difunctional monomers increased, except when the *exo*-C6D was used. The data to hand are insufficient to explain this observation in detail. The effect of the spacer length between the reactive imidonorbornene units of difunctional monomers and the length of N-alkyl pendant groups of monofunctional monomers on the thermal and mechanical properties of the crosslinked materials were investigated and are discussed in section 5.3.1 and 5.3.2 respectively. Subsequently, the effect of the curing conditions were investigated and these experiments are discussed in section 5.3.3.

5.3.1 Effect of the spacer length between the reactive imidonorbornene units of difunctional monomers on gel content and product properties

The monomer (*exo*-C6M, 5 g) and crosslinking agent (*exo*-CnD where n = 5, 9 and 12, 5% by mole) were mixed and stirred at room temperature in a small reaction vessel until the crosslinking agent dissolved completely. The initiator (4-5 mg, monomer/initiator ratio ~ 4,000/1) was added into the mixed monomers and stirred for 15 minutes. The reacting mixture was transferred into a glass mould using a syringe. The filled mould was placed in an oven at 60 °C for 20 minutes and then at 160 °C for 60 minutes (this procedure will be called 'fast curing conditions' in section 5.3.3). All the crosslinked samples were obtained as clear pale yellow hard materials. The crosslinked polymers which are expected to be obtained are shown in Figure 5.9. The moulded articles were characterised using sol-gel extraction and the DMTA technique.

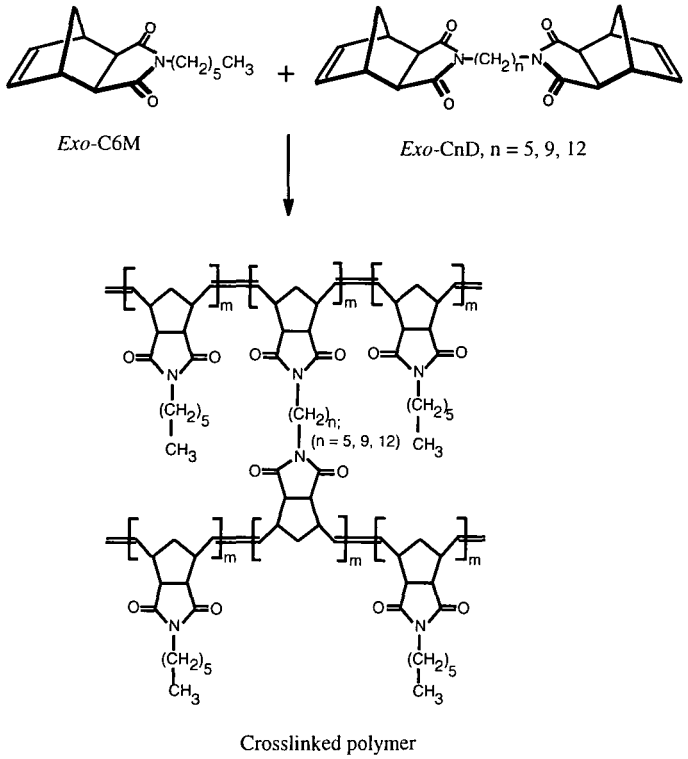

Figure 5.9 A schematic representation of the crosslinked polymers produced by varying the spacer between the main chains.

The results from sol-gel extraction experiments showed that the gel fraction of the crosslinked product increases when crosslinkers with shorter spacers between the reactive imidonorbornene units were used. The ^{1}H nmr spectrum of the sol fraction from sample number 3 is shown in Figure 5.10. It is apparent that there was linear and branched polymer, about 7.2%, in the sol fraction, which was about 3-4% of the crude material. The rest of the sol was unreacted monomer. This result is consistent with the results from section 3.3.1.2, where it was concluded that sol fractions consist mostly of unreacted monomer with a small proportion of linear and branch polymers. This indicates that monofunctional monomer gives material with a higher conversion than the crosslinked system under similar conditions. This might be because the gelation time was shorter in the latter system. Access of monomer to active chain ends might be inhibited and the polymerisation would not go to completion.

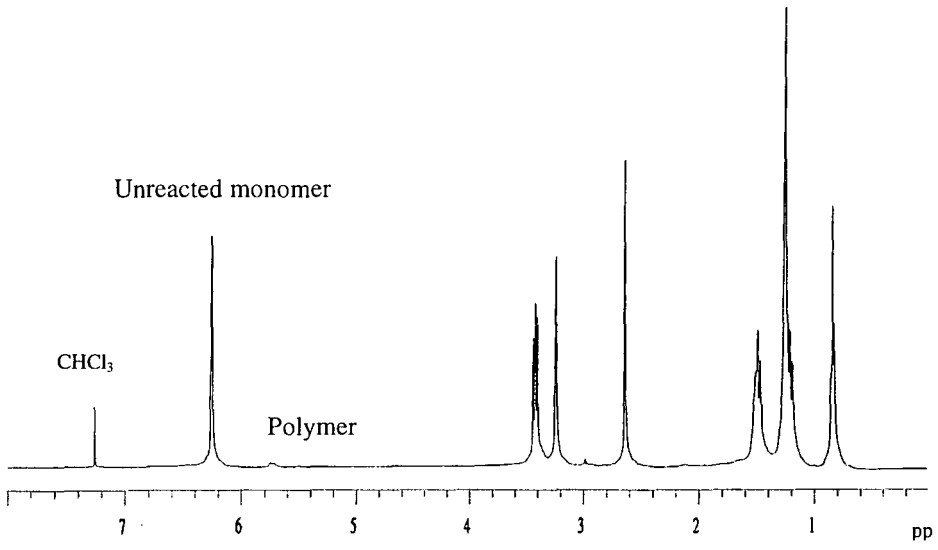

Figure 5.10 ^{1}H Nmr spectra of the sol fraction of sample derived from *exo*-C6M crosslinked with 5% loading of *exo*-C9D.

Pieces of the plaques derived from *exo*-C6M crosslinked with 5% loading of *exo*-CnD, where n = 5, 9 and 12, were cut for the DMTA analysis. The dynamic modulus and damping (tanδ) curves as a function of temperature are shown in Figure 5.11a and b respectively and the determined parameters are recorded in Table 5.10.

(a)

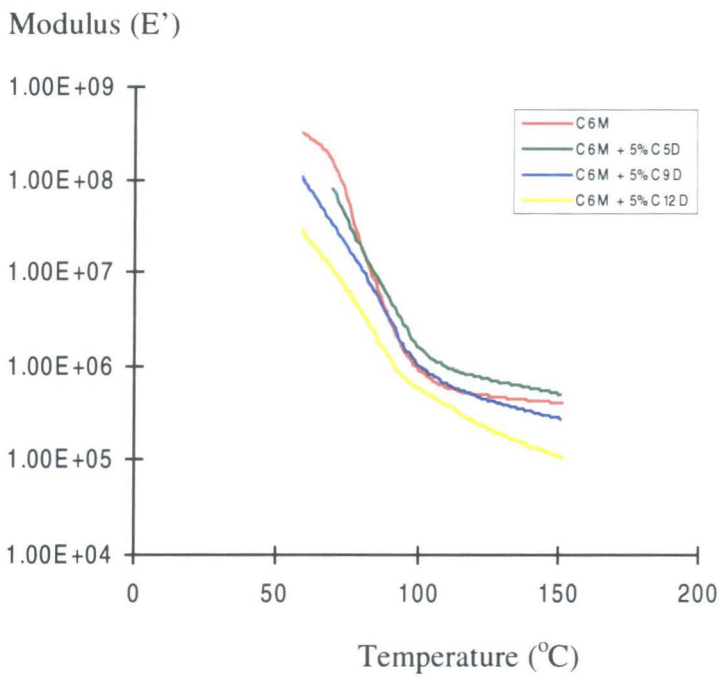

(b)

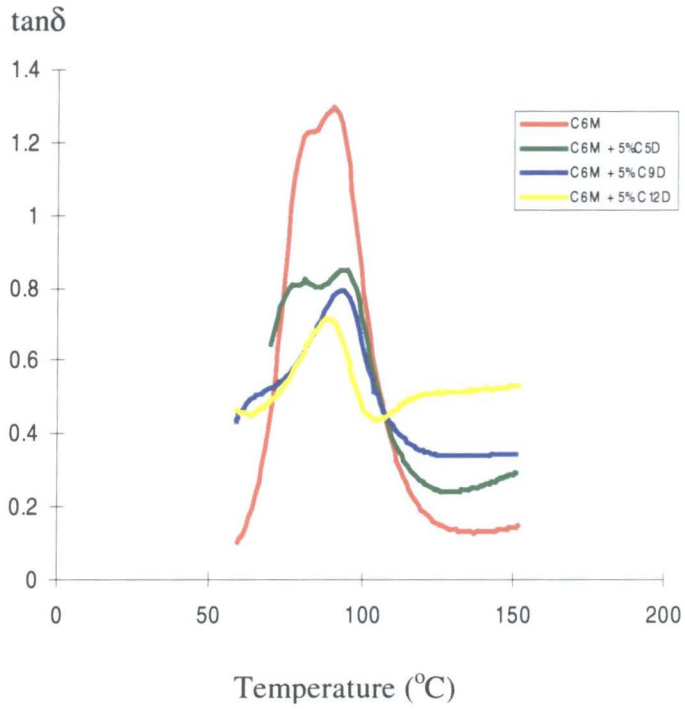

Figure 5.11 (a) The modulus curves and (b) damping (tanδ) curves as a function of temperature for moulded articles derived from *exo*-C6M crosslinked with 5 mole% loading of *exo*-CnD, where n = 5, 9, and 12.

Sample no.	% gel feaction	DMTA				Ratio Mc(Th.)/ Mc(Expt.)
		Tg (°C)	Shear modulus (G, MPa) at Tg + 50°C	Mc (kg/mol) at Tg + 50°C		
				Theory	Expt.	
1 *exo*-C6M	98*	87-93	0.19	-	-	-
2 *exo*-C6M + 5% *exo*-C5D	71	78-94	0.56-0.69	2.47	6.62	0.37
3 *exo*-C6M + 5% *exo*- C9D	59	92	0.31	2.47	12.46	0.20
4 *exo*-C6M + 5% *exo*-C12D	42	89	0.15	2.47	26.45	0.09

Table 5.10 The analysis of the moulded articles using *exo*-C6M as a monomer varying the crosslinking agent. * %conversion was determined from ^{1}H nmr analysis.

The mechanical analysis of crude materials which were obtained from *exo*-C6M, sample number 1, and *exo*-C6M crosslinked with a 5 mole% loading of *exo*-C5D, sample number 2, showed a broad transition with two peaks between 78 and 93 °C, indicating that inhomogeneous products were obtained. When 5 mole% loading of *exo*-C9D and *exo*-C12D were included in the feed stocks, samples number 3 and 4 respectively, the mechanical analysis of crude materials exhibited one relatively narrow peak which occurred within the same transition temperature range as samples number 1 and 2. These results indicate that the linear and crosslinked materials showed similar thermal property under the conditions studied. However, it is interesting to note that all the crosslinked products had an increase amount of unreacted monomer in comparison with the experiment in the absence of crosslinking agent in the monomer feed. As expected, the glass transition temperature of the crosslinked materials increases as the gel fraction increases. The shear modulus and the ratio Mc(theory)/Mc(expt.) (see page 65 chapter 3 for the details) increases as the spacer length between the functional groups in *exo*-CnD gets shorter. This indicates that a more crosslinked structure was obtained when the crosslinking agent with the shorter

spacer was used. This result is consistent with the result from section 4.5 where it was established that the difunctional monomer with shorter methylene spacer between the reactive imidonorbornene units reacted much more quickly than those with longer spacers. However, we were unable to determined the amount of the crosslinker which had reacted at both ends.

5.3.2 Effect of the length of N-alkyl pendant group of monofunctional monomer on gel content and product properties

The monomer (*exo*-CnM where n = 5, 6 and 8, 5 g) and crosslinking agent (*exo*-C5D, 5% by mole) were mixed at room temperature in a small reaction vessel and stirred until the crosslinking agent dissolved completely. In the experiment using *exo*-C4M as monomer feed, *exo*-C5D was dissolved in *exo*-C4M at 35 °C by placing the reaction vessel in an oil bath. The initiator (4-5 mg, monomer/initiator ratio ~ 4,000/1) was added into the mixed monomers and stirred for 15 minutes. The reacting mixture was transferred into a glass mould using a syringe. The filled mould was placed in an oven at 60 °C for 20 minutes and then at 160 °C for 60 minutes. The crosslinked polymers which are expected to be obtained are shown in Figure 5.12, below.

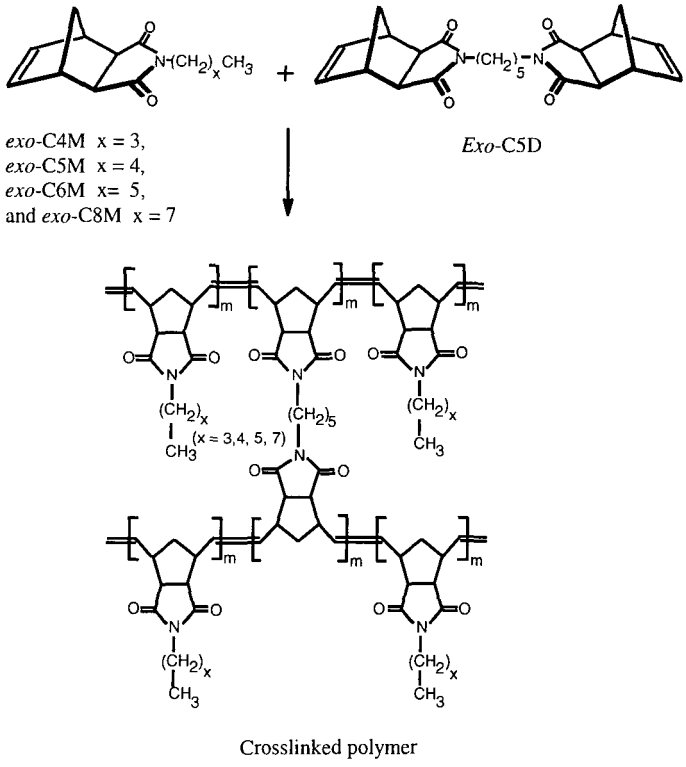

Figure 5.12 A schematic representation of the crosslinked polymers varying the length of the pendant groups on the main chain.

All the crosslinked samples were obtained as clear yellow hard solids, except for the sample using *exo*-C8M as monomer which was obtained as a rubbery solid, indicating low conversion. The crude samples were characterised using sol-gel extraction and the DMTA technique. All the parameters determined are recorded in Table 5.11 and the dynamic modulus and damping (tanδ) curves as a function of temperature are shown in Figure 5.13.

Sample no.	% gel feaction	DMTA				Ratio [Mc(th.)/ Mc(expt.)]
		Tg (°C)	Shear modulus (G, MPa) at Tg + 50°C	Mc (kg/mol) at Tg + 50°C		
				Theory	Expt.	
1 *exo*-C4M + 5% *exo*-C5D	91	130	0.32	2.19	13.20	0.17
2 *exo*-C5M + 5% *exo*-C5D	88	80-109	0.52	2.33	7.73	0.30
3 *exo*-C6M + 5% *exo*-C5D	71	77-94	0.56-0.69	2.47	6.62	0.37
4 *exo*-C8M + 5% *exo*-C5D	37	-14	-	2.75	-	-

Table 5.11 The analysis of moulded articles produced using *exo*-C5D as the crosslinking agent and varying the monomer.

The results from sol-gel extraction experiments showed that the gel fraction in the final products increased when monomers with shorter N-alkyl pendant groups were used. The material derived from *exo*-C8M, sample number 4, showed both very low conversion and Tg. This result is consistent with the results from section 5.2.5 where it was established that the *exo*-C8M showed a very low reactivity in this polymerisation system. The mechanical analysis of crude materials which were obtained from *exo*-CnM, where n = 5 and 6, crosslinked with a 5 mole% loading of *exo*-C5D showed a broad transition with two peaks at approximately 80 &109 and 77 & 94°C respectively, indicating that inhomogeneous crosslinked products were obtained. It is apparent that the thermal property of the crosslinked materials is affected by the amount of the gel

fraction and the flexibility of the N-alkyl pendant group on the main chain. The glass transition of the material is increased when the material has a greater amount of gel fraction and a shorter N-alkyl pendant group on the main chain. This is because the sol fraction acts as a plasticiser and long pendant groups increase the flexibility of the polymer chain.

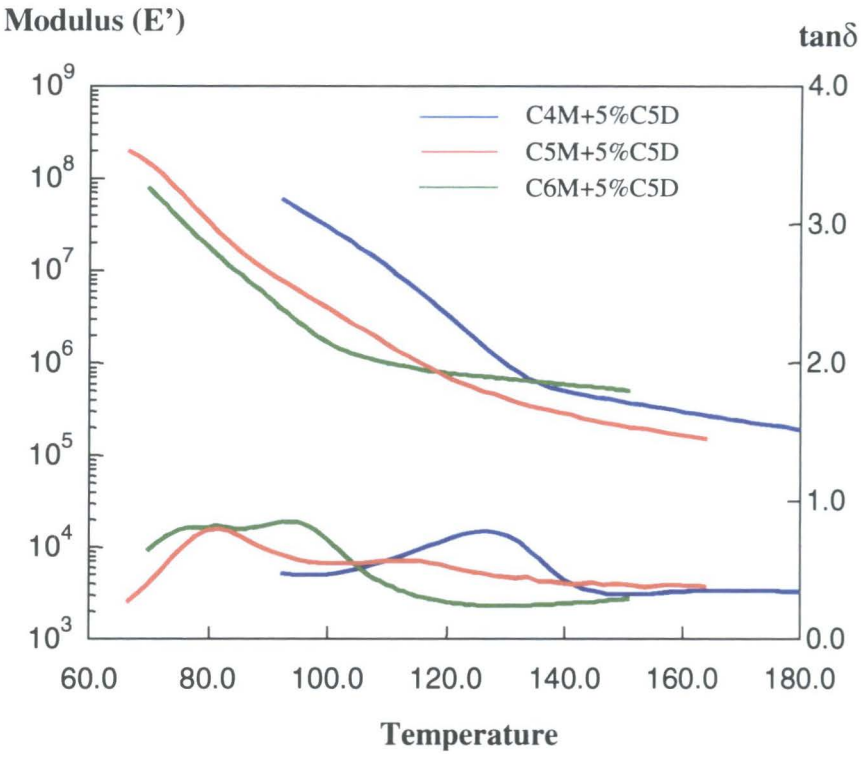

Figure 5.13 The modulus and damping curves as a function of temperature for mould articles derived from *exo*-CnM, where n = 4, 5, and 6, crosslinked with 5 mole% loading of *exo*-C5D.

The shear modulus and the ratio Mc(theory)/Mc(expt.) increased, whereas the molecular weight between the crosslink (Mc) decreased, when monomer with a longer N-alkyl group was used, see experiments 1, 2 and 3 respectively. We were unable to determined the shear modulus and the Mc of the material derived from *exo*-C8M crosslinked with 5mole% loading of *exo*-C5D, sample number 4, since it was too fluid at the temperature of measurement. The increase in the molecular weight between the crosslink (Mc) of the product derived from monomer with the shorter N-alkyl group crosslinked with a 5 mole% loading of the difunctional reagent, experiment 1, indicates that this polymerisation results a crosslinked polymer with longer monomer sequence

between crosslinks than those obtained from the polymerisations of the monomer with longer N-alkyl groups, sample number 2 and 3 respectively. It seems reasonable to suggest that the monomer with the shorter N-alkyl group is more reactive than those with the longer N-alkyl groups although this has not been proved.

5.3.3 Effect of curing condition and post cure on gel content and product properties

The monomer (*exo*-C6M, 5 g) and the crosslinking agent (*exo*-C6D, 1% by mole) were mixed and stirred in a small reaction vessel at room temperature until the crosslinking agent dissolved completely. The initiator was added into the mixed monomers and stirred for 15 minutes. For the fast curing experiment 1, the reacting mixture was transferred into a glass mould using a syringe. The filled mould was placed in an oven at 60 °C for 20 minutes and then at 160 °C for 60 minutes. For the slow curing experiment 3, the same procedure as fast curing experiment was used but the filled mould was kept at room temperature for an hour before was placed in the oven at 100 °C for 60 minutes. The samples were cut up and characterised using DMTA technique. Two other samples were treated in the same way except that the samples were kept in the oven at 160°C for 2 hours, experiments 2 and 4, to examine the effect of post cure. The modulus and damping (tanδ) curves as a function for temperature for the materials produced under slow and fast curing condition are shown in Figure 5.13a and b respectively and the parameters determined are recorded in Table 5.12.

The experimental results showed that slower curing and post curing conditions seem to be beneficial. The glass transition temperature of the material derived from *exo*-C6M with a 1% loading of *exo*-C6D under fast curing experiment 1 exhibited a lowering of Tg of about 16°C, in comparison with experiment 3 conducted under slow curing conditions. The shear modulus and the ratio Mc(theory)/Mc(expt.) increased, whereas the molecular weight between the crosslink (Mc) decreased, when the polymerisation was carried out under the slow curing condition, indicating a more crosslinked structure had been formed. The ratio of Mc(theory)/Mc(expt.) of the samples obtained under slow curing conditions, experiment 3, is close to unity, indicating near perfect crosslinking. This indicates that the amount of the crosslinker which has both ends reacted is increased in the materials obtained under slow curing condition as the

gelation was delayed during the period when the filled mould was kept at room temperature.

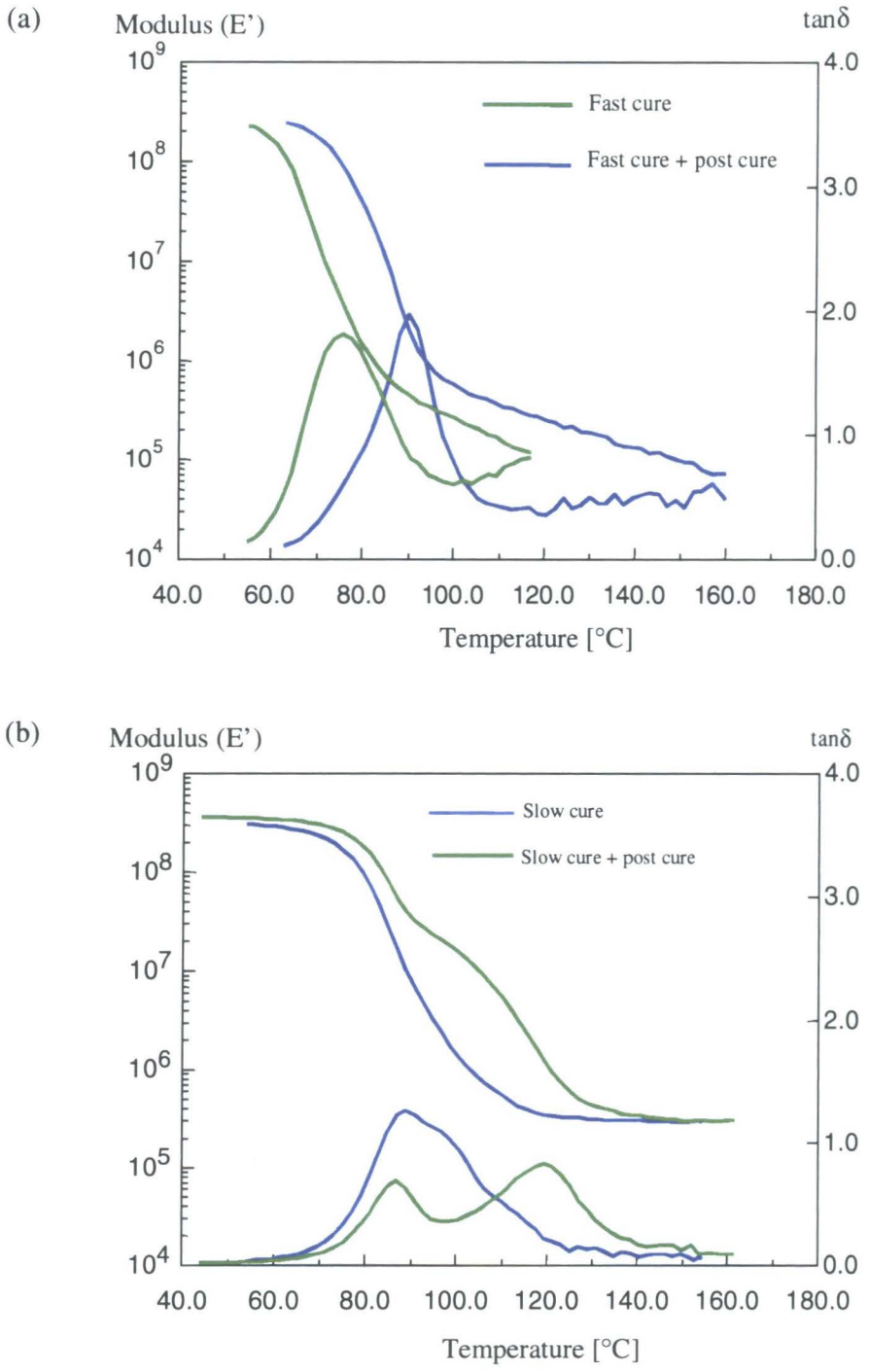

Figure 5.13 The modulus and damping (tanδ) curves as a function of temperature for materials produced from *exo*-C6M crosslinked with a 1 mole% loading of *exo*-C6D under (a) fast curing and (b) slow curing conditions.

experiment	Gel fraction	DMTA				ratio Mc(theory)/ Mc (Expt)
		Tg (°C)	Shear modulus (G, MPa) at Tg+50	Mc (kg/mol) At Tg + 50°C		
				Theory	Expt.	
1 *exo*-C6M+1%*exo*-C6D fast cure	35	76	0.09	12.35	41.06	0.30
2 *exo*-C6M+1%*exo*-C6D fast cure + post cure	76	92	0.10	12.35	25.60	0.48
3 exo-C6M+1%*exo*-C6D slow cure	97	92	0.31	12.35	12.62	0.98
4 *exo*-C6M+1%*exo*-C6D slow cure + post cure	98	92 & 119	0.31	12.35	13.36	0.92

Table 5.12 The analysis of the 'as-made' samples from in-mould processing under different curing conditions.

The gel content and the Tg of the fast curing sample, experiment 1, are increased by a factor of two after the material was post cured at 160 °C for 2 hours, experiment 2. As expected, the shear modulus and the ratio Mc(theory)/Mc(expt.) increased as well, whereas the molecular weight between the crosslink (Mc) decreased, indicating a more crosslinked structure was formed during the post curing. These results suggest that the unreacted monomer and the crosslinker which had one end unreacted may have reacted further during the post curing. It can be concluded that post curing is desirable to bring the sample to its final dimensionally stable state and to minimise the residual unreacted monomer, which is indicated by the increase in Tg.

The analysis of the crude material, experiment 4, which was obtained after the post curing of the slow curing sample, experiment 3, at 160 °C for 2 hours was similar in amount of the gel fraction, mechanical properties, Mc and ratio Mc(theory)/Mc(expt.) as the material obtained before post curing. These results suggest that the crosslinked

structure cannot be increased by post curing in the material which already has near perfect crosslinking. However, the post curing experiment did result in structural changes in the material as the glass transition temperature increased. The material, which was obtained after post curing the slow curing sample, exhibited two broad transition peaks after post curing for 2 hours at 160 °C. The second transition peak occurs at 119 °C, about 30°C higher temperature than the first transition temperature. The data to hand are insufficient to explain this observation satisfactorily; however, it may be that post curing at 160 °C for 2 hours was not long enough to bring the sample to the final stable state. It is clear that the cure protocol adopted in this last series of experiments gives a fully crosslinked product. This is indicated by the near 100% gel content, the approach of Mc(theory)/Mc(expt.) to unity and the constant plateau modulus above Tg.

5.4 Reference for Chapter 5

[1] 'Polymer Characterisation', B. J. Hunt and M. I. James, Blackie Academic & Professional, London, 1993.

[2] 'Mechanical Properties of Polymers and Composites', L. E. Nielsen, Marcel Dekker, Inc., New York, 1974.

[3] 'Encyclopedia of Polymer Science and Engineering', H. F. Mark, N. M. Bikales, C. G. Overberger, G. Menges, Volume 9, John Wiley & Son, New York, 1987.

Chapter 6

Overall conclusions and proposals for future work

6.1 Overall Conclusions

The work described in this thesis indicates that new polymeric materials using N-alkylnorbornene-5,6-dicarboxyimide as monomer and N,N'-alkylene-di(norbornene-5,6-dicarboxyimides) as crosslinking agent can be prepared via ROMP-processing. ROMP in bulk of *exo*- and *endo*-N-hexylnorbornene-5,6-dicarboxyimide (*exo*- and *endo*-C6M) using a well-defined ruthenium carbene initiator has been investigated. It was found that the *endo*-isomer is much less reactive than the corresponding *exo*-isomer in both linear and crosslinking polymerisations and largely fails to undergo ring-opening polymerisation in bulk under the condition studied. The relative reactivity of the *exo*- and *endo*-C6M was investigated using the ^{1}H nmr technique since the initiation and propagation steps of the polymerisations can be followed by this technique. The results from the nmr scale polymerisations confirms that the polymerisations are living and the order of the reactivity of chain end propagation and initiating alkylidene species was: *exo* derived alkylidene more reactive than initiator, which was more reactive than *endo* chain end species and that the *exo*-isomer was more reactive than *endo*-isomer. The process of producing triblock (*exo-endo-exo*) copolymer by sequential addition of *exo*- and *endo*-C6M was not well controlled and resulted in mostly diblock(*exo-endo*) copolymer with a small proportion of triblock material having very few long *exo*-sequences. The copolymerisation using an *exo-/endo*-C6M mixture produced block or blocky copolymers rather than statistical copolymers, which indicated that the ratio (r) of the reactivity of the *exo*-propagating species with *exo*-monomer to the reactivity of the *exo*-propagating species with *endo*-monomer $>>1$, or $r_x = k_{pxx}/k_{pxn} >>1$ and the ratio of the reactivity of the *endo*-propagating species with *endo*-monomer to the reactivity of the *endo*-propagating species with *exo*-monomer $<<1$, or $r_n = k_{pnn}/k_{pnx} <<1$.

The results from the preparative scale homo and block copolymerisation of *exo*- and *endo*-C6M indicates that inclusion of the *endo*-monomer in the feed results in poor reactivity and low conversion. The *cis/trans* content and the thermal properties of the resulting polymers depends upon the amount of each monomer isomer incorporated into the polymer chain. Polymers derived from *exo*-isomer were recovered in high conversion (>90%) and showed the majority of double bonds having the *trans* configuration in the linear polymer generally about 80%. Block copolymers

were recovered in moderate conversion (65-75%) and showed *trans* vinylene configurations of between 90-95%. Whereas, under similar conditions with pure *endo*-isomer only *trans* stereochemistry was observed and conversion was low (<20%). The glass transition temperature of these pure linear polymers correlated with the *trans* content rather than the molecular weight. The *endo*-polymers, which are all *trans* at the vinylenes, exhibited the highest Tg at about 115-118 °C, where as the *exo*-homopolymer and copolymers exhibit glass transitions at about 85-88 °C.

Pure linear polymers, poly(*exo*-CnM) where n = the number of carbon atoms in the alkyl group, can be obtained without residual unreacted monomer from solution polymerisation. It was found that the thermal properties of the polymers are affected by the length of the N-alkyl pendant group but not by the number average molecular weight (Mn) in the range of Mn investigated. However, the Mn of the linear polymers can be controlled and showed a roughly linear relationship with the [M]/[I] ratio. Highly crosslinked polymers, poly(*exo*-CnD) where n = the number of methylene unit separating the reactive imidonorbornene units, were successfully prepared in high conversion (>90%) from solution polymerisation of the difunctional monomers. The degree of swelling and crosslink density are affected by the length of methylene spacer between the polymer chain. Polymers with shorter methylene spacer showed higher degrees of swelling than those with longer methylene spacer, indicating a lower crosslink density in such products.

The optimal conditions for preparing the linear and crosslinked polymeric materials via ROMP-processing have been developed. Only *exo*-monomers were used as the monomers feed in these experiments, since in bulk polymerisation the *endo*-monomer was found to terminate the chain growth and the unreacted monomer was found to be a very effective plasticiser and permanently plasticised the final products. The conversions and the properties of the materials are affected by the polymerisation formulation, initial mixing time and temperature, curing conditions, the length of the pendant N-alkyl groups on the main chain and the spacer length between the functional groups in the crosslinker. A monomer/initiator ratio of about 4,000 was found to be optimal for in-mould processing. The monomer and the initiator should be mixed efficiently for about 20 minutes in order to dissolve the initiator at low temperature, it was established that, under these conditions, the monomer did not react appreciably

before being transferred to a mould. A curing time of about 60 minutes at high temperature, 160 °C, seems to be beneficial for producing linear material. The overall extent of the polymerisation is increased at high curing temperature and showed a roughly linear relationship with the curing time. However, it was found that the materials with the highest conversions were obtained when the mixtures were allowed to polymerise at moderate polymerisation rates, at 60°C for 20 minutes, before rapid reaction took place at high temperature, 160 °C for an hour. By using these optimal conditions, the linear polymeric materials derived from the *exo*-monofunctional monomers, *exo*-C4M, C5M and C6M, were obtained in high conversion (94 to 98%), whereas low conversion material was obtained when *exo*-C8M was used as monomer feed. All the crude materials showed *cis* vinylene contents generally of about 24 to 26% which are not affected by the length of the N-alkyl pendant groups. The thermal and mechanical properties, Tg, flexural modulus, flexural strength and shear modulus, of the linear materials decrease as the N-alkyl pendant group gets longer.

Crosslinked materials can be obtained by polymerising a difunctional monomer with a monofunctional monomer in a manner where the difunctional monomer acts as a crosslinker. The solid difunctional monomer was dissolved in liquid monofunctional monomer prior to addition of the initiator. Shorter N-alkyl pendant groups on the main chain and shorter methylene spacer length between the reactive functionalities of the crosslinker lead to an increase in the glass transition temperature of the crosslinked materials. By contrast, the mechanical properties and the Mc(theory)/Mc(expt.) ratios were increased when materials were obtained using crosslinking agents with shorter spacers and monomers with longer N-pendant groups. It was found that the optimal conditions for producing linear materials were not appropriate for preparing good crosslinked materials. For well-cured crosslinked materials, the reacting mixture should be allowed to polymerise under slow curing conditions in a mould at room temperature for an hour before rapid reaction takes place at high temperature, 100 °C. The crosslinked material which was obtained in this way showed improved thermal and physical properties. The post curing experiments have been shown to be desirable to bring the sample to its final dimensionally stable form and/or to minimise the amount of unreacted monomer in the product.

6.2 Proposals for future work

The work described in this thesis involved preparing the linear and crossliked materials of imidonorbornene derivatives using Grubbs' ruthenium carbene as an initiator. This work illustrated that slow reaction rate at low temperature and rapid reaction at high temperature in these polymerisation systems allows the preparation of moulded materials with high conversion and good properties. The system has potential for the preparation of products ranging in properties from soft elastomers to brittle and highly crosslinked materials. This was achieved by changing the polymerisation formulation, i.e. the monomer, the crosslinker and the polymerisation conditions. The characteristics of this system lead to the possibility of producing materials by RTM (Resin Transfer Moulding)[1-3] in which the low viscosity of the mixture at low temperature allows the reactive mixture to infuse the reinforced shape in the mould completely.

In this thesis only 1 and 5 mole% loading of the crosslinking agent has been investigated in any detail. Thus it would be worth exploring the effect of different loadings of crosslinking agents in the feed, and further exploration of the cure protocol. ROMP in this work was initiated using a well-defined ruthenium carbene initiator namely, $Cl_2[(C_6H_{11})_3P]_2Ru{=}CHC_6H_5$ **(a)**. However, it would be interesting to ROMP these imidonorbornene derivatives using monosubstitued imidazolinylidene as a ligand at the metal centre **(b)**. The resulting initiator is less reactive at room temperature but displays greater reactivity at high temperature than **(a)**.[4]

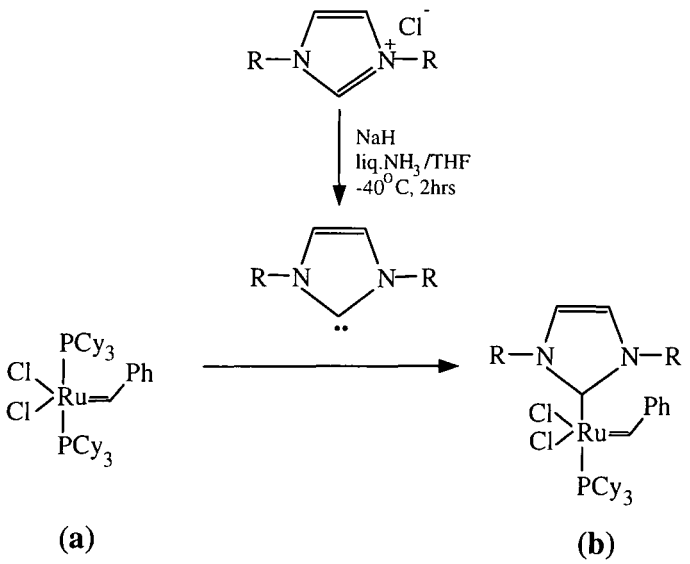

New derivatives of norbornene could be explored as monomers, e.g. ester, ketone and other functionalities, and this would extend the range of materials available via this relatively simple procedure.

6.3 References for Chapter 6

[1] C. D. Rudd, E. V. Rice, L. J. Bulmer, and A. C. Long, *Plast., Rubb. and Compos. Process. Appl.*, **20**, 67, 1993.

[2] 'Liquid Moulding technologies' , C. D. Rudd, A. C. Long, K. N. Kendall, and C. G. E. Mangin, Woodhead Publishing Limited, London, 1997.

[3] K. N. Kendall and C. D. Rudd, *Polym. Compos.*, **15**(5), 334, 1994.

[4] M. Scholl, T. M. Trnka, J. P. Morgan, and R. H. Grubbs, Tetrahedron Letters, 40, 2247, 1999.

Appendix 1

Instrumentation and procedures for measurements

- **NMR** ^{1}H, ^{13}C, COSY, HETCOR, and DEPT spectra were recorded either on a Varian VXR 400 nmr spectrometer at 399.953 MHz (^{1}H) and 100.577 (^{13}C) or Varian Gemini nmr spectrometer at 199.532 MHz (^{1}H) and 50.289 MHz (^{13}C); deuterated chloroform, deuterated dichloromethane, deuterated acetone were used as solvents.

- **INFRARED SPECTRA (IR)** were recorded on a Perkin Elmer 1600 series FTIR. The spectra were recorded as solvent (chloroform) cast films (polymers) or KBr discs.

- **ELEMENTAL ANALYSIS** were carried out on a Exeter Analytical, Inc. CE-440 elemental analyser.

- **MASS SPECTRA (MS)** were recorded on a VG analytical model 7070E mass spectrometer or VG TRIO 1000 mass spectrometer coupled to HP5890 SERIES II gas chromatrography.

- **GEL PERMEATION CHROMATOGRAPHY (GPC)** analyses were performed on chloroform solutions using a Knauer HPLC pump (Model 64), water Model R401 differential refractometer detector and 3 PLgel columns with pore size of 10^2, 10^3, and 10^5 ^{o}A (column packing PL gel 5 μm mixed styrene-divinyl benzene beads). The sample solutions (concentration 0.2%) were filtrated through a Whatman WTP type 0.2 μm filter to remove any particulate before injection. The columns were calibrated using Polymer Laboratories polystyrene standards.

- **DIFFERENTIAL SCANNING CALORIMETRY (DSC)** was carried out using a Perkin Elmer DSC 7 or a Pyris 1 differential scanning calorimeter over the temperature range of 25 to 200 ^{0}C (heating rate 10 ^{0}C min^{-1}).

- **THERMOGRAVIMETRIC ANALYSIS (TGA)** was performed using a Stanton Redcroft TG 760 thermobalance. TGA traces were recorded by increasing the sample temperature from 20 ^{o}C to 650 ^{o}C by 10 ^{o}C per minute under a nitrogen atmosphere and the 2% weight loss temperature was taken as the decomposition temperature.

The following measurements were carried out by Drs. P. Hine and R. A. Duckett in the Physics Department, Leeds University.

- **DENSITY COLUMN** was used to determine the density of the materials.

- **THREE POINT BENDING GEOMETRY** was used to determine the flexural strength in accordance with ASTM D790. The span was 23.2 mm and the specimens were 35 to 50 mm long, 3 to 4 mm wide and 4 to 5 mm thick depending upon the plaque size available. The cross head speed was 0.5 mm/minute which is equivalent to a strain rate of $1x10^{-5}$ S^{-1}. The following equation was used to calculate the flexural strength:

$\sigma = 6PL / 4WT^2$ where σ = Flexural stress, L= Span between loading points, W = sample width, T = Sample thickness and P = Load at the centre point.

- **DYNAMIC MECHANICAL THERMAL ANALYSIS (DMTA)**

Dynamic mechanical analysis measures the deformation of a material in response to a periodic force. The measurements are generally made to calculate an elastic modulus and a mechanical damping or dissipation of energy as heat. Viscous liquids can not store potential energy like elastic materials, for example a spring or rubber band, do when they are stretched. All the energy used in deforming them is dissipated into heat and the amount of energy dissipated as heat is called the mechanical damping. Polymers are viscoelastic materials which have both characteristics of elastic material and viscous liquid. Dynamic mechanical tests are useful for studying the mechanical properties of the polymers since the mechanical properties of the polymer are very sensitive to glass transition, crystallinity, crosslinking and phase separation. At low temperature, the molecular motion of the polymer chain is low, so the modulus is high. The material then shows nearly perfect elastic behaviour, like a stiff spring, thus it shows low damping. At temperatures above the glass transition temperature, the molecular segments are free to move, so the modulus is lower. The material is in a rubbery stage which stores energy without dissipating it to heat, thus the damping is also low. The damping peak occurs in the transition region where some of the frozen segments become free to move. The frozen segments store much more energy than the rubbery segments and the excess energy is dissipated as heat. At the glass transition

temperature the polymer has expanded to the extent that there is enough free volume available in the material to begin the molecular motion. In this work DMTA was measured using a Rheometrics Dynamic Mechanical Spectrometer. The behaviour of the materials at temperatures below their glass transition temperature (Tg) was studied using a RSAII dynamic analyser using a dual cantilever beam geometry while near and above Tg a RDAII dynamic analyser using a parallel plate geometry was used.

Dual Cantilever Beam Geometry

The dual cantilever beam geometry was used to measure the flexural modulus, E, of the materials at 20 ^{o}C and any relaxations below the glass transition. The sample was clamped at both ends and in the centre from where a dynamic displacement is applied. The test frequency was 10 rads and the dynamic strain was 0.005.

Parallel Plate Geometry

The parallel plate geometry was used to determine the glass transition temperature and the shear modulus at and above the Tg of the materials. The plate diameter was 10 mm and the gap between the plates was approximately 3 mm.

Appendix 2

Analytical data for Chapter 2

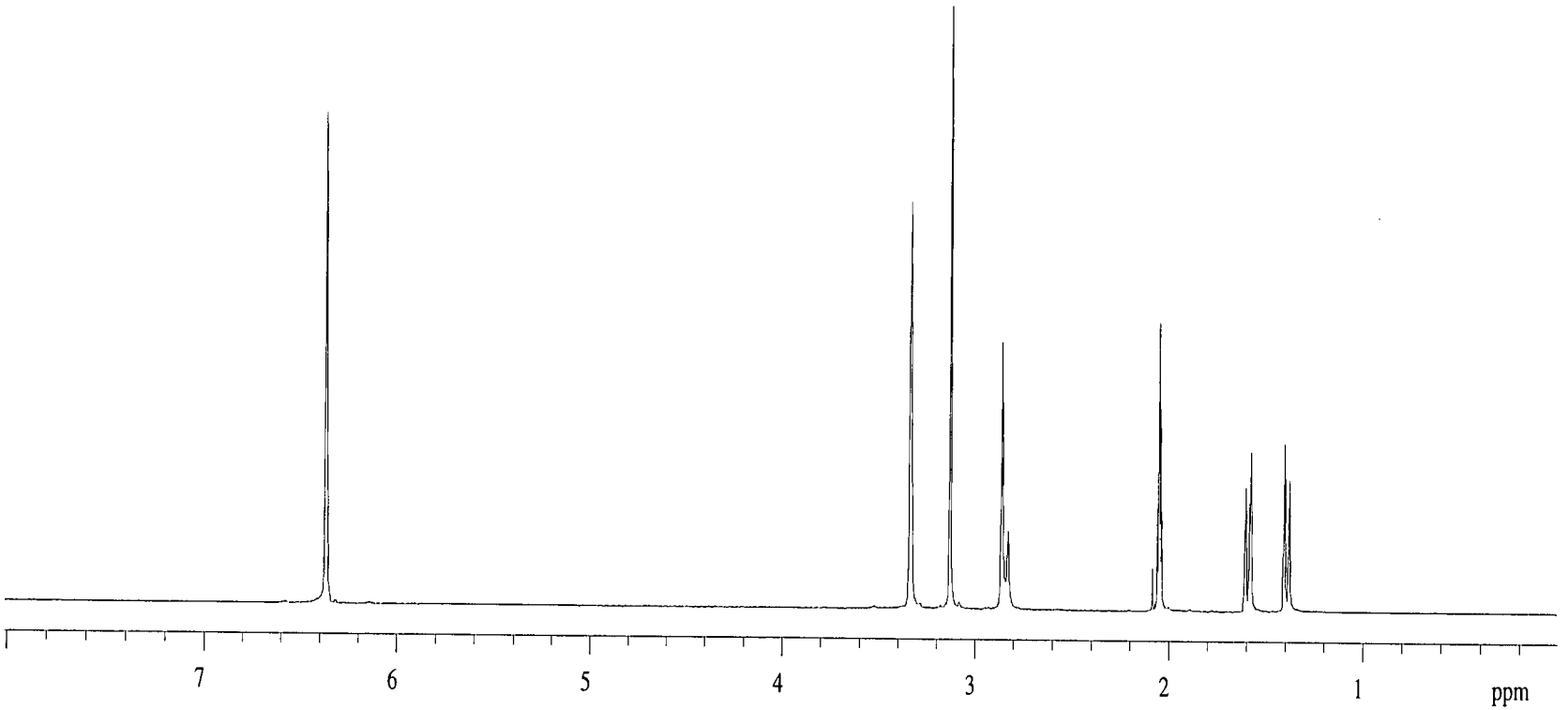

Appendix 2.1 ^{1}H nmr spectrum of *exo*-AN.

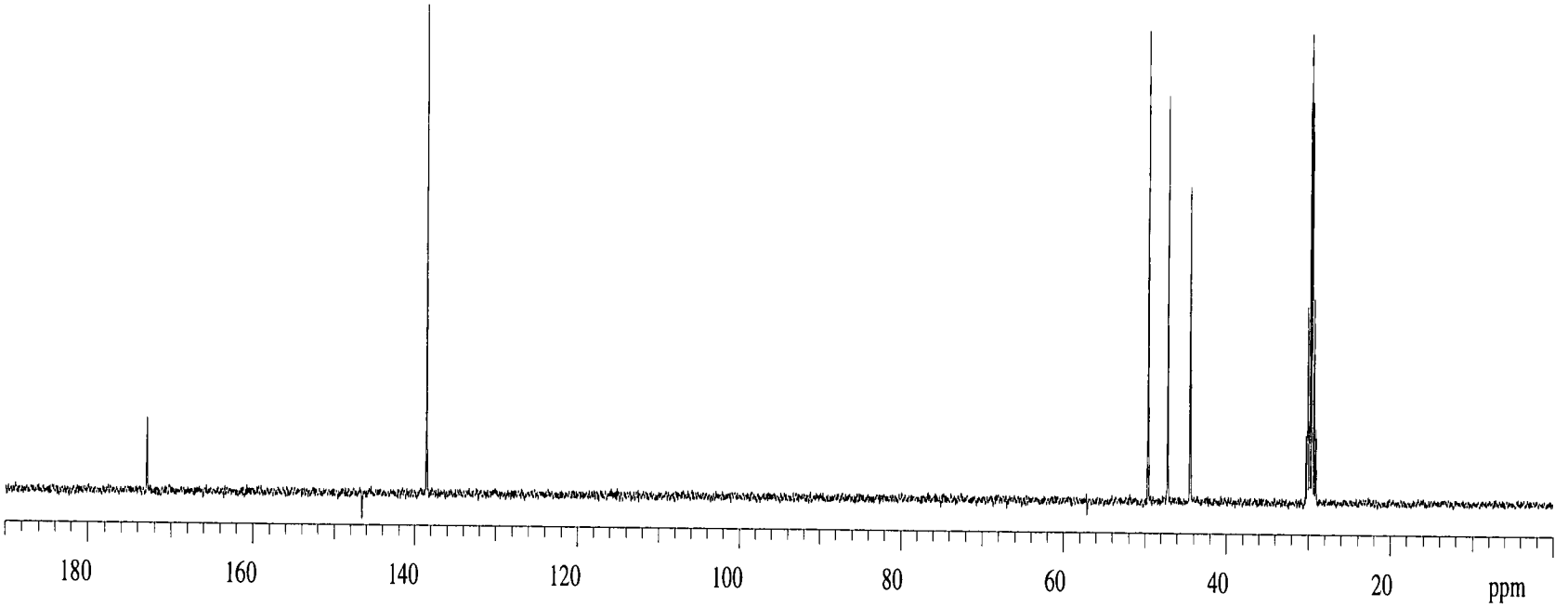

Appendix 2.2 ^{13}C nmr spectrum of *exo*-AN.

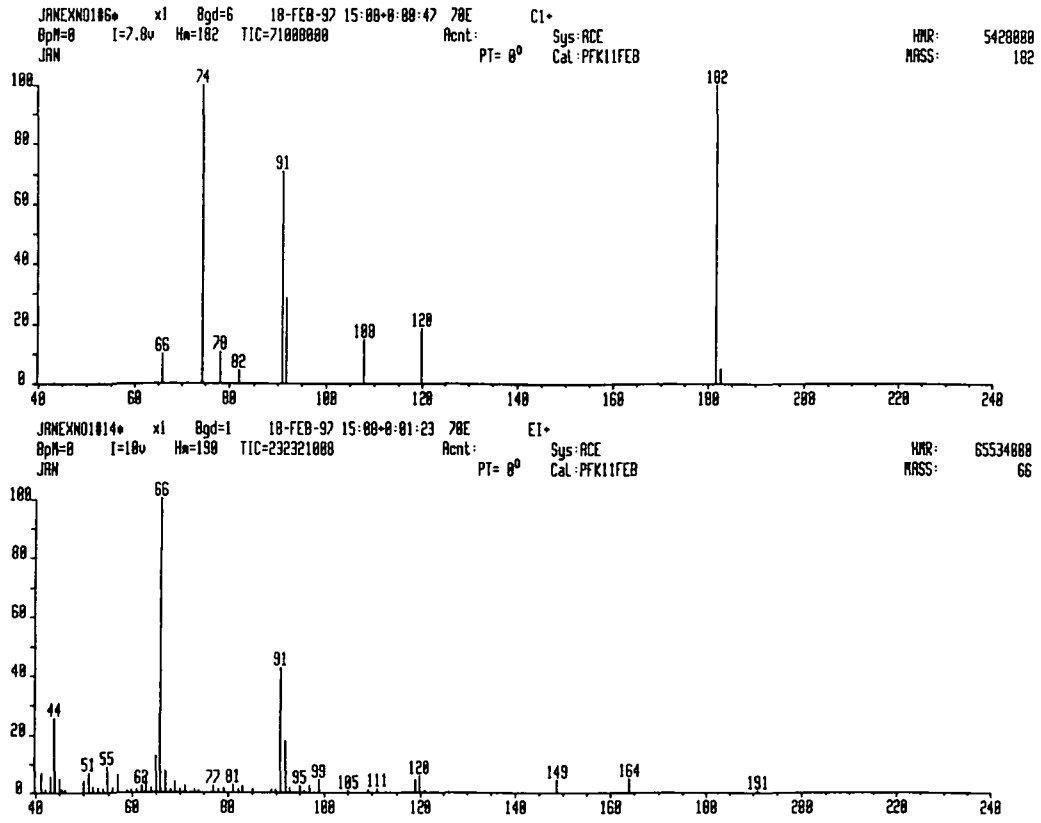

Appendix 2.3 Mass spectrum of *exo*-AN.

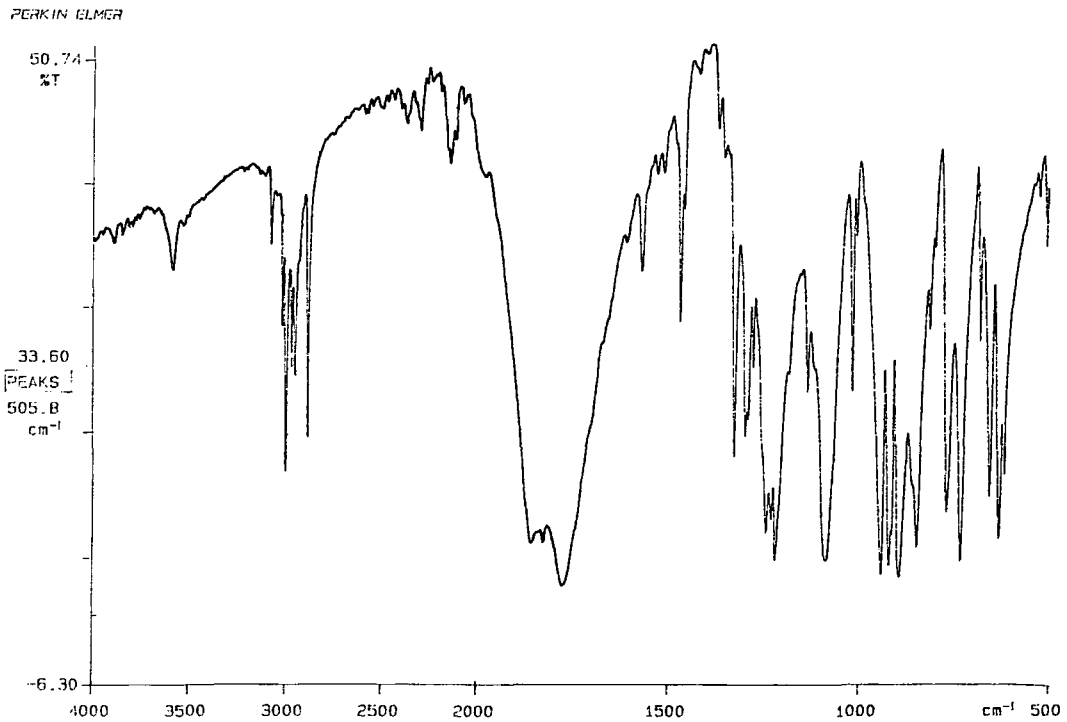

Appendix 2.4 Infrared spectrum of *exo*-AN.

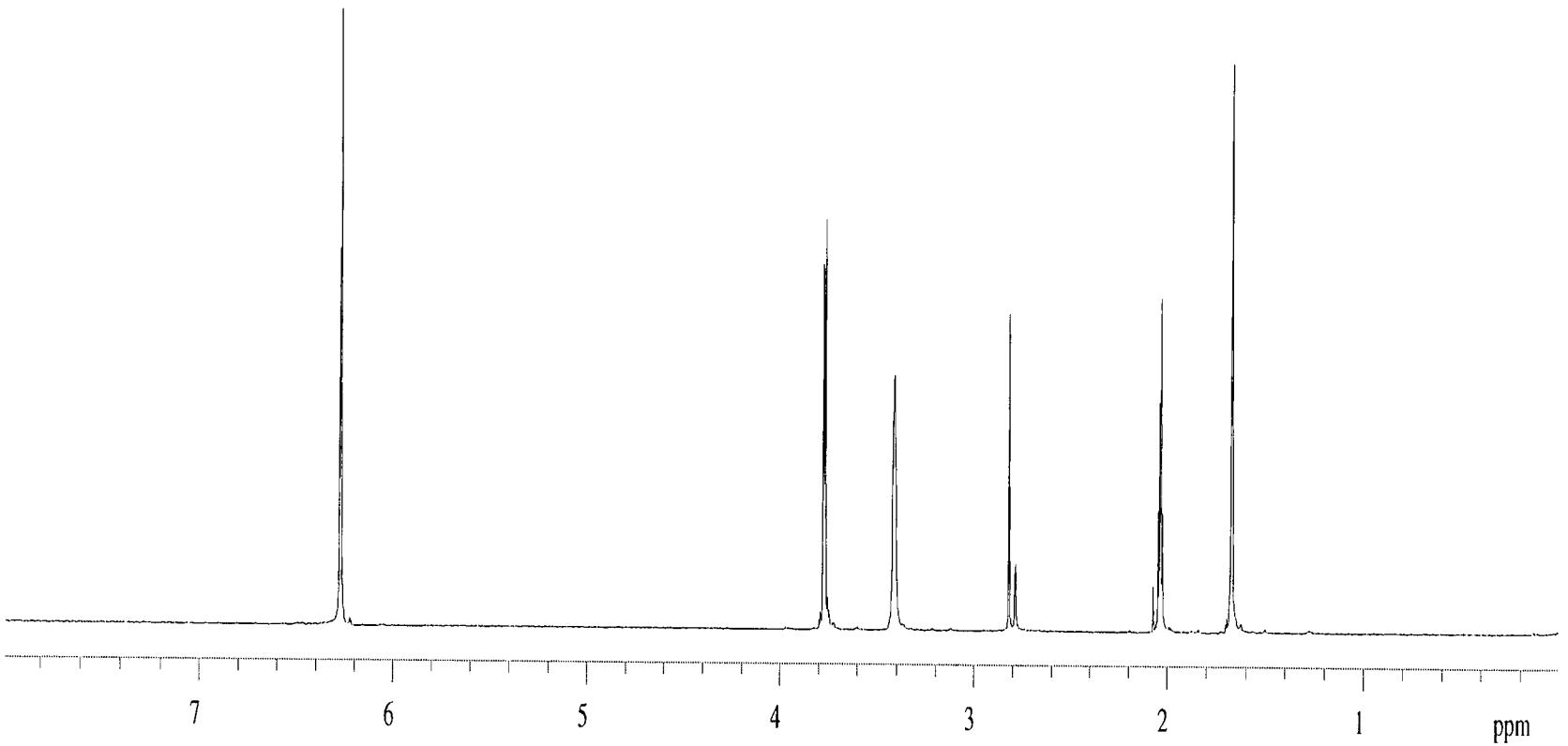

Appendix 2.5 ^{1}H nmr spectrum of *endo*-AN.

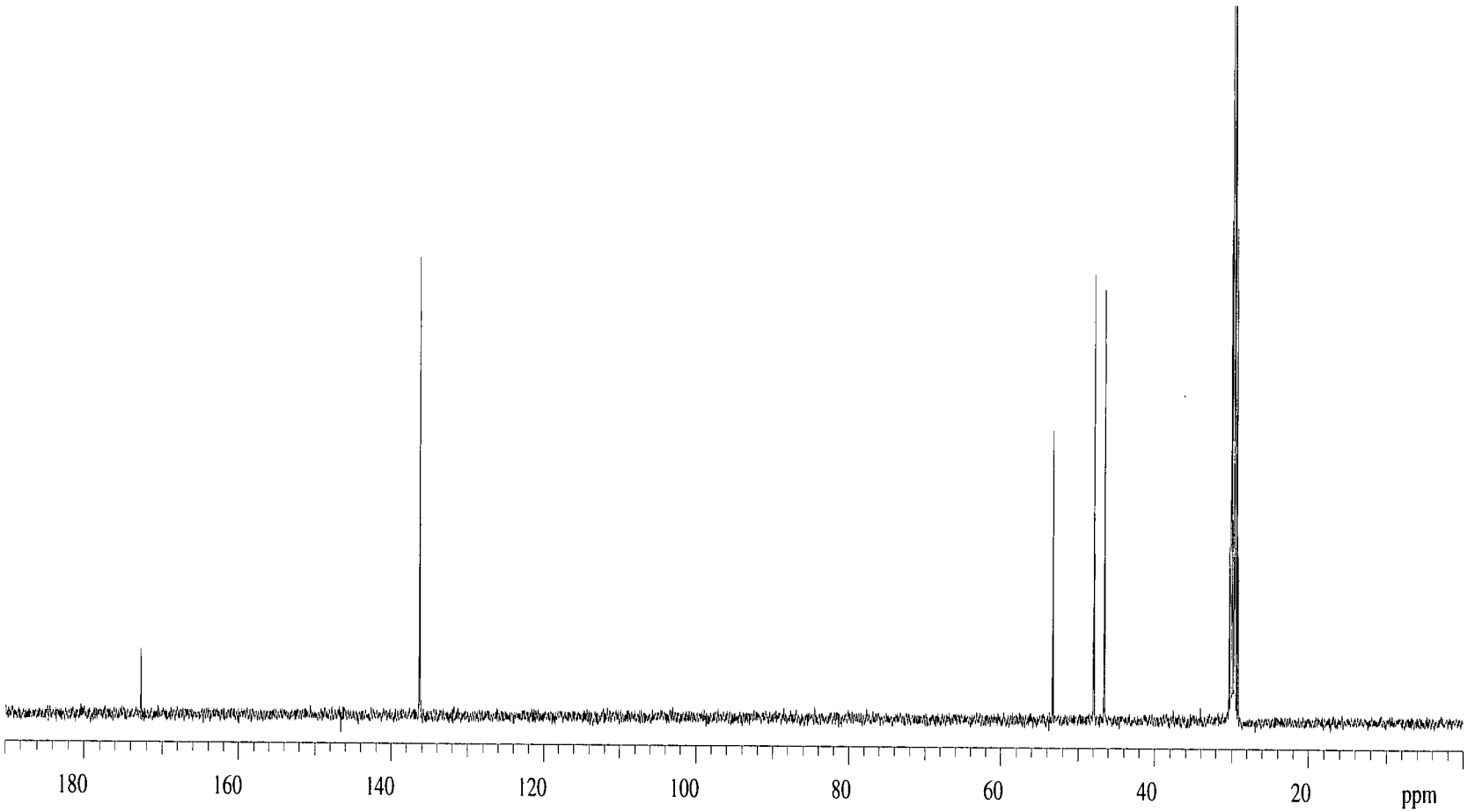

Appendix 2.6 ^{13}C nmr spectrum of *endo*-AN.

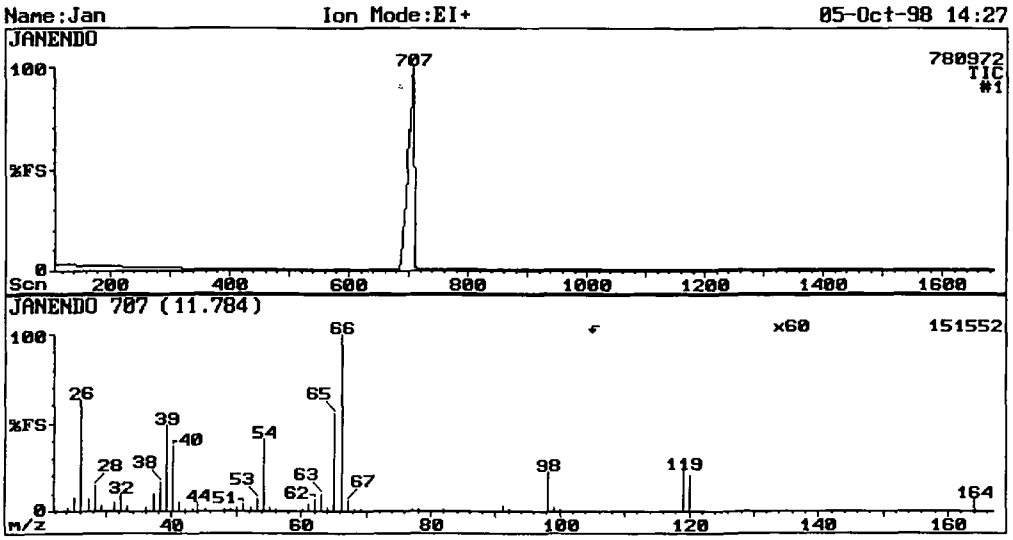

Appendix 2.7 GC-Mass spectrum of *endo*-AN.

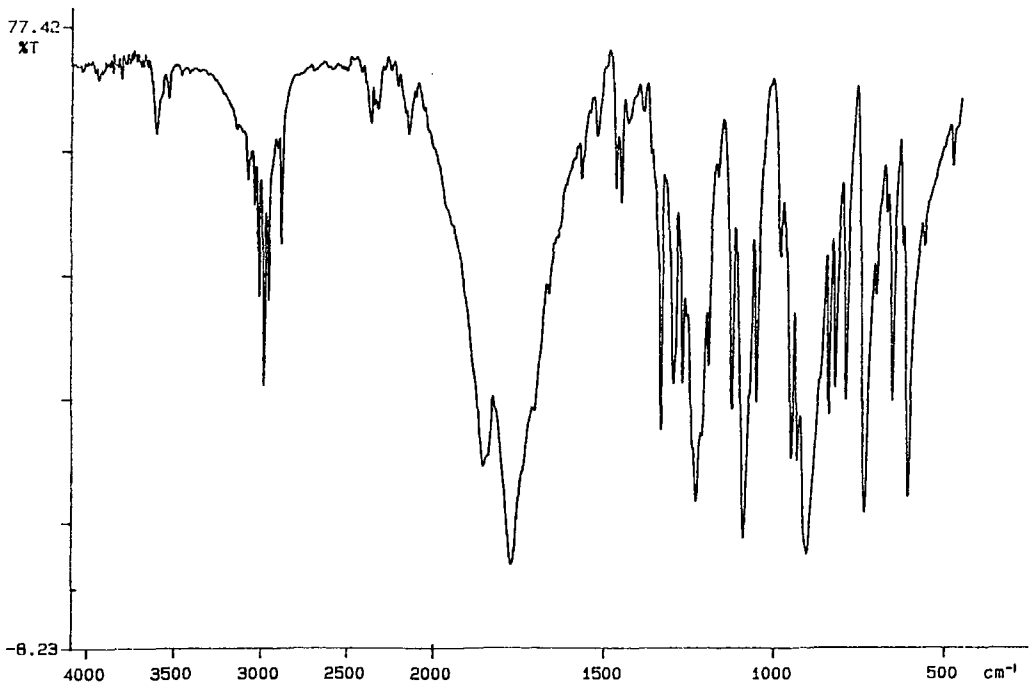

Appendix 2.8 Infrared spectrum of *endo*-AN.

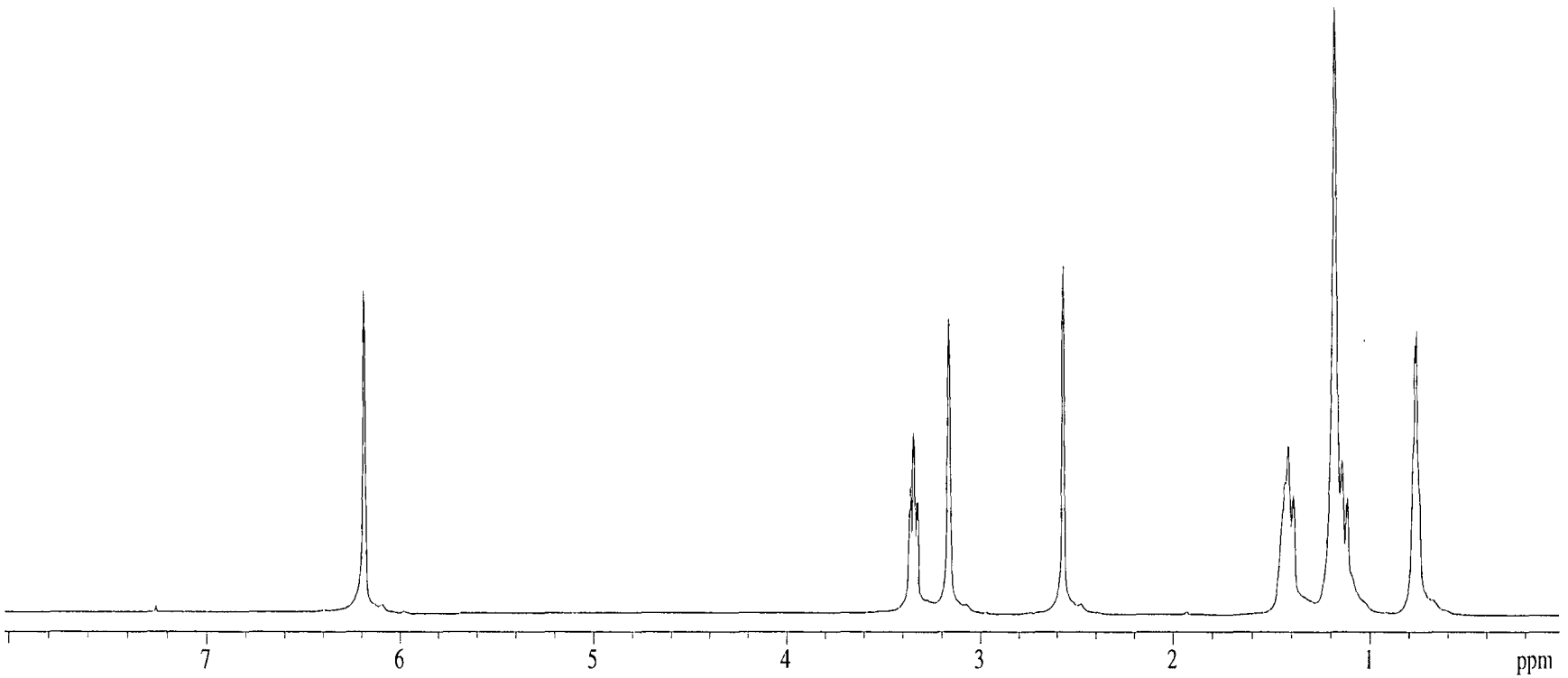

Appendix 2.9 ^{1}H nmr spectrum of *exo*-C6M.

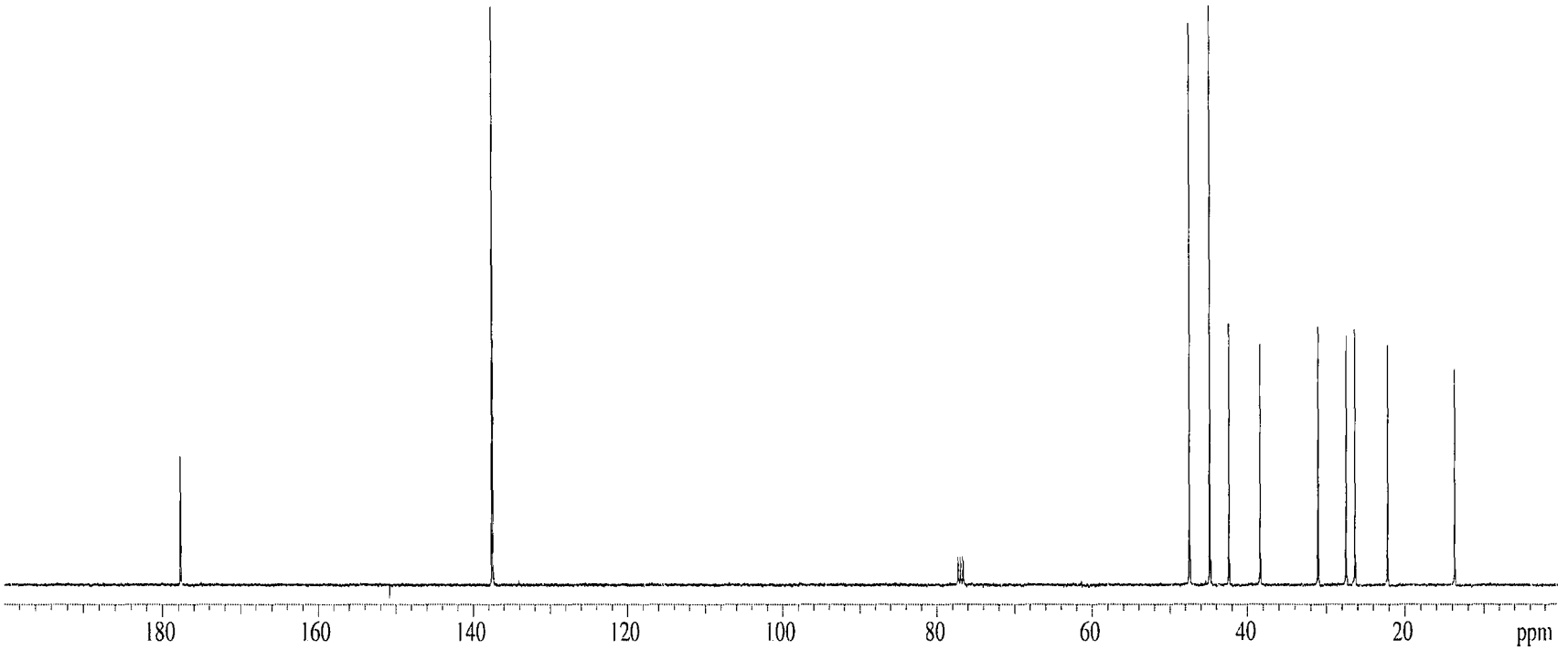

Appendix 2.10 ^{13}C nmr spectrum of *exo*-C6M.

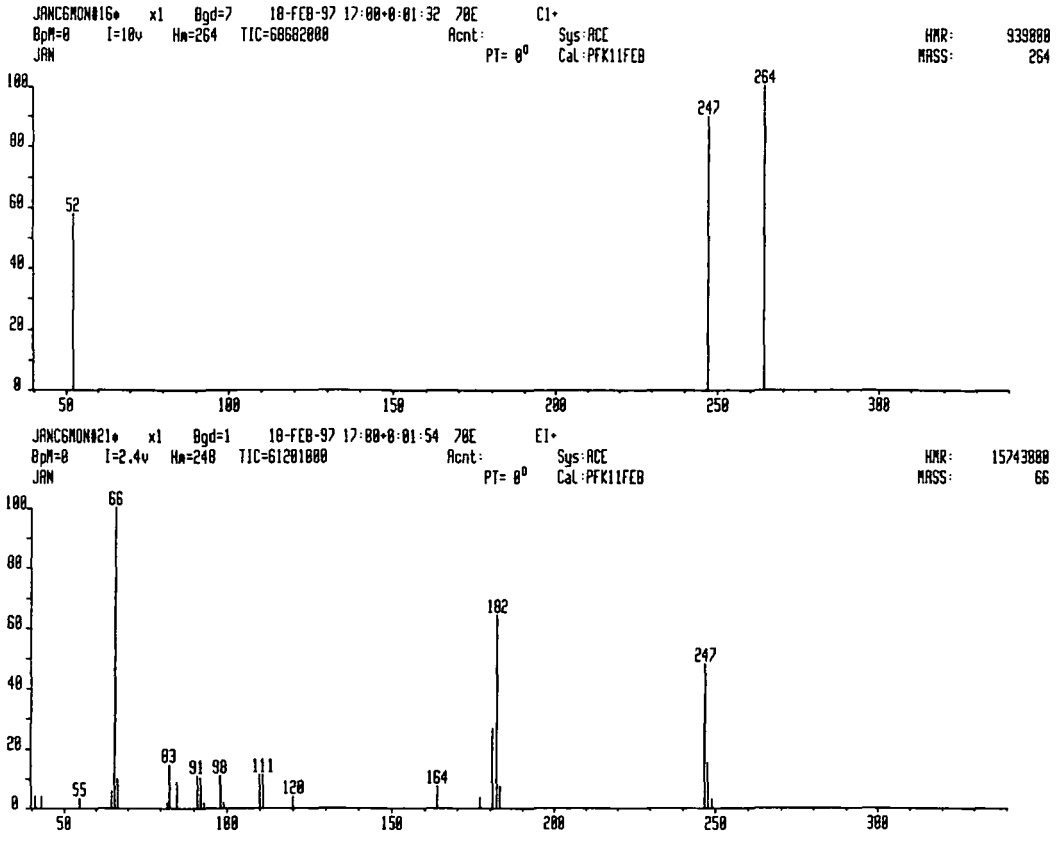

Appendix 2.11 Mass spectrum of *exo*-C6M.

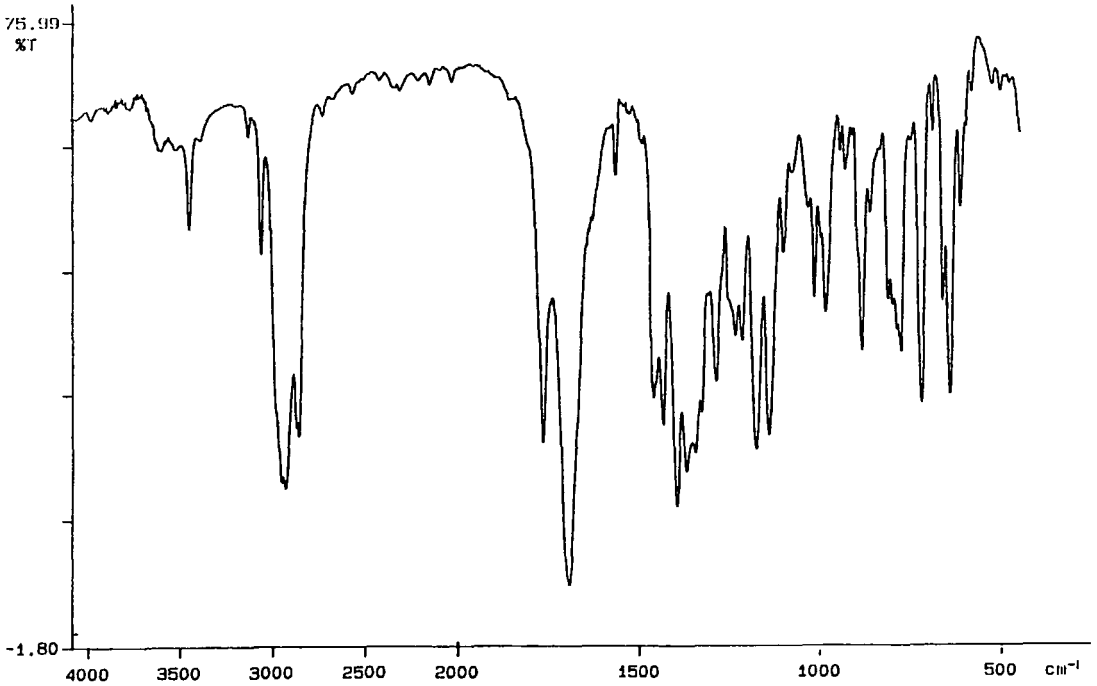

Appendix 2.12 Infrared spectrum of *exo*-C6M.

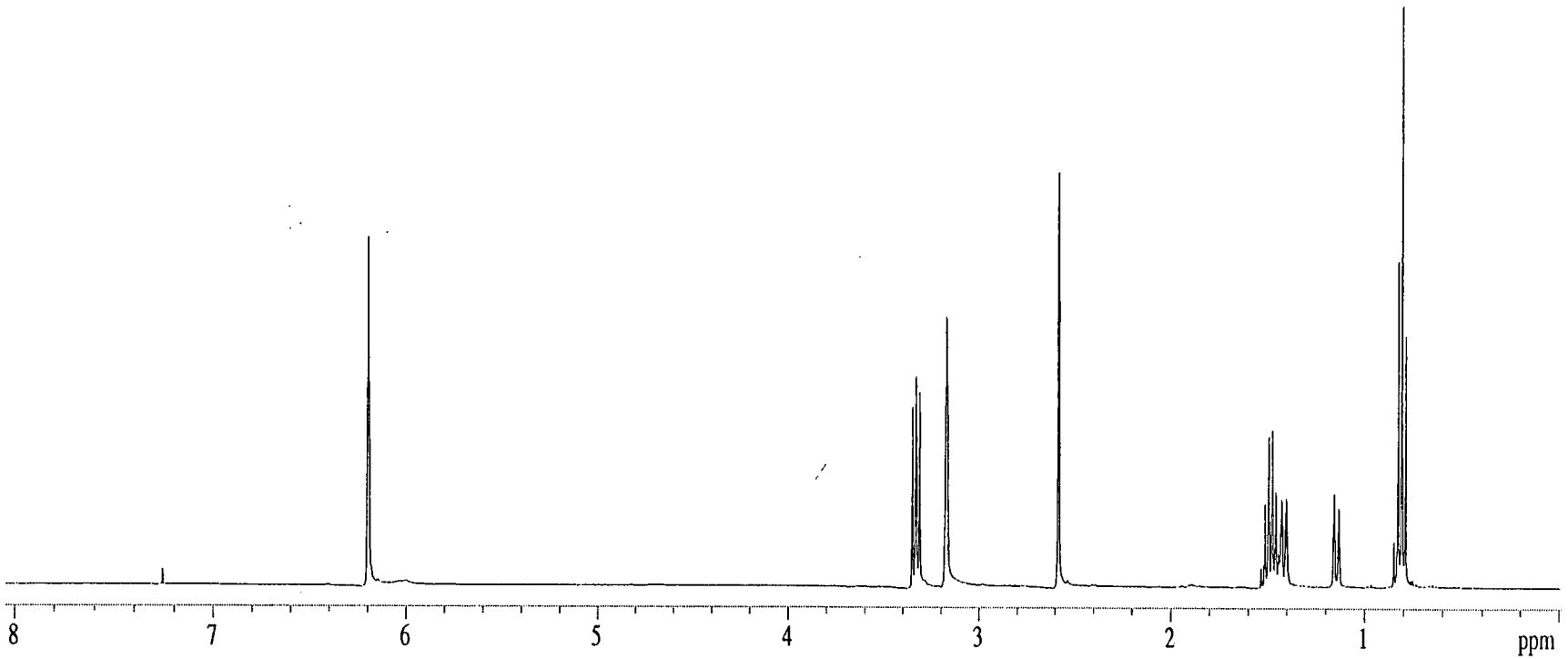

Appendix 2.13 ^{1}H nmr spectrum of *exo*-C3M.

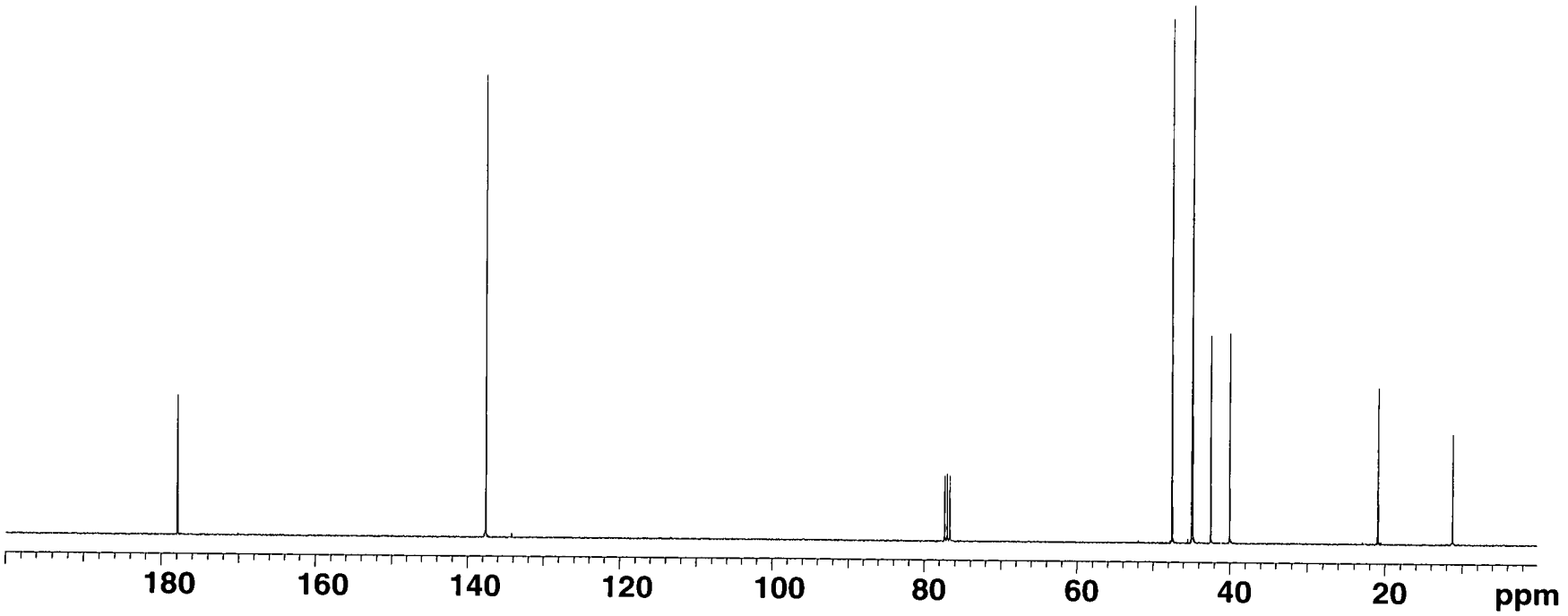

Appendix 2.14 ^{13}C nmr spectrum of *exo*-C3M.

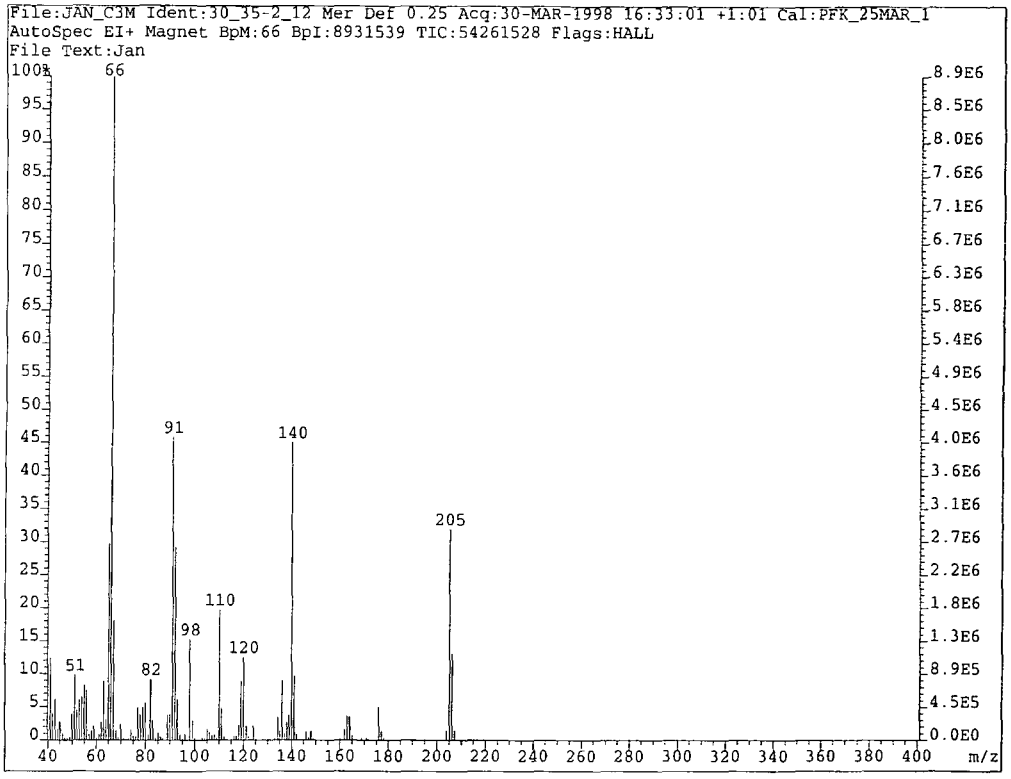

Appendix 2.15 Mass spectrum of *exo*-C3M.

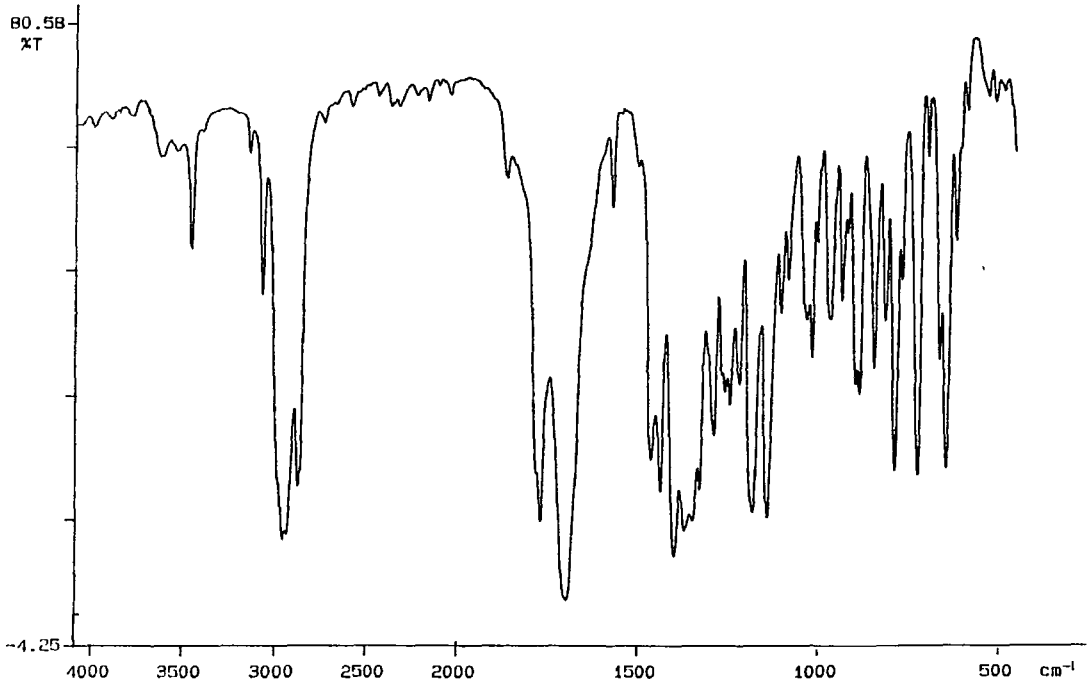

Appendix 2.16 Infrared spectrum of *exo*-C3M.

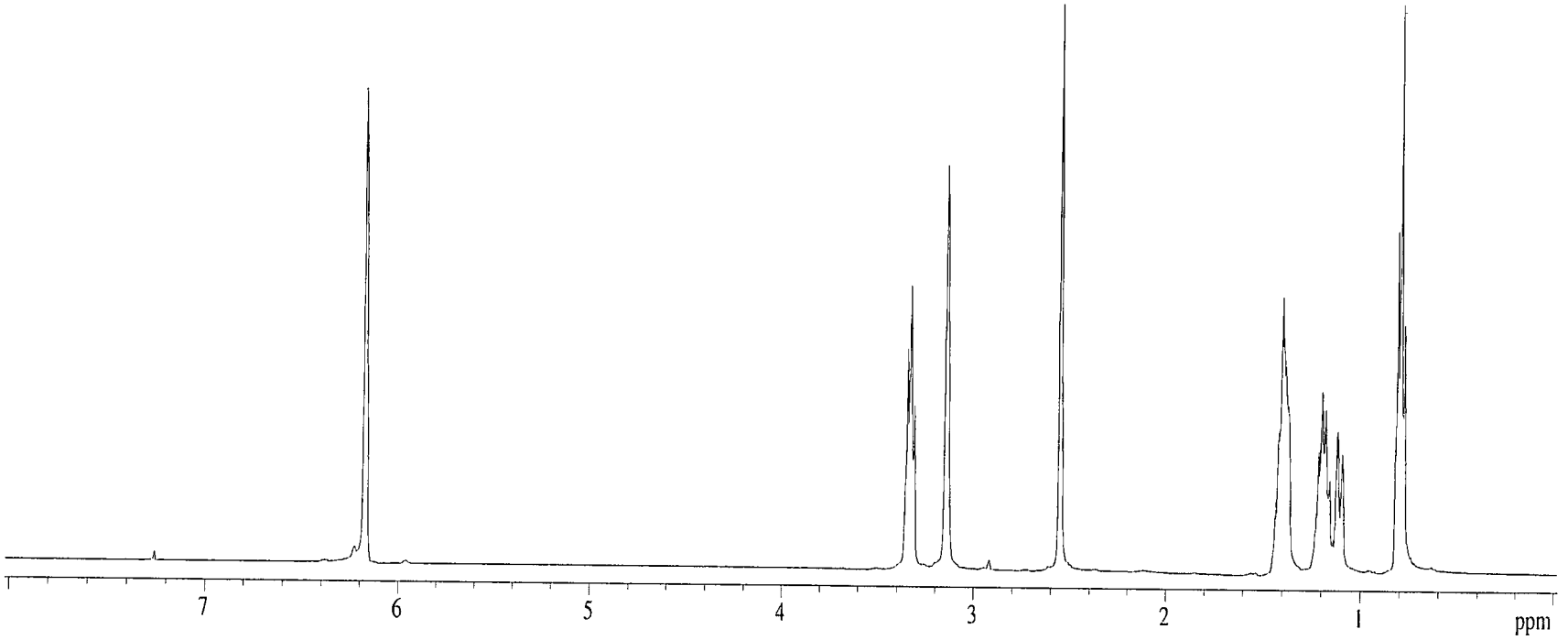

Appendix 2.17 ^{1}H nmr spectrum of *exo*-C4M.

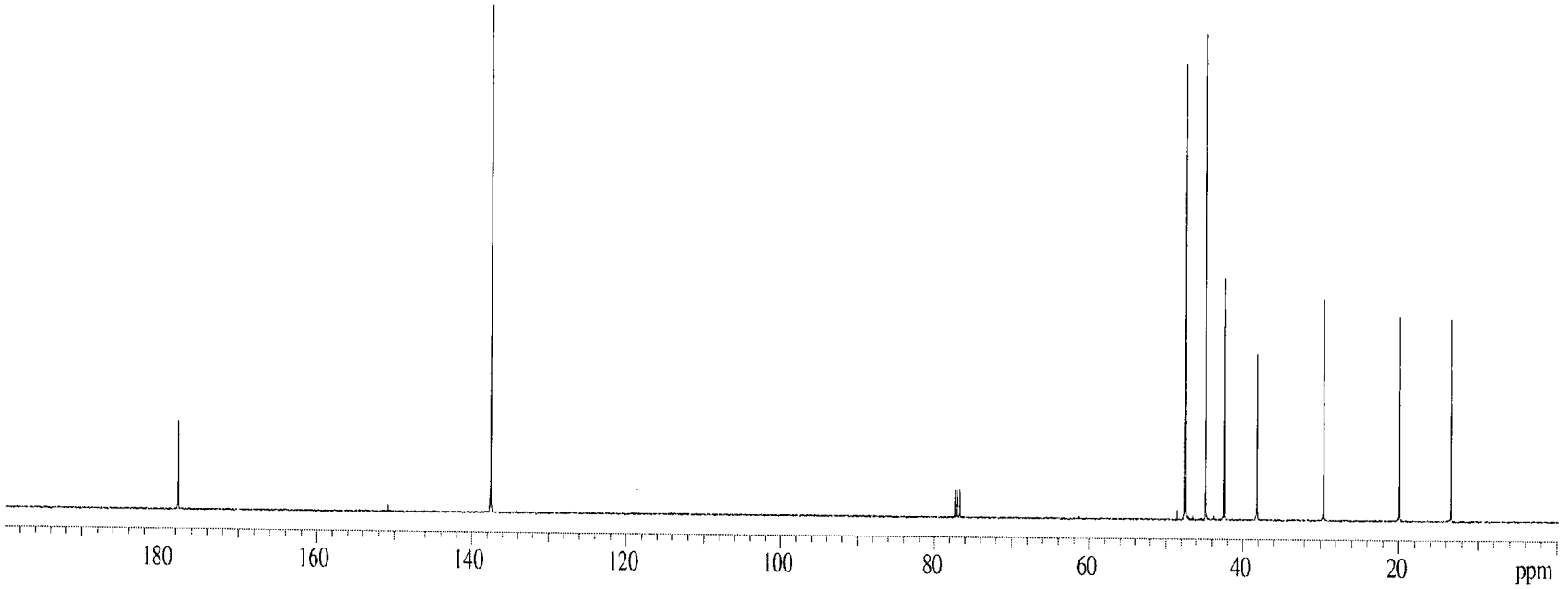

Appendix 2.18 ^{13}C nmr spectrum of *exo*-C4M.

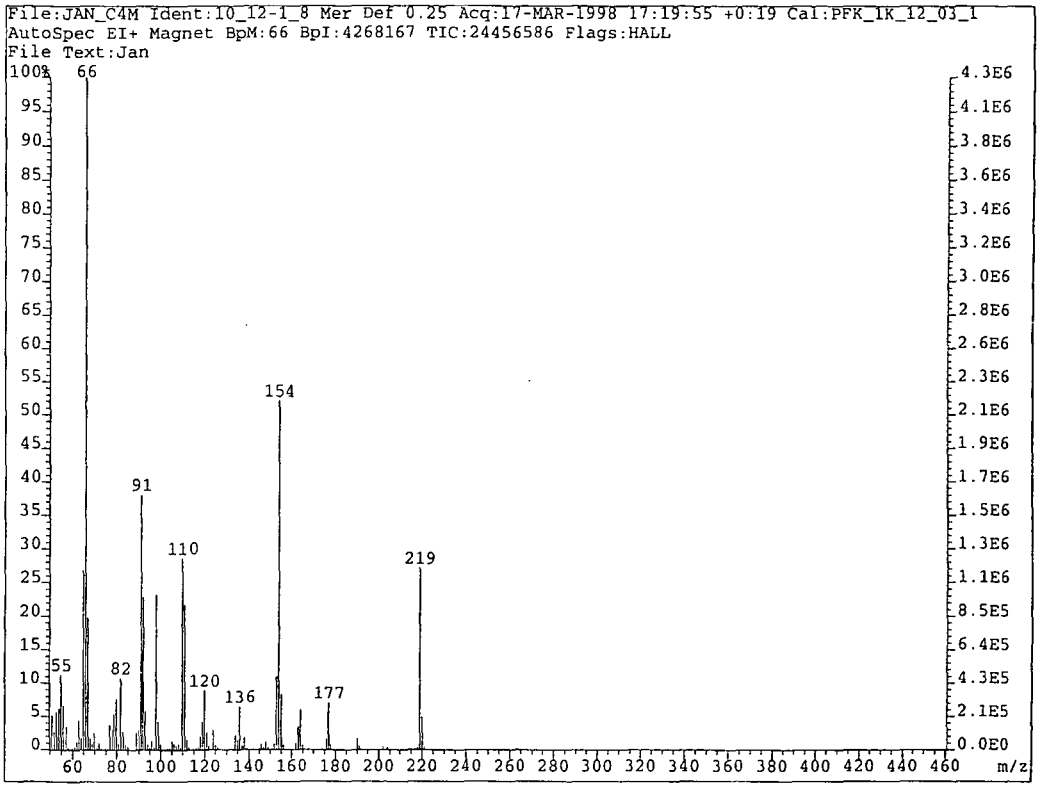

Appendix 2.19 Mass spectrum of *exo*-C4M.

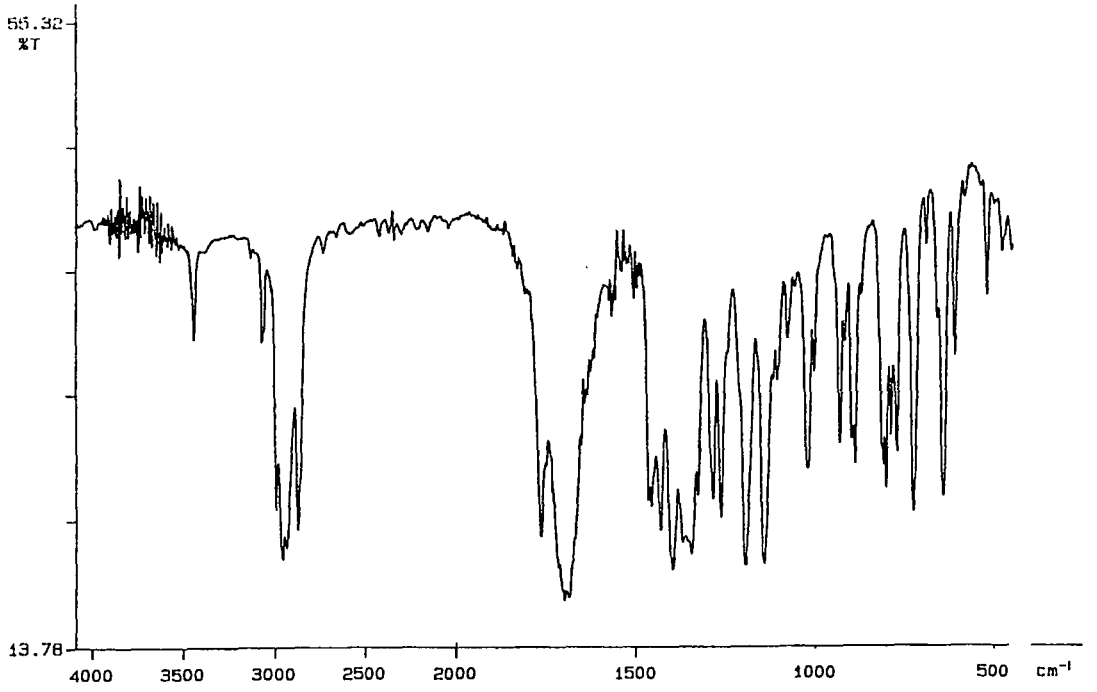

Appendix 2.20 Infrared spectrum of *exo*-C4M.

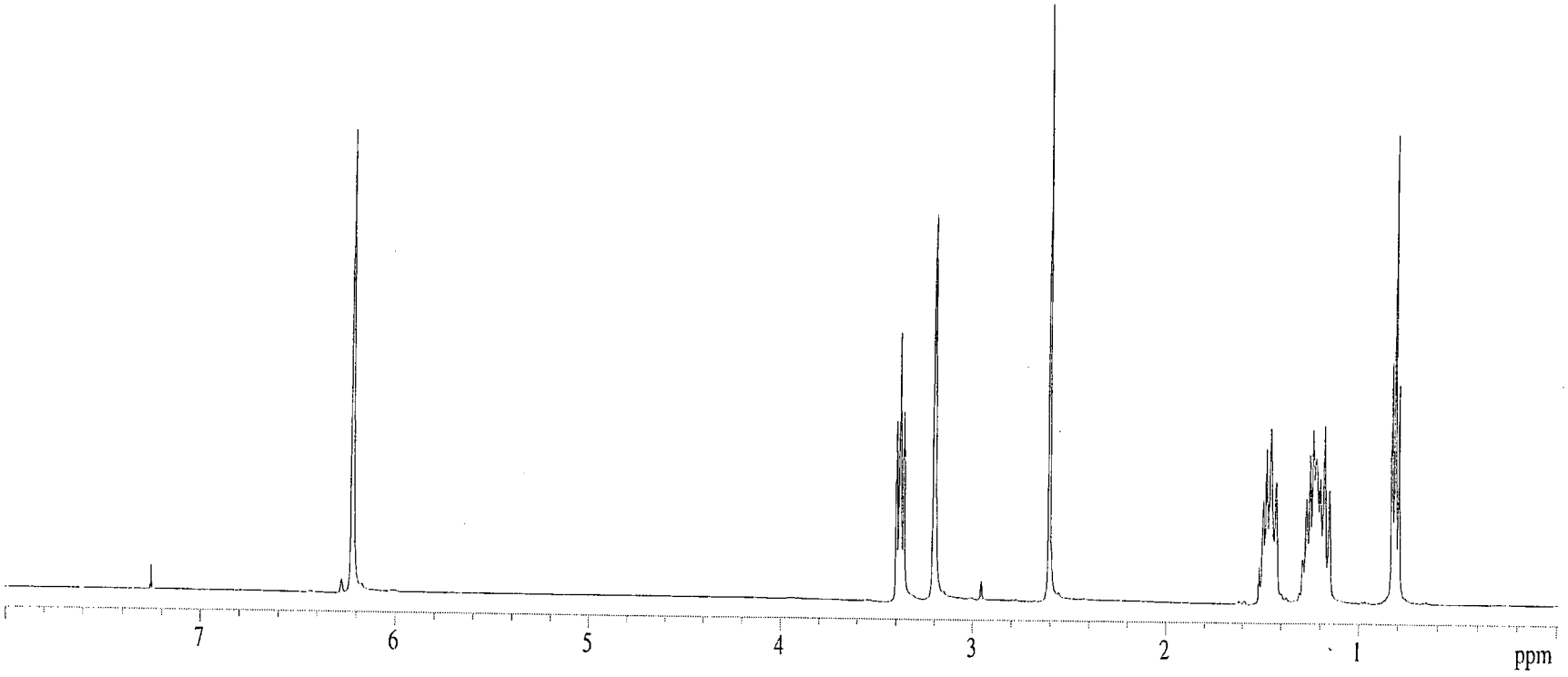

Appendix 2.21 ^{1}H nmr spectrum of *exo*-C5M.

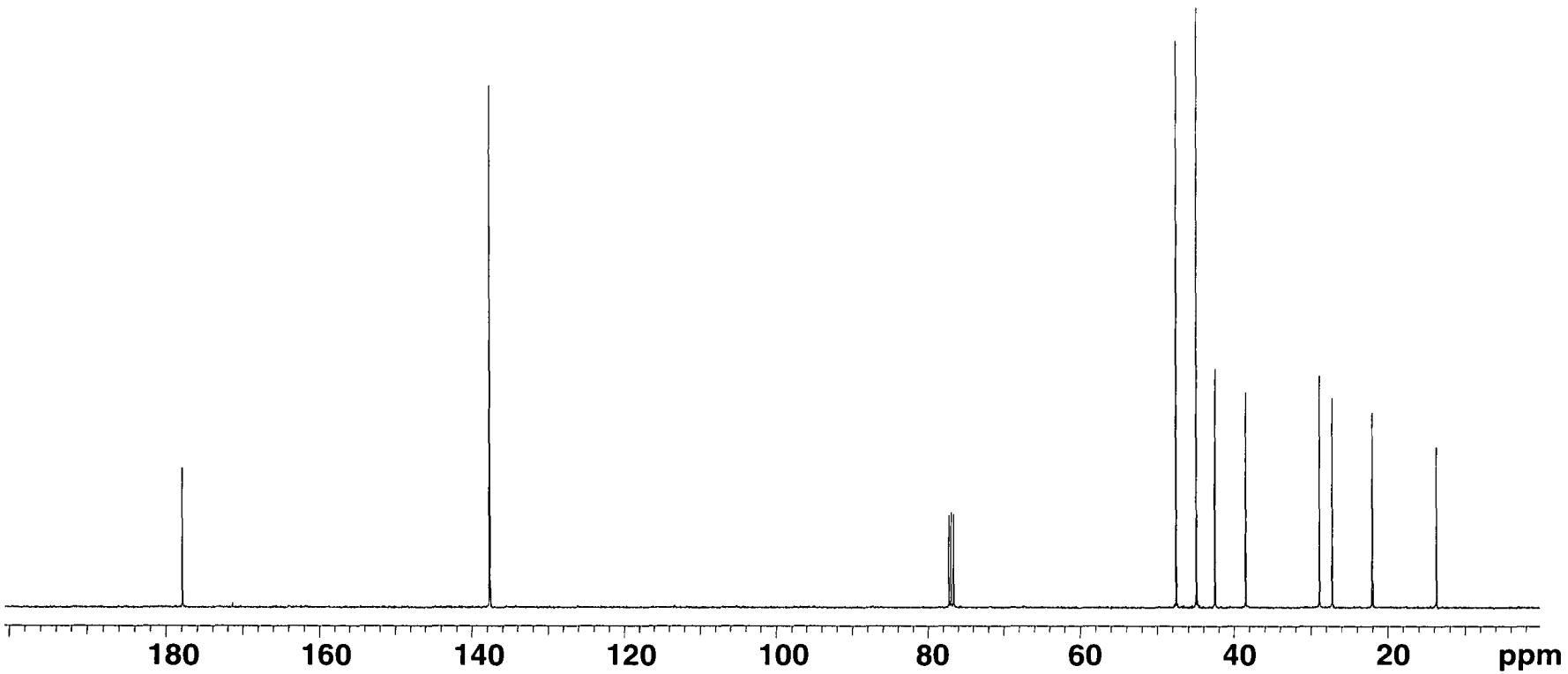

Appendix 2.22 ^{13}C nmr spectrum of *exo*-C5M.

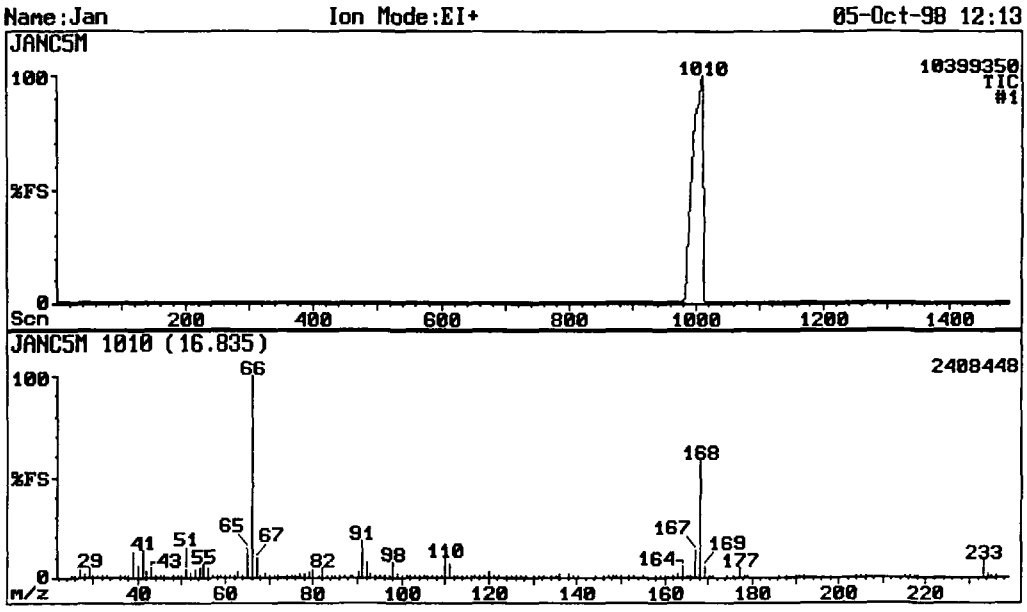

Appendix 2.23 GC-Mass spectrum of *exo*-C5M.

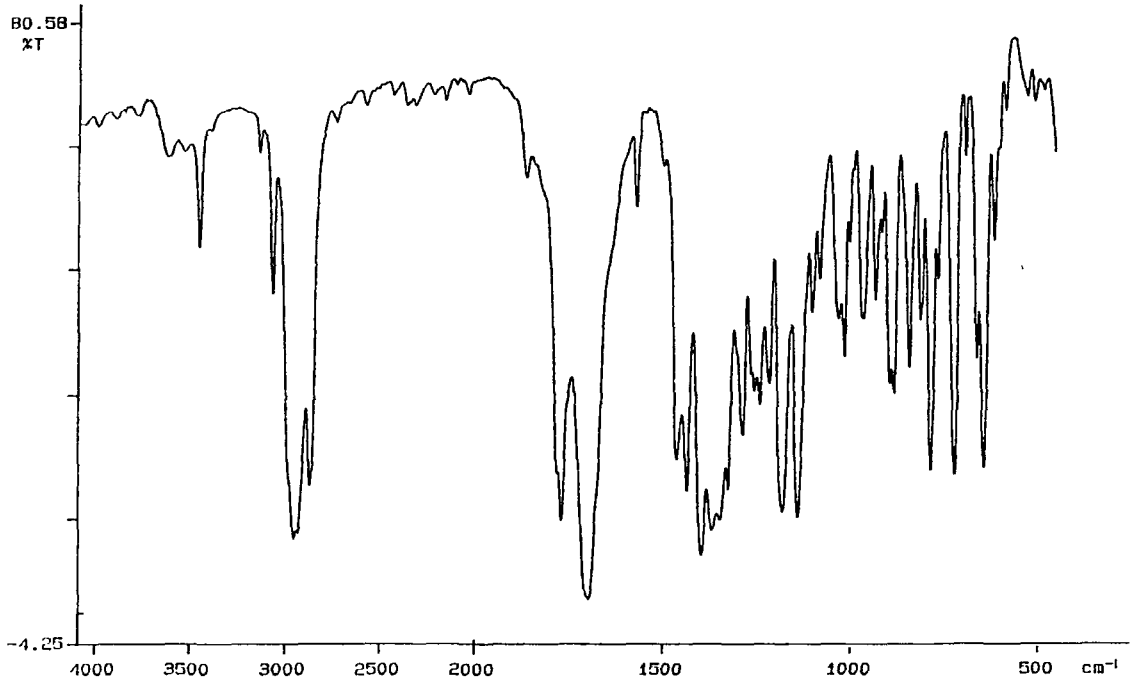

Appendix 2.24 Infrared spectrum of *exo*-C5M.

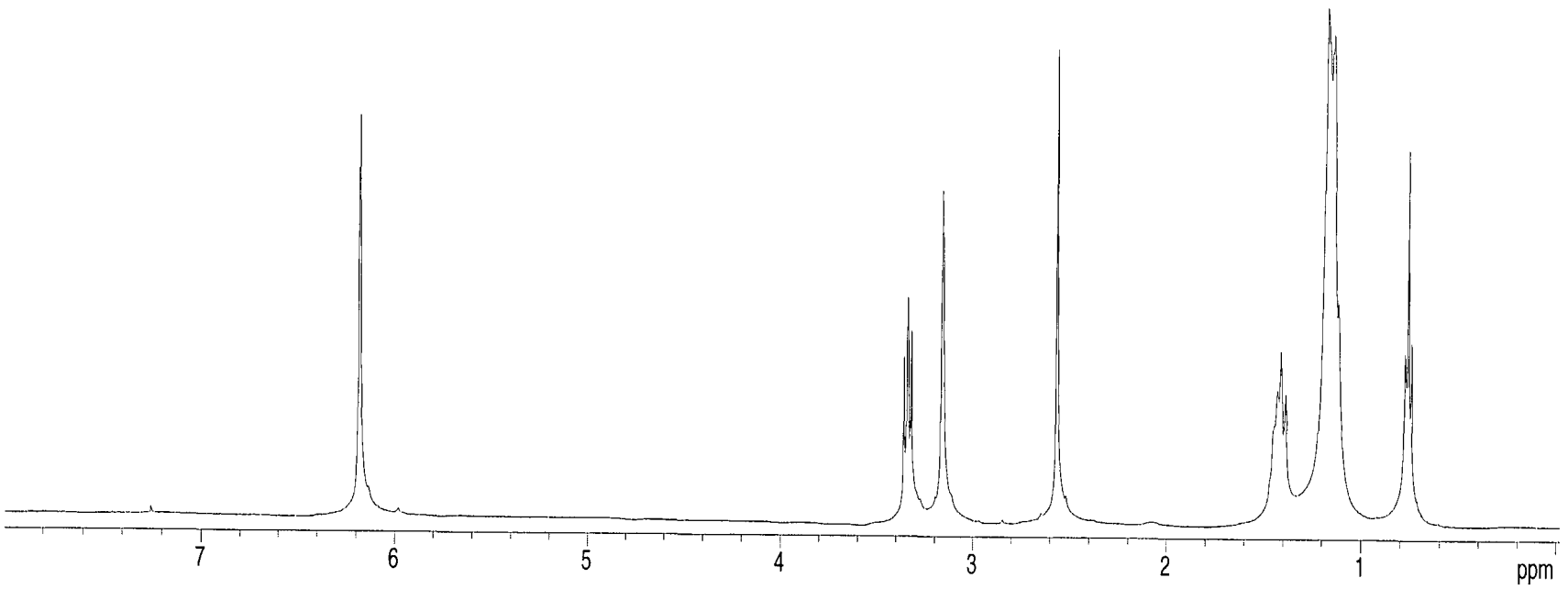

Appendix 2.25 ^{1}H nmr spectrum of *exo*-C8M.

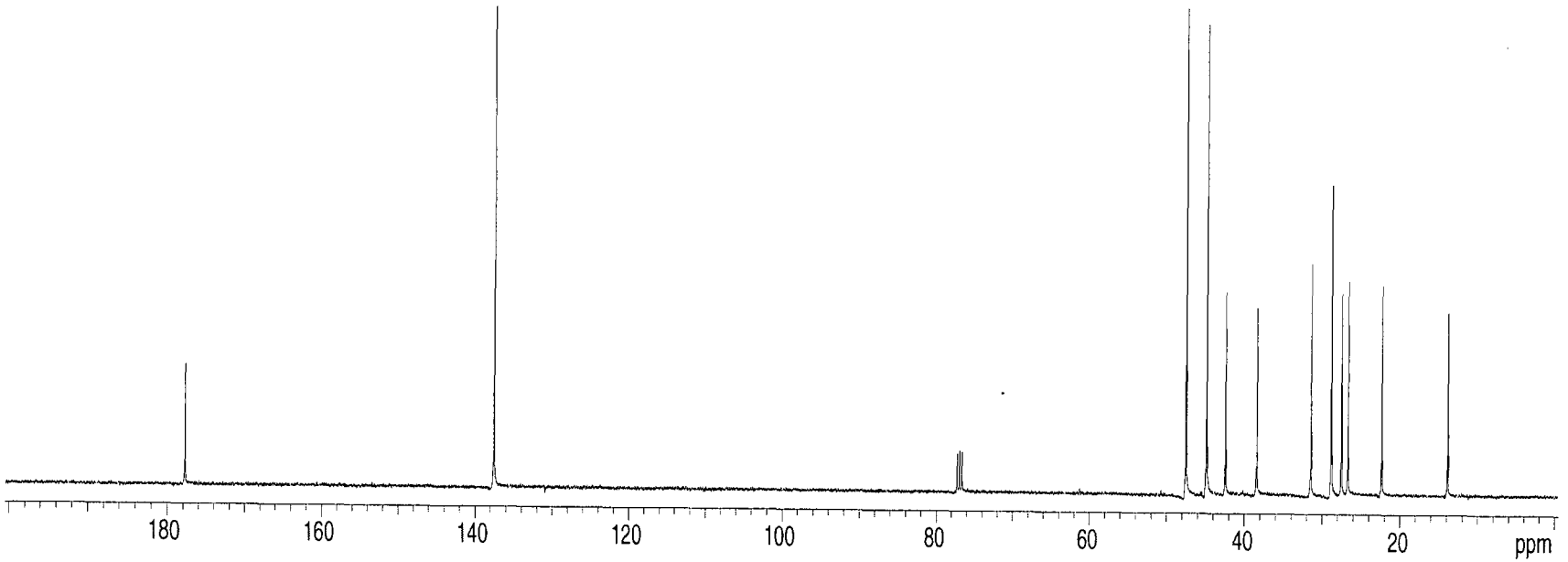

Appendix 2.26 ^{13}C nmr spectrum of *exo*-C8M.

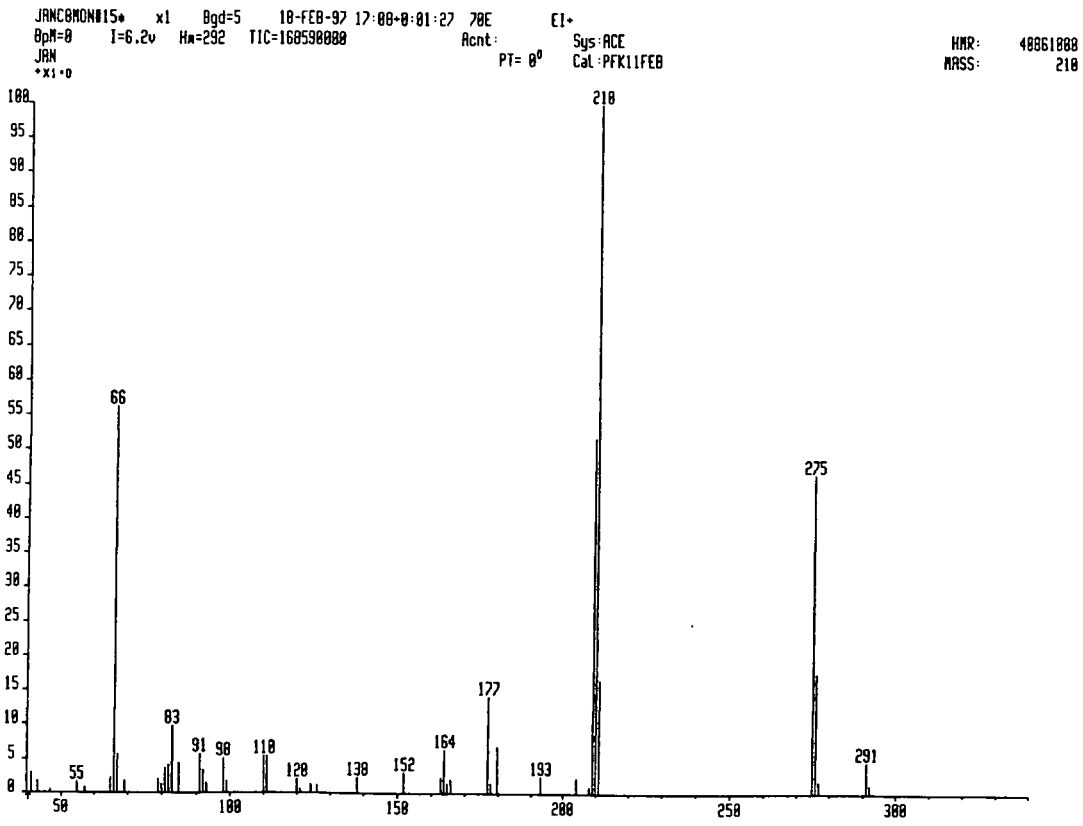

Appendix 2.27 Mass spectrum of *exo*-C8M.

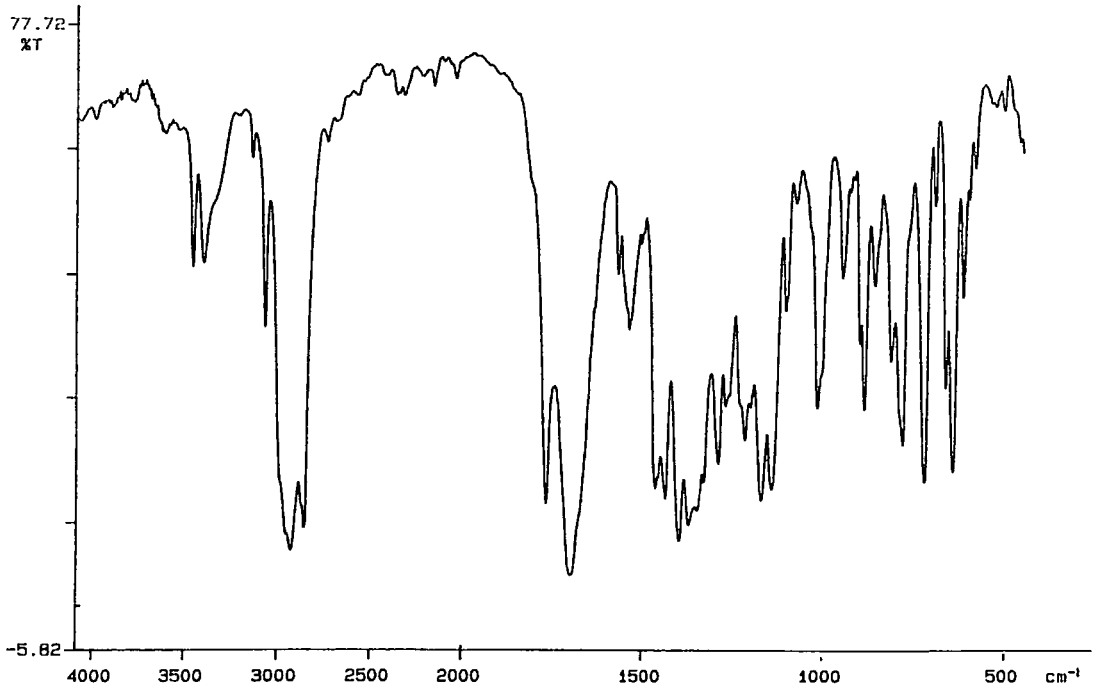

Appendix 2.28 Infrared spectrum of *exo*-C8M.

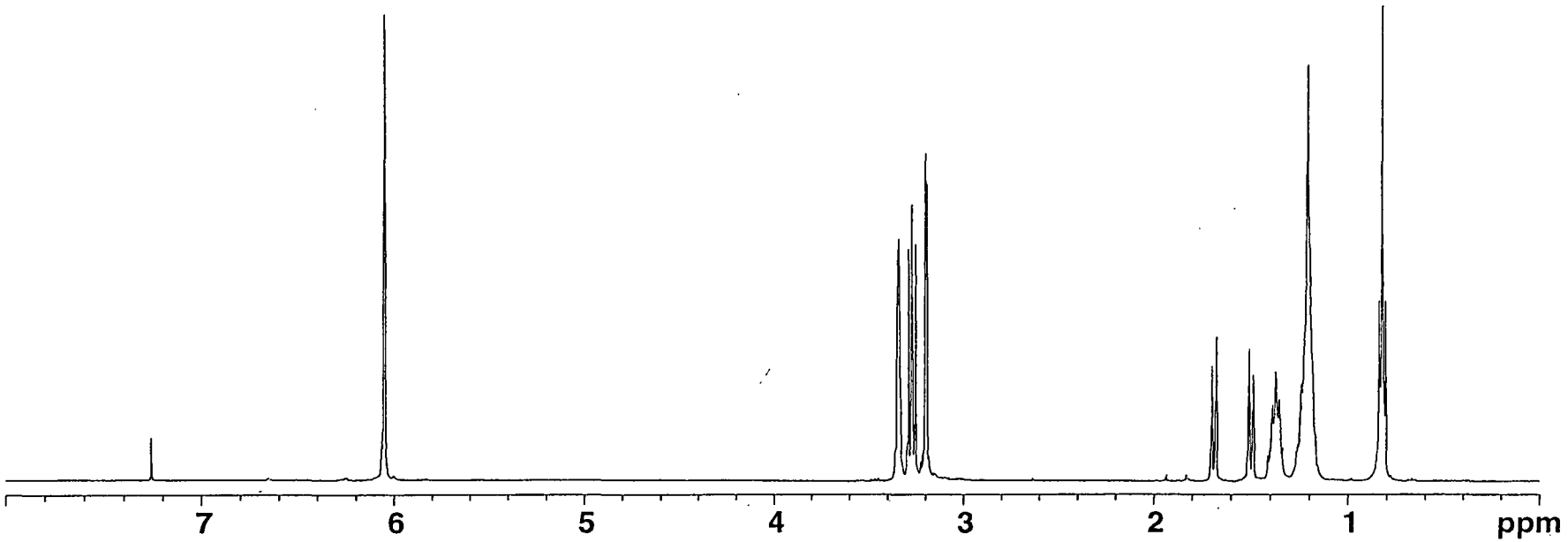

Appendix 2.29 ^{1}H nmr spectrum of *endo*-C6M.

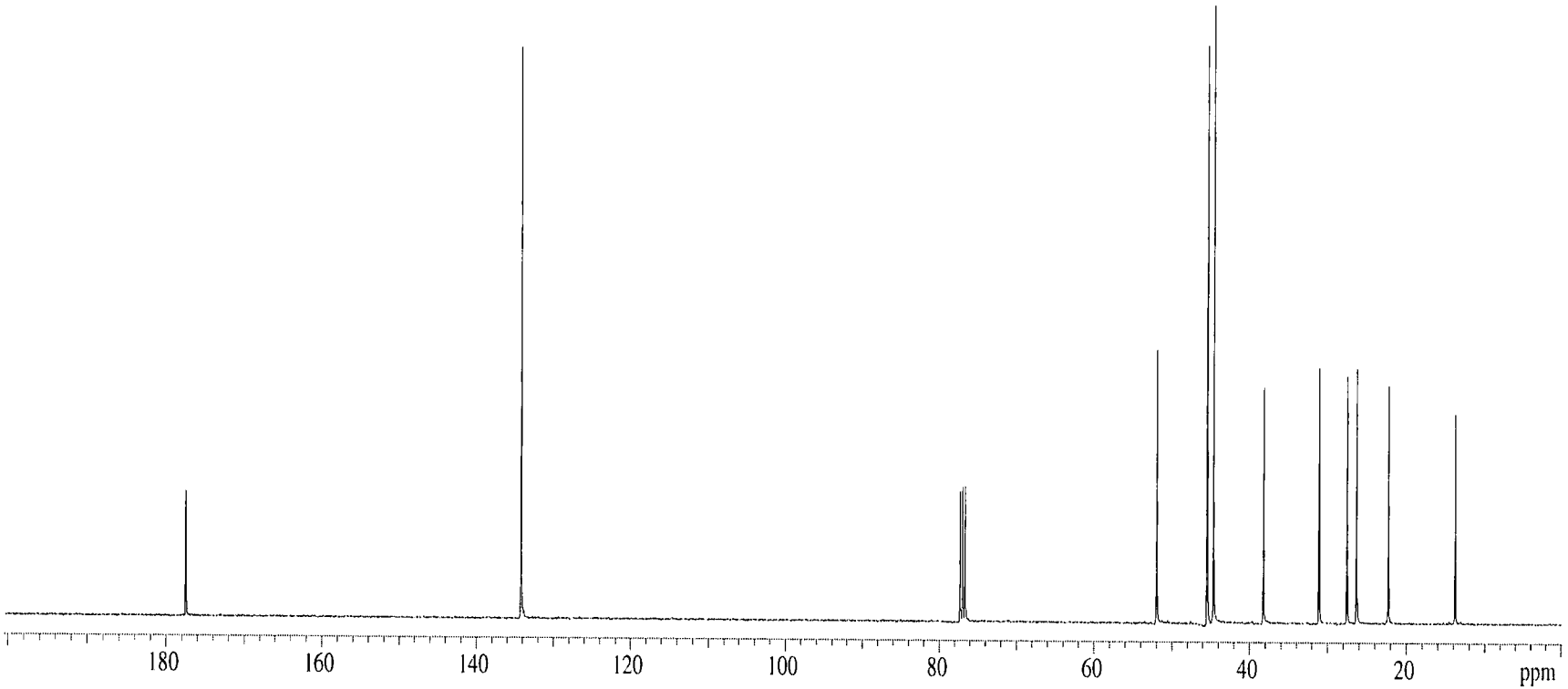

Appendix 2.30 ^{13}C nmr spectrum of *endo*-C6M.

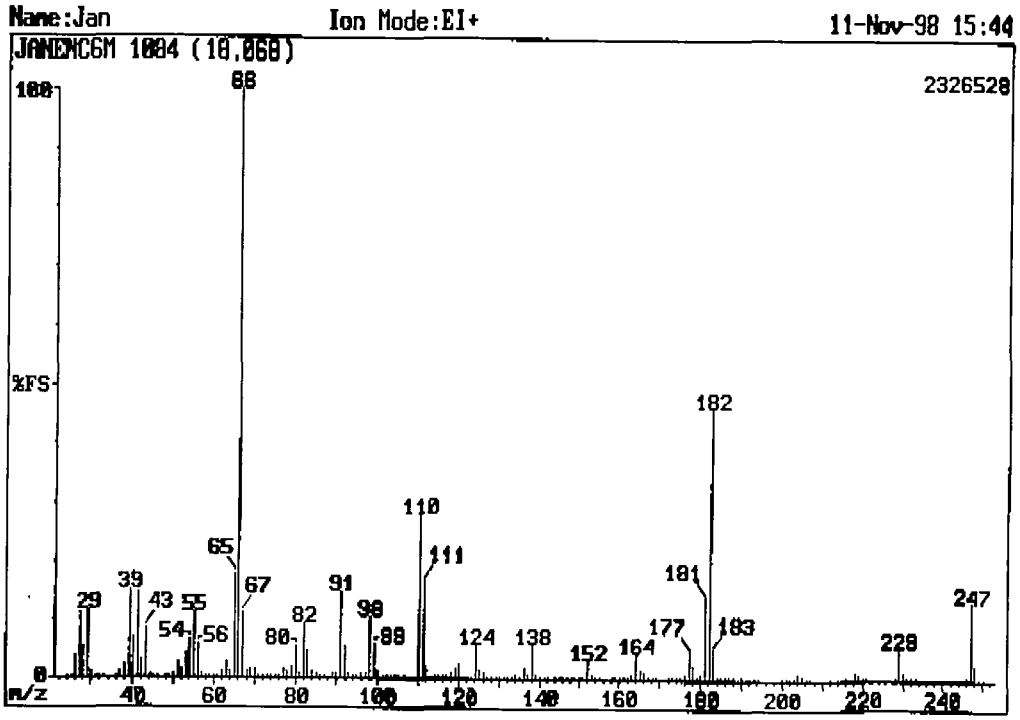

Appendix 2.31 Mass spectrum of *endo*-C6M.

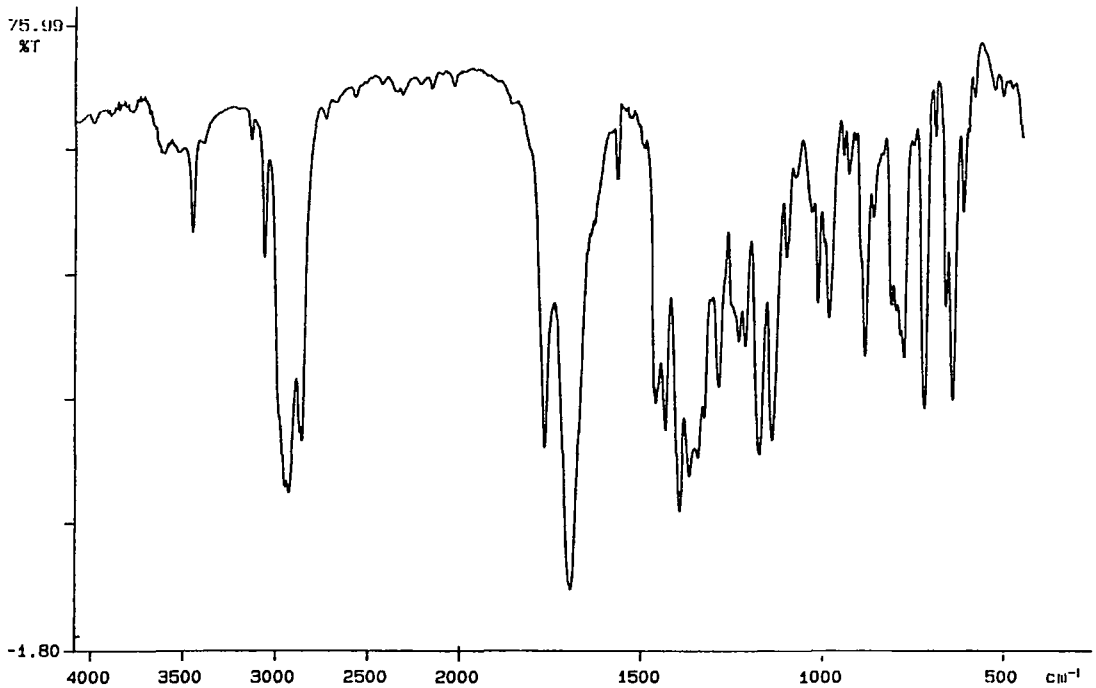

Appendix 2.32 Infrared spectrum of *endo*-C6M.

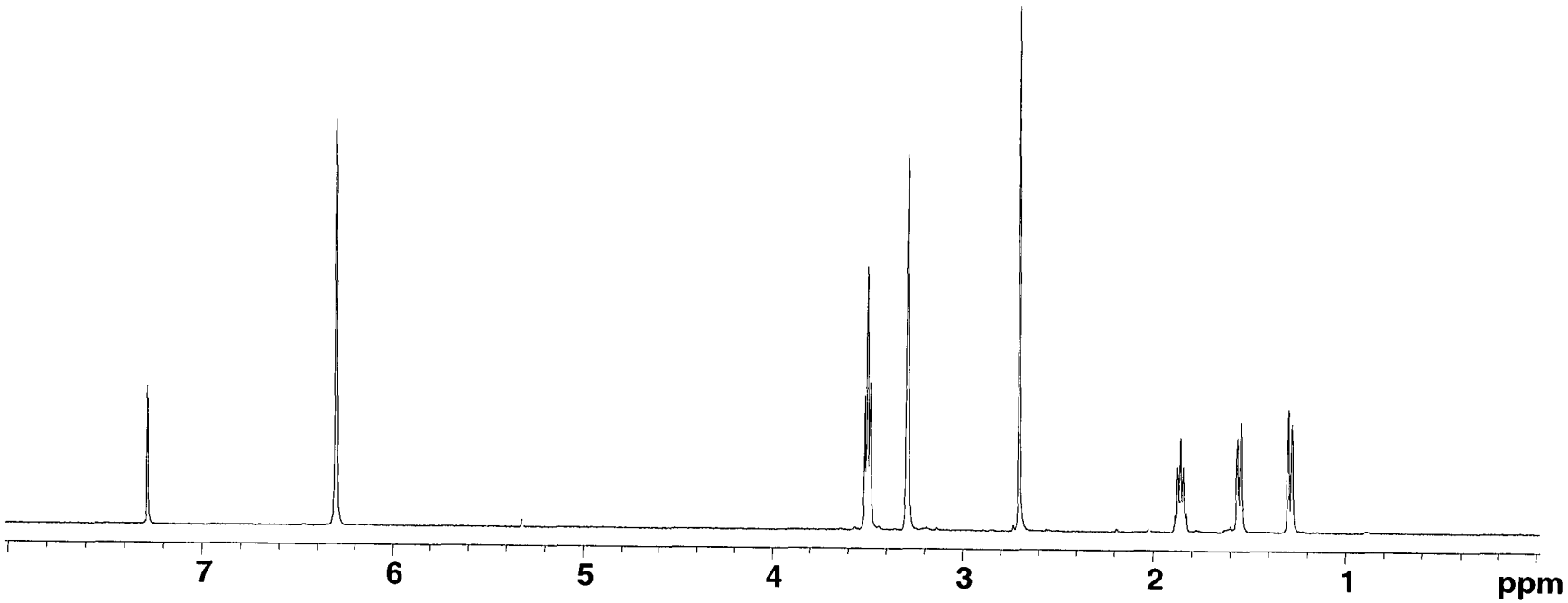

Appendix 2.33 ^{1}H nmr spectrum of *exo*-C3D.

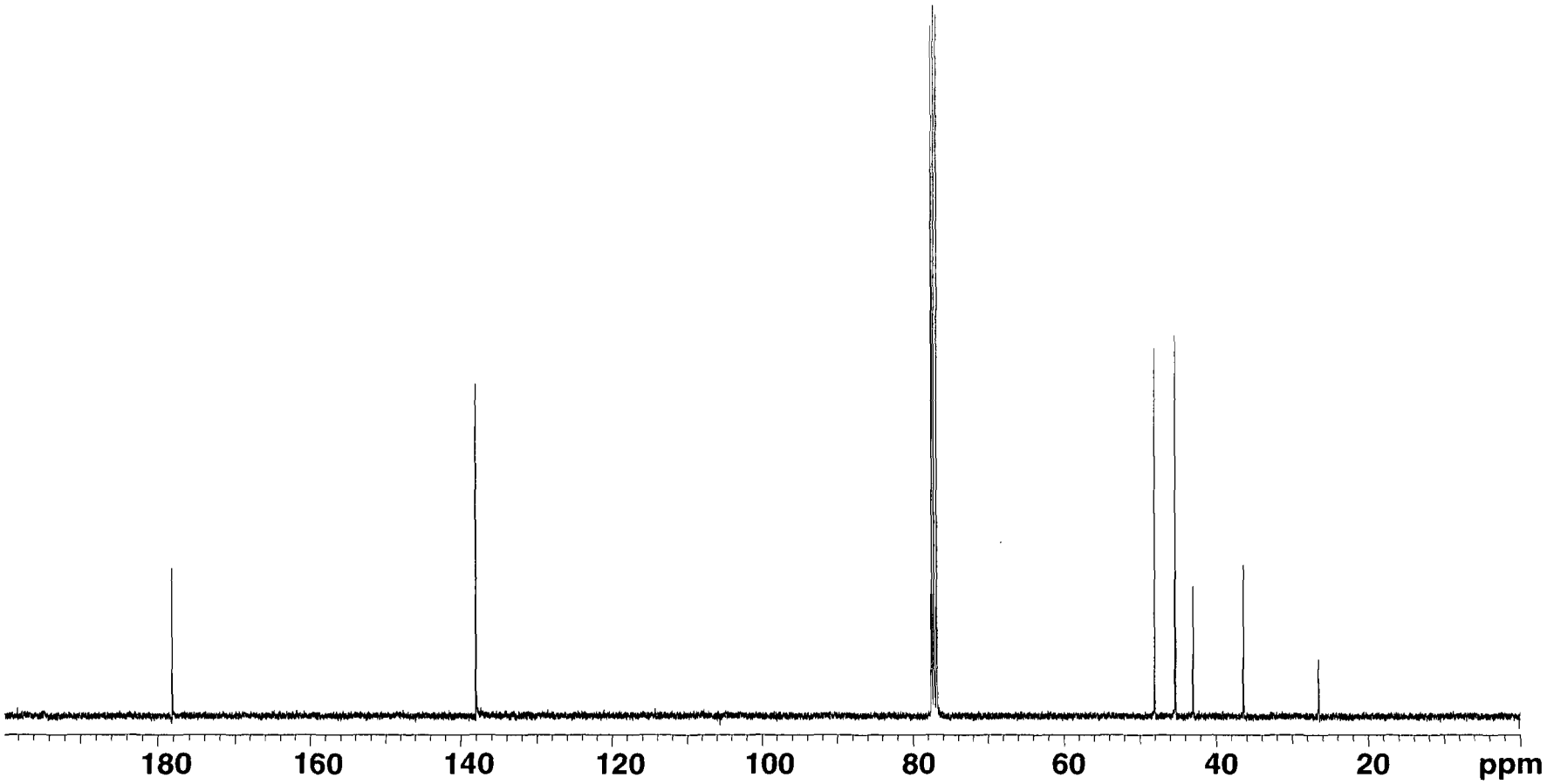

Appendix 2.34 ^{13}C nmr spectrum of *exo*-C3D.

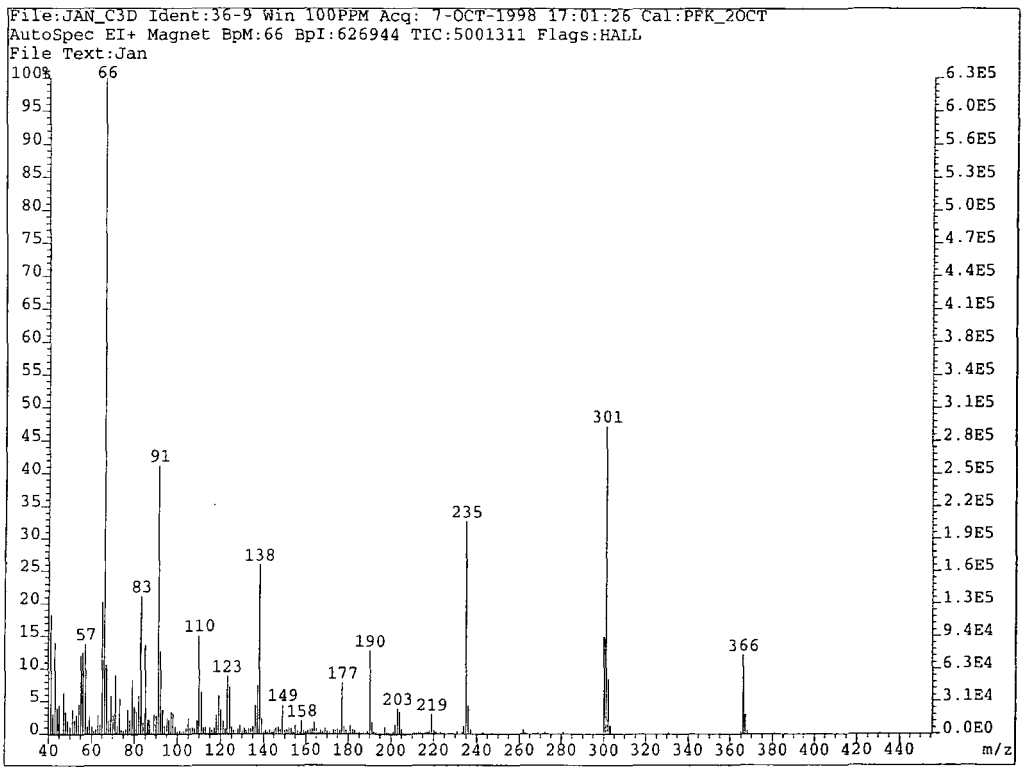

Appendix 2.35 Mass spectrum of *exo*-C3D.

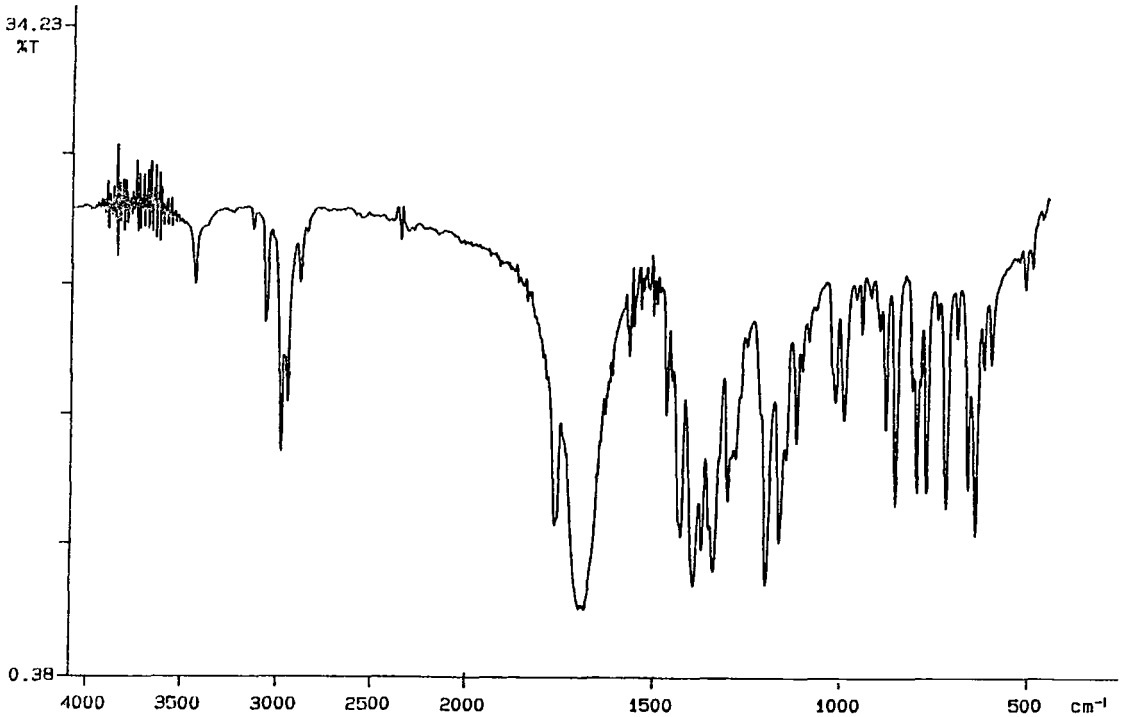

Appendix 2.36 Infrared spectrum of *exo*-C3D.

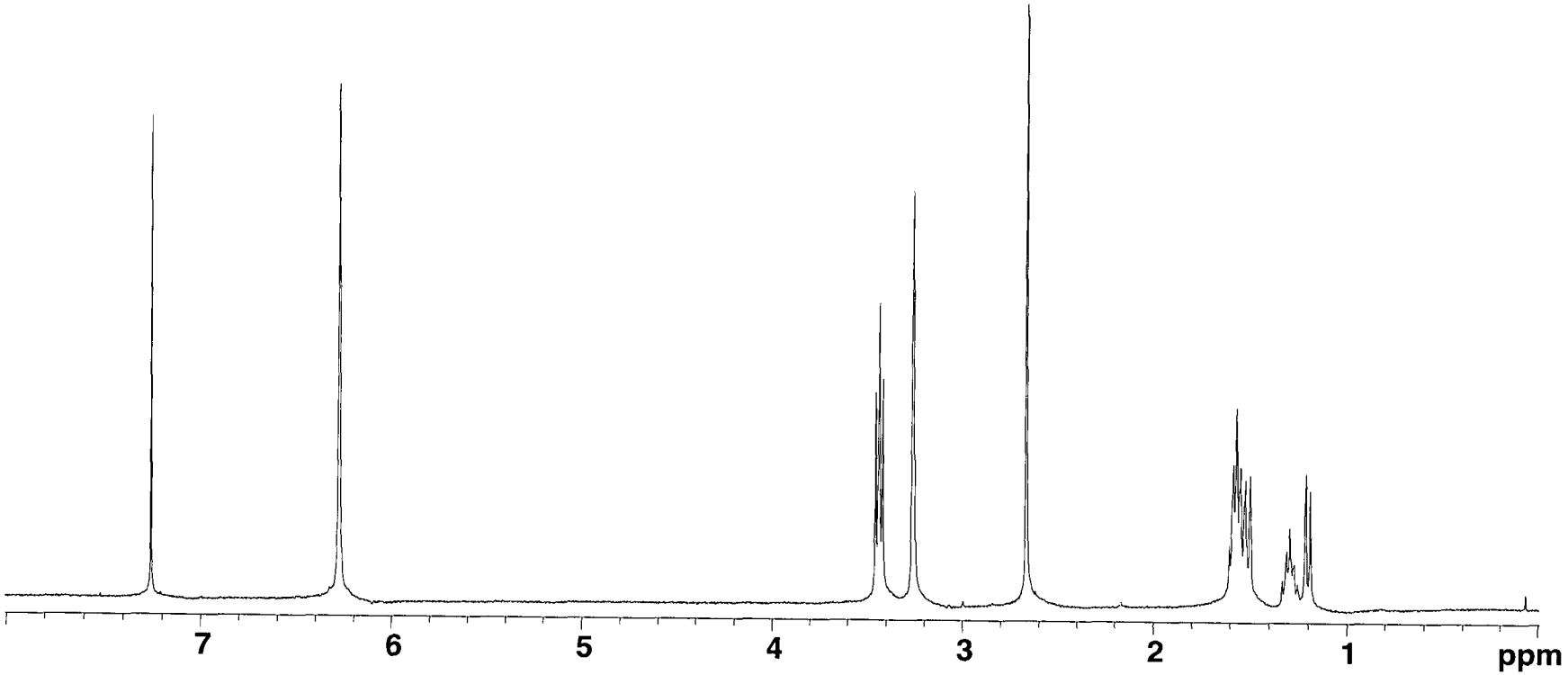

Appendix 2.37 ^{1}H nmr spectrum of *exo*-C5D.

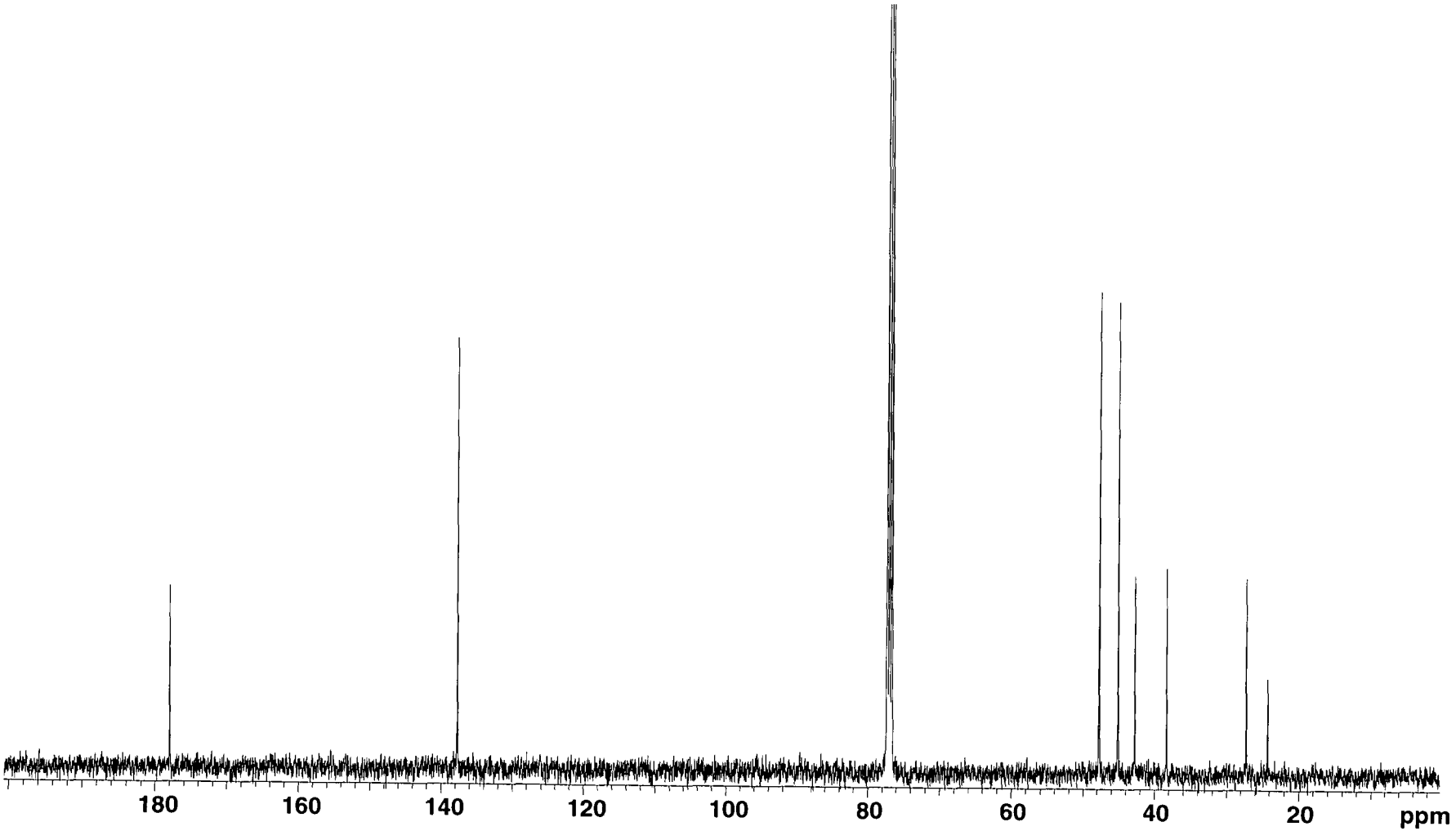

Appendix 2.38 ^{13}C nmr spectrum of *exo*-C5D.

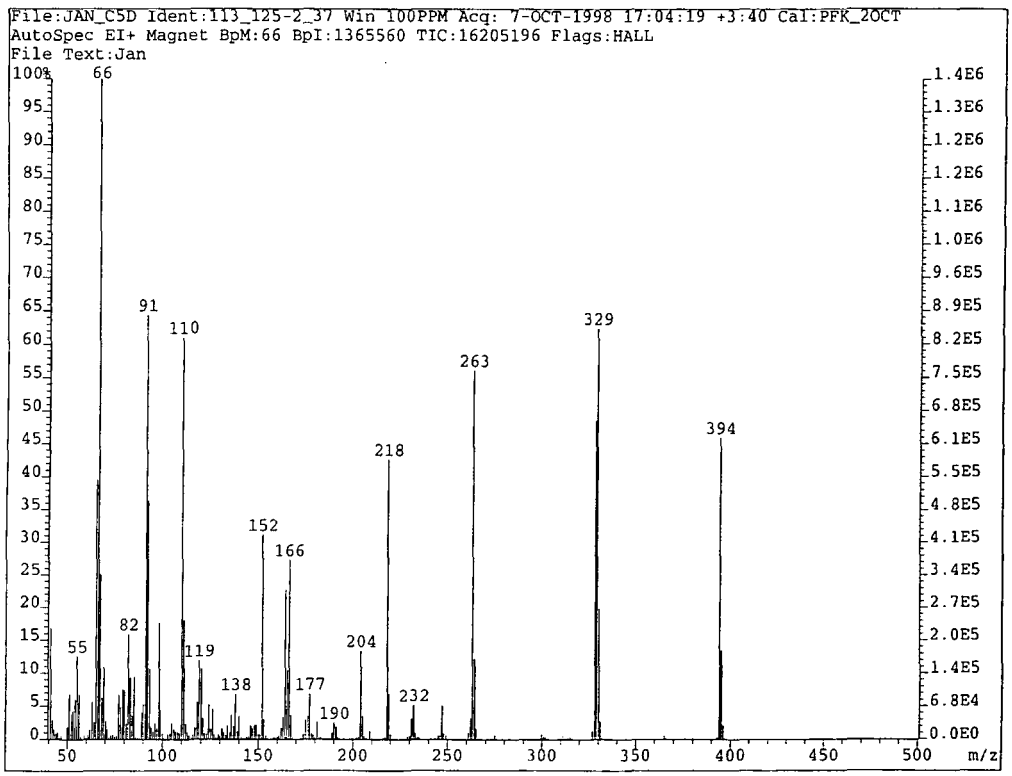

Appendix 2.39 Mass spectrum of *exo*-C5D.

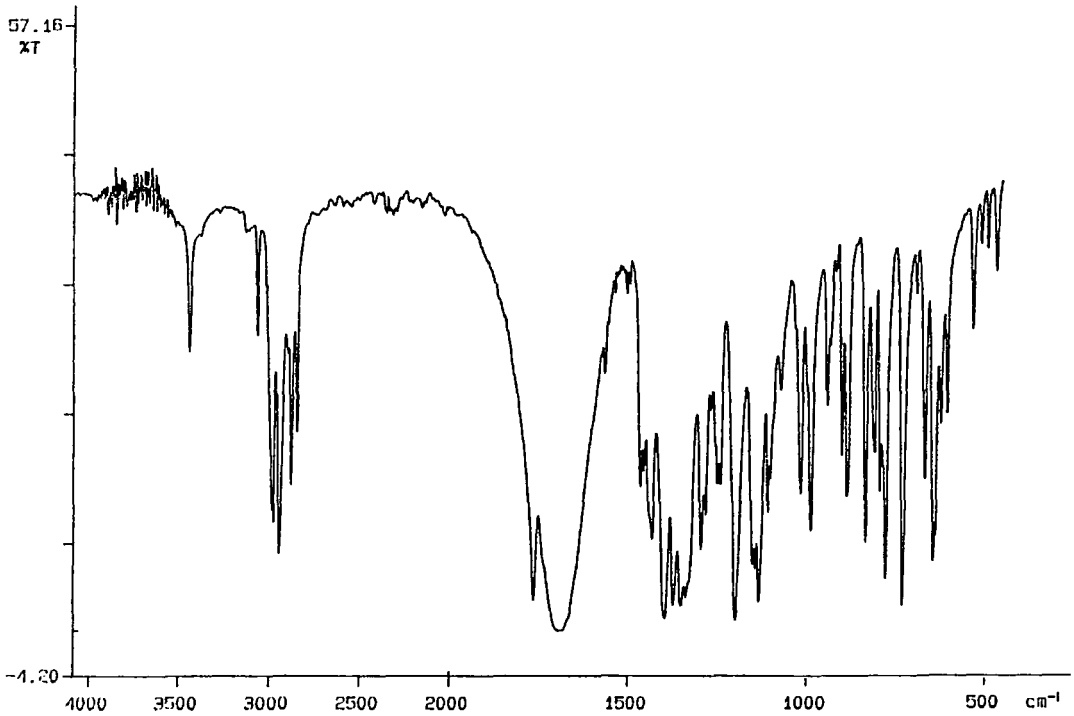

Appendix 2.40 Infrared spectrum of *exo*-C5D.

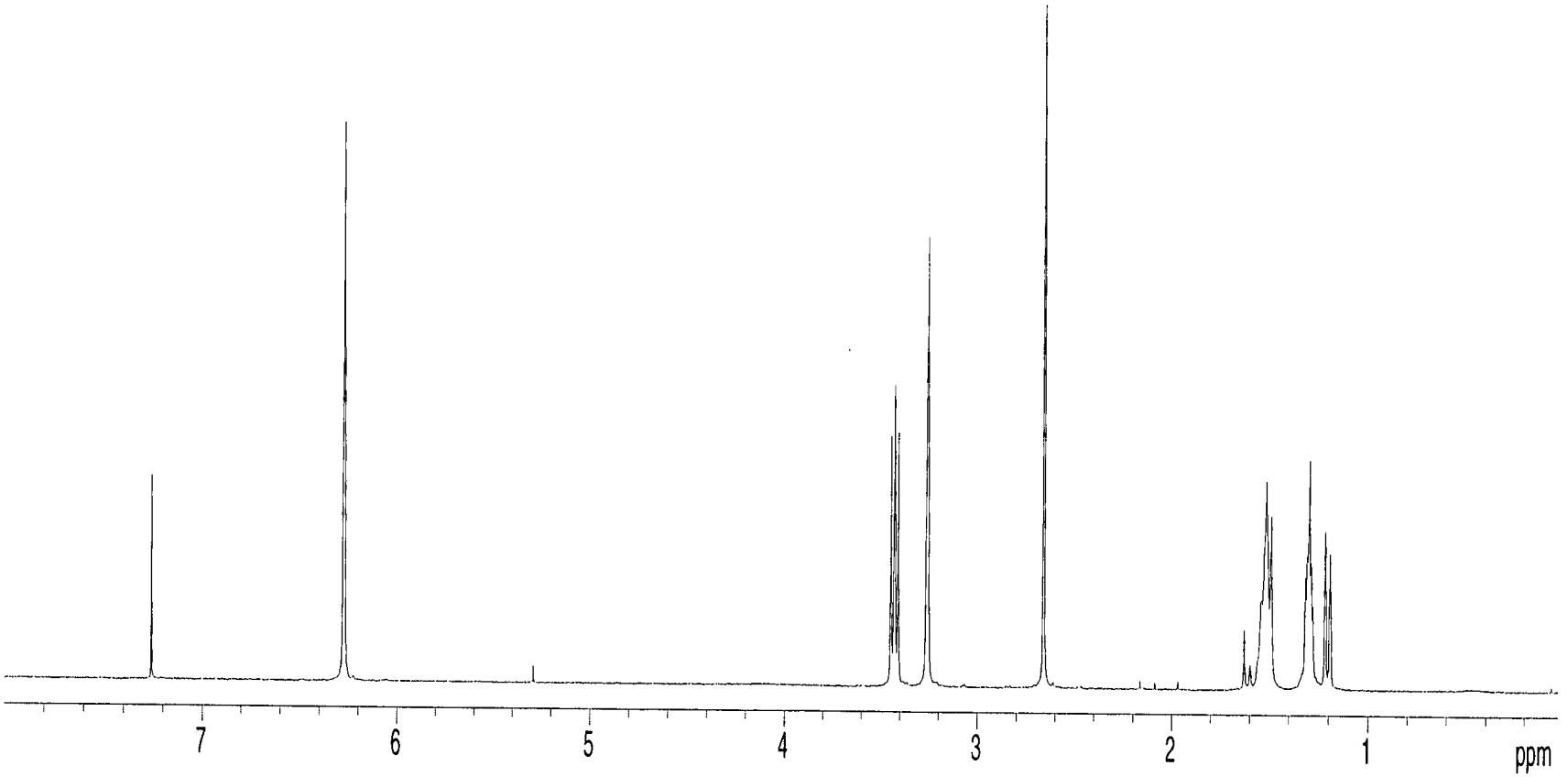

Appendix 2.41 ^{1}H nmr spectrum of *exo*-C6D.

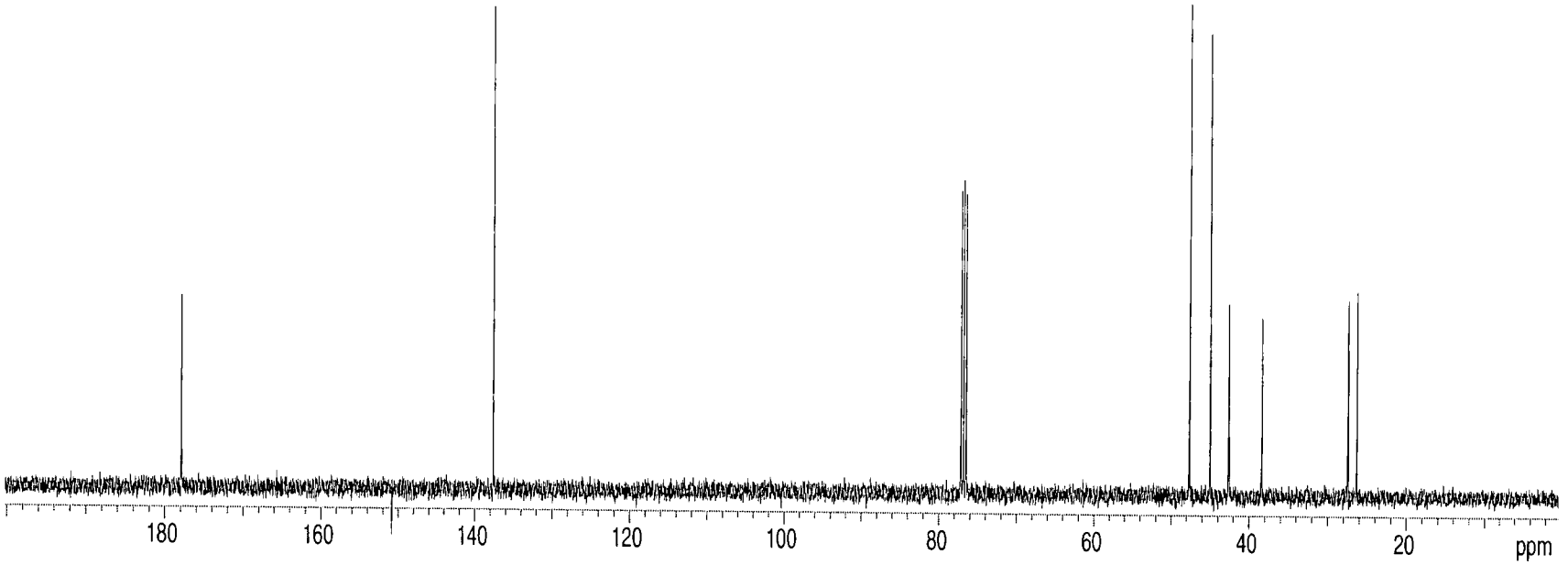

Appendix 2.42 ^{13}C nmr spectrum of *exo*-C6D.

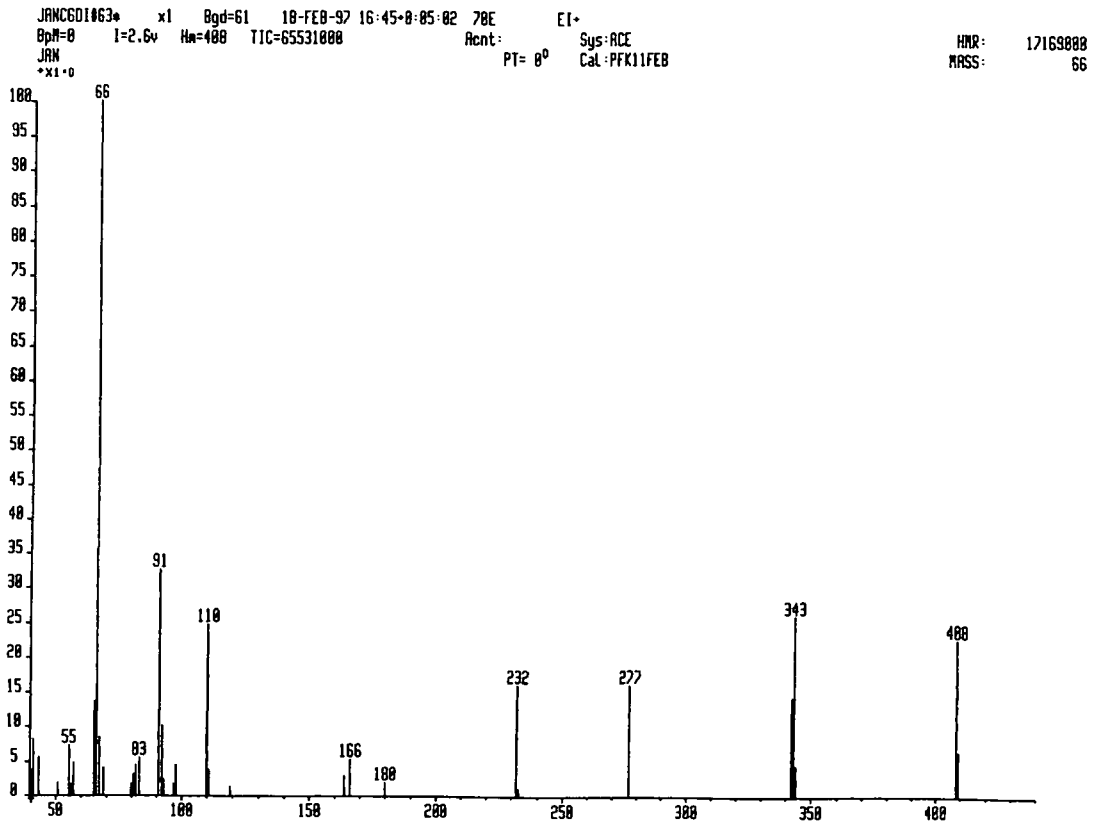

Appendix 2.43 Mass spectrum of *exo*-C6D.

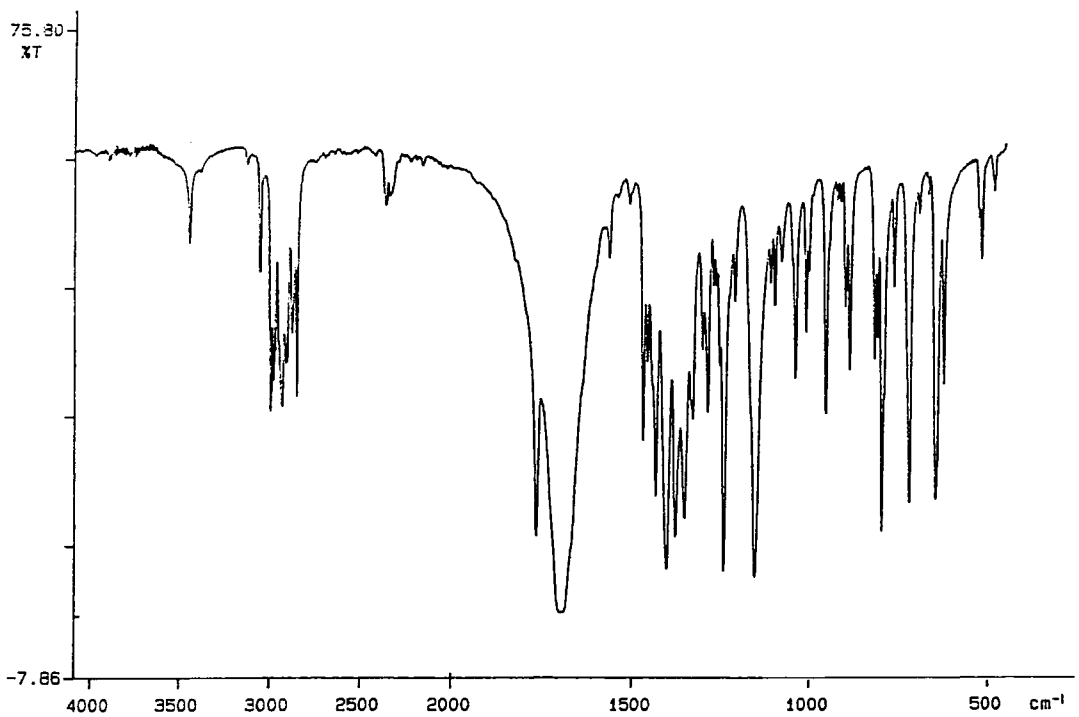

Appendix 2.44 Infrared spectrum of *exo*-C6D.

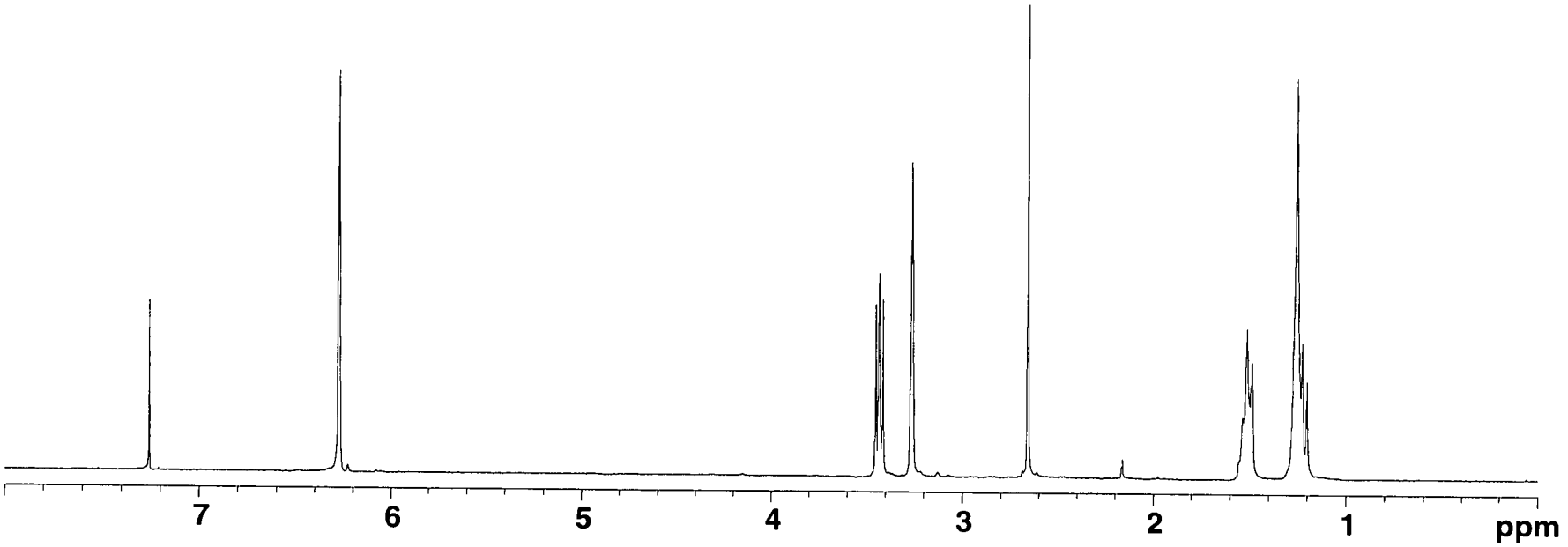

Appendix 2.45 ^{1}H nmr spectrum of *exo*-C9D.

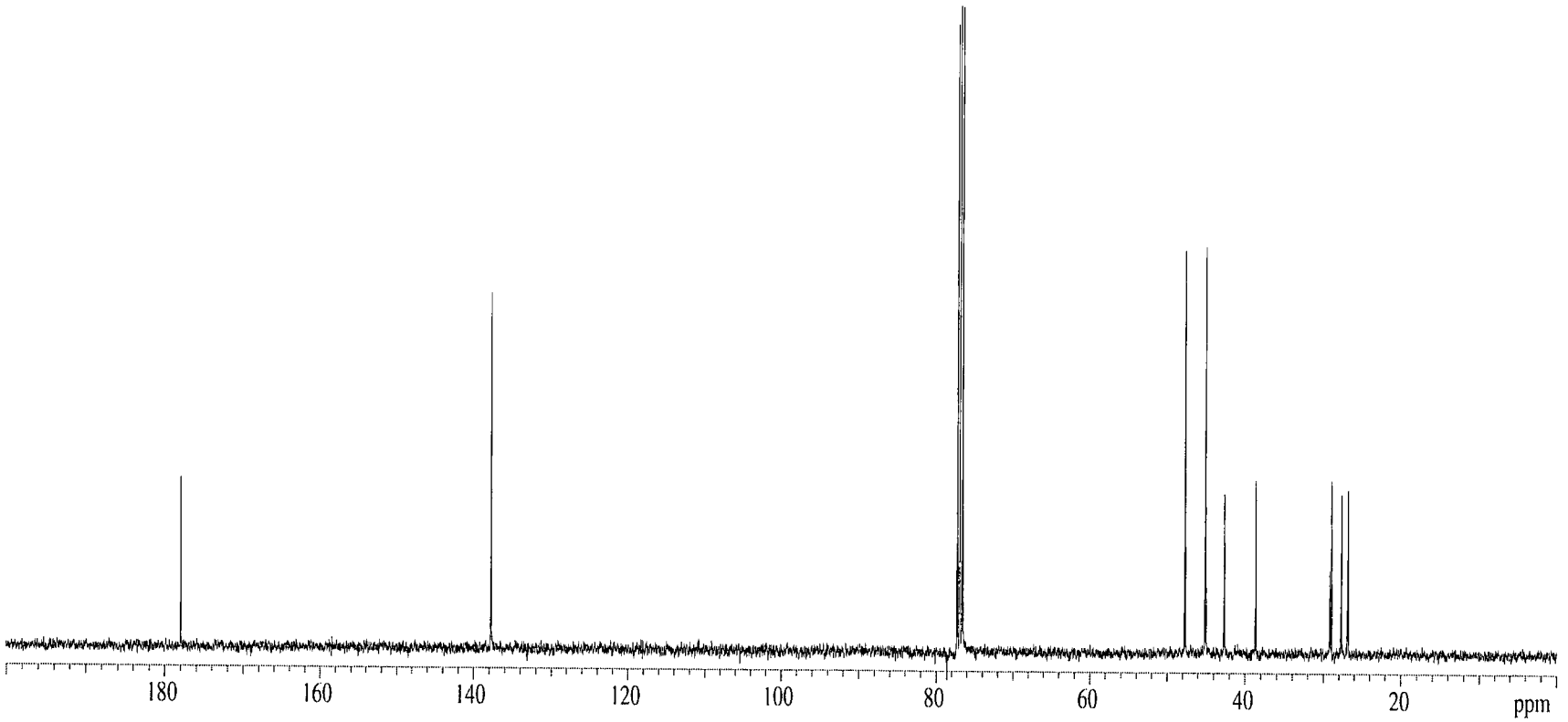

Appendix 2.46 ^{13}C nmr spectrum of *exo*-C9D.

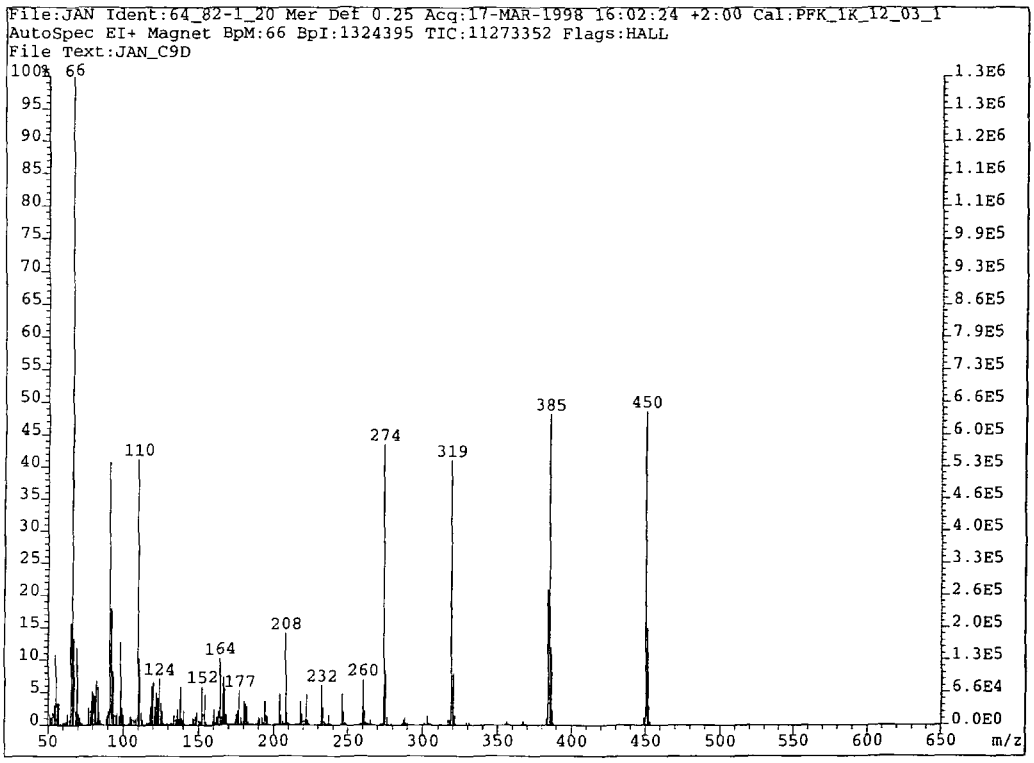

Appendix 2.47 Mass spectrum of *exo*-C9D.

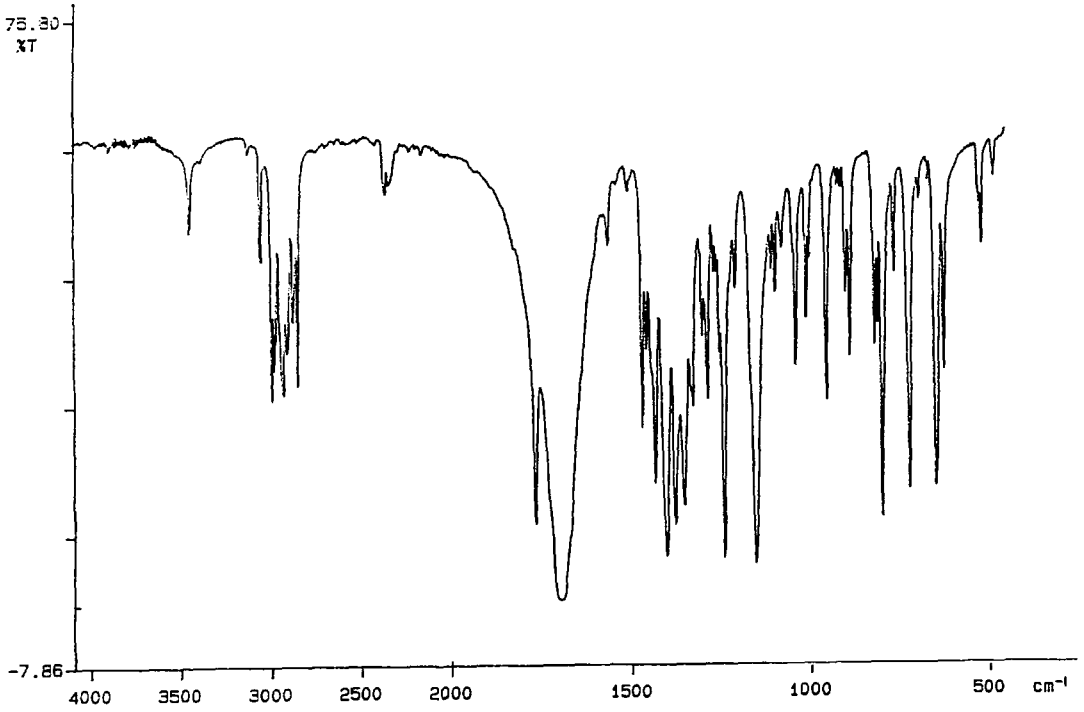

Appendix 2.48 Infrared spectrum of *exo*-C9D.

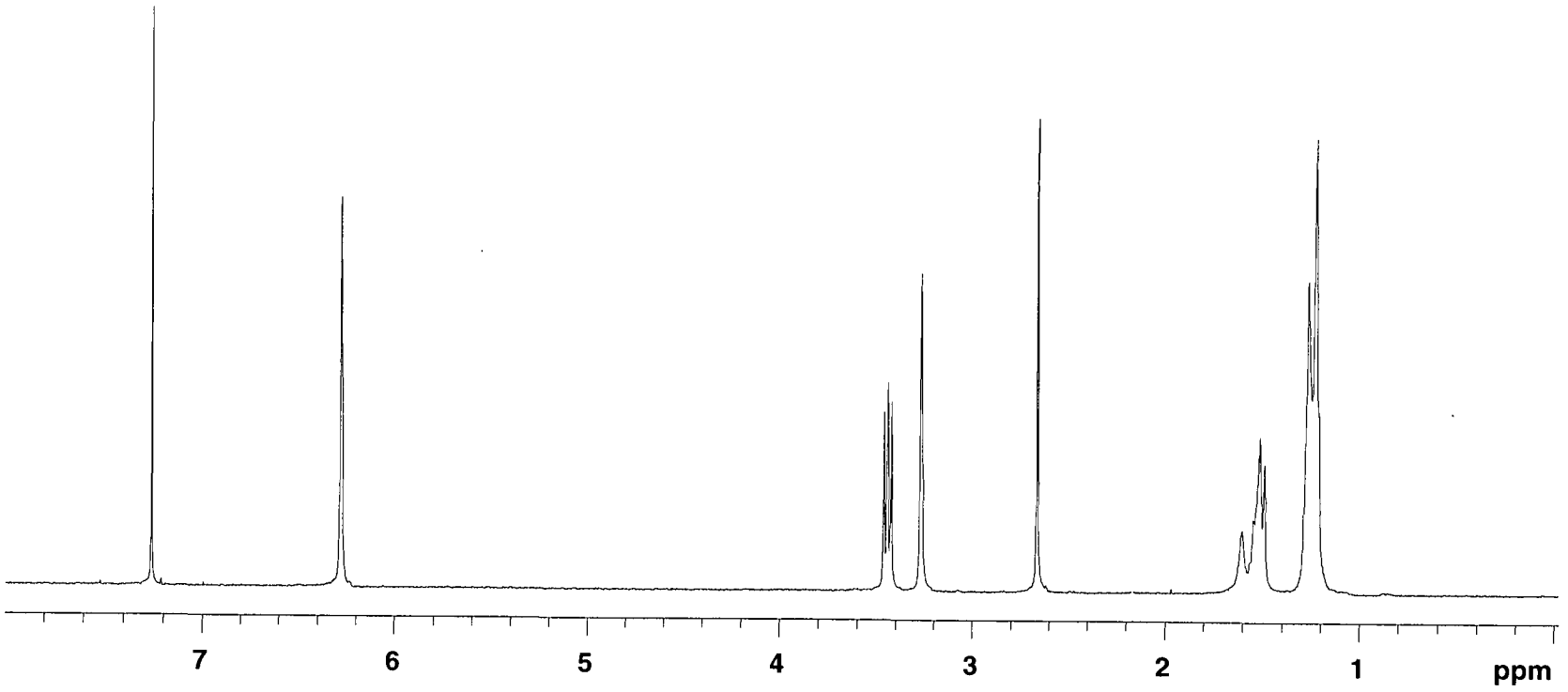

Appendix 2.49 ^{1}H nmr spectrum of *exo*-C12D.

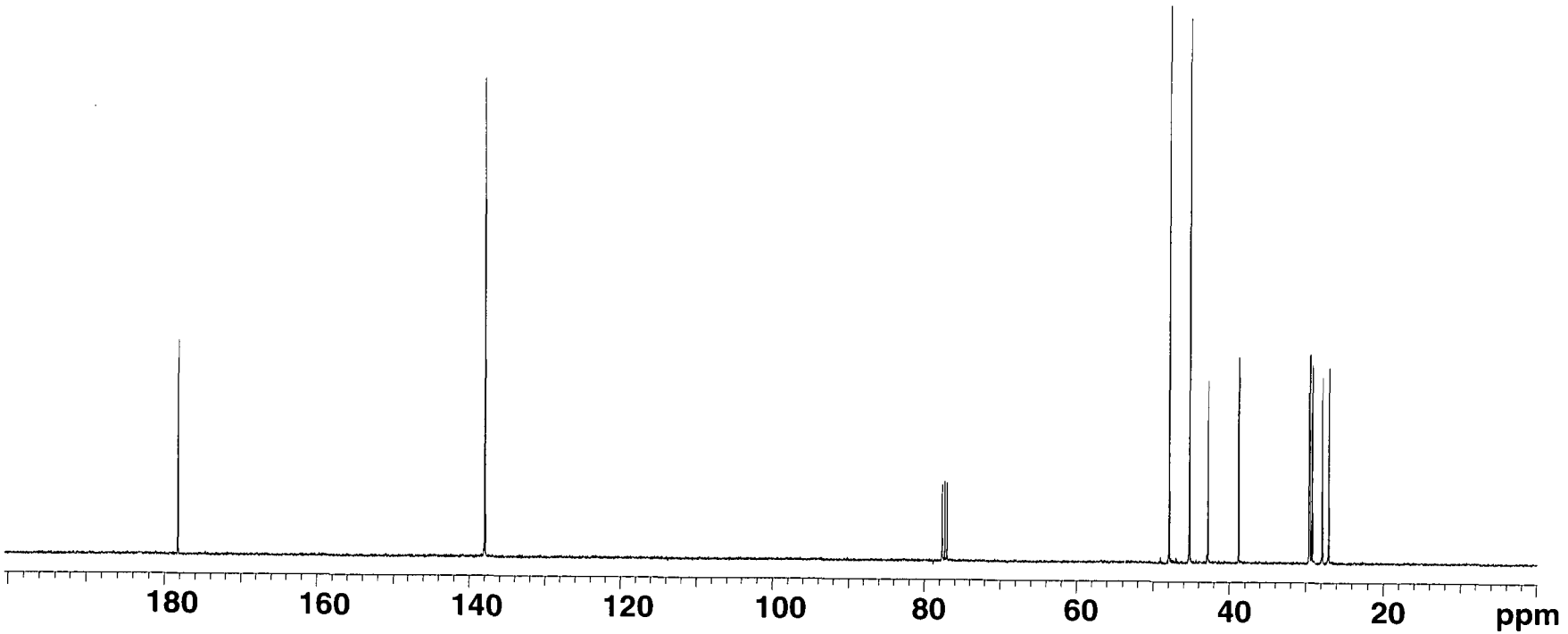

Appendix 2.50 ^{13}C nmr spectrum of *exo*-C12D.

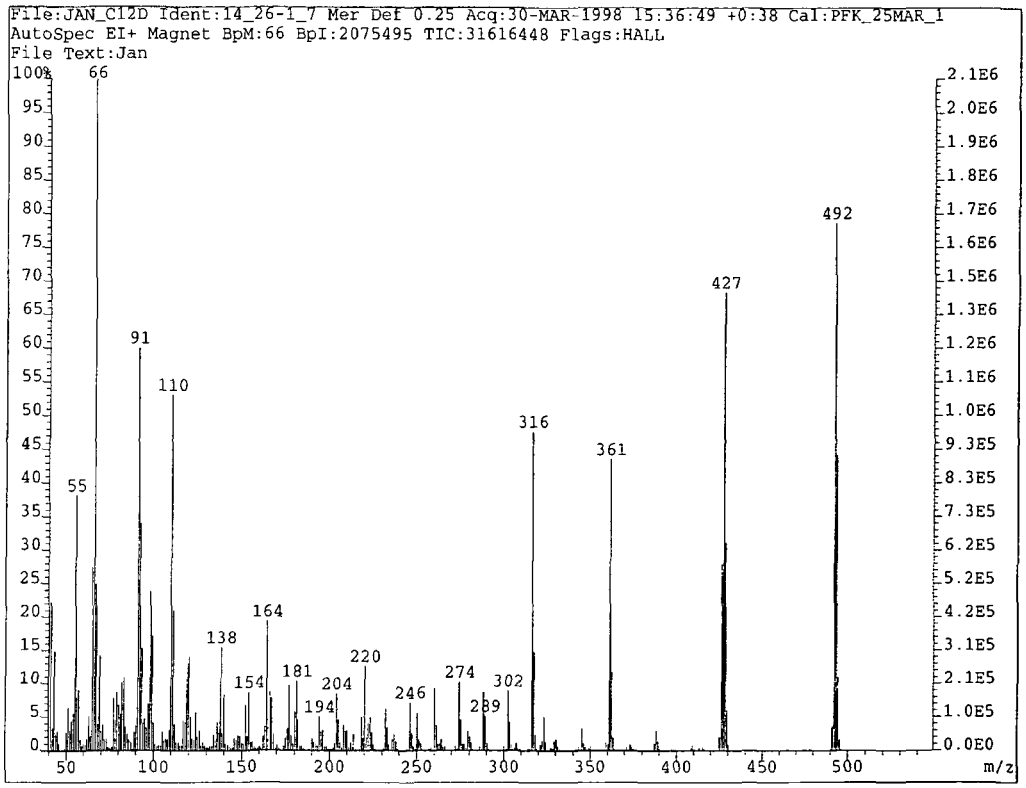

Appendix 2.51 Mass spectrum of *exo*-C12D.

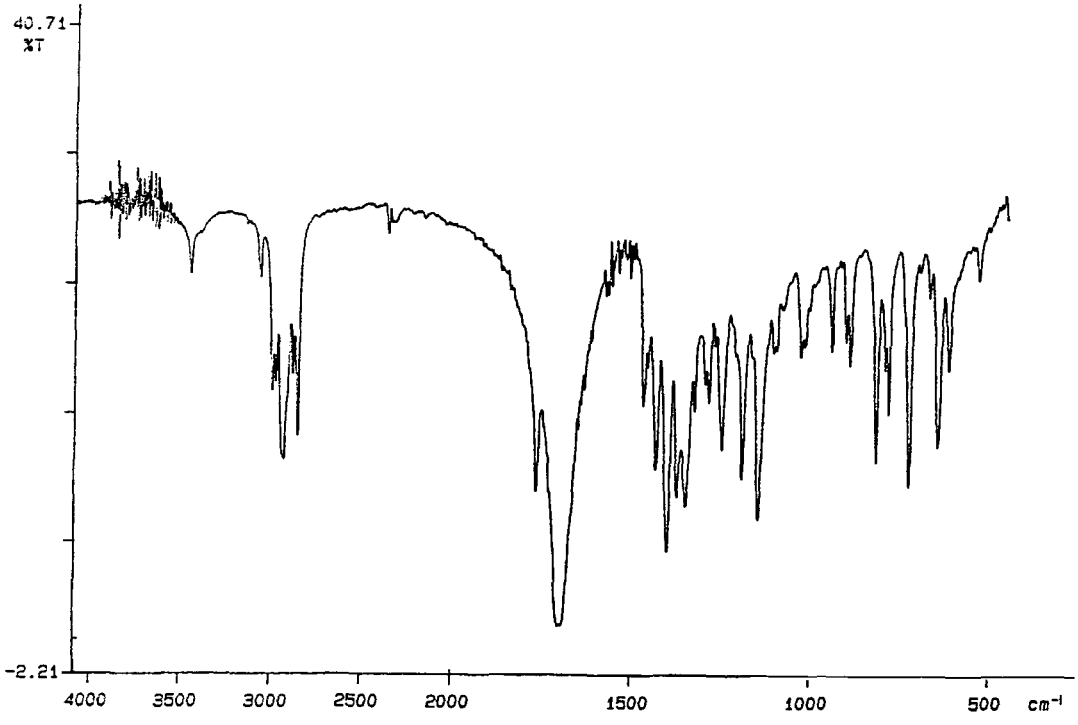

Appendix 2.52 Infrared spectrum of *exo*-C12D.

Appendix 3

Analytical data for Chapter 3

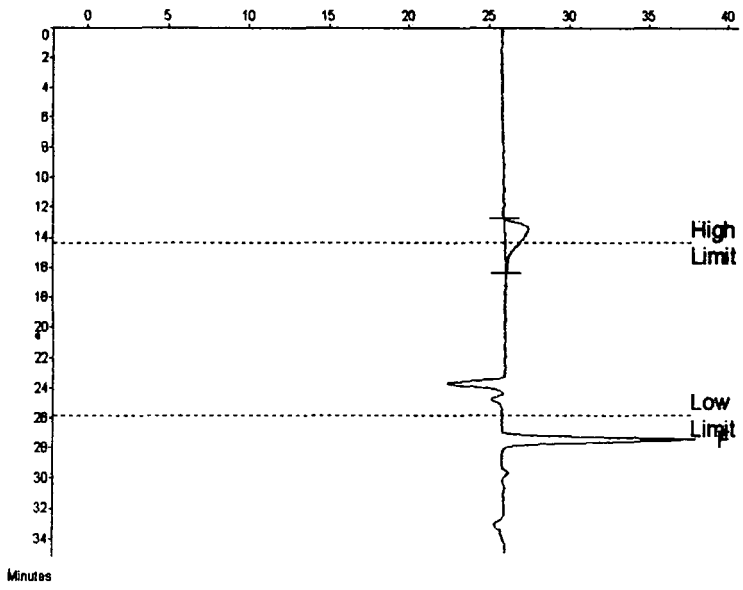

Molecular Weight Averages

Mn = 1,413,246

Mw = 1,934,585

Mz = 2,372,093

Polydispersity = 1.339

Appendix 3.1 GPC trace of crude polymeric material obtained from ROMP in bulk of 100% *exo*-C6M.

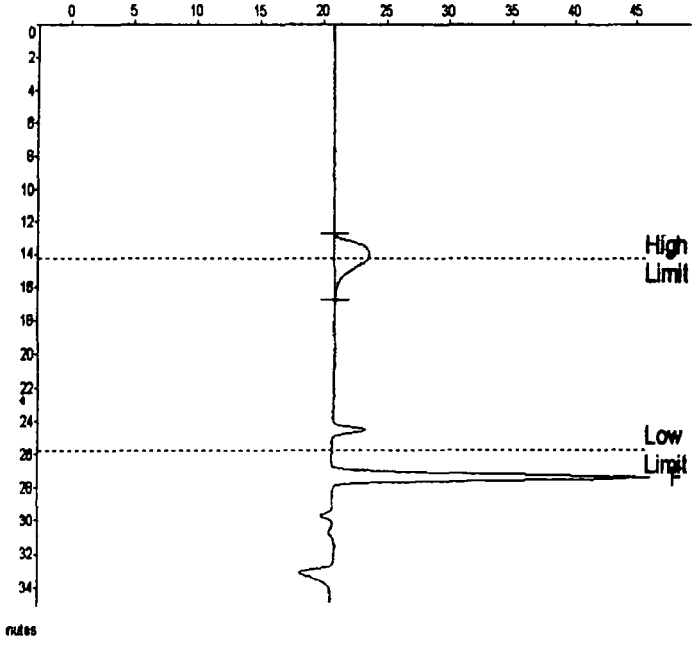

Molecular Weight Averages

Mn = 843,274

Mw = 1,386,014

Mz = 1,950,819

Polydispersity = 1.644

Appendix 3.2 GPC trace of crude polymeric material obtained from ROMP in bulk of 90% *exo*/10% *endo*-C6M.

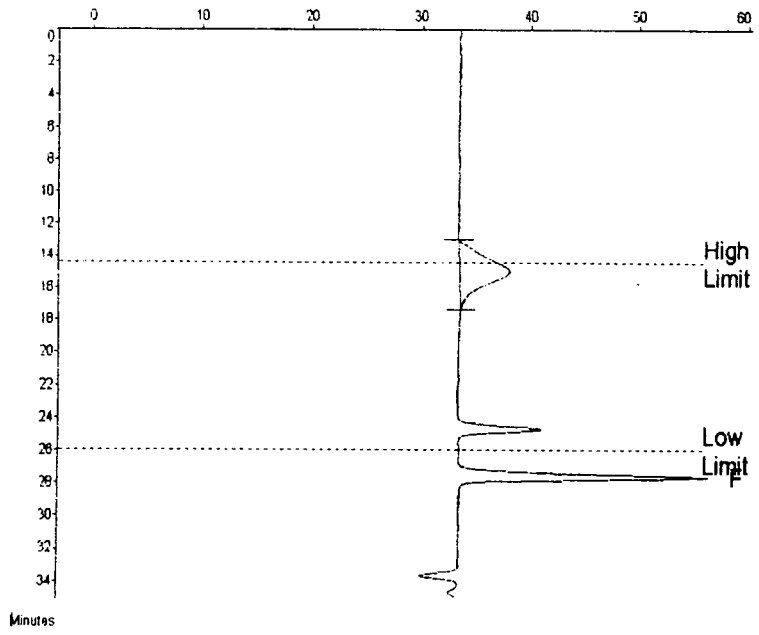

Molecular Weight Averages

Mn = 453,506

Mw = 800,289

Mz = 1,330,765

Polydispersity = 1.735

Appendix 3.3 GPC trace of crude polymeric material obtained from ROMP in bulk of 80% *exo*/20% *endo*-C6M.

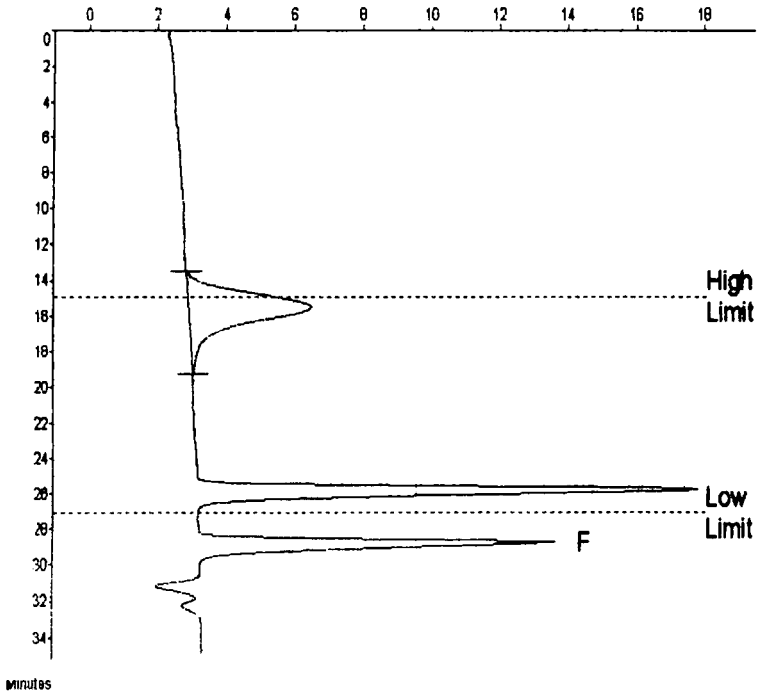

Molecular Weight Averages

Mn = 344,553

Mw = 618,067

Mz = 928,198

Polydispersity = 1.794

Appendix 3.4 GPC trace of crude polymeric material obtained from ROMP in bulk of 56% *exo*/44% *endo*-C6M.

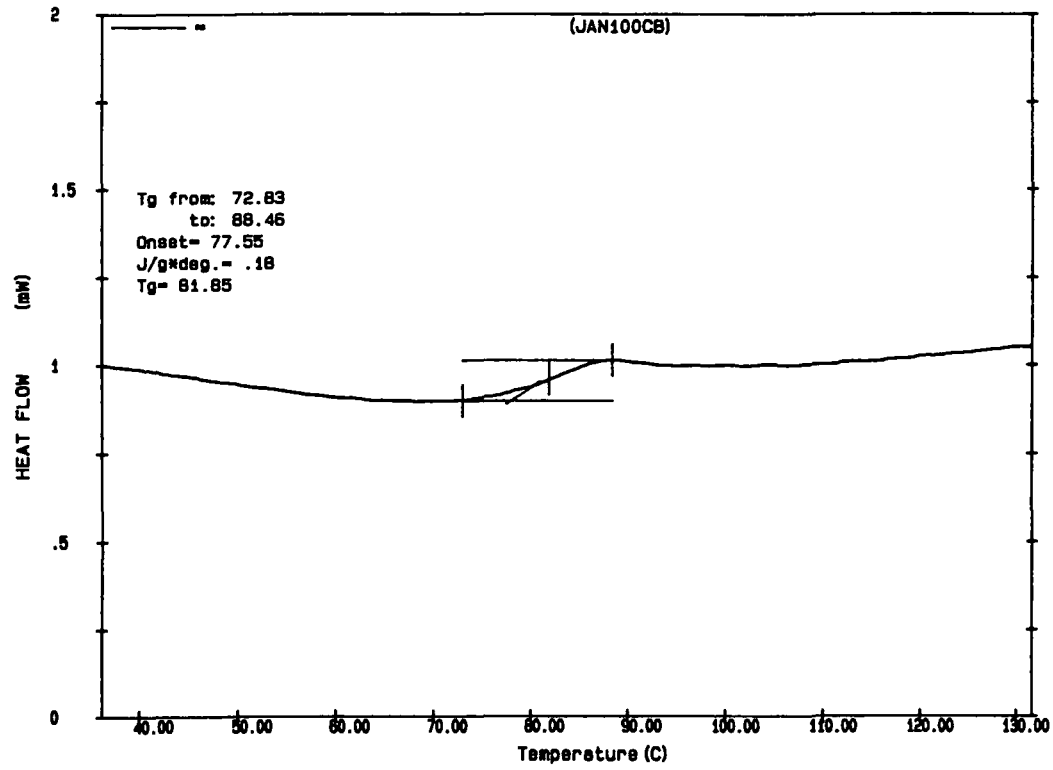

Appendix 3.5 DSC trace of crude polymeric material obtained from ROMP in bulk of 100% *exo*-C6M.

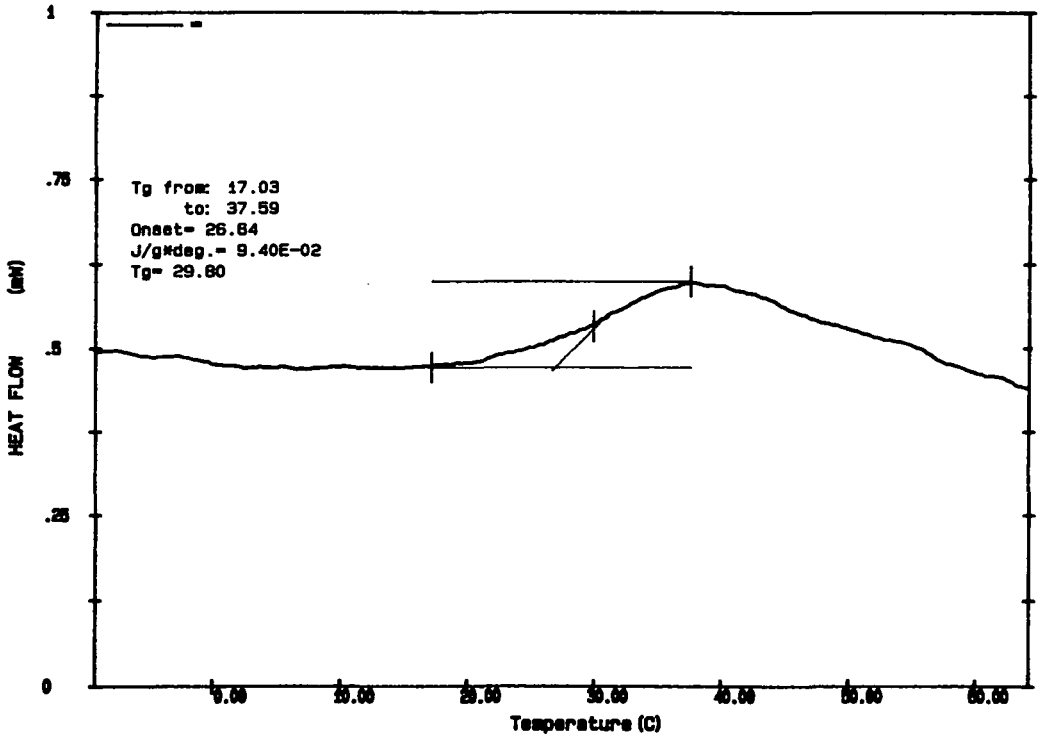

Appendix 3.6 DSC trace of crude polymeric material obtained from ROMP in bulk of 90% *exo*/ 10% *endo*-C6M.

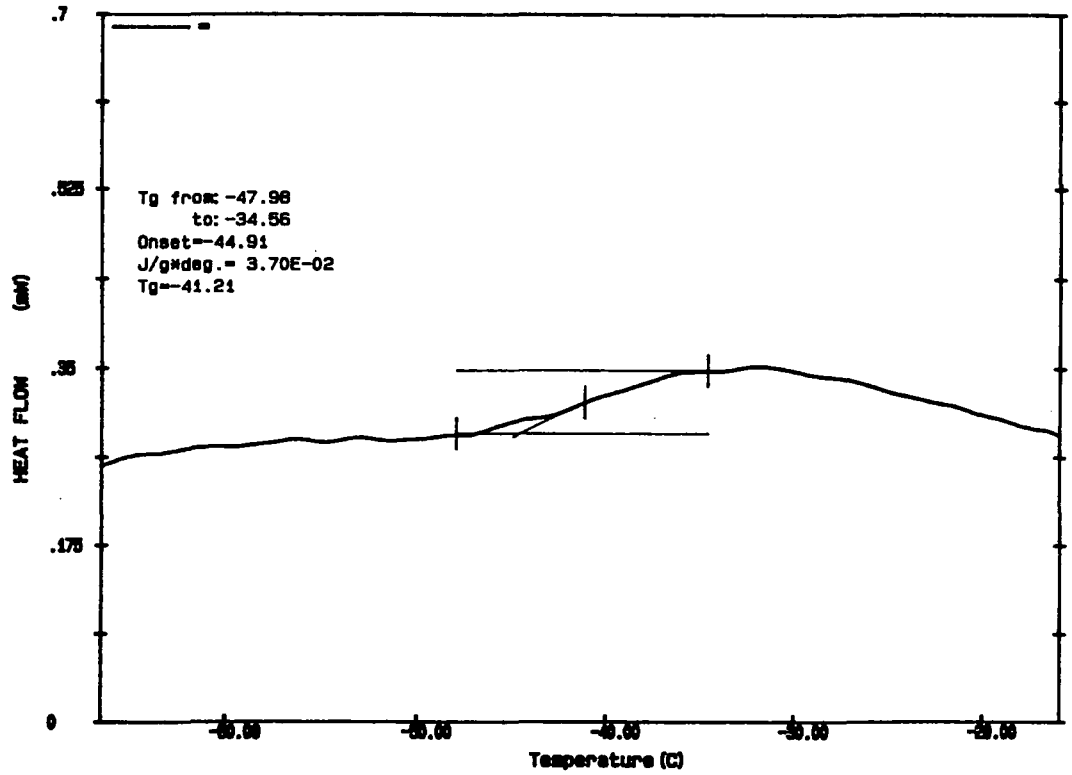

Appendix 3.7 DSC trace of crude polymeric material obtained from ROMP in bulk of 80% *exo*/ 20% *endo*-C6M.

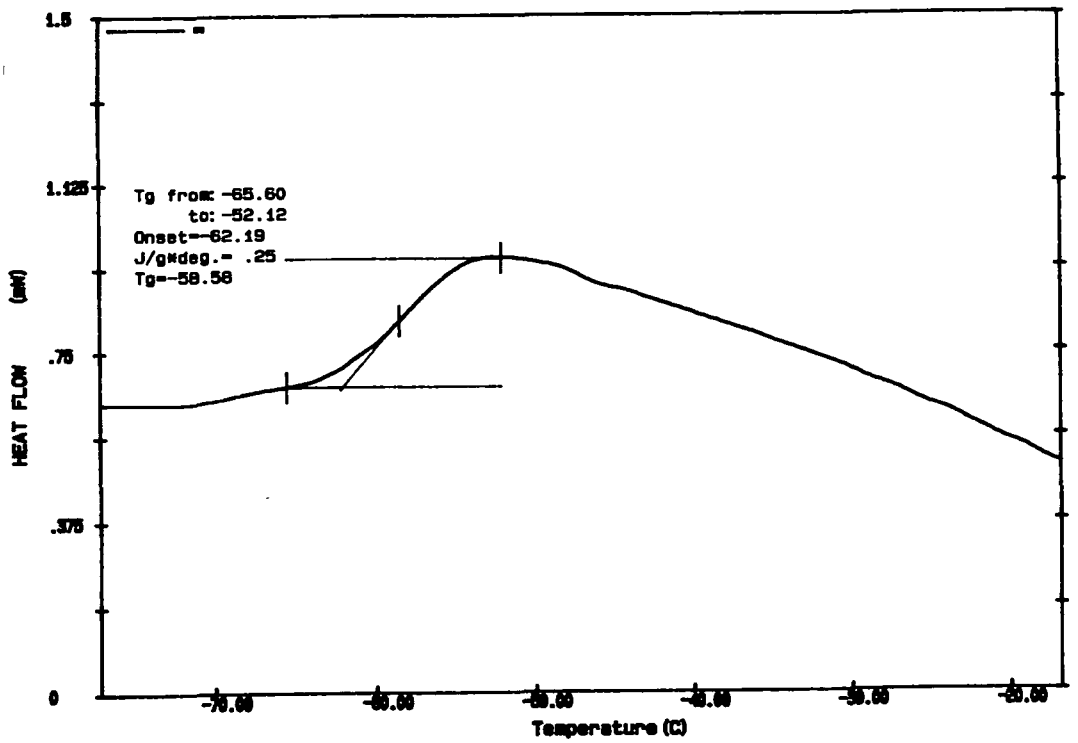

Appendix 3.8 DSC trace of crude polymeric material obtained from ROMP in bulk of 56% *exo*/ 44% *endo*-C6M.

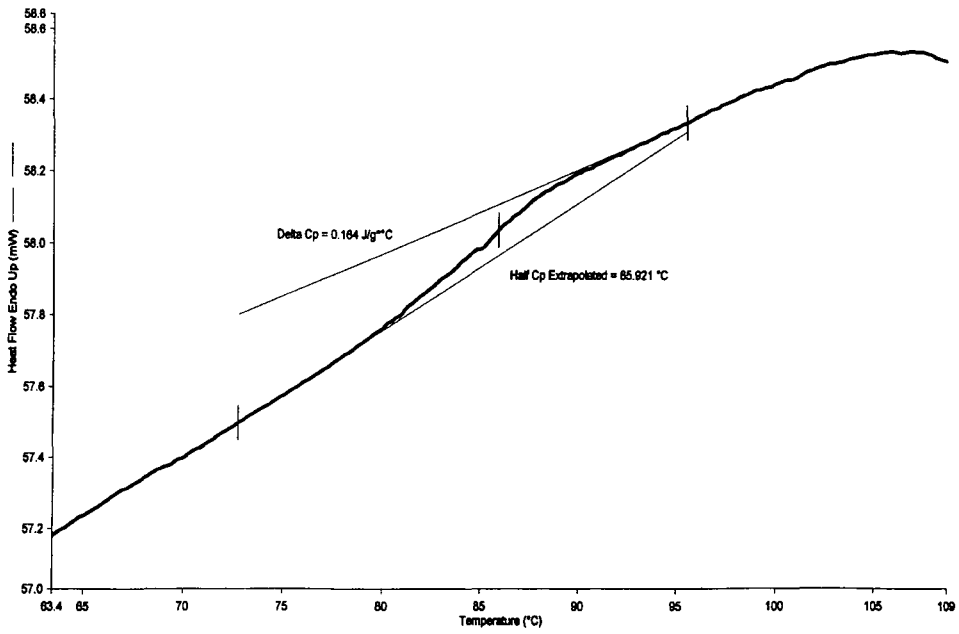

Appendix 3.9 DSC trace of pure polymeric material obtained from ROMP in bulk of 100% *exo*-C6M.

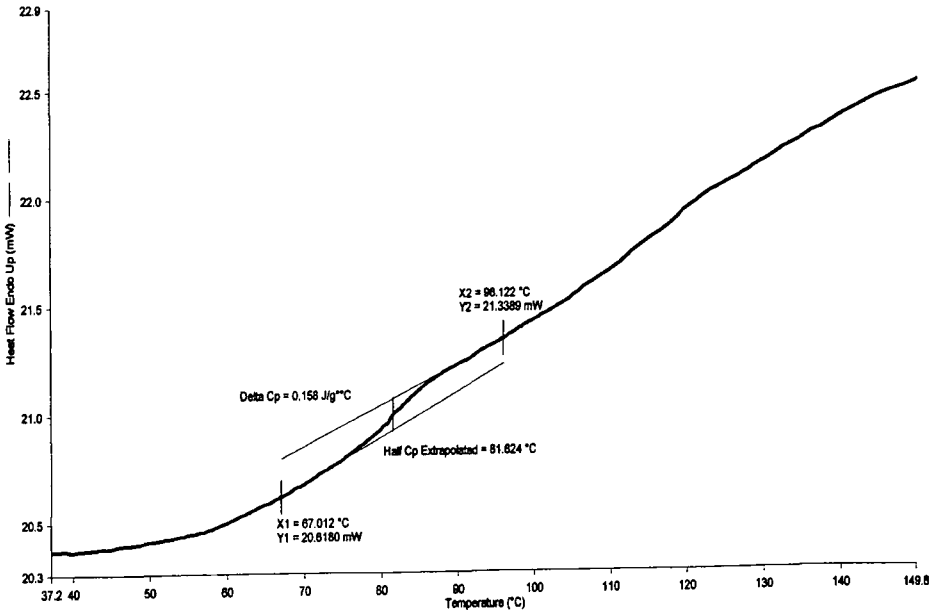

Appendix 3.10 DSC trace of pure polymeric material obtained from ROMP in bulk of 90% *exo*/10% *endo*-C6M.

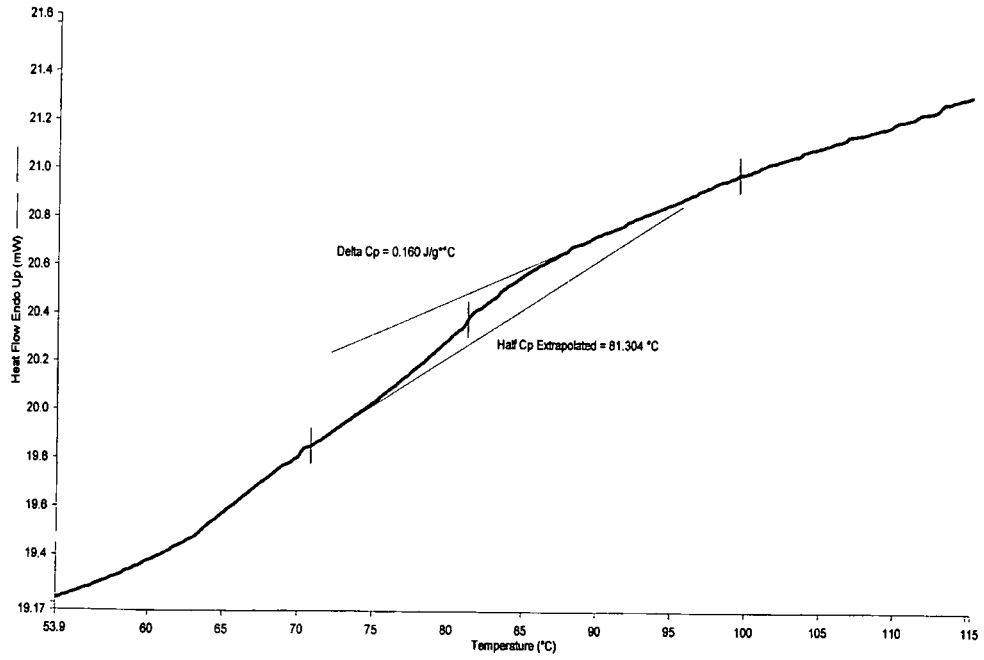

Appendix 3.11 DSC trace of pure polymeric material obtained from ROMP in bulk of 80% *exo*/20% *endo*-C6M.

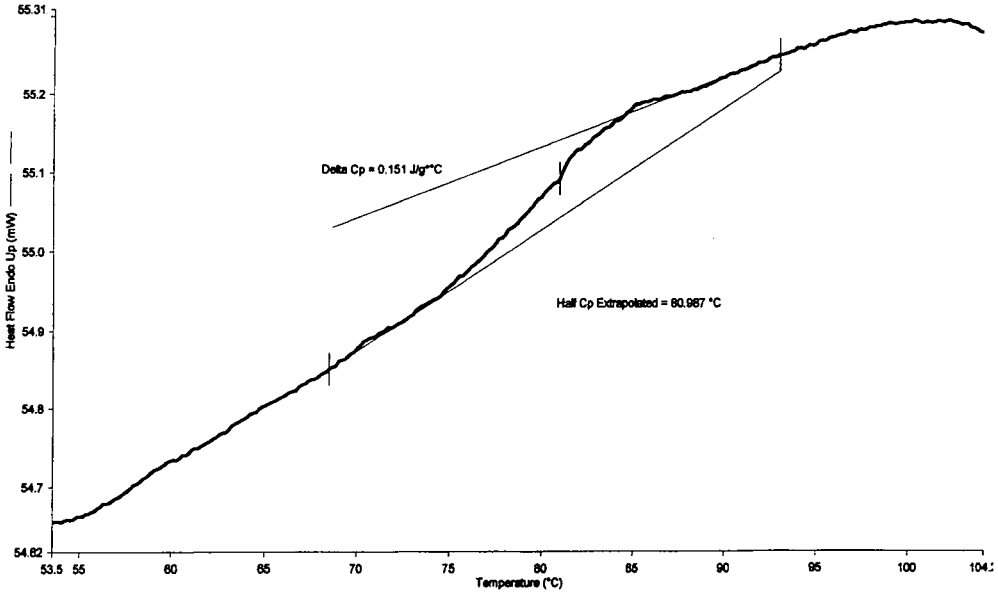

Appendix 3.12 DSC trace of pure polymeric material obtained from ROMP in bulk of 56% *exo*/44% *endo*-C6M.

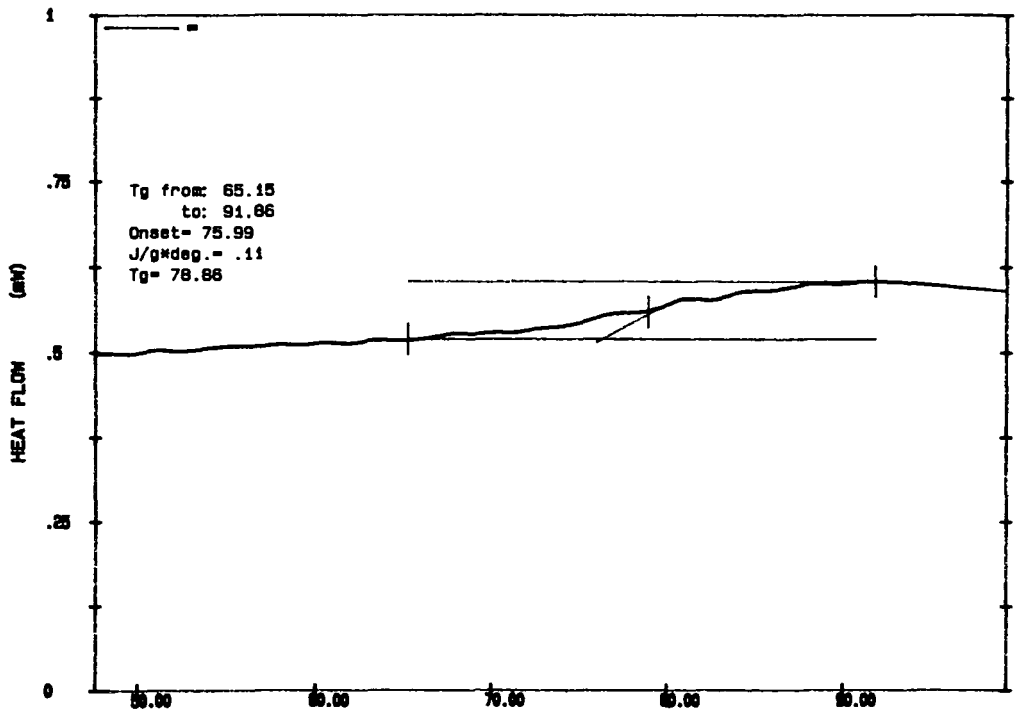

Appendix 3.13 DSC trace of crude polymeric material obtained from ROMP in bulk of 97% *exo*-C6M / 3% exo-C6D.

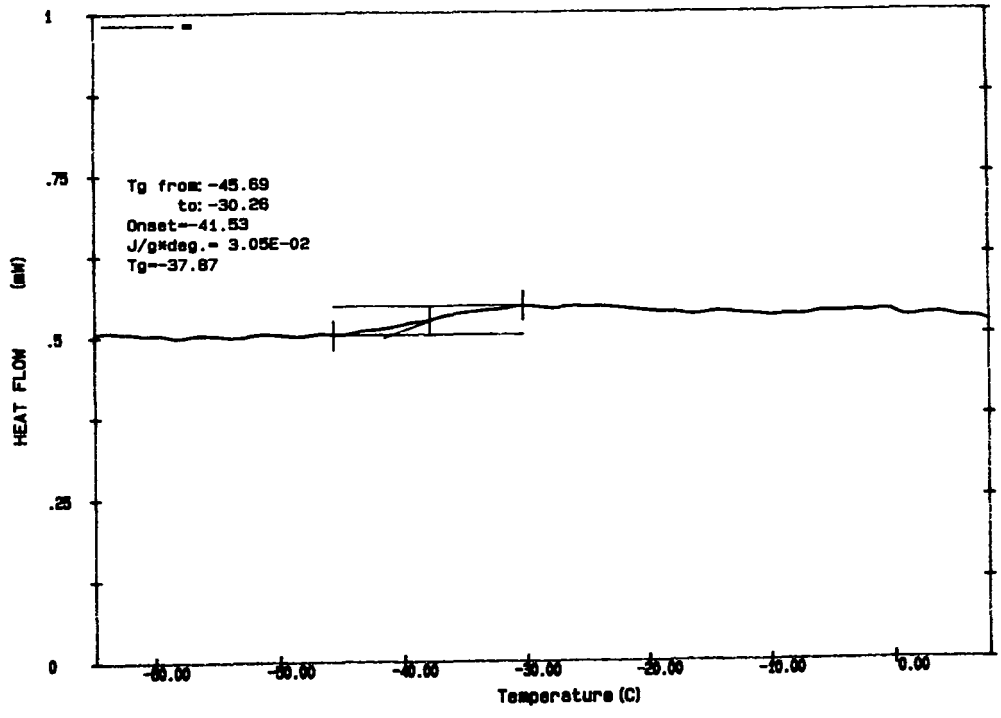

Appendix 3.14 DSC trace of crude polymeric material obtained from ROMP in bulk of 78% *exo*-C6M / 19% *endo*-C6M/ 3% exo-C6D.

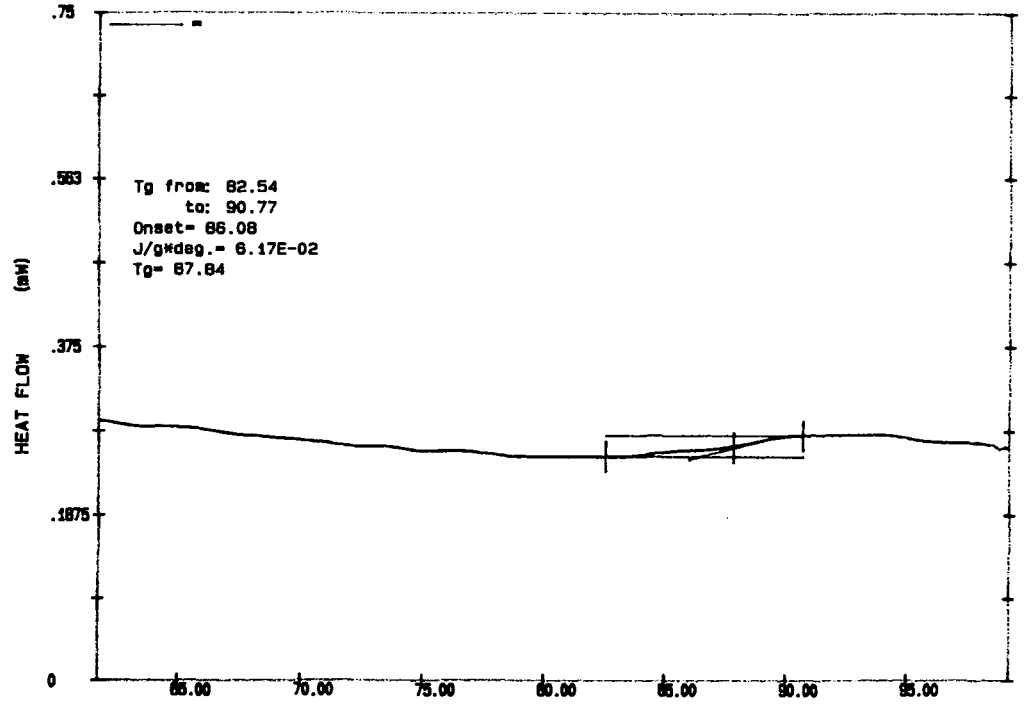

Appendix 3.15 DSC trace of gel fraction of material obtained from ROMP in bulk of 97% *exo*-C6M / 3% exo-C6D.

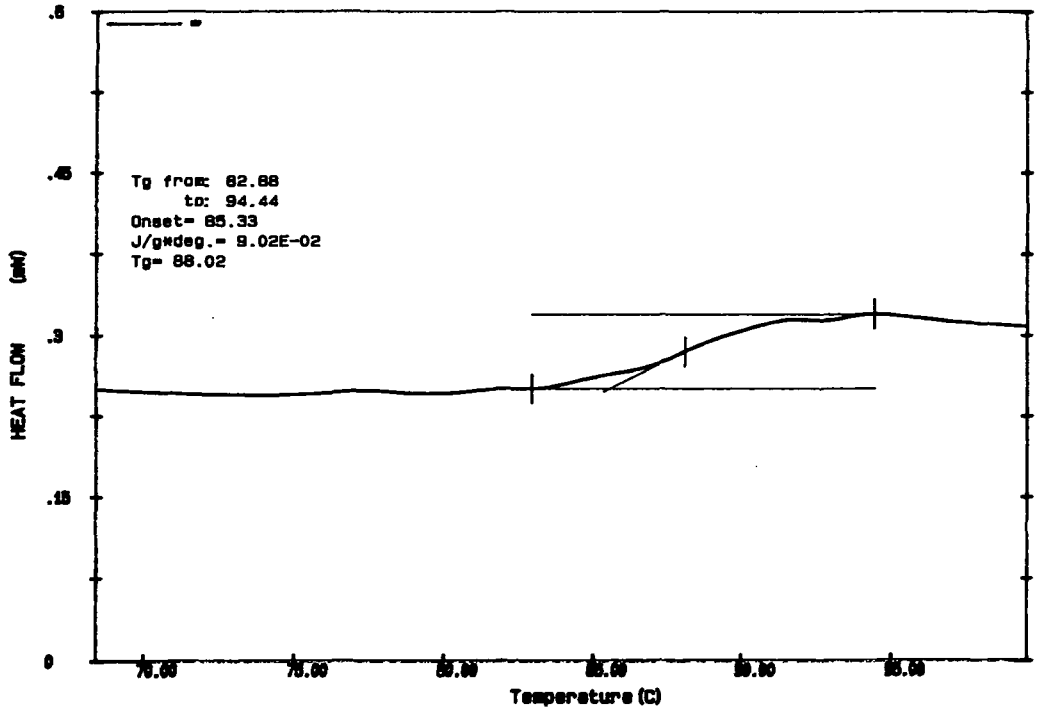

Appendix 3.16 DSC trace of gel fraction of material obtained from ROMP in bulk of 97% *exo*-C6M /19% *endo*-C6M/ 3% exo-C6D.

Appendix 4

Analytical data for Chapter 4

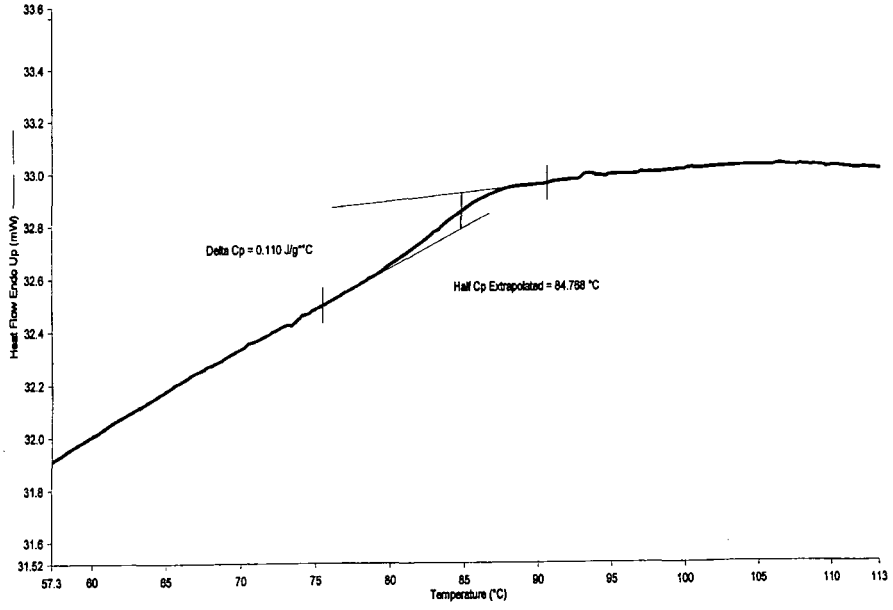

Appendix 4.1 DSC trace of poly(*exo*)

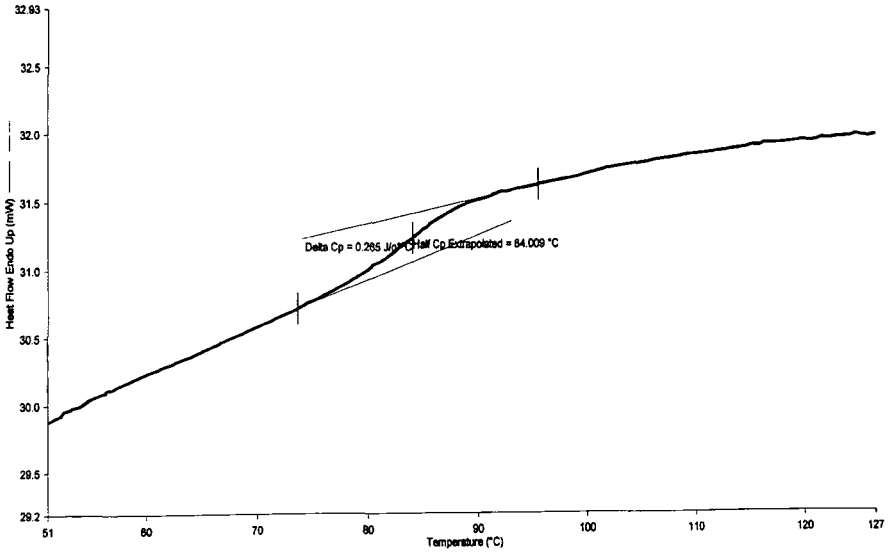

Appendix 4.2 DSC trace of poly(*exo* + *exo*)

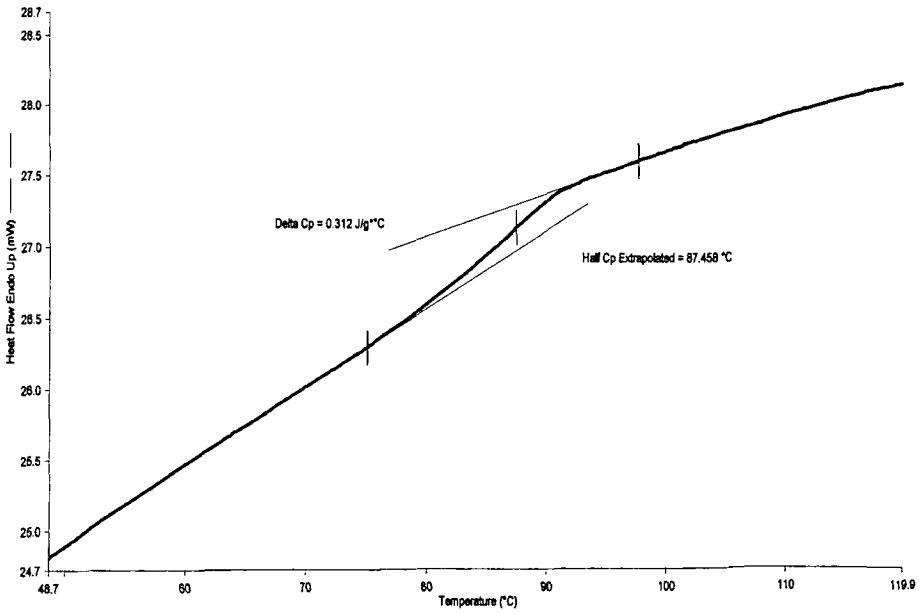

Appendix 4.3 DSC trace of poly(*exo+endo*).

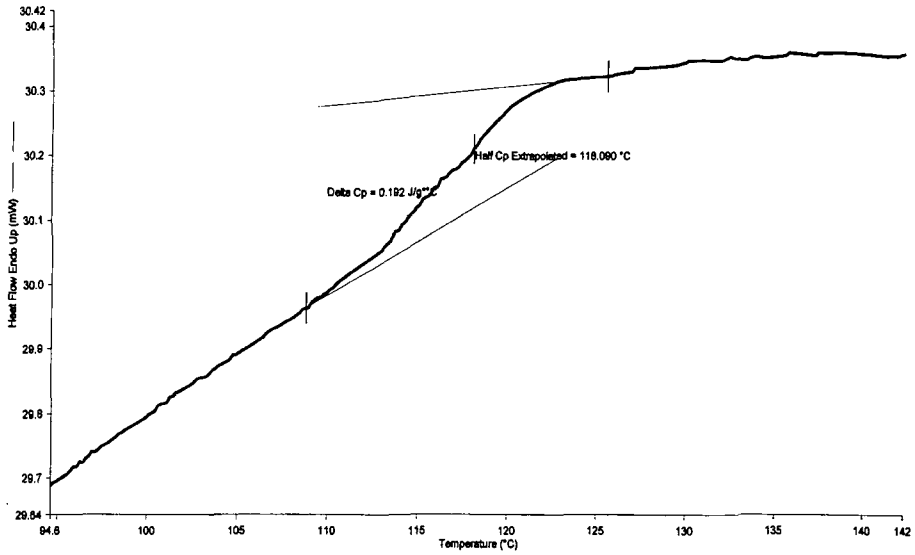

Appendix 4.4 DSC trace of poly(*endo*).

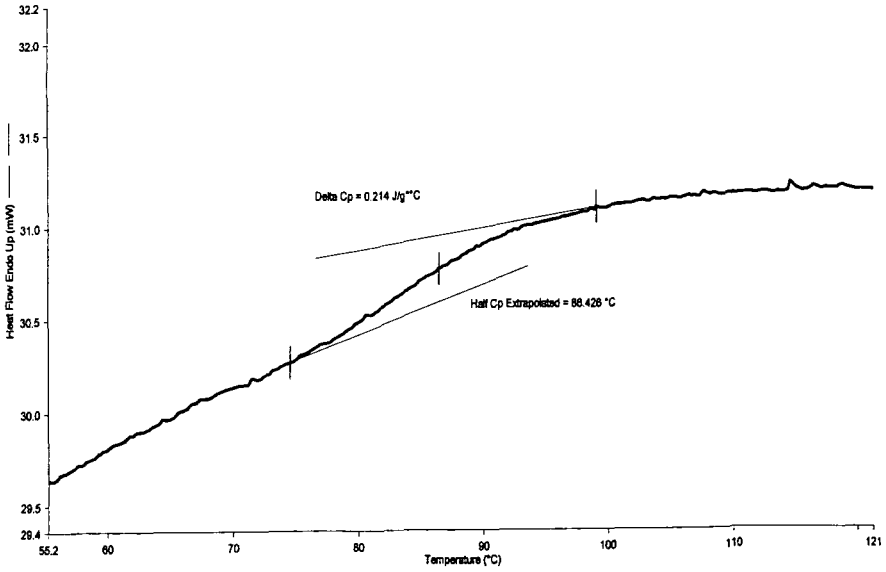

Appendix 4.5 DSC trace of poly(*endo*+*exo*).

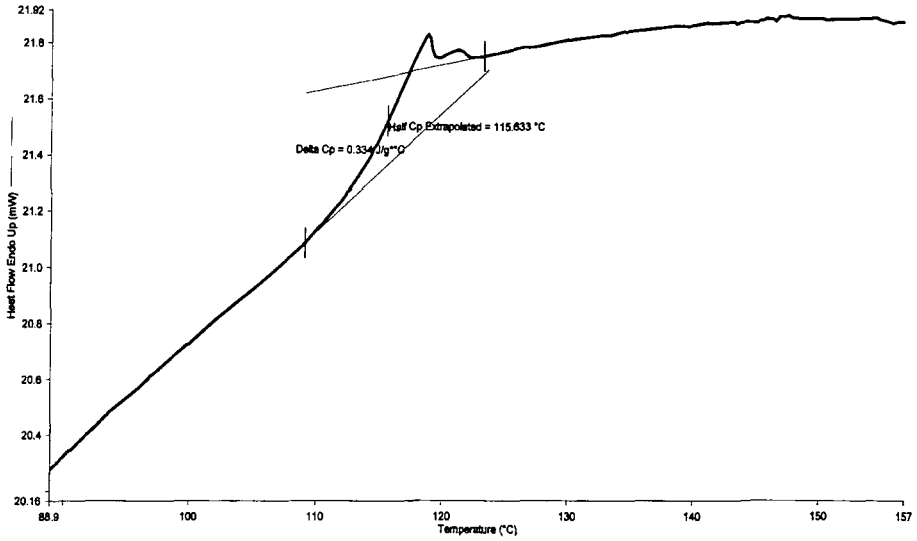

Appendix 4.6 DSC trace of poly(*endo*+*endo*).

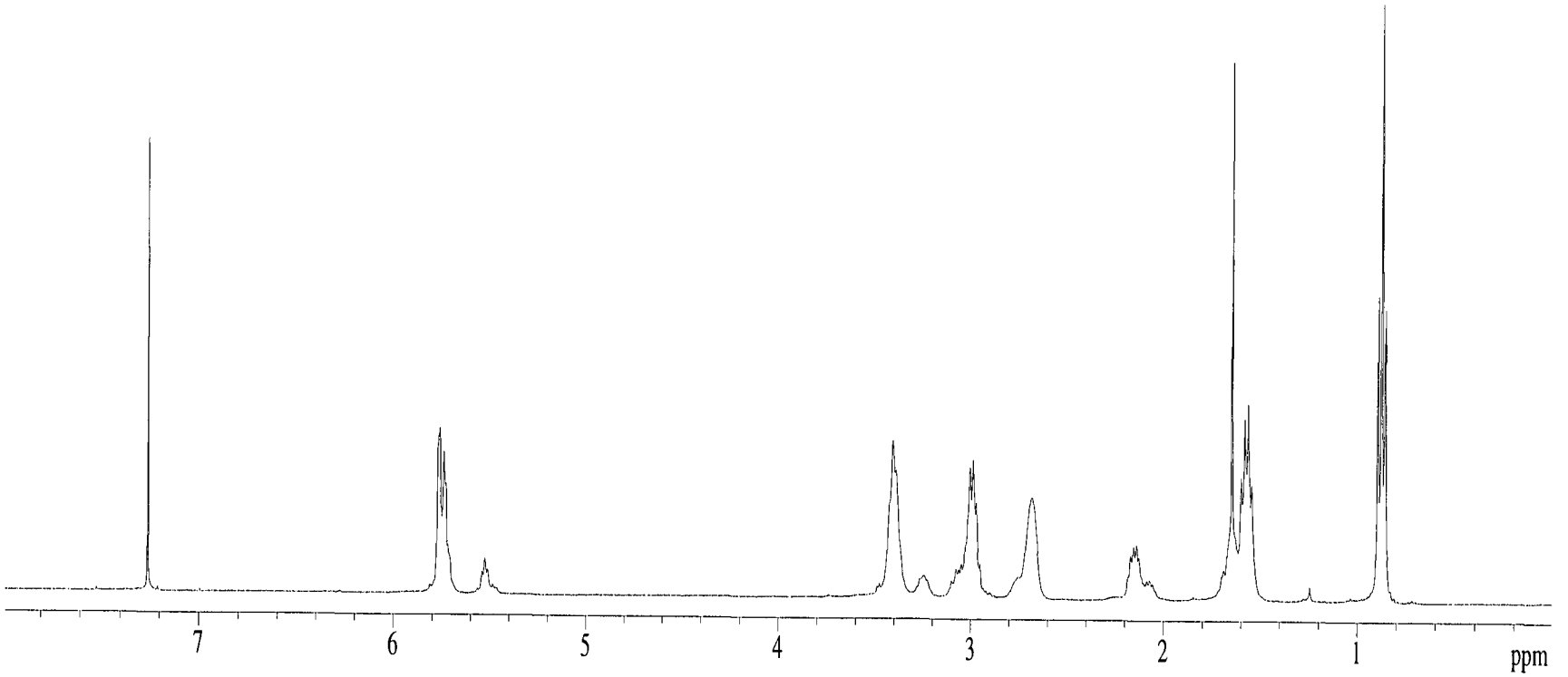

Appendix 4.7 ^{1}H nmr spectrum of poly(*exo*-C3M).

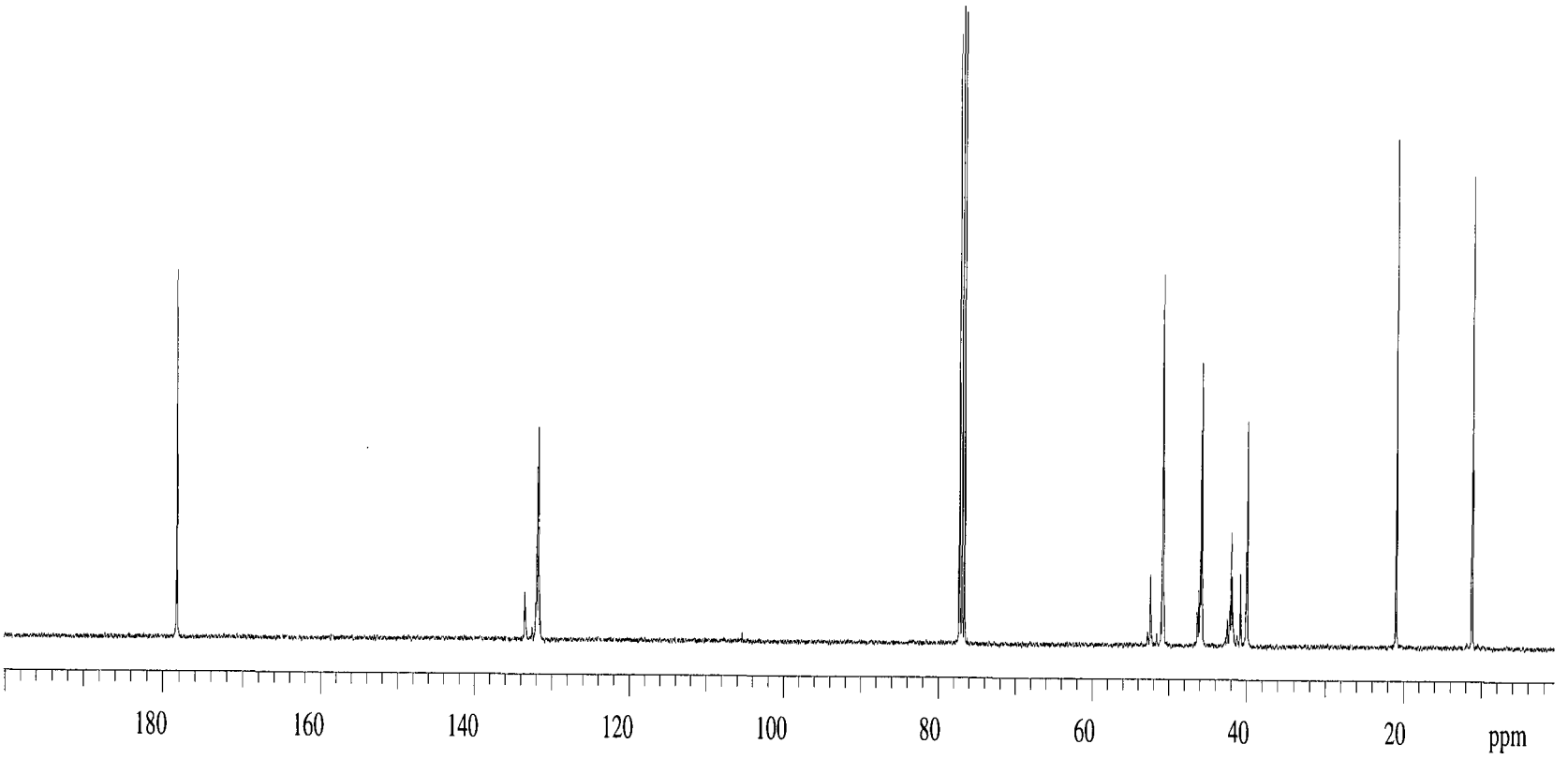

Appendix 4.8 ^{13}C nmr spectrum of poly(*exo*-C3M).

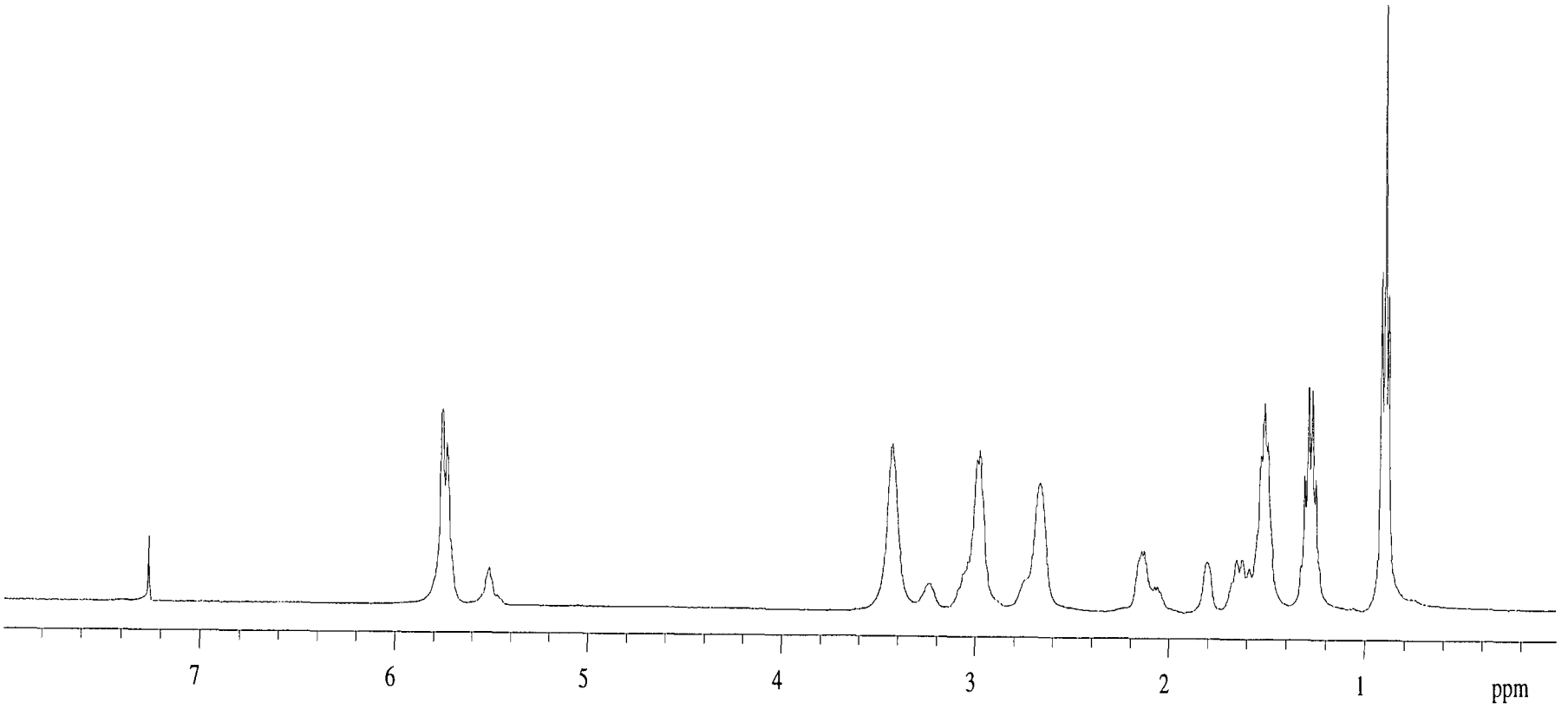

Appendix 4.9 ^{1}H nmr spectrum of poly(*exo*-C4M).

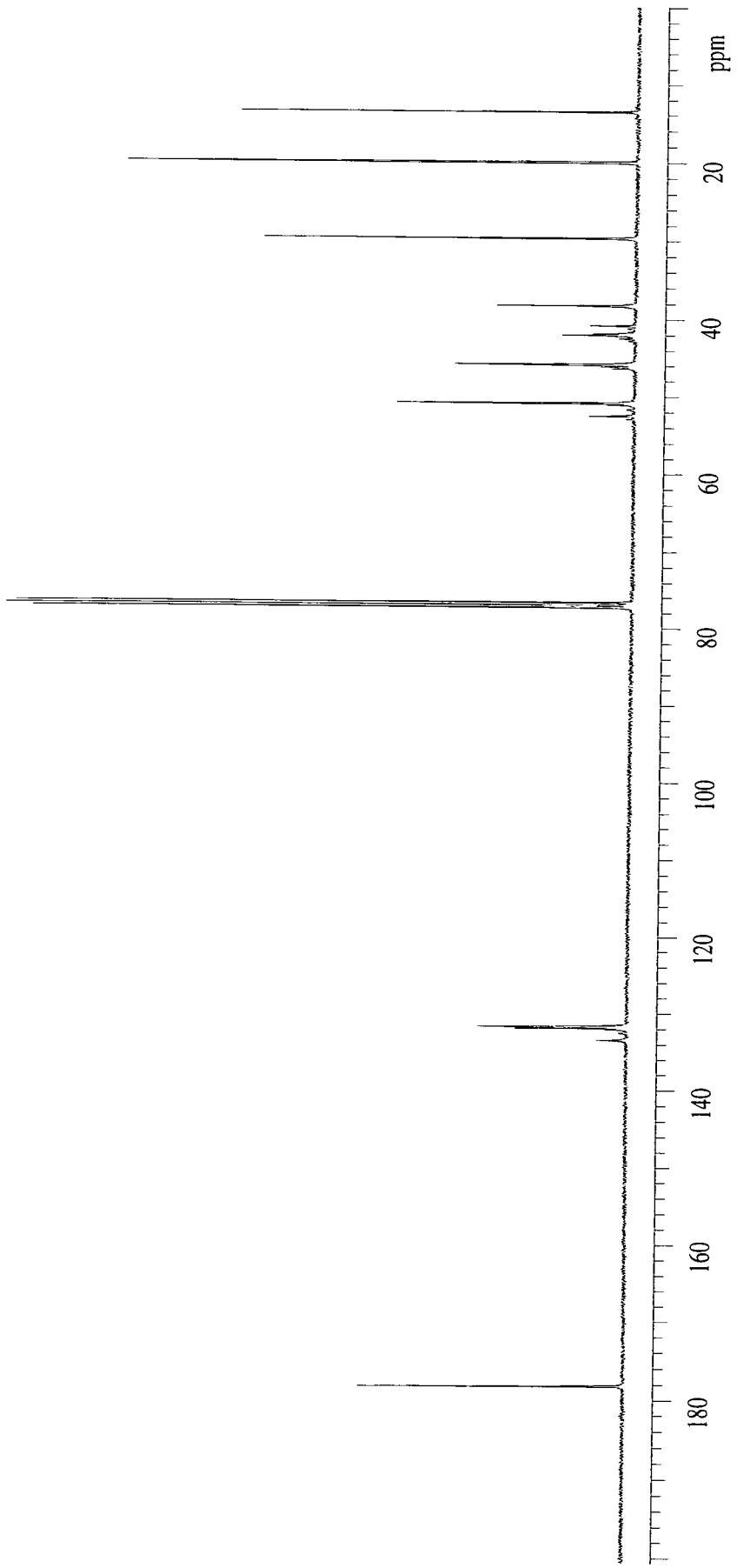

Appendix 4.10 ^{13}C nmr spectrum of poly(*exo*-C4M).

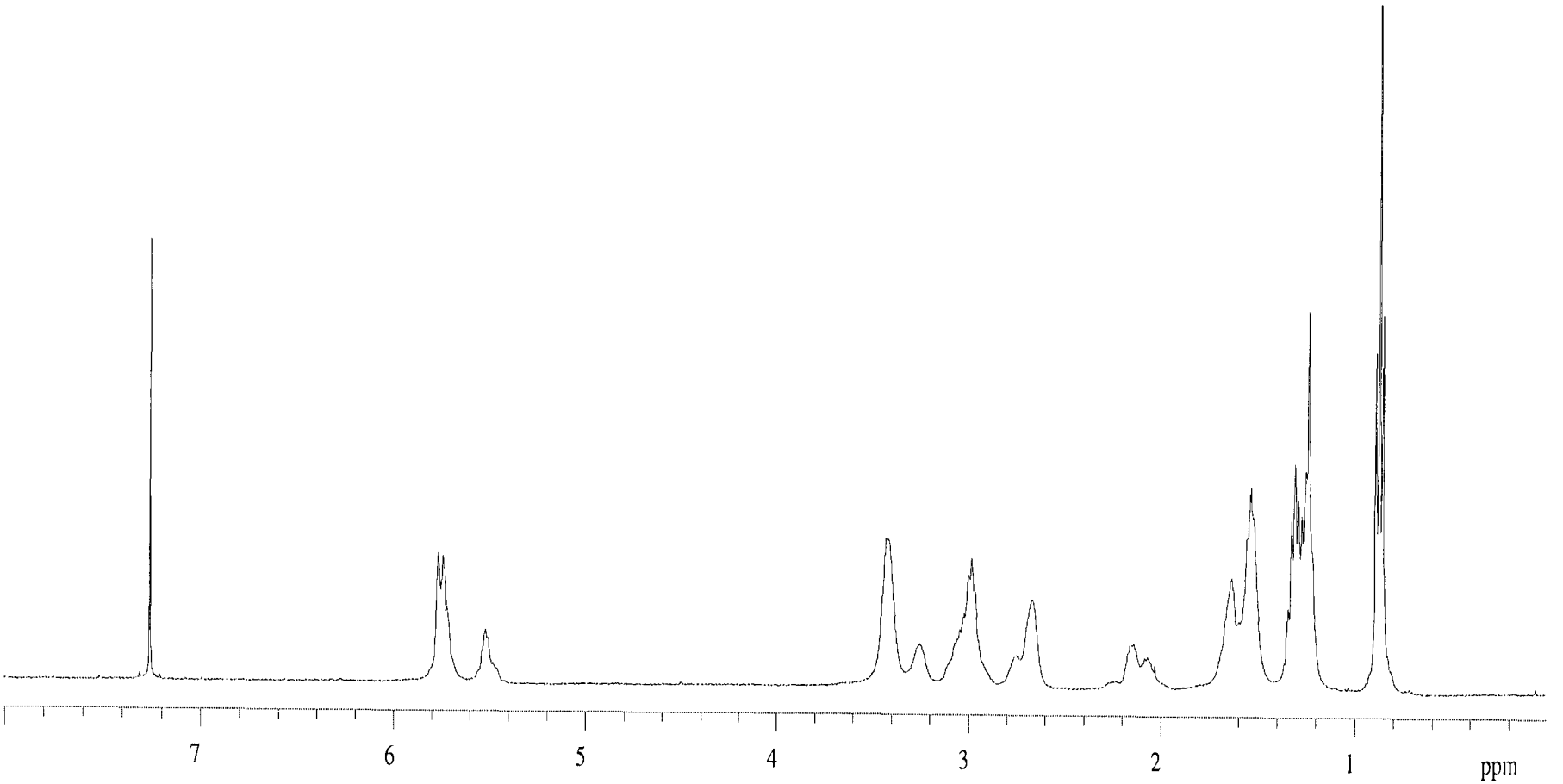

Appendix 4.11 ^{1}H nmr spectrum of poly(*exo*-C5M).

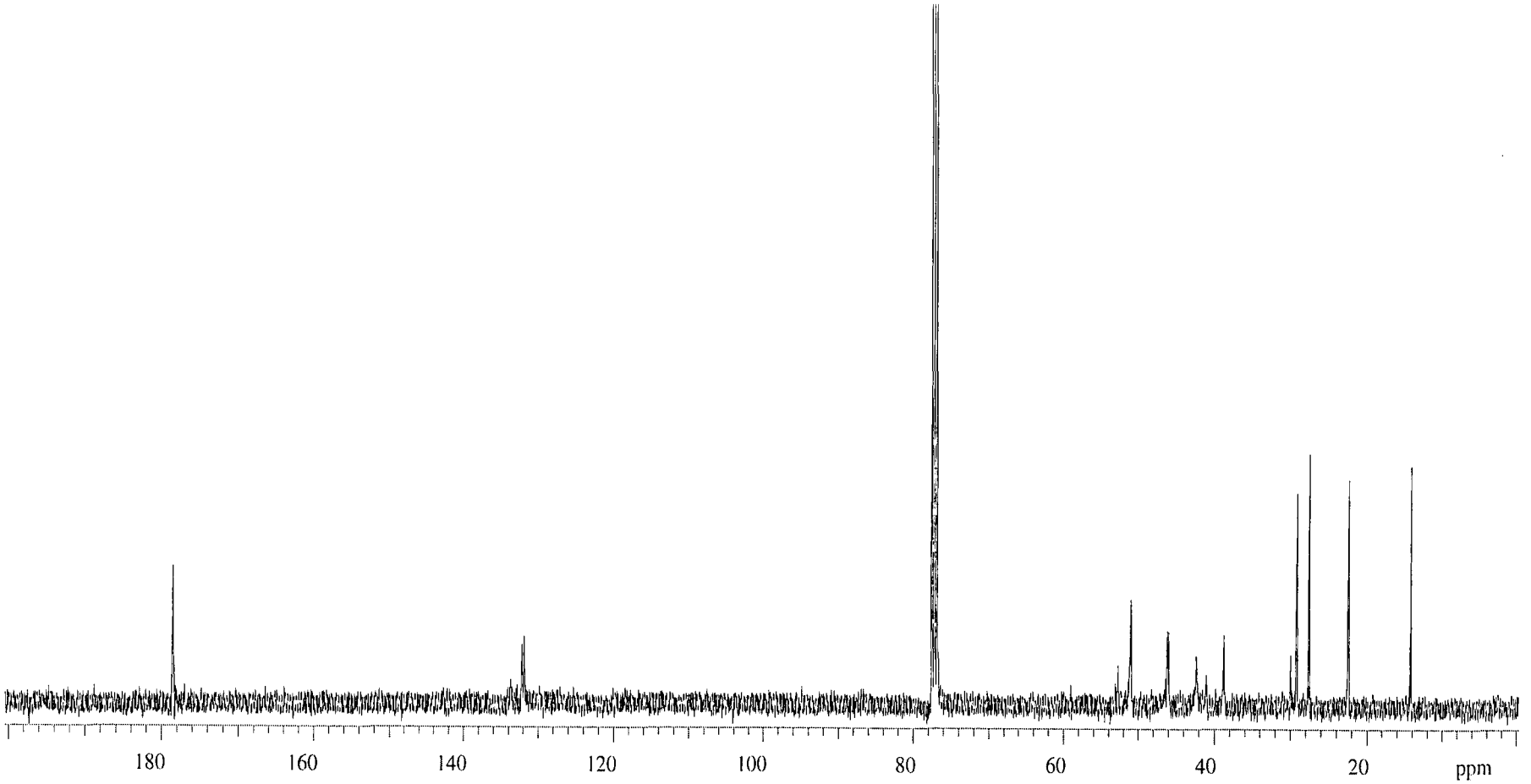

Appendix 4.12 ^{13}C nmr spectrum of poly(*exo*-C5M).

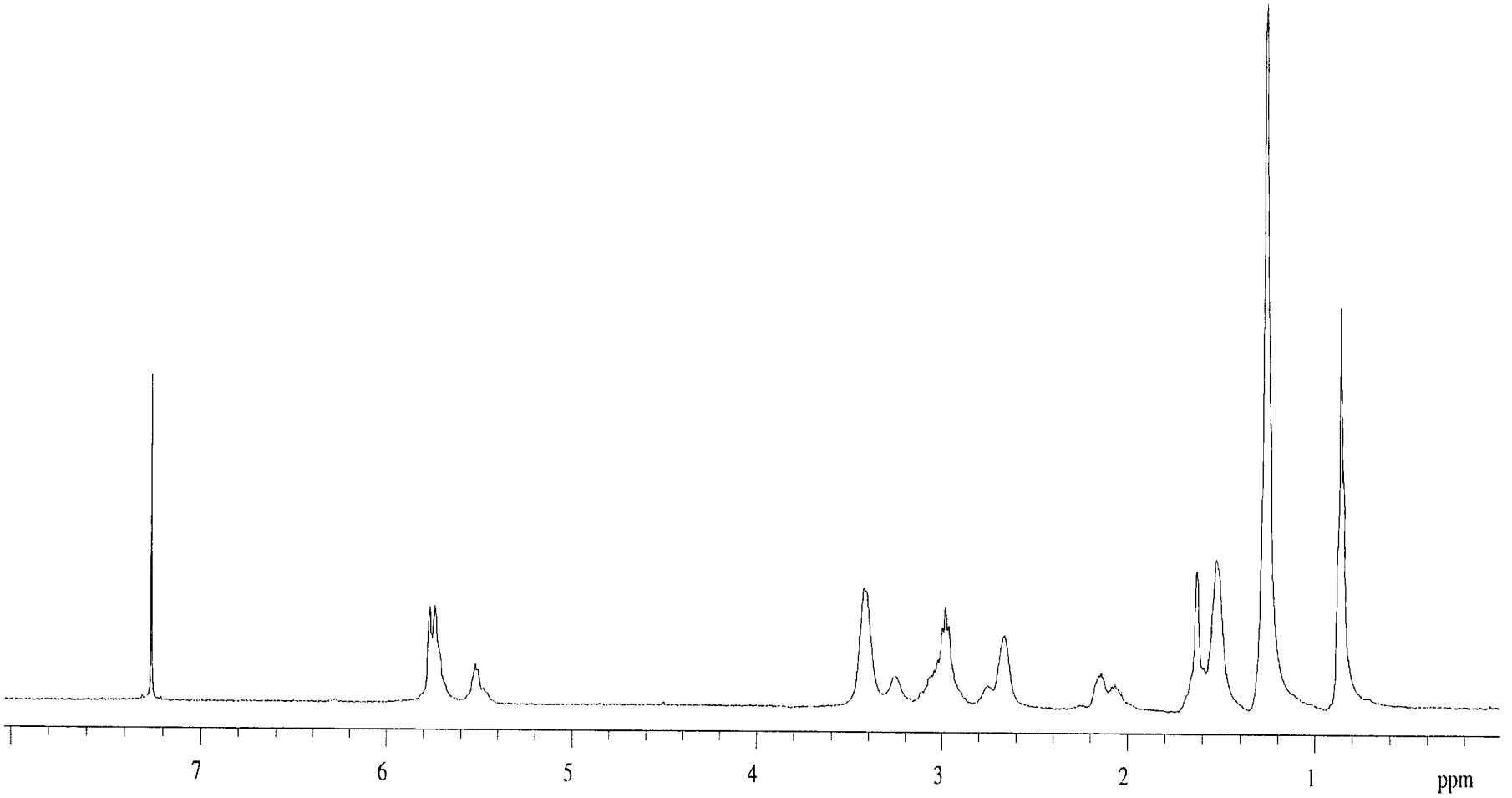

Appendix 4.13 ^{1}H nmr spectrum of poly(*exo*-C6M).

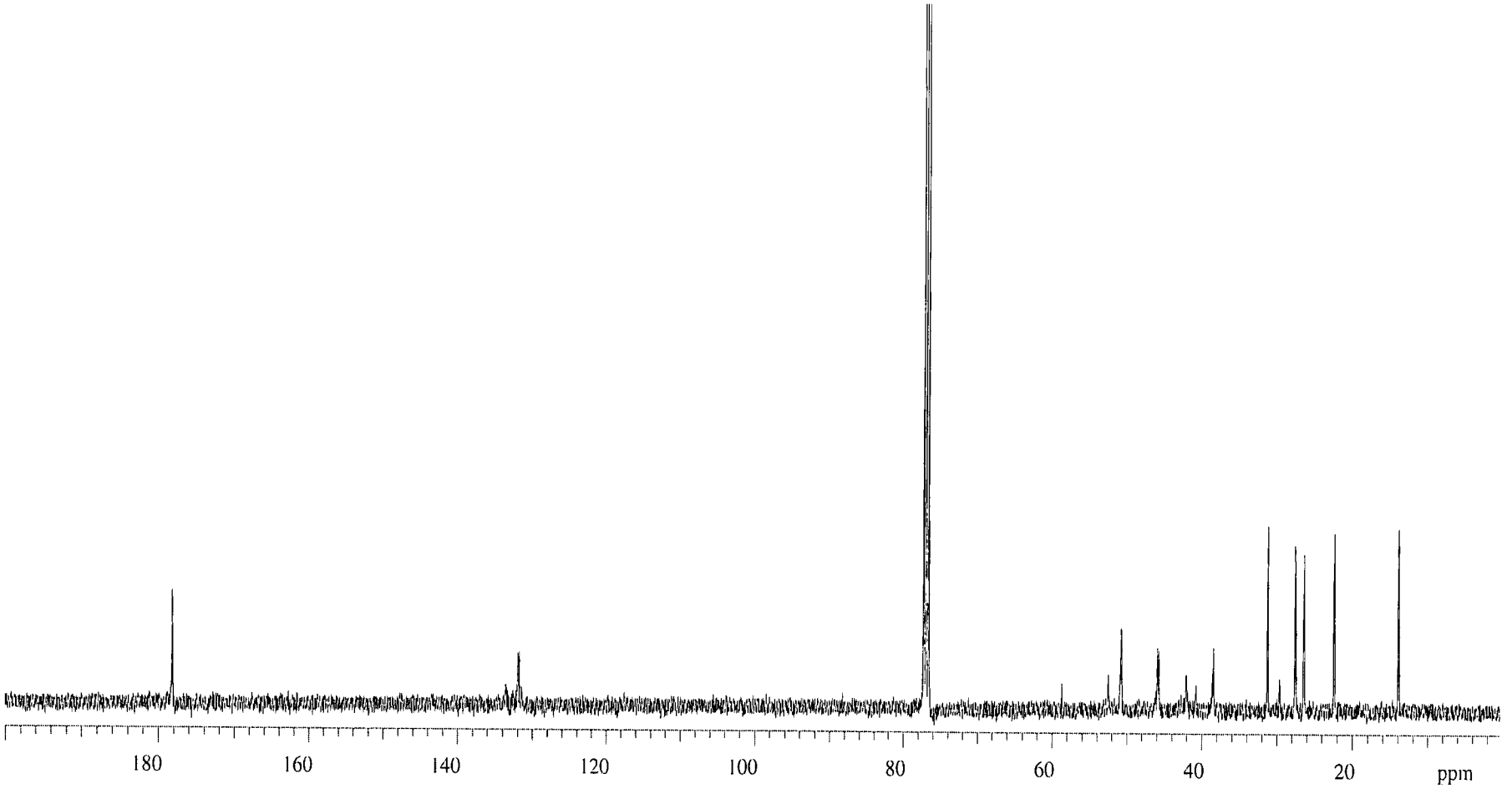

Appendix 4.14 ^{13}C nmr spectrum of poly(*exo*-C6M).

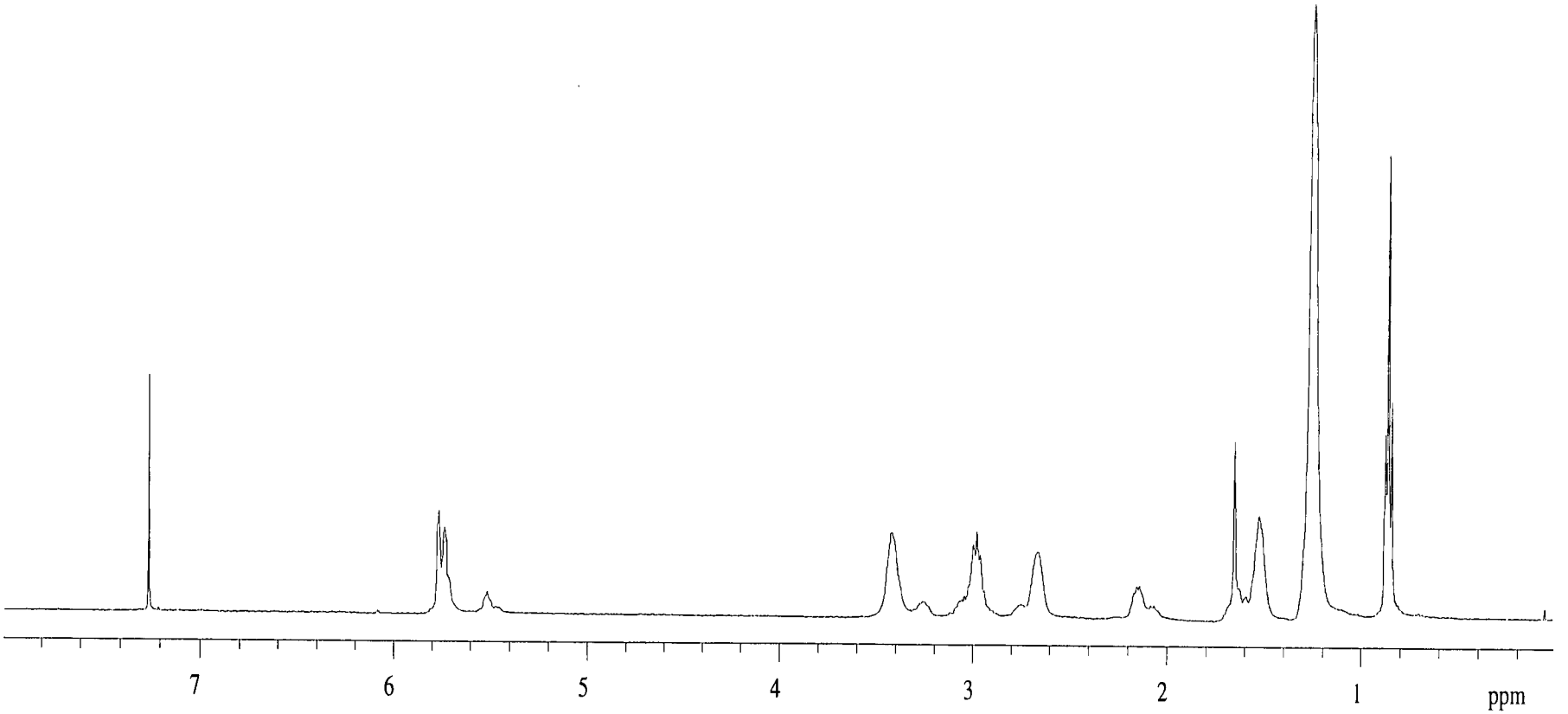

Appendix 4.15 ^{1}H nmr spectrum of poly(*exo*-C8M).

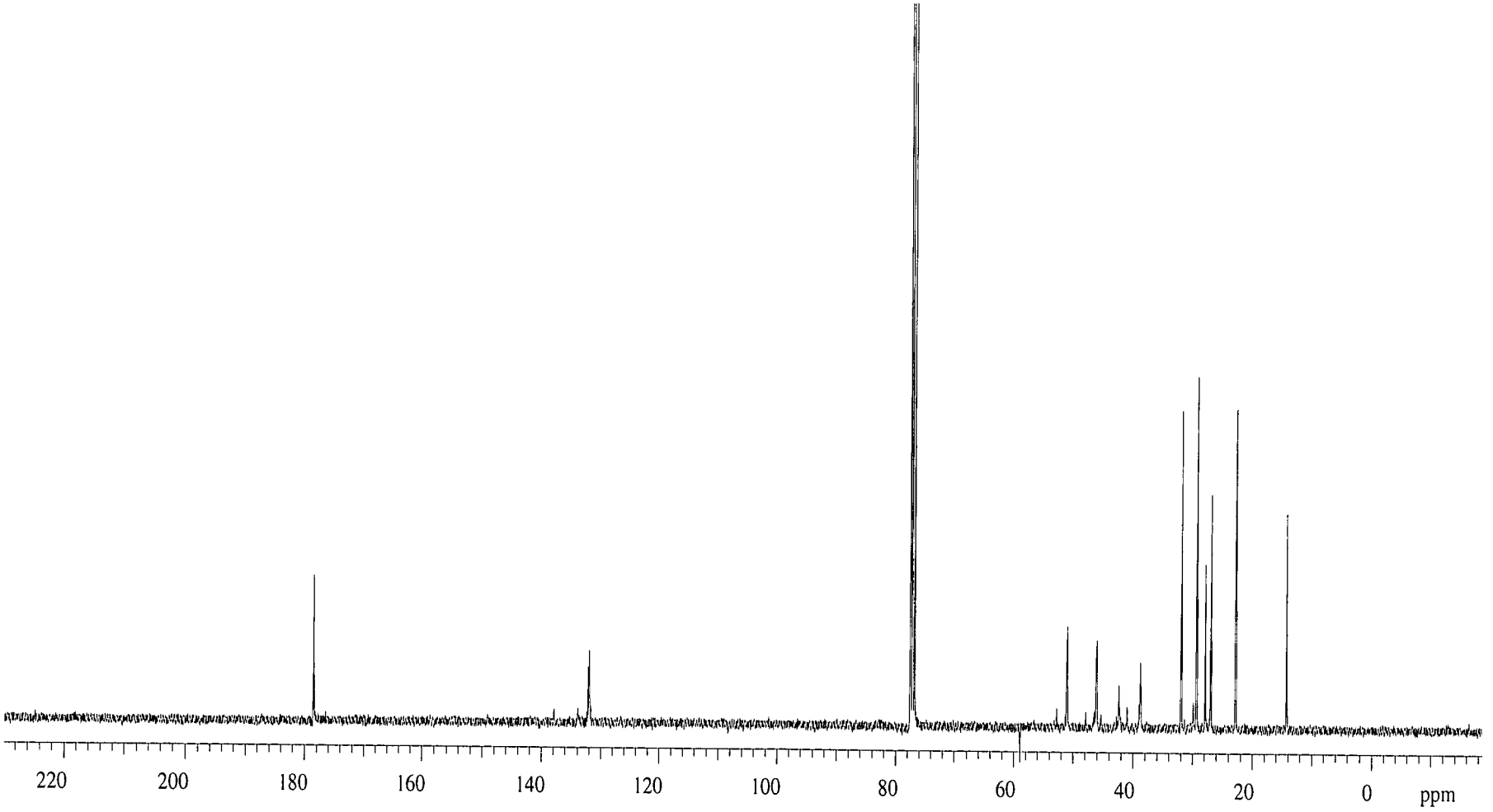

Appendix 4.16 ^{13}C nmr spectrum of poly(*exo*-C8M).

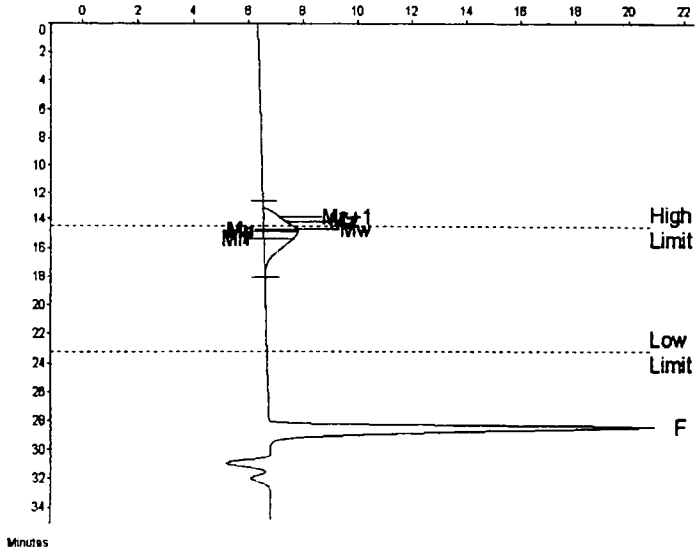

Molecular Weight Averages

Mn = 452,725

Mw = 860,207

Mz = 1,435,024

Polydispersity = 1.900

Appendix 4.17 GPC trace of poly(*exo*-C3M).

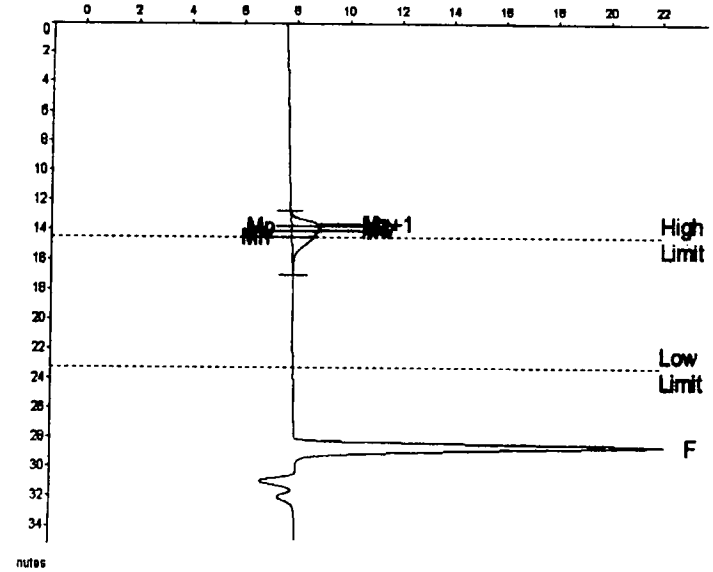

Molecular Weight Averages

Mn = 1,032,745

Mw = 1,558,181

Mz = 2,059,252

Polydispersity = 1.609

Appendix 4.18 GPC trace of poly(*exo*-C4M)-H.

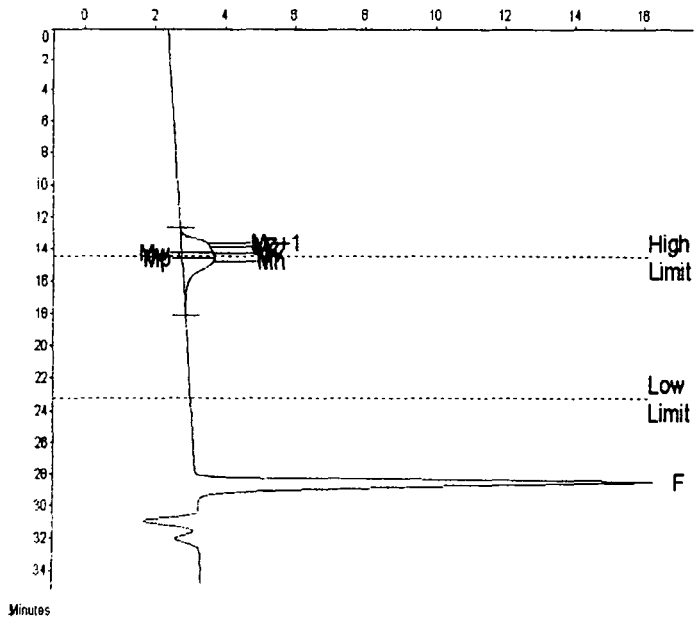

Molecular Weight Averages

Mn = 736,380

Mw = 1,296,250

Mz = 1,913,012

Polydispersity = 1.760

Appendix 4.19 GPC trace of poly(*exo*-C4M)-M.

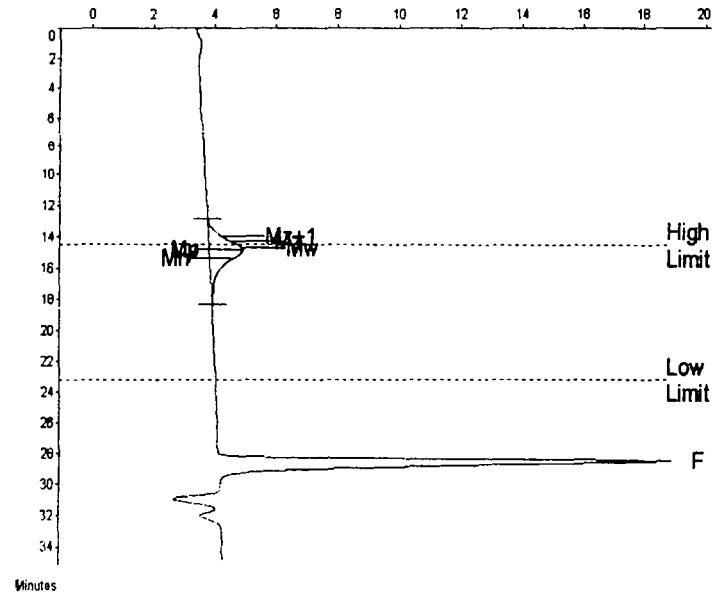

Molecular Weight Averages

Mn = 461,588

Mw = 834,924

Mz = 1,291,869

Polydispersity = 1.809

Appendix 4.20 GPC trace of poly(*exo*-C4M)-L.

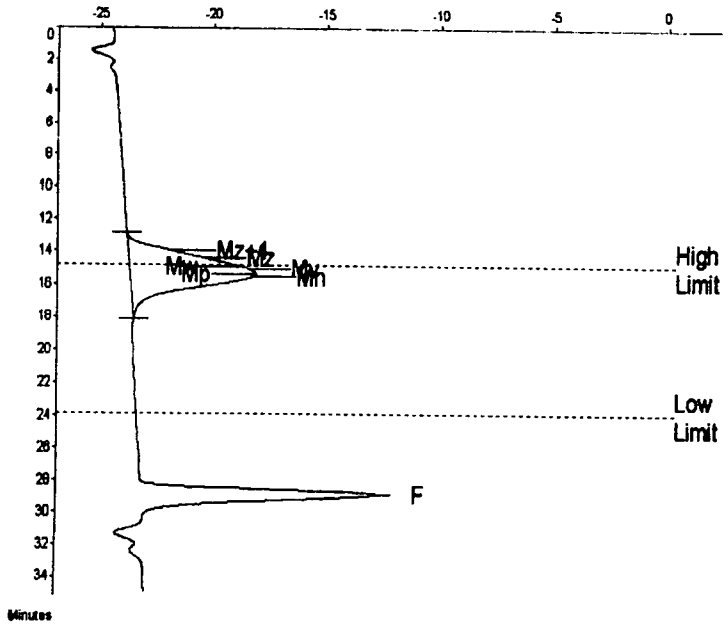

Molecular Weight Averages

Mn = 497,537

Mw = 888,398

Mz = 1,530,370

Polydispersity = 1.786

Appendix 4.21 GPC trace of poly(*exo*-C5M).

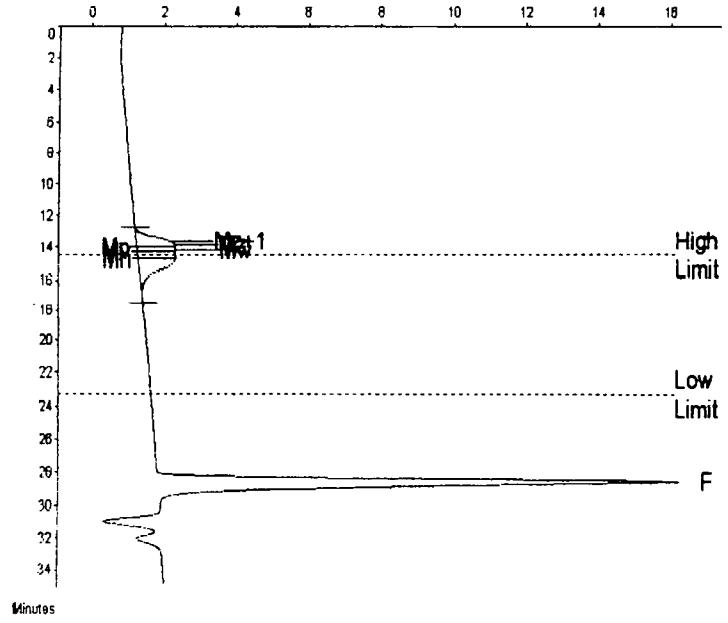

Molecular Weight Averages

Mn = 820,313

Mw = 1,354,389

Mz = 1,963,033

Polydispersity = 1.651

Appendix 4.22 GPC trace of poly(*exo*-C6M).

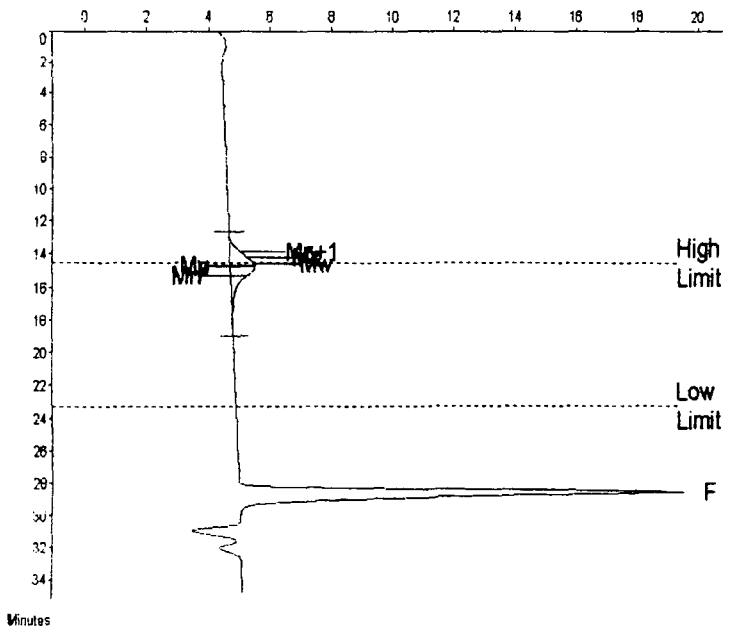

Molecular Weight Averages

Mn = 491608

Mw = 941015

Mz = 1405800

Polydispersity = 1.914

Appendix 4.23 GPC trace of poly(*exo*-C8M).

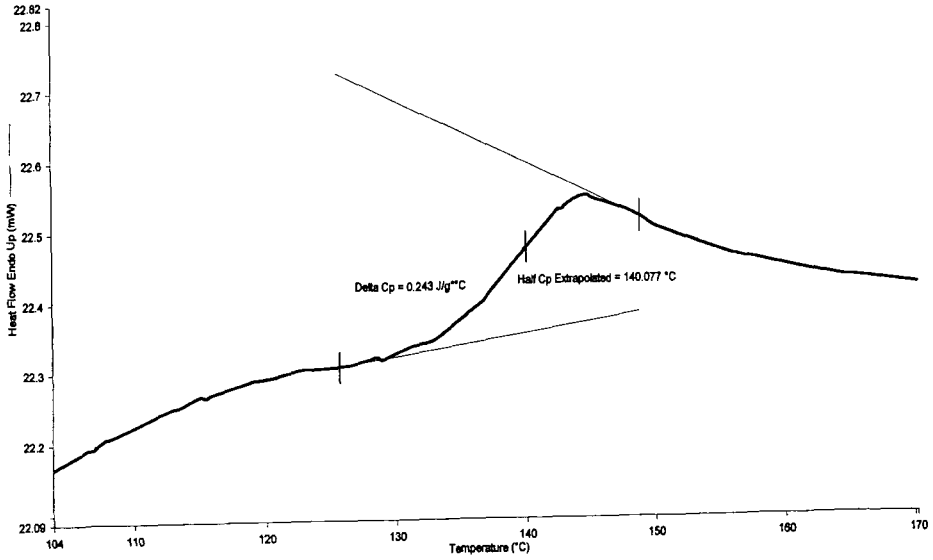

Appendix 4.24 DSC trace of poly(*exo*-C3M).

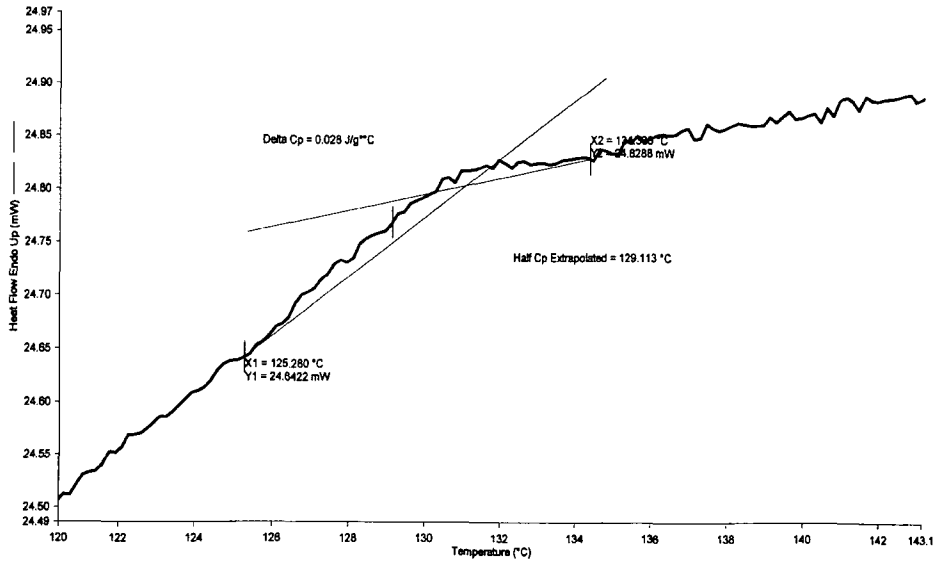

Appendix 4.25 GPC trace of poly(*exo*-C4M)-H.

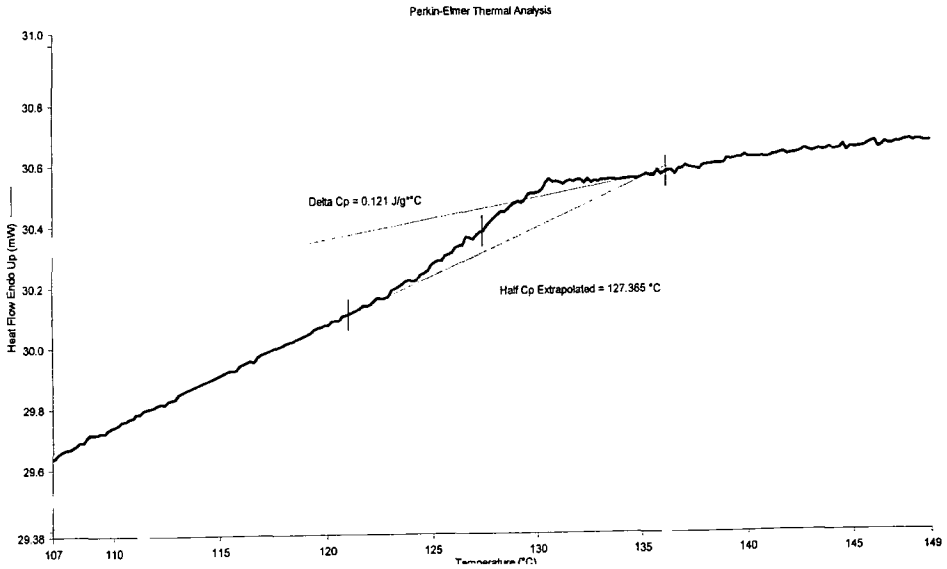

Appendix 4.26 GPC trace of poly(*exo*-C4M)-M.

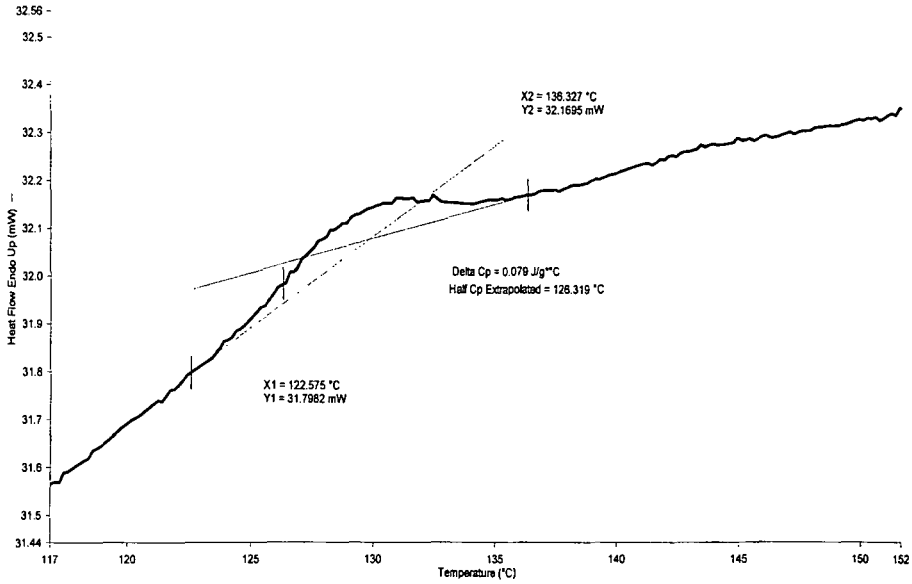

Appendix 4.27 GPC trace of poly(*exo*-C4M)-L.

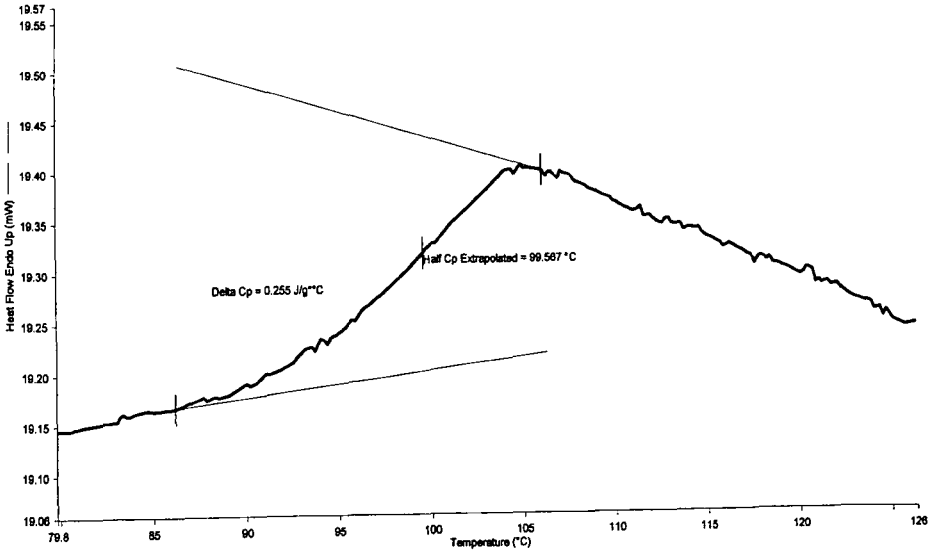

Appendix 4.28 GPC trace of poly(*exo*-C5M).

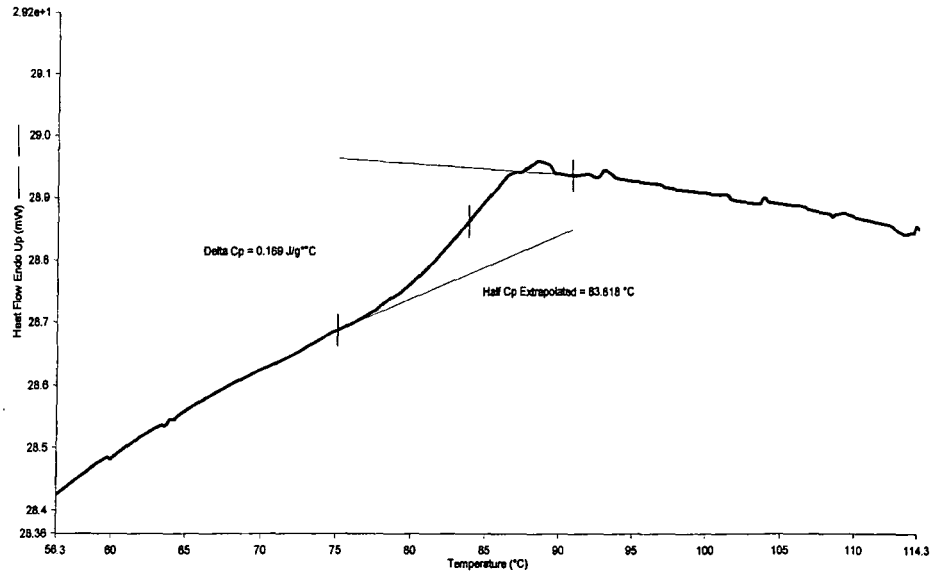

Appendix 4.29 GPC trace of poly(*exo*-C6M).

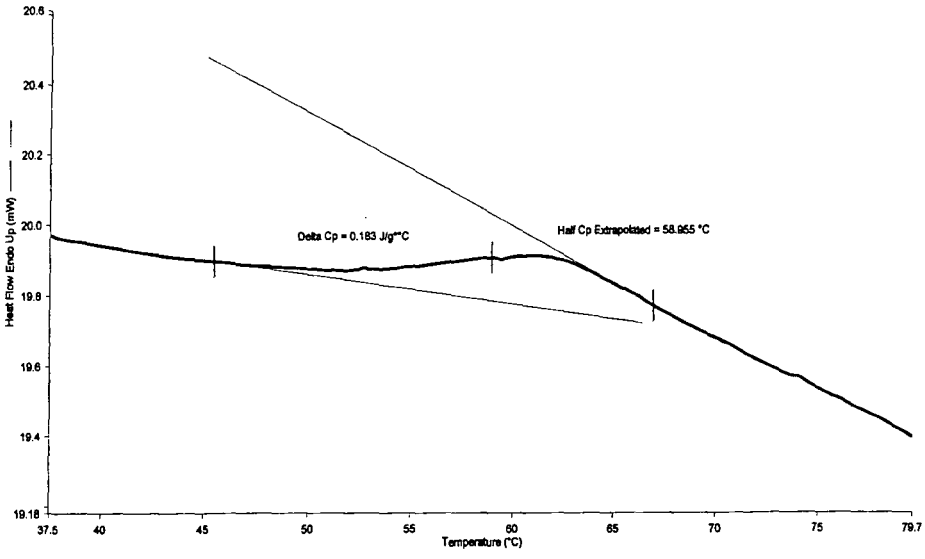

Appendix 4.30 GPC trace of poly(*exo*-C8M).

Appendix 5

Conferences attended

April 1996 Macro Group Family Meeting, Manchester University.

July 1997 The International Meeting on Methathesis and Related Chemistry-ISOM-12, St. Augustine, Florida USA.

July 1998 World Polymer Congress, 37th International Symposium on Macromolecules, Gold Coast, Australia.

July 1999 International Symposium on Olefin Metathesis and Related Chemistry, ISOM'99, Rolduc, Kerkrade, The Netherlands.

September 1999 IRC Industrial Club Meeting, , Leeds and Bradford University.